Effective field theories of strong-interacting systems in nucleon scattering and heavy-quark bound states

Mario Sanchez Sanchez

université PARIS-SACLAY

NNT:
2017SACLS419

Thèse de doctorat

UNIVERSITÉ PARIS SUD
Comprendre le monde, construire l'avenir

Théories effectives des champs pour systèmes avec interaction forte : diffusion des nucléons et états liés de quarks lourds

Thèse de doctorat de l'Université Paris-Saclay
préparée à l'Université Paris-Sud

École doctorale n°576 – *Particules, Hadrons, Énergie, Noyau, Instrumentation, Imagerie, Cosmos et Simulation (PHENIICS)*
Spécialité de doctorat : Physique hadronique

Thèse présentée et soutenue à Orsay, le 20 Novembre 2017, par

M. Sánchez Sánchez Mario

Composition du Jury :

M. Carbonell Jaume Directeur de Recherche, IPN, *Orsay (France)*	Président
M. Frederico Tobias Professeur, ITA, *São José dos Campos (Brésil)*	Rapporteur
M. Hammer Hans-Werner Professeur, Institut für Kernphysik, *Darmstadt (Allemagne)*	Rapporteur
M. Pavón Valderrama Manuel Chargé de Recherche, Université Beihang, *Beijing (Chine)*	Examinateur
M. Somà Vittorio Ingénieur de Recherche, IRFU, *Gif-sur-Yvette (France)*	Examinateur
M. van Kolck Ubirajara Directeur de Recherche, IPN, *Orsay (France)*	Directeur de thèse

Acknowledgements

In these lines I would like to remark my gratitude towards those who, one way or another, contributed to make this thesis possible, and also made my life during the last three years more enjoyable and less tough than it would have been without them.

In particular, I will always be grateful to Bira, my advisor, whose vast knowledge, deep physical intuition, and strong "EFTism" have been, and keep being, a fundamental inspiration for me. I have learned a lot from enlightening discussions with him —and if I couldn't learn more, this was due to my own limitations, which he helped me to overcome during these years. By the way, talking with him about any topic, no matter whether we coincided in our viewpoints or not, was always instructive and pleasant. I should also acknowledge his patience and care in reading the endless drafts of the thesis manuscript.

Heartily thanks also to Manolo for his guidance, patience and generosity, which includes having been a great host during my stay in China at the very end of my Ph.D. I will never forget that he taught me much of the physics included in these pages, and supported and trusted in me when concerns and doubts assailed me.

Thank you to Jerry and Bingwei, with whom it was a pleasure to collaborate, discuss and start growing as a researcher —I really hope we keep working together for many years—; to the people in the committee of my thesis defense for their generosity and kindness; to the members of the *Physique théorique* and *Physique hadronique* groups at the IPNO (Michael, Marcella, Dennis, Elias, Paolo, Giai, Véronique, Bachir..., and the junior researchers as well) for being there when I needed them with kind and warm words and for those enjoyable discussions at lunchtime; to my former professors in Murcia for having contributed in the process that drove me to this Ph.D. adventure, and in particular to José Antonio, whose intervention in that regard was key.

Pasaré a mi lengua materna para dar las gracias a mis amigos de toda la vida, *Pepaco*, *Pancho* y *Edgardo*, con quienes tantos momentos entrañables, alegrías y penas he compartido

desde que era un crío de la escuela primaria. Más de una vez en que estaba abrumado por la cantidad de trabajo o saturado por algún cálculo duro de roer, entrar en nuestro grupo de *whatsapp* y leer las tonterías que escribían y añadir las mías me ayudó a desconectar y a echar unas risas. Me alegra poder decir que nuestra amistad no se ha perdido por el hecho de que yo tuviera que abandonar la ciudad y el país donde crecimos juntos, sino que se ha fortalecido y espero que siga viva por mucho tiempo.

Nunca podré estar lo bastante agradecido a mis padres. Ellos me dieron la vida y jamás me fallaron. Su apoyo —emocional y financiero— ha sido, es y será un ingrediente indispensable en todos los éxitos que haya alcanzado o pueda alcanzar en el futuro. Por ello, deseo corresponderles y trabajar cada día para que puedan sentirse orgullosos de mí. Gracias también a mi hermana Cristina, que estuvo a mi lado en más de un momento duro; a mis tías Consuelo y María José, por su bondad desprendida y risueña; a mis abuelos Lorenzo e Isabel donde quiera que estén.

Y, desde luego, gracias a Uly, mi mujer, por su sacrificio y su amor. Sé que a menudo no ha sido fácil, pero has sido paciente y comprensiva; has permanecido a mi lado pese a mis (muchos) defectos y a las (demasiadas) veces en que mi trabajo ha interferido en nuestra vida familiar; has sacrificado tus propias ambiciones personales en pro de nuestro proyecto común... y me has regalado lo mejor que me ha pasado en mi vida, nuestro precioso hijo Jaime, a quien, juntos, hemos visto crecer, no tan de cerca como habría deseado en mi caso, durante los dos últimos años, y que tantos momentos de dicha nos ha de regalar todavía. A ti y a él, os llevo en mi corazón, y a vosotros os dedico cada línea de este trabajo.

A Jaime y Uly

Contents

Chapter 1

Introduction

1.1 Effective field theory

1.1.1 What is it?

Problems displaying separation of momentum (or distance) scales constantly appear in physics. Among many examples of this fact, we could recall that one does not need to describe how atoms or molecules interact with each other to study the macroscopic properties of a fluid, nor to have a precise knowledge of what is going on in the atomic nucleus to make predictions about atomic or molecular systems. Given two theories, A and B, such that the momentum and energy regimes of the theory A lie far above the ones of the theory B (the typical distances that concern the theory A are much smaller than the ones of the theory B, put in other words), the theory B is said to be "less fundamental" than (or to "emerge" from) the theory A; however, it is clear that, *within its own territory*, the theory B is a self-contained, useful theory from where concrete predictions can be made. Putting it short:

"High-energy details are inconsequential if we stick to a low-energy description of nature."

(Actually, if this were not the case, physicists could not make any progress in their respective fields of expertise until some "theory of everything" was finally established.) The effect of the theory A at large distances may thus be parametrized by the so-called *low-energy couplings* of the theory B. Sometimes, the couplings can be derived from the theory A, either explicitly or by means of numerical calculations ("top-down strategy"); however, often this task is

not feasible and one needs to determine the couplings from the available empirical data ("bottom-up strategy").

The ideas above are very powerful, and the effective field theory (EFT) approach (see Refs. [1–5] for general and pedagogical reviews) exploits them in a *systematic* way. Indeed, this last feature of any EFT is essential, and what distinguishes it from models. We say that an EFT is "systematic" in the sense that, at least *a priori*, its predictions can be made as accurate as one wants by going one step further in a power series whose expansion parameter is usually given by the ratio of two physical scales, such as the typical external momentum of a physical process amenable to the EFT over the momentum scale at which the EFT stops working and needs to be replaced by some other EFT that underlies the former. At the same time, the EFT expansion offers one the possibility of always keeping under control the *uncertainties* of its predictions at a given order.

There are two more basic ingredients that one needs to add to cook a proper EFT. These are *renormalization-group* (RG) *invariance* and *power counting* (PC):

- The emergence of ultraviolet infinities from loop diagrams was discovered several decades ago, in the context of quantum electrodynamics (QED). Such divergences may be healed via the introduction of a cutoff Λ that separates "low" and "high" loop momenta (*regularization*). But, given the arbitrariness of this separation, the low-energy couplings of the theory must run with Λ in such a way that *all* the resulting predictions of observable quantities exhibit a mild and controlled cutoff dependence, remaining well-defined in the $\Lambda \to \infty$ limit (*renormalization*).

- In EFT, *any* interaction that is not forbidden by symmetry requirements will take place; consequently, an infinite number of interactions will occur. The role of PC rules is to discriminate *which* of these interactions should be used when doing calculations at a given order in the EFT expansion. These rules also tell us whether a given interaction term should be taken as non-perturbative (infinitely iterated) or perturbative.

The two key notions above —RG invariance and PC— are not independent of each other, but actually intimately intertwined. On the one hand, the traditional sense of renormalization can be reinterpreted —from "global" to "order-by-order"— thanks to PC, as the latter guarantees that a *finite* number of interaction terms suffices to achieve, at a given order in the expansion, the desired accuracy, thus allowing for a *finite* number of low-energy couplings to circumvent cutoff dependence of observables. On the other hand, a consistent PC needs

to provide all the necessary low-energy couplings to ensure that the RG invariance principle is truly satisfied by the EFT. As we will see, this requirement on the PC rules can be quite delicate sometimes (most particularly, when some of the effective interaction terms are to be fully iterated).

1.1.2 Why is it useful in nuclear and hadronic physics?

For many years already, it has been established that quantum chromodynamics (QCD) is the fundamental theory of the strong interaction (see Ref. [6] for a nice review). The pure QCD Lagrangian is [1]

$$\mathcal{L}_{\rm QCD} = \sum_f \bar{q}_f^i \left(i\gamma_\mu D^\mu_{ij} - m_f \delta_{ij} \right) q_f^j - \tfrac{1}{2}{\rm Tr}\left(\mathcal{G}_{\mu\nu}\mathcal{G}^{\mu\nu} \right), \tag{1.1}$$

where q_f^i is the spin-1/2 quark field, with dimension of mass$^{3/2}$ ($[q_f^i] = 3/2$), f standing for a flavor index that can be u ("up"), d ("down"), s ("strange"), c ("charm"), b ("bottom"), or t ("top"), and $i = \mathrm{r}, \mathrm{g}, \mathrm{b} \equiv 1, 2, 3$ being a color index. Here, the sum over both greek and latin indices is implied, γ_μ is a Dirac matrix whose (omitted) indices are contracted with the spinor indices of the quark fields, and m_f is the quark mass. Besides, $D^\mu_{ij} = \partial^\mu \delta_{ij} - ig A^\mu_a \mathcal{T}^a_{ij} \equiv \partial^\mu \delta_{ij} - ig \mathcal{A}^\mu_{ij}$ is the covariant derivative matrix element in color space, g being the strong coupling constant, $A^\mu_1, \ldots, A^\mu_8$ being the gluon fields, and $\mathcal{T}^1, \ldots, \mathcal{T}^8$ being the matrix generators of $\mathrm{SU}(3)_{\rm color}$. Finally, $\mathcal{G}^{\mu\nu} = \partial^\mu \mathcal{A}^\nu - \partial^\nu \mathcal{A}^\mu - ig\left[\mathcal{A}^\mu, \mathcal{A}^\nu\right]$ is the gluon strength tensor.

The strong coupling g is not exactly "constant", but subject to RG invariance, thus dependent upon the characteristic energy scale of a given strong process. As the energy is increased (much above the infrared QCD scale $\Lambda_{\rm QCD} \sim 300\,\mathrm{MeV}$), the coupling gets smaller and smaller, implying a very perturbative color interaction (*asymptotic freedom*). In perturbative QCD, it is convenient to take gluons and quarks as the explicit degrees of freedom of the theory. Conversely, in the low-energy regime (below $\Lambda_{\rm QCD}$) the theory gets highly non-perturbative, as manifest in the fact that the QCD spectrum cannot be written in terms of gluons and quarks anymore, but in terms of hadrons —mesons and baryons— into which those remain tightly bound (*confinement*).

[1] All through this work we will use natural units, thus set the reduced Planck constant $\hbar$ and the speed of light c equal to 1.

The most stable baryons are the nucleons (protons and neutrons), which bind into the atomic nuclei that, together with the electrons, constitute ordinary matter. Other hadrons, like pions or hyperons, also interact with each other through the strong force. Nuclear and hadronic forces can thus be seen as a residual effect of the strong interactions that keep gluons and quarks confined, much like atomic and molecular forces emerge from the electromagnetic interactions that combine nuclei and electrons into atoms. Thus, a complete theoretical understanding of nuclear and hadronic physics demands to bridge their gap with the underlying QCD. Even though physical models —some of which were posed before the discovery of QCD— can sometimes reproduce successfully several empirically observed features of nuclear and hadronic systems, they miss the connection above. This makes necessary to look for alternative strategies. Nowadays, among such strategies the most promising are lattice QCD (LQCD) and EFT:

- In LQCD, one aims at calculating nuclear and hadronic properties *directly* from QCD, by means of computationally expensive simulations on a discretized space-time grid. It is only since a few years that LQCD has started to obtain quantitative properties of light nuclei, few-nucleon scattering, and other hadronic systems, even though still for unphysically large quark masses (see *e.g.* Refs. [7, 8] for overviews and references). Indeed, LQCD is not yet able to explain the systems above in the physical world, *i.e.* for the physical pion mass ($m_\pi \approx 140\,\text{MeV}$). Still, the current situation invites us to think that such objective will be reached soon.

- Conversely, the EFT formulation avoids the requirement of complex numerical calculations by establishing the connection with the underlying QCD in an *indirect* way (see Refs. [9–11] for reviews concerning nuclear forces). The basic idea is to exploit the (either exact or approximate) *symmetries* of the Lagrangian (1.1), and write down the most general effective Lagrangian involving the low-energy degrees of freedom (*i.e.* hadrons) and preserving such symmetries. In this regard, nuclear and hadronic EFTs are nothing but the RG evolution of QCD at low, non-perturbative energies.

(The two approaches above are not in contradiction to each other. In fact, they can be seen as complementary; for example, the so-called chiral extrapolations allow for the determination of the effective couplings from LQCD results.)

In this work, we will follow the second approach. This can be done thanks to the separation of scales that is inherent to nuclear and hadronic physics —while hadrons are no longer

valid degrees of freedoms at momenta above a characteristic hard scale $M_{\rm QCD} \sim 1\,\text{GeV}$, most processes of interest occur at a softer momentum scale $Q \sim 100\,\text{MeV}$ or less. Then, PC rules dictate which terms in the effective Lagrangian (out of an infinite number) are to be taken into account when computing observables at a given order in an expansion in powers of the small parameter $Q/M_{\rm QCD}$. The systematicity of this expansion represents another important advantage of the EFT method with respect to models when facing nuclear and hadronic systems. Thanks to the recent development of *ab initio* methods, which bridge the gap between nuclear forces and currents on one hand and nuclear structure and reactions on the other (see Ref. [12] for an overview), nuclear EFT is now better exploited than ever.

In this chapter, we will present two EFTs that are widely used nowadays in the study of nuclear forces, that is to say *chiral EFT* (Section 1.2) and *pionless EFT* (Section 1.3), plus another EFT which is particularly useful when applied to exotic hadronic systems, namely *heavy-quark EFT* (Section 1.4). At the end of the chapter, an outline of the rest of the present work will be given (Section 1.5).

1.2 Chiral EFT

1.2.1 A brief primer to chiral perturbation theory

Chiral perturbation theory (χPT) is the oldest, best-established example of low-energy EFT of the strong interaction (see Ref. [13] for a pedagogical introduction). As such, this theory needs to preserve the same symmetries as QCD does at high energies. To show how χPT emerges from QCD, let us consider the QCD Lagrangian (1.1) restricted to the two lightest quark flavors u and d. Taking $\gamma^5 = i\gamma^0\gamma^1\gamma^2\gamma^3$, decompose the up-quark spinor field as the sum

$$u = u_L + u_R, \quad \text{with} \quad u_L = \tfrac{1}{2}\left(1+\gamma^5\right)u \quad \text{and} \quad u_R = \tfrac{1}{2}\left(1-\gamma^5\right)u, \tag{1.2}$$

and similarly for the down-quark spinor field [2]. In the limit of vanishing $\bar{m} = (m_u + m_d)/2$, the QCD Lagrangian will become

$$\mathcal{L}_{\rm QCD}|_{\bar{m}=0} = \bar{u}_L i\not{D} u_L + \bar{u}_R i\not{D} u_R + \bar{d}_L i\not{D} d_L + \bar{d}_R i\not{D} d_R - \tfrac{1}{2}\text{Tr}\left(\mathcal{G}_{\mu\nu}\mathcal{G}^{\mu\nu}\right), \tag{1.3}$$

[2] To see the physical meaning of these definitions, consider the spin operator $\boldsymbol{S}$ of u and d. If these are assumed to be massless, *i.e.* to move with unambiguous three-velocity $\boldsymbol{v}$ ($|\boldsymbol{v}| = 1$), then u_L and d_L (u_R and d_R) will be eigenstates of $\boldsymbol{S}\cdot\boldsymbol{v}$ with eigenvalue $-1/2$ ($+1/2$).

where the color indices were now omitted for simplicity, and we abbreviated $\not{D} = \gamma_\mu D^\mu$. As a consequence of the full decoupling between the right- and the left-handed components of the quark fields, the massless QCD Lagrangian (1.3) is *chirally symmetric*, *i.e.* invariant under the independent flavor rotations

$$\begin{pmatrix} u_L & d_L \end{pmatrix}^{\mathrm{T}} \mapsto U_L \begin{pmatrix} u_L & d_L \end{pmatrix}^{\mathrm{T}} \quad \text{and} \quad \begin{pmatrix} u_R & d_R \end{pmatrix}^{\mathrm{T}} \mapsto U_R \begin{pmatrix} u_R & d_R \end{pmatrix}^{\mathrm{T}}, \tag{1.4}$$

where "T" refers to the transpose matrix, and $U_{L,R} \in \mathrm{SU}(2)_{L,R}$ may be parametrized up to the linear term in $\epsilon \to 0$ as

$$U_{L,R} = 1 + i\epsilon^a_{L,R}\tau^a, \tag{1.5}$$

with τ^1, τ^2, τ^3 the Pauli matrices in flavor space. Then, taking

$$\epsilon^a_V = \tfrac{1}{2}\left(\epsilon^a_L + \epsilon^a_R\right) \quad \text{and} \quad \epsilon^a_A = \tfrac{1}{2}\left(\epsilon^a_L - \epsilon^a_R\right), \tag{1.6}$$

Eq. (1.4) yields

$$\begin{pmatrix} u & d \end{pmatrix}^{\mathrm{T}} \mapsto U \begin{pmatrix} u & d \end{pmatrix}^{\mathrm{T}} \quad \text{with} \quad U = 1 + i\left(\epsilon^a_V + \gamma_5\epsilon^a_A\right)\tau^a. \tag{1.7}$$

When $\epsilon^a_A = 0$ ($U_L = U_R$), $U_V = 1 + i\epsilon^a_V\tau^a$ belongs to $\mathrm{SU}(2)_V$, the group of isospin rotations, corresponding to the internal symmetry of the nucleon isodoublet $N = (p\,n)^{\mathrm{T}}$. When $\epsilon^a_V = 0$ ($U_L^\dagger = U_R$), $U_A = 1 + i\gamma_5\epsilon^a_A\tau^a$ is an axial rotation [3].

If the invariance under $\mathrm{SU}(2)_L \times \mathrm{SU}(2)_R$ had been fully respected by the massless theory, then the expectation value of the bilinear operators $\bar{u}u$ and $\bar{d}d$ at the ground state —its so-called vacuum expectation value (VEV)— would have identically vanished. However, as it has been repeatedly checked in lattice calculations (see *e.g.* Ref. [15]),

$$\langle \bar{q}_k q_l \rangle = 2\left\langle \left(\bar{q}_k\right)_L \left(q_l\right)_R \right\rangle = v^3\delta_{kl} \quad \text{with} \quad q_1 = u \quad \text{and} \quad q_2 = d, \tag{1.8}$$

where the magnitude of v has the same size as Λ_{QCD}. The non-vanishing of the VEV $\langle \bar{q}q \rangle$, also known as the chiral condensate, illustrates the spontaneous symmetry breakdown (SSB) of $SU(2)_L \times SU(2)_R$ by massless QCD (see Appendix A for a short review on SSB) [4]. Applying

[3] Actually, the Lagrangian (1.3) is also invariant under $\mathrm{U}(1)_V$, $(u\,d)^{\mathrm{T}} \mapsto (1 + i\epsilon_V)\,(u\,d)^{\mathrm{T}}$ (which is an exactly fulfilled symmetry even away from the massless limit), as a reflection of the baryon number conservation. Finally, its invariance under $\mathrm{U}(1)_A$, $(u\,d)^{\mathrm{T}} \mapsto (1 + i\gamma_5\epsilon_A)\,(u\,d)^{\mathrm{T}}$, is verified, too; however, this one is not a true symmetry of the massless theory due to quantum effects known as *anomalies* [14].

[4] The Big Bang cosmology accepts that the SSB of chiral symmetry emerged in the very early Universe (less than a millionth of a second after the bang), when its temperature became $\lesssim \Lambda_{\mathrm{QCD}} \sim 10^{12}\,\mathrm{K}$. At this point, the thermal energy of the sea of quarks was overcome by their binding energies, so quarks could coalesce into hadrons.

Eq. (1.4) to Eq. (1.8) gives

$$\langle \bar{q}_k q_l \rangle \mapsto (U_L)_{km} \left(v^3 \delta_{mn}\right) \left(U_R^\dagger\right)_{nl} = v^3 \left(U_L U_R^\dagger\right)_{kl}, \tag{1.9}$$

from where we see that only for an isospin transformation U_V does the chiral condensate remain invariant; in any other case where $\epsilon_L^a \neq \epsilon_R^a$, the chiral transformation will produce a different VEV which will be degenerate in energy with the previous one —in a word, the chiral condensate spontaneously breaks $G \equiv \mathrm{SU}(2)_L \times \mathrm{SU}(2)_R$ down to $H \equiv \mathrm{SU}(2)_V$. This corresponds to the presence of $2^2 - 1 = 3$ broken generators, which in virtue of the Goldstone theorem implies the emergence of three massless Goldstone bosons. These turn out to be the pion triplet.

Of course, all the discussion up to now has ignored that $m_{u,d} \neq 0$. Away from the massless limit, the term $-m_k \bar{q}_k q_k = -m_k[(\bar{q}_k)_L (q_k)_R + (\bar{q}_k)_R (q_k)_L]$ in the Lagrangian (1.1) mixes the left- and the right-handed components of the quarks, so the two-flavor theory is not invariant anymore under Eq. (1.4) —that is to say, chiral symmetry is also *explicitly* broken. But, as $m_{u,d}/\Lambda_{\mathrm{QCD}} \ll 1$ ($m_u \sim 2\,\mathrm{MeV}$, $m_d \sim 5\,\mathrm{MeV}$ [16]), it happens that $\mathcal{L}_{\mathrm{QCD}}$ is, up to a very good approximation, invariant under Eq. (1.4). Besides, even though the isospin symmetry is not manifest at the quark level (as the relative mass splitting $|m_u - m_d| \,/\, (m_u + m_d) \sim 1/3$ is not so small), the relation $\langle \bar{u}u \rangle = \langle \bar{d}d \rangle$ keeps being very approximately valid.

In the same way, the three bosons emerging from SSB are not truly massless as they would be in the $\bar{m} \to 0$ limit, but they are rather light ($m_{\pi^\pm} \approx 140\,\mathrm{MeV}$, $m_{\pi^0} \approx 135\,\mathrm{MeV}$ [16]) when compared to the hadron masses ($\sim 1\,\mathrm{GeV}$), so they go under the name of pseudo-Goldstone bosons. Again, the smallness of their relative mass splitting is a reflection of the goodness of isospin symmetry at the hadron level. Actually, neglecting the quark mass splitting, the non-vanishing squared pion mass can be postdicted, up to a dimensionful proportionality constant, as the product of the two ways in which chiral symmetry breaks down —explicit and spontaneous—

$$m_\pi^2 = -\tfrac{2}{f_\pi^2}\, \bar{m}\, v^3 + \mathcal{O}(\bar{m}^2), \quad \bar{m} = m_u = m_d, \tag{1.10}$$

where $f_\pi \simeq 93\,\mathrm{MeV}$ can be empirically measured through the leptonic decay of the pion [17]. This is the celebrated Gell-Mann–Oakes–Renner relation [18], which holds within $\sim 10\%$ approximation in the real world.

χPT is an EFT for low external momenta ($Q \sim m_\pi$) that focuses on the purely pionic sector, just ignoring all the remaining, heavier modes of QCD. The fields $\pi^1(x)$, $\pi^2(x)$, $\pi^3(x)$ are the coordinates associated to the Goldstone fields living in the quotient group G/H,

which is itself SU(2), hence spanned by three generators $\mathcal{T}^1$, $\mathcal{T}^2$, $\mathcal{T}^3$. In the defining representation, the latter are a triplet of traceless, Hermitian matrices which we choose to obey the convenient normalization $\mathrm{Tr}\,(\mathcal{T}^a\mathcal{T}^b) = \delta^{ab}$, thus we take $\mathcal{T}^a = \tau^a/\sqrt{2}$, with τ^a a Pauli matrix. This allows us to define the pion matrix $\Pi(x)$,

$$\Pi(x) = \pi^a(x)\mathcal{T}^a = \begin{pmatrix} \frac{1}{\sqrt{2}}\pi^3(x) & \frac{1}{\sqrt{2}}[\pi^1(x) - i\pi^2(x)] \\ \frac{1}{\sqrt{2}}[\pi^1(x) + i\pi^2(x)] & -\frac{1}{\sqrt{2}}\pi^3(x) \end{pmatrix} \equiv \begin{pmatrix} \frac{1}{\sqrt{2}}\pi^0(x) & \pi^+(x) \\ \pi^-(x) & -\frac{1}{\sqrt{2}}\pi^0(x) \end{pmatrix}, \tag{1.11}$$

which, according to the chosen normalization, can be inverted through $\pi^a(x) = \mathrm{Tr}\,[\Pi(x)\mathcal{T}^a]$. Then, the unimodular, unitary matrix $\mathcal{U}(x)$,

$$\mathcal{U}(x) = e^{\sqrt{2}i\,\Pi(x)/f_\pi}, \tag{1.12}$$

will transform linearly under G,

$$\mathcal{U}(x) \mapsto U_L\,\mathcal{U}(x)\,U_R^\dagger. \tag{1.13}$$

To see how the pion fields should change under some transformation living in G/H, say a pure axial rotation, expand the exponentials in Eq. (1.13) and truncate both sides at the linear order in ϵ or $\Pi(x)/f_\pi$. This yields $1 + \sqrt{2}i\Pi(x)/f_\pi \mapsto 1 + \sqrt{2}i\,[\Pi(x)/f_\pi + \sqrt{2}\epsilon^a\tau^a]$, or equivalently, $\pi^a(x) \mapsto [\pi^a(x) + 2\epsilon^a f_\pi]$. The change in $\pi^a(x)$ is not linear in $\pi^a(x)$, which is a sign of SSB [19].

The exponential representation (1.12) of the pion fields is not the only valid one; other commonly used choices include the so-called sigma parametrization

$$\mathcal{U}(x) = \sigma(x) + i\tau^a\,\tfrac{\pi^a(x)}{f_\pi}, \quad \sigma(x) = \left[1 - \tfrac{\pi^a(x)\pi^a(x)}{f_\pi^2}\right]^{1/2}. \tag{1.14}$$

Of course, predictions of observables can never depend on the chosen representation. This is explicitly proven by the Callan–Coleman–Wess–Zumino construction [20, 21] —all realizations of the chiral group are equivalent to each other up to non-linear redefinitions of the fields, which do not affect the results for observables.

The analysis performed up to now could have been extended beyond the u and d quark flavors to include the s quark. In that case, the spontaneous breakdown of chiral symmetry would have been $\mathrm{SU}(3)_L \times \mathrm{SU}(3)_R \to \mathrm{SU}(3)_V$, implying the emergence of $3^2 - 1 = 8$ pseudo-Goldstone bosons. Everything would have worked out essentially the same way, but the pion

matrix (1.11) would have been replaced by the meson-octet matrix,

$$\Pi(x) = \begin{pmatrix} \frac{1}{\sqrt{2}}\pi^0(x) + \frac{1}{\sqrt{6}}\eta(x) & \pi^+(x) & K^+(x) \\ \pi^-(x) & -\frac{1}{\sqrt{2}}\pi^0(x) + \frac{1}{\sqrt{6}}\eta(x) & K^0(x) \\ K^-(x) & \bar{K}^0(x) & -\sqrt{\frac{2}{3}}\,\eta(x) \end{pmatrix}, \tag{1.15}$$

where the five new pseudo-Goldstone bosons are significantly heavier than the three old ones ($m_K \sim m_\eta \sim 500\,\mathrm{MeV}$), as $m_s \sim 100\,\mathrm{MeV} \gg m_{u,d}$ [16]. In other words, the explicit breaking of $\mathrm{SU}(3)_L \times \mathrm{SU}(3)_R$ is much more severe than the one of $\mathrm{SU}(2)_L \times \mathrm{SU}(2)_R$. Consequently, throughout this Section 1.2 we will stick to u and d as "light" quarks and simply ignore the strange sector, contrary to what will be done in Section 1.4. There, we will explore as well how to treat the heaviest quarks (c, b, t), whose mass is much larger than Λ_{QCD}.

On the basis of the transformation rule (1.13), together with the cyclicity of the trace, one can use $\mathcal{U}$, $\mathcal{U}^\dagger$, and their derivatives as building blocks of a chiral-invariant effective Lagrangian that describes pion interactions in the chiral (massless) limit,

$$\mathcal{L}_\pi|_{\bar{m}=0} = \sum_{n=0}^{\infty} \mathcal{L}_\pi^{[2n]}|_{\bar{m}=0}, \tag{1.16}$$

where $\mathcal{L}_\pi^{[2n]}|_{\bar{m}=0}$ includes all allowed terms given by a coupling $g^{[2n]}$, $[g^{[2n]}] = 4 - 2n$, times an operator $O^{[2n]}$, $[O^{[2n]}] = +2n$, with $n = 0, 1, \ldots$ as a consequence of Lorentz invariance. Since $\mathcal{U}^\dagger = \mathcal{U}^{-1}$, $\mathcal{L}_\pi^{[0]}|_{\bar{m}=0}$ cannot exhibit any dependence on the fields; it thus represents a contribution to the cosmological constant with no relevance in this context. Hence, the lowest contribution to $\mathcal{L}_\pi|_{\bar{m}=0}$ will be

$$\mathcal{L}_\pi^{[2]}|_{\bar{m}=0} = g^{[2]}\,\mathrm{Tr}\left[\partial_\mu \mathcal{U}(x)\,\partial^\mu \mathcal{U}^\dagger(x)\right]. \tag{1.17}$$

Some other possible terms with two derivatives, *e.g.* $\mathrm{Tr}\,[\mathcal{U}(x)\partial_\mu\mathcal{U}^\dagger(x)]\,\mathrm{Tr}\,[\mathcal{U}(x)\partial^\mu\mathcal{U}^\dagger(x)]$, will not contribute (as $\mathrm{Tr}\,[\mathcal{U}(x)\partial_\mu\mathcal{U}^\dagger(x)] = 0$), while pieces such as $\mathrm{Tr}\,[\mathcal{U}(x)\partial_\mu\partial^\mu\mathcal{U}^\dagger(x)]$ are actually equivalent to the one given in Eq. (1.17) (as total derivatives can be safely dropped from the Lagrangian). Expanding Eq. (1.17) at low momenta,

$$\mathcal{L}_\pi^{[2]}|_{\bar{m}=0} = \tfrac{1}{2}\partial_\mu\pi^a\partial^\mu\pi^a + \tfrac{1}{6f_\pi^2}\Big[(\pi^a\partial_\mu\pi^a)\,(\pi^b\partial^\mu\pi^b) - (\pi^a\pi^a)(\partial_\mu\pi^b\partial^\mu\pi^b)\Big] + \ldots, \tag{1.18}$$

where the arbitrary normalization of the field was used to fix $g^{[2]} = f_\pi^2/4$ so that the kinetic term is canonically normalized. This result illustrates how the imposed symmetry constrains all vertices with increasing number of pions in the LO Lagrangian.

The expansion (1.16) can be extended beyond the chiral limit, so that $(\mathcal{L}_\pi^{[2n]} - \mathcal{L}_\pi^{[2n]}|_{\bar{m}=0})$ includes all allowed terms given by an operator $\tilde{O}^{[2n]}$ that contains $2a$ derivative insertions and $b \geqslant 1$ quark-mass insertions, $[\tilde{O}^{[2n]}] = n + a$, multiplied by a coupling constant $\tilde{g}^{[2n]}$, $[\tilde{g}^{[2n]}] = 4 - n - a$. Here we used the restriction $a + b = n$, due to the fact that one single power of $\bar{m}$ is standardly counted in χPT as *two* powers of m_π (see Eq. (1.10)), *i.e.* two powers of p, implying that finite-$\bar{m}$ effects should enter in $\mathcal{L}_\pi^{[2]}$ already [5]. A convenient way of finding out *how* they must enter is to treat the quark mass matrix $\mathcal{M}_{kl} = \bar{m}\,\delta_{kl}$ as a fictitious ("spurion") field that follows the transformation rule $\mathcal{M} \mapsto U_L \mathcal{M} U_R^\dagger$ under $\mathrm{SU}(2)_L \times \mathrm{SU}(2)_R$. Hence,

$$\mathcal{L}_\pi^{[2]} - \mathcal{L}_\pi^{[2]}|_{\bar{m}=0} = \tilde{g}^{[2]}\,\mathrm{Tr}\left[\mathcal{M}\mathcal{U}^\dagger(x) + \mathrm{H.c.}\right]. \tag{1.19}$$

Now, one comes back to the real world where $\mathcal{M}$ does not preserve the transformation rule above due to the non-vanishing of $\bar{m}$. Then, expanding $\mathcal{U}^\dagger(x)$ and $\mathcal{U}(x)$ up to two pion fields and fixing $\tilde{g}^{[2]} = f_\pi^2 m_\pi^2/(4\bar{m}) = -v^3/2$ (see Eq. (1.10)) gives (modulo an irrelevant constant)

$$\mathcal{L}_\pi^{[2]} - \mathcal{L}_\pi^{[2]}|_{\bar{m}=0} = -\tfrac{1}{2} m_\pi^2 \pi^a \pi^a + \ldots, \tag{1.20}$$

which is the canonically normalized pion-mass term.

Combining Eqs. (1.18) and (1.20),

$$\mathcal{L}_\pi^{[2]} = \tfrac{1}{2}\left(\partial_\mu \vec{\pi} \cdot \partial^\mu \vec{\pi} - m_\pi^2 \vec{\pi}^2\right) + \ldots, \tag{1.21}$$

where $\vec{\pi} = (\pi^1, \pi^2, \pi^3)$, and the dots refer to terms with at least four pion insertions (including the one appearing in Eq. (1.18)). Coming back to the resummation of the pion fields,

$$\mathcal{L}_\pi^{[2]} = \tfrac{1}{4} f_\pi^2 \left\{\mathrm{Tr}\left[\partial_\mu \mathcal{U}(x)\, \partial^\mu \mathcal{U}^\dagger(x)\right] + m_\pi^2\,\mathrm{Tr}\left[\mathcal{U}(x) + \mathcal{U}^\dagger(x)\right]\right\}. \tag{1.22}$$

The next contributions will enter at $\mathcal{L}_\pi^{[4]}$. They will include $g_1^{[4]}\,\mathrm{Tr}\left[\partial^\mu \partial^\nu \mathcal{U}(x)\, \partial_\mu \partial_\nu \mathcal{U}(x)\right]$, as well as other operators, each of them multiplied by some coupling constant $g_i^{[4]}$, containing either four derivatives, four powers of the pion mass, or two derivatives and two powers of the pion mass. As we will see, such contributions are parametrically suppressed with respect to the ones in Eq. (1.22). Consequently, $\mathcal{L}_\pi^{[2]}$ and $\mathcal{L}_\pi^{[4]}$ go under the names of leading order (LO) and next-to-leading order (NLO) chiral Lagrangians, respectively.

[5] In Refs. [22, 23] an alternative approach based on the assumption $\bar{m} = \mathcal{O}(p)$ was proposed. However, after the determination of the S-wave two-pion scattering length from K_{e4} decay [24], such an approach was discarded [25].

The Feynman diagrams describing two-pion interactions will then arise from the truncated $\mathcal{L}_\pi$ according to the usual rules of quantum field theory. Take a diagram contributing to the total amplitude $\mathcal{A} = i(S-1)$, S being the scattering matrix, with L relativistic loop integrations, I_π internal pion lines, and V_i vertices of tipe i, each of them associated with d_i derivative/pion-mass insertions. These numbers verify the topological relation

$$L - I_\pi + \sum_i V_i = 1, \tag{1.23}$$

which may be deduced from Euler's formula relating the number of vertices, edges, and faces of a convex polyhedron. The diagram can be assigned a *chiral power* ν such that its contribution to the amplitude scales as Q^ν, Q generically denoting the pion momenta and the pion mass. If each relativistic loop counts as Q^4, each relativistic pion propagator counts as $1/Q^2$, and each derivative/pion-mass insertion counts as Q, then it follows

$$\nu = 4L - 2I_\pi + \sum_i d_i V_i = 2 + 2L + \sum_i \Delta_i V_i, \quad \Delta_i = d_i - 2, \tag{1.24}$$

$\Delta \geqslant 0$ being the so-called *chiral index* of the vertex V.

From Eq. (1.24), one finds out that the chiral power of a four-pion vertex emerging from $\mathcal{L}_{4\pi}^{[2]}$ ($d_1 = 2$, $V_1 = 1$, $L = 0$) is $\nu = 2$, while for a four-pion vertex emerging from $\mathcal{L}_{4\pi}^{[4]}$ ($d_1 = 4$, $V_1 = 1$, $L = 0$) it turns out $\nu = 4$. In particular,

$$\mathcal{A}_{4\pi}^{[2]} \sim Q^2/f_\pi^2 \quad \text{and} \quad \mathcal{A}_{4\pi}^{[4]} \sim g_i^{[4]} Q^4/f_\pi^4. \tag{1.25}$$

But, for the diagram expansion to be consistent, we require

$$\mathcal{A}_{4\pi}^{[4]}/\mathcal{A}_{4\pi}^{[2]} \sim (Q/M_{\rm hi})^2 \quad \Rightarrow \quad M_{\rm hi} \sim (g_i^{[4]})^{-1/2} f_\pi, \tag{1.26}$$

where $M_{\rm hi}$ is the breakdown scale of the expansion, whose size we want to estimate. With that purpose, consider the diagram of Figure 1.1, whose vertices emerge from $\mathcal{L}_\pi^{[2]}$ ($d_1 = 2$, $V_1 = 2$, $L = 1$). Its chiral power turns out to be $\nu = 4$; more precisely,

$$\mathcal{A}_{4\pi}^{[1\mathrm{L}]} \sim \int \frac{Q^4}{(4\pi)^2} \times \left(\frac{Q^2}{f_\pi^2}\right)^2 \times \left(\frac{1}{Q^2}\right)^2 = \frac{1}{(4\pi f_\pi^2)^2} \int Q^4, \tag{1.27}$$

where the replacement $Q^4/(2\pi)^4 \to Q^4/(4\pi)^2$ has accounted for the integration over the solid angle. Then, $\mathcal{A}_{4\pi}^{[2]}$ and $\mathcal{A}_{4\pi}^{[4]}$ will absorb the two ultraviolet divergences, quadratic and logarithmic respectively, that result from $\mathcal{A}_{4\pi}^{[1\mathrm{L}]}$, *i.e.*

$$\mathcal{A}_{4\pi}^{[1\mathrm{L}]}|_{\rm quad} \sim \frac{Q^2}{(4\pi f_\pi^2)^2}\Lambda^2 \quad \text{and} \quad \mathcal{A}_{4\pi}^{[1\mathrm{L}]}|_{\log} \sim \frac{Q^4}{(4\pi f_\pi^2)^2}\ln(\Lambda/\mu), \tag{1.28}$$

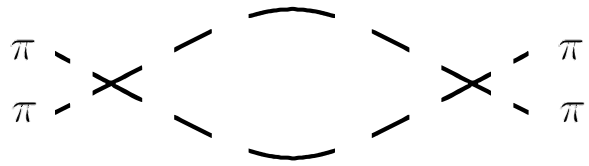

Figure 1.1: Pion loop.

where μ is some infrared subtraction point. Hence, the renormalized four-pion amplitude at second order in perturbation theory will be, roughly,

$$\mathcal{A}_{4\pi}^{[2+4]} \sim \frac{Q^2}{f_\pi^2} + \left[\bar{g}^{[4]}(\mu) + \frac{\ln(Q/\mu)}{(4\pi)^2}\right]\frac{Q^4}{f_\pi^4}, \tag{1.29}$$

where the renormalized coupling $\bar{g}^{[4]}$ is given by some combination of the Λ-independent parts of the $g_i^{[4]}$'s. Now, change the renormalization scale by some factor $\varphi = \mathcal{O}(1)$, say $\varphi = e^{-1}$. Since $\mathcal{A}_{4\pi}^{[2+4]}$ needs to remain the same,

$$\bar{g}^{[4]}(e^{-1}\mu) + \frac{1+\ln(Q/\mu)}{(4\pi)^2} = \bar{g}^{[4]}(\mu) + \frac{\ln(Q/\mu)}{(4\pi)^2} \quad \Rightarrow \quad (4\pi)^2\left[\bar{g}^{[4]}(\varphi\mu) - \bar{g}^{[4]}(\mu)\right] = \mathcal{O}(1). \tag{1.30}$$

Therefore, it is *natural* to conclude that

$$(4\pi)^2\bar{g}^{[4]}(\mu) = \mathcal{O}(1), \tag{1.31}$$

as if there was some μ_1 such that $(4\pi)^2|\bar{g}^{[4]}(\mu_1)| \ll 1$ or $(4\pi)^2|\bar{g}^{[4]}(\mu_1)| \gg 1$, then there would be some other μ_2, $\mu_2/\mu_1 = \mathcal{O}(1)$, for which such inequalities could not hold. Combining Eqs. (1.26) and (1.31) yields finally our guess for the χPT breakdown scale [26],

$$M_{\rm hi} \sim M_{\rm QCD} \sim 4\pi f_\pi \sim 1\,{\rm GeV}, \tag{1.32}$$

where the characteristic QCD scale $M_{\rm QCD}$ was introduced in Section 1.1.2. Quite consistently, such a result is not far from the mass of the vector meson ρ ($M_\rho \approx 770\,{\rm MeV}$), the nucleon N ($M_N \approx 940\,{\rm MeV}$), and other non-Goldstone hadrons that are not considered the χPT action. At the same time, the estimate above anticipates a nice convergence of the EFT expansion, as $M_{\rm hi}$ might be $\gtrsim 5$ times larger than the pion mass.

The analysis above can be generalized to yield the so-called *naturalness* condition, also known as naive dimensional analysis (NDA) *à la* Georgi–Manohar [27, 28]: Write a given term of the Lagrangian as some coupling constant g times an operator O with dimensions of mass^d, and let n be the number of strongly interacting fields contained in O. Define the reduced (dimensionless) coupling constant g_R as

$$g_R \equiv M_{\rm QCD}^{d-n-2} f_\pi^{n-2} g \sim \frac{M_{\rm QCD}^{d-4}}{(4\pi)^{n-2}} g. \tag{1.33}$$

The NDA hypothesis consists of assuming that g_R has the same size as the product of the corresponding reduced couplings of the underlying theory. Later we will come back to such an assumption.

1.2.2 Bringing nucleons into the picture

At this point, we aim at generalizing χPT to include the nucleon field. In order to do so, first we must give an effective Lagrangian that encodes the coupling between a relativistic pseudo-Goldstone boson (pion) with momentum $\mathcal{O}(m_\pi)$ and a non-relativistic heavy baryon (nucleon) with three-momentum $\mathcal{O}(m_\pi)$. It is customary to introduce the auxiliary SU(2) matrix $\xi(x)$,

$$\xi(x) = e^{i\Pi(x)/(\sqrt{2}f_\pi)} = \mathcal{U}^{1/2}(x) \tag{1.34}$$

(see Eq. (1.12)), whose transformation law under G is easily inferred from Eq. (1.13),

$$\xi(x) \mapsto \left[U_L \xi^2(x) U_R^\dagger\right]^{1/2} = \mathfrak{h}(x)\xi(x)U_R^\dagger = U_L \xi(x) \mathfrak{h}^\dagger(x), \tag{1.35}$$

where we introduced the unitary ("compensator") matrix

$$\mathfrak{h}(x) = \left[U_L \xi^2(x) U_R^\dagger\right]^{-1/2} U_L \xi(x). \tag{1.36}$$

For a pure isospin rotation, Eq. (1.36) will simply give

$$\mathfrak{h}(x) = U_V. \tag{1.37}$$

When $\epsilon_L^a \neq \epsilon_R^a$, conversely, $\mathfrak{h}(x)$ exhibits complicated non-linear dependence on the pion fields. For instance, if $\epsilon_L^a + \epsilon_R^a = 0$, Eq. (1.36) will yield

$$\mathfrak{h}(x) = U_A^{-1/2} \xi^{-1}(x) U_A^{1/2} \xi(x) \equiv e^{i\mathfrak{m}_A(x)}, \tag{1.38}$$

where, recalling that $U_A = 1 + i\gamma_5\epsilon_A^a\tau^a$,

$$\mathfrak{m}_A(x) \propto i\gamma_5\left[\epsilon_A^a\tau^a, \tfrac{\Pi(x)}{f_\pi}\right] + \mathcal{O}\left(\epsilon^2, \pi^2\right). \tag{1.39}$$

Similarly to what we did in the purely pionic sector, we require that the relativistic nucleon isodoublet $\Psi(x)$ transforms non-linearly under the chiral group G, but linearly under the isospin subgroup H. Given Eq. (1.37), the transformation

$$\Psi(x) \mapsto \mathfrak{h}(x)\Psi(x) \tag{1.40}$$

is manifestly linear for $\epsilon_L^a = \epsilon_R^a$. Conversely, for some transformation in the coset G/H, say a pure axial rotation, Eq. (1.39) illustrates that the above rule multiplies the nucleon field by functions of the pion fields, which reflects the well-known fact that chiral transformations correspond to the emission/absorption of Goldstone bosons.

Due to the locality of Eq. (1.40), a standard kinetic piece like $\bar\Psi(i\not\partial - M_N)\Psi$ will not be chiral-invariant in general. The ordinary derivative ∂^μ needs to be promoted to a covariant derivative $\mathcal{D}^\mu = \partial^\mu + V^\mu$, where

$$V^\mu(x) = \tfrac{1}{2}\left[\xi^\dagger(x), \partial^\mu\xi(x)\right] = \mathcal{O}(\pi^2) \tag{1.41}$$

—the so-called *vector pion current*— transforms under G as $V^\mu \mapsto \mathfrak{h}\left(V^\mu + \partial^\mu\right)\mathfrak{h}^\dagger$, thus guaranteeing the invariance of $\bar\Psi(i\not{\mathcal{D}} - M_N)\Psi$. A term such as $\bar\Psi\gamma^5\not{A}\Psi$ ($\gamma^5 = -\gamma_5$) turns out to be invariant, too, since

$$A^\mu(x) = \tfrac{i}{2}\left\{\xi^\dagger(x), \partial^\mu\xi(x)\right\} = -\tfrac{1}{2}\vec\tau\cdot\partial^\mu\tfrac{\vec\pi(x)}{f_\pi} + \mathcal{O}(\pi^3) \tag{1.42}$$

—known as the *axial-vector pion current*— transforms as $A^\mu \mapsto \mathfrak{h}A^\mu\mathfrak{h}^\dagger$. The LO relativistic pion-nucleon Lagrangian proposed in Ref. [29] with such building blocks reads

$$\mathcal{L}_{\pi N}^{[\mathrm{LO}]}|_{\mathrm{GSS}} = \bar\Psi\left[i\not{\mathcal{D}} - M_N + g_A\gamma^5\not{A}\right]\Psi = \bar\Psi\left[i\not\partial - M_N - \tfrac{1}{2}g_A\gamma^5\vec\tau\cdot\not\partial\tfrac{\vec\pi}{f_\pi} + \ldots\right]\Psi, \tag{1.43}$$

where $g_A \simeq 1.26$ is the axial coupling constant, and the ellipsis refer to terms with at least two pion insertions. (Note that the LO contribution to the pure pion Lagrangian (1.21) has been made implicit.) But M_N, unlike m_π, is not small compared to the hard scale M_{QCD} and does not vanish in the chiral limit. Treating the nucleon as a relativistic field is, thus, problematic. As an example of this, let us note that we could have included in $\mathcal{L}_{\pi N}^{[\mathrm{LO}]}|_{\mathrm{GSS}}$ some other chiral-invariant piece such as the pion-nucleon coupling

$$\tilde{\mathcal{L}}_{\pi N} = \bar\Psi\left[\tilde g_A M_{\mathrm{QCD}}^{-2}\gamma^5\not{A}\not{\mathcal{D}}_\mu\mathcal{D}^\mu\right]\Psi = \bar\Psi\left[-\tfrac{1}{2}\tilde g_A M_{\mathrm{QCD}}^{-2}\gamma^5\vec\tau\cdot\not\partial\tfrac{\vec\pi}{f_\pi}\,\partial_\mu\partial^\mu + \ldots\right]\Psi, \tag{1.44}$$

with $\tilde{g}_A = \mathcal{O}(1)$ some dimensionless coupling. The insertion of two negative powers of M_{QCD} comes with the two extra derivatives, in analogy with what it is done in χPT. But each time derivative acting on Ψ brings down one positive power of M_N, implying that the pion-nucleon coupling included in Eq. (1.44) has a size of $\mathcal{O}(M_N^2/M_{\text{QCD}}^2) = \mathcal{O}(1)$ compared to the one given in Eq. (1.43), and thus it is not suppressed. This illustrates that there is no clear way to organize the derivative expansion anymore; such an observation also applies to contributions from loops enhanced by powers of M_N. The moral is that we cannot rely on a particular hierarchy of terms in the Lagrangian *before taking the non-relativistic limit*. We will see that, once this is done, the Lagrangian coming out from $\mathcal{L}_{\pi N}^{[\text{LO}]}|_{\text{GSS}}$ will appear as LO in virtue of consistent PC rules.

It is customary to decompose the nucleon four-momentum p_μ as

$$p_\mu = M_N v_\mu + q_\mu, \tag{1.45}$$

where v_μ and q_μ are the nucleon four-velocity and the nucleon residual momentum, verifying $v^\mu v_\mu = 1$ and $v^\mu q_\mu / M_N \ll 1$ respectively. Then, separate out the kinematical dependence on the nucleon mass exhibited by Ψ,

$$\Psi(x) = e^{-iM_N v^\mu x_\mu} \psi(x), \tag{1.46}$$

which, once plugged into Eq. (1.43), gives

$$\mathcal{L}_{\pi N}^{[\text{LO}]}|_{\text{GSS}} = \bar{\psi}\left[i\partial\!\!\!/ + (v\!\!\!/ - 1) M_N - \tfrac{1}{2} g_A \vec{\tau} \cdot (\gamma^5 \partial\!\!\!/) \tfrac{\vec{\pi}}{f_\pi} + \dots \right] \psi. \tag{1.47}$$

This can be simplified by introducing the projection operators

$$P_\pm^v = \tfrac{1}{2}(1 \pm v\!\!\!/), \tag{1.48}$$

thus decomposing the four-spinor ψ as the sum

$$\psi(x) = N(x) + h(x) \quad \text{with} \quad N(x) = P_+^v \psi(x) \quad \text{and} \quad h(x) = P_-^v \psi(x). \tag{1.49}$$

Consider the rest frame of the nucleon, $v_\mu = (1, \mathbf{0})$. Then, $N(x)$ and $h(x)$ correspond (up to a phase) to the upper and lower components of the positive-frequency solution of the free Dirac equation. Neglecting terms suppressed by powers of M_N, the upper component collapses to a bispinor, while the lower one vanishes. Hence, Eq. (1.47) becomes

$$\mathcal{L}_{\pi N}^{[\text{LO}]}|_{\text{GSS}} \to \mathcal{L}_{\pi N}^{[\text{LO}]} = N^\dagger \left[i\partial_0 - \tfrac{1}{2} g_A \vec{\tau} \cdot (\boldsymbol{\sigma} \cdot \boldsymbol{\nabla}) \tfrac{\vec{\pi}}{f_\pi} + \dots \right] N, \tag{1.50}$$

where the "→" indicates that pieces proportional to some positive power of $1/M_N$ are not included anymore as omitted terms labeled as "...". Below, we will see that $\mathcal{L}_{\pi N}^{[\mathrm{LO}]}$ represents indeed the LO contribution to the pion-nucleon Lagrangian. Being suppressed by M_N, the piece proportional to $\bar{\psi}[\vec{\tau}\cdot(\gamma^5\gamma^0\partial_0)\vec{\pi}]\psi$ in Eq. (1.47) needs to be included in $\mathcal{L}_{\pi N}^{[\mathrm{NLO}]}$, just like the first correction to the kinetic part of the nucleon. The remaining terms contained in $\mathcal{L}_{\pi N}^{[\mathrm{NLO}]}$ have, at least, two pion-field or two pion-mass insertions.

Similarly to the purely pionic sector, the full πN coupling gives rise to an infinite series of Feynman diagrams that, according to their increasing chiral power ν, can be organized as decreasingly important in the low-momentum regime of the EFT. For a given πN graph with L loops, I_f (I_π) fermion (pion) propagators, and V_i vertices, each of them associated with d_i derivative/pion-mass insertions and f_i fermion legs,

$$\nu = 4L - 2I + I_f + \sum_i d_i V_i, \quad I = I_f + I_\pi, \tag{1.51}$$

since each loop counts as Q^4, each fermion (pion) internal line counts as $1/Q$ ($1/Q^2$), and each derivative/pion-mass insertion counts as Q. Using

$$L - I + \sum_i V_i = 1, \tag{1.52}$$

which generalizes Eq. (1.23), and

$$\tfrac{1}{2}\sum_i f_i V_i - I_f = 1, \tag{1.53}$$

which is a consequence of the fact that V_i connects f_i nucleon lines in a diagram with two external nucleon legs, Eq. (1.51) becomes

$$\nu = 1 + 2L + \sum_i \Delta_i V_i, \quad \Delta_i = \tfrac{1}{2} f_i + d_i - 2. \tag{1.54}$$

Then, the only πN term that contains one single pion-field insertion and whose chiral index is minimized ($\Delta = 0$) is the axial-vector coupling that has been made explicit in Eq. (1.50).

There is a vast literature on the successful application of the χPT approach to the purely pionic and one-nucleon sectors. For reviews, the interested reader may consult Refs. [30–32].

1.2.3 Chiral EFT of two-nucleon systems

Now, what will come up if a second nucleon enters the scene? From what we have just seen, in the low-momentum regime $Q \ll M_{\mathrm{QCD}}$, the nucleon-nucleon (NN) interaction will

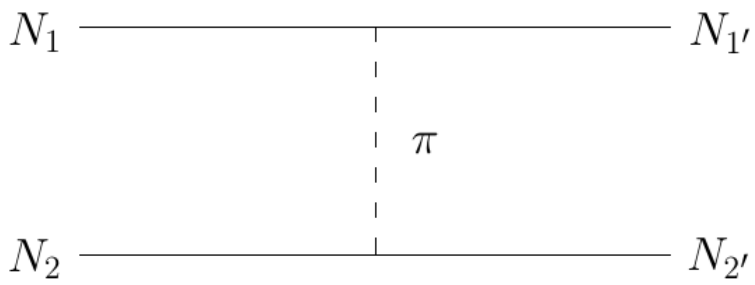

Figure 1.2: Diagrammatic exchange of a virtual pion in a two-nucleon process.

be mediated by the exchange of off-shell (virtual) pions [6]. Here, we will first derive in detail the expression of the one-pion-exchange (OPE) NN potential. (As we will see, interactions due to the exchange of two or more pions are parametrically suppressed in comparison.) Let $\boldsymbol{p}$ ($\boldsymbol{p}'$) be the relative three-momentum of the incoming (outcoming) nucleons. The pion-nucleon vertex $v_{N\to\pi N}$ is readily obtained from Eq. (1.50) in terms of the three-momentum $\boldsymbol{q} = \boldsymbol{p}' - \boldsymbol{p}$ carried by the pion,

$$v_{N\to\pi^a N} = -i\,\frac{g_A}{2f_\pi}\,\langle N|N^\dagger\vec{\tau}\cdot(\boldsymbol{\sigma}\cdot\boldsymbol{\nabla})\,\vec{\pi}N|\pi^a N\rangle = -i\,\frac{g_A}{2f_\pi}\,\tau^a\,\boldsymbol{\sigma}\cdot(-i\boldsymbol{q}) = -v_{\pi^a N\to N}, \tag{1.55}$$

while the pion propagator is found from Eq. (1.21),

$$\mathcal{P}_\pi^{ab} = -\frac{\delta^{ab}}{q_\mu q^\mu - m_\pi^2} \approx \frac{\delta^{ab}}{\boldsymbol{q}^2 + m_\pi^2}, \tag{1.56}$$

as $q_0 \sim \boldsymbol{q}^2/M_N$ is negligible at LO. The OPE potential in momentum space then reads

$$V_{\rm OPE}(\boldsymbol{q}) \;=\; v_{N_1\to\pi^a N_{1'}}\,\mathcal{P}_\pi^{ab}\,v_{\pi^b N_2\to N_{2'}} \;=\; -\,\vec{\tau}_1\cdot\vec{\tau}_2\,\frac{g_A^2}{4f_\pi^2}\,\frac{\boldsymbol{\sigma}_1\cdot\boldsymbol{q}\,\boldsymbol{\sigma}_2\cdot\boldsymbol{q}}{\boldsymbol{q}^2+m_\pi^2} \tag{1.57}$$

(see Figure 1.2). Its coordinate counterpart is recovered through the inverse Fourier transform,

$$\mathcal{V}_{\rm OPE}\,(\boldsymbol{r}) = \int\frac{\mathrm{d}^3q}{(2\pi)^3}\,e^{i\boldsymbol{q}\cdot\boldsymbol{r}}\,V_{\rm OPE}(\boldsymbol{q}). \tag{1.58}$$

Introducing the so-called tensor operator,

$$S_{12}(\hat{\boldsymbol{r}}) = 3\,\boldsymbol{\sigma}_1\cdot\hat{\boldsymbol{r}}\,\boldsymbol{\sigma}_2\cdot\hat{\boldsymbol{r}} - \boldsymbol{\sigma}_1\cdot\boldsymbol{\sigma}_2, \quad \hat{\boldsymbol{r}} = \frac{\boldsymbol{r}}{r}, \tag{1.59}$$

[6] Funnily enough, this confirms the old proposal by Yukawa, made many years before the discovery of QCD and χEFT [33].

together with the dimensionless functions

$$T(x) = 1 + \frac{3}{x} + \frac{3}{x^2} \quad \text{and} \quad Y(x) = \frac{e^{-x}}{x}, \tag{1.60}$$

it turns out that

$$\mathcal{V}_{\rm OPE}(\boldsymbol{r}) = \frac{g_A^2 m_\pi^3}{48\pi f_\pi^2}\, \vec{\tau}_1 \cdot \vec{\tau}_2 \left\{ [S_{12}(\hat{\boldsymbol{r}}) T(m_\pi r) + \boldsymbol{\sigma}_1 \cdot \boldsymbol{\sigma}_2] Y(m_\pi r) - \frac{4\pi}{m_\pi^3}\, \boldsymbol{\sigma}_1 \cdot \boldsymbol{\sigma}_2\, \delta(\boldsymbol{r}) \right\}. \tag{1.61}$$

Integrating S_{12} over the unit sphere, we compute its projection onto the S wave, which turns out to be zero, implying that, for transitions with $\ell = \ell' = 0$,

$$\mathcal{V}^{(S)}_{\rm OPE}(\boldsymbol{r}) = \frac{g_A^2 m_\pi^3}{48\pi f_\pi^2}\, \boldsymbol{\sigma}_1 \cdot \boldsymbol{\sigma}_2\, \vec{\tau}_1 \cdot \vec{\tau}_2 \left[Y(m_\pi r) - \frac{4\pi}{m_\pi^3}\, \delta(\boldsymbol{r}) \right]. \tag{1.62}$$

(For details associated with transitions between the S and D waves, belonging to the spin-triplet $S = 1$, see Appendix B.) But, for a system composed of two nucleons, the intrinsic spin (isospin) numbers are $S_1 = S_2 = 1/2$ ($I_1 = I_2 = 1/2$), thus $\boldsymbol{S}_{1,2} = \boldsymbol{\sigma}_{1,2}/2$ ($\vec{I}_{1,2} = \vec{\tau}_{1,2}/2$) for the corresponding spin (isospin) operators, so that

$$\begin{aligned} \boldsymbol{\sigma}_1 \cdot \boldsymbol{\sigma}_2 &= 4\, \boldsymbol{S}_1 \cdot \boldsymbol{S}_2 = 2 \left[(\boldsymbol{S}_1 + \boldsymbol{S}_2)^2 - \boldsymbol{S}_1^2 - \boldsymbol{S}_2^2 \right] \\ &= 2 \left[S(S+1) - S_1(S_1+1) - S_2(S_2+1) \right] = 2S(S+1) - 3, \end{aligned} \tag{1.63}$$

$$\begin{aligned} \vec{\tau}_1 \cdot \vec{\tau}_2 &= 4\, \vec{I}_1 \cdot \vec{I}_2 = 2 \left[\left(\vec{I}_1 + \vec{I}_2 \right)^2 - \vec{I}_1^{\,2} - \vec{I}_2^{\,2} \right] \\ &= 2 \left[I(I+1) - I_1(I_1+1) - I_2(I_2+1) \right] = 2I(I+1) - 3, \end{aligned} \tag{1.64}$$

in terms of the total spin S (isospin I). Because of the addition rules for angular momenta, both S and I are either 0 or 1; however, given that nucleons are fermions, we also know that, for what concerns the S wave, $S + I$ is odd. Hence,

$$S = 0 \;\equiv\; \left\{ \tfrac{1}{\sqrt{2}} \left(|{\uparrow\downarrow}\rangle - |{\downarrow\uparrow}\rangle \right) \right\} \;\Leftrightarrow\; I = 1 \;\equiv\; \left\{ |pp\rangle\,, |nn\rangle\,, \tfrac{1}{\sqrt{2}} \left(|pn\rangle + |np\rangle \right) \right\}, \tag{1.65}$$

$$S = 1 \;\equiv\; \left\{ |{\uparrow\uparrow}\rangle\,, |{\downarrow\downarrow}\rangle\,, \tfrac{1}{\sqrt{2}} \left(|{\uparrow\downarrow}\rangle + |{\downarrow\uparrow}\rangle \right) \right\} \;\Leftrightarrow\; I = 0 \;\equiv\; \left\{ \tfrac{1}{\sqrt{2}} \left(|pn\rangle - |np\rangle \right) \right\}, \tag{1.66}$$

respectively for the spin-singlet (isospin-triplet) ${}^1S_0$ and the spin-triplet (isospin-singlet) ${}^3S_1$, implying that $(\boldsymbol{\sigma}_1 \cdot \boldsymbol{\sigma}_2\, \vec{\tau}_1 \cdot \vec{\tau}_2)_{{}^1S_0} = (\boldsymbol{\sigma}_1 \cdot \boldsymbol{\sigma}_2\, \vec{\tau}_1 \cdot \vec{\tau}_2)_{{}^3S_1} = -3$, *i.e.*

$$\mathcal{V}^{(S)}_{\rm OPE}(\boldsymbol{r}) = \frac{4\pi}{M_N \Lambda_{NN}} \left(\delta(\boldsymbol{r}) - \frac{m_\pi^3}{4\pi}\, Y(m_\pi r) \right), \tag{1.67}$$

or, back to momentum space through Fourier transform,

$$V_{\rm OPE}^{(S)}(\boldsymbol{q}) = \frac{4\pi}{M_N \Lambda_{NN}} \left(1 - \frac{m_\pi^2}{\boldsymbol{q}^2 + m_\pi^2}\right), \tag{1.68}$$

where we introduced the characteristic momentum scale of OPE [34, 35]

$$\Lambda_{NN} \equiv \frac{16\pi f_\pi^2}{g_A^2 M_N} \approx 290\,\text{MeV}. \tag{1.69}$$

OPE is supplemented by the pure contact part of the NN interaction, consisting of four-nucleon vertices without pseudo-Goldstone fields. These terms "parametrize our ignorance", as they emerge from the short-distance (high-energy) physics that, being inherent to the nuclear interaction, remains unresolved by our EFT. According to the PC rules we will discuss later on, the S-wave projected LO NN contact Lagrangian reads [9]

$$\mathcal{L}_{NN}^{[\rm LO]}\big|_{\rm ct}^{(S)} = N^\dagger\Big(i\partial_0 + \frac{\boldsymbol{\nabla}^2}{2M_N}\Big)N - C_{^1S_0}(N^{\rm T}\vec{P}_{^1S_0}N)^\dagger\cdot(N^{\rm T}\vec{P}_{^1S_0}N) - C_{^3S_1}(N^{\rm T}\boldsymbol{P}_{^3S_1}N)^\dagger\cdot(N^{\rm T}\boldsymbol{P}_{^3S_1}N), \tag{1.70}$$

where the ${}^1S_0$ (${}^3S_1$) projector is expressed in terms of the Pauli matrices $\boldsymbol{\sigma}$ and $\vec{\tau}$ acting on spin and isospin space as $\vec{P}_{^1S_0} = \sigma_2\vec{\tau}\tau_2/\sqrt{8}$ ($\boldsymbol{P}_{^3S_1} = \tau_2\boldsymbol{\sigma}\sigma_2/\sqrt{8}$). Then, the NN LO potential becomes

$$V_{\rm LO}^{(S)}(\boldsymbol{p}',\boldsymbol{p}) = C_S - \frac{4\pi}{M_N\Lambda_{NN}}\frac{m_\pi^2}{(\boldsymbol{p}'-\boldsymbol{p})^2 + m_\pi^2}, \quad C_S \to C_S + \frac{4\pi}{M_N\Lambda_{NN}}, \tag{1.71}$$

with $S = \{{}^1S_0, {}^3S_1\}$. The bare couplings $C_{^1S_0}$ and $C_{^3S_1}$, unknown *a priori*, must be determined through fitting to the available low-energy data.

Remarkably, and contrary to what we saw for the one-nucleon sector, the kinetic piece $N^\dagger[\boldsymbol{\nabla}^2/(2M_N)]N$ has now been included in the LO Lagrangian, in correspondence to the "infrared enhancement" of those NN diagrams containing purely nucleonic intermediate states —the so-called "reducible" (or iterative) graphs. The infrared enhancement was pointed out by Weinberg [36, 37] in order to explain the non-perturbative nature of the NN system, which is manifest in the presence of a loosely bound state (the deuteron) in the spin-triplet and a very shallow virtual state in the spin-singlet. Explicitly, the LO S-wave scattering amplitude at the scattering energy $E = k^2/M_N$ is obtained from the Lippmann–Schwinger (LS) equation

$$\begin{aligned} T_{\rm LO}^{(S)}(\boldsymbol{p}',\boldsymbol{p},k) &= V_{\rm LO}^{(S)}(\boldsymbol{p}',\boldsymbol{p}) + \int \frac{\mathrm{d}^3 l}{(2\pi)^3}\, V_{\rm LO}^{(S)}(\boldsymbol{p}',\boldsymbol{l})\, G_0^{(\pm)}(\boldsymbol{l},k)\, T_{\rm LO}^{(S)}(\boldsymbol{l},\boldsymbol{p},k) \\ &= V_{\rm LO}^{(S)}(\boldsymbol{p}',\boldsymbol{p}) + \int \frac{\mathrm{d}^3 l}{(2\pi)^3}\, V_{\rm LO}^{(S)}(\boldsymbol{p}',\boldsymbol{l})\, G_0^{(\pm)}(\boldsymbol{l},k)\, V_{\rm LO}^{(S)}(\boldsymbol{l},\boldsymbol{p}) + \ldots, \end{aligned} \tag{1.72}$$

where the Schrödinger propagator is found from the kinetic term in Eq. (1.70),

$$G_0^{(\pm)}(\boldsymbol{l}, k) = \frac{M_N}{k^2 - \boldsymbol{l}^2 \pm i0^+} = \mathcal{O}(4\pi f_\pi / Q^2); \tag{1.73}$$

therefore, assuming that the contact part of $V_{\rm LO}^{(S)}$ follows the same scaling as its long-range part,

$$T_{\rm LO}^{(S)} \sim \frac{1}{f_\pi^2} + \frac{Q^3}{4\pi} \times \frac{1}{f_\pi^2} \times \frac{4\pi f_\pi}{Q^2} \times \frac{1}{f_\pi^2} + \cdots \sim \frac{1}{f_\pi^2}\left(1 - \frac{Q}{f_\pi}\right)^{-1}, \tag{1.74}$$

which is compatible with the emergence of a (real or virtual) bound state or a resonance at $Q \sim f_\pi$.

1.2.3.1 Weinberg power counting

Much like it happens in the purely pionic and the one-nucleon sectors, the only restriction that binds the construction of the χEFT Lagrangian is the preservation of the symmetries of the underlying QCD. Otherwise, such Lagrangian is the most general one, implying that it contains an infinite number of terms and thus gives rise to an infinite number of Feynman diagrams. Hence, again we need, for our approach to be useful, a set of PC rules that tell us which diagrams should be kept when computing observables at a given order in the EFT expansion. A series of pioneering works at the early and middle 90s [36–41] postulates that the full NN effective potential in momentum space, found through the sum of all those diagrams that are not infrared enhanced —known as "irreducible" graphs—, is amenable to the decomposition

$$V_{NN} = \sum_{\nu=0}^{\infty} V_{NN}^{[\nu]} \sim M_{\rm lo}^{-2} \sum_{\nu=0}^{\infty} c_\nu \left(Q/M_{\rm hi}\right)^\nu, \quad c_\nu = \mathcal{O}(1), \tag{1.75}$$

where the chiral power ν of a given NN irreducible diagram is found through inserting Eq. (1.52) and the topological relation

$$\tfrac{1}{2}\sum_i f_i V_i - I_f = 2 \tag{1.76}$$

—emerging from the fact that V_i connects f_i nucleon lines in a diagram with four external nucleon legs— into Eq. (1.51),

$$\nu = 2L + \sum_i \Delta_i V_i, \quad \Delta_i = \tfrac{1}{2} f_i + d_i - 2. \tag{1.77}$$

The generalization of this prescription to the three-nucleon sector and beyond ($A \geqslant 3$) illustrates in a simple way the hierarchical suppression of A-body forces when A is increased. Even more importantly, for any given ν, there is only a *finite* number of diagrams giving rise to $V_{NN}^{[\nu]}$:

- Comparing Eqs. (1.71) and (1.75), we identify $V_{\rm LO}^{(S)} \equiv V_{NN}^{[0]}$. This is so because the short-range part of $V_{\rm LO}^{(S)}$ comes from the four-nucleon vertex without derivative/pion-mass insertions ($L = 0$, $V_1 = 1$, $f_1 = 4$, $d_1 = 0$), while its long-range part arises from the OPE diagram at tree-level ($L = 0$, $V_1 = 2$, $f_1 = 2$, $d_1 = 1$). According to Eq. (1.77), both graphs verify $\nu = 0$.

- No NN diagram with $\nu = 1$ is allowed by time-reversal and parity symmetries. NLO is thus an empty order in Weinberg PC, which is the reason why some authors call the $\nu = 2$ order "NLO" instead of N^{2}LO (next-to-next-to-leading order). Here we will refrain from using such terminology, though, and simply adopt as a general rule that N$^\nu$LO is the order suppressed by $\mathcal{O}(Q/M_{\rm hi})$ with respect to N$^{\nu-1}$LO.

- The two-pion-exchange (TPE) interaction emerges at N^{2}LO, as any leading TPE diagram entering here has $L = 1$, $f_1 = 2$, $d_1 = 1$. Besides, if the delta isobar $\Delta(1232)$ —the lowest nucleon resonance, with excitation energy $\delta M_{\Delta N} = M_\Delta - M_N \gtrsim 2m_\pi$— is taken as another degree of freedom of the EFT [9], then it will appear in diagrams with $L \geqslant 1$, thus enter at N^{2}LO, too [7]. Finally, when diagrams with $L = 0$, $f_1 = 4$, $d_1 = 2$ are considered, one needs to keep seven contact terms provided with two derivatives, which contribute in S and P waves, plus two derivative-independent contact terms proportional to m_π^2 that affect S waves.

It is useful to note that, for what concerns the scaling of the parameters in the theory, the Weinberg rules are equivalent to the naturalness condition of the dimensionless coupling g_R (see Eq. (1.33)). To check this, decompose the total effective Lagrangian in the NN sector as

$$\mathcal{L}_{\rm eff}^{(A=2)} = \mathcal{L}_{\rm free} + \mathcal{L}_{\pi\pi} + \mathcal{L}_{N\pi N} + \mathcal{L}_{C_0} + \mathcal{L}_{C_2} + \mathcal{L}_{D_2} + \ldots , \tag{1.78}$$

[7] In terms of PC, the explicit inclusion of the delta amounts to assuming $\delta M_{\Delta N} = \mathcal{O}(M_{\rm lo})$. Conversely, integrating it out corresponds to the case $\delta M_{\Delta N} \to \infty$, in which the extraction of the pion-nucleon couplings contained in $\mathcal{L}_{\pi N}^{[\rm NLO]}$ will be biased by a relative error $\mathcal{O}(M_{\rm lo}/\delta M_{\Delta N})$. Not being numerically negligible, this has some significant effect in the nuclear potential [42].

with

$$\begin{aligned} \mathcal{L}_{\text{free}} &\sim \tfrac{1}{M_N} N\partial^2 N, \quad \mathcal{L}_{N\pi N} \sim \tfrac{g_A}{f_\pi} N\partial\pi N, \qquad \mathcal{L}_{\pi\pi} \sim m_\pi^2\pi^2, \\ \mathcal{L}_{C_0} &\sim C_0 N^4, \qquad \mathcal{L}_{C_2} \sim C_2 (N\partial N)^2, \quad \mathcal{L}_{D_2} \sim D_2 m_\pi^2 N^4. \end{aligned} \tag{1.79}$$

From $\mathcal{L}_{\text{free}}$, $\mathcal{L}_{N\pi N}$, and $\mathcal{L}_{\pi\pi}$, one confirms

$$\left(\tfrac{1}{M_N}\right)_R \sim \tfrac{M_{\text{QCD}}^{5-4}}{(4\pi)^{2-2}} \tfrac{1}{M_N} = \mathcal{O}(1) \quad \Rightarrow \quad M_N = \mathcal{O}(M_{\text{QCD}}), \tag{1.80}$$

$$\left(\tfrac{g_A}{f_\pi}\right)_R \sim \tfrac{M_{\text{QCD}}^{5-4}}{(4\pi)^{3-2}} \tfrac{g_A}{f_\pi} = \mathcal{O}(1) \quad \Rightarrow \quad g_A = \mathcal{O}(1), \tag{1.81}$$

$$\left(m_\pi^2\right)_R \sim \tfrac{M_{\text{QCD}}^{2-4}}{(4\pi)^{2-2}} m_\pi^2 \sim \bar{m}_R \sim \tfrac{M_{\text{QCD}}^{3-4}}{(4\pi)^{2-2}} \bar{m} \quad \Rightarrow \quad m_\pi^2 = \mathcal{O}(M_{\text{QCD}}\bar{m}), \tag{1.82}$$

where we used that $\mathcal{L}_{qq} \sim \bar{m} q^2$, while from $\mathcal{L}_{C_0}$, $\mathcal{L}_{C_2}$, and $\mathcal{L}_{D_2}$, one gets

$$(C_0)_R \sim \tfrac{M_{\text{QCD}}^{6-4}}{(4\pi)^{4-2}} C_0 = \mathcal{O}(1) \quad \Rightarrow \quad C_0 = \mathcal{O}(f_\pi^{-2}), \tag{1.83}$$

$$(C_2)_R \sim \tfrac{M_{\text{QCD}}^{8-4}}{(4\pi)^{4-2}} C_2 = \mathcal{O}(1) \quad \Rightarrow \quad C_2 = \mathcal{O}(M_{\text{QCD}}^{-2} f_\pi^{-2}), \tag{1.84}$$

$$\left(D_2 m_\pi^2\right)_R \sim \tfrac{M_{\text{QCD}}^{6-4}}{(4\pi)^{4-2}} D_2 m_\pi^2 \sim \bar{m}_R = \mathcal{O}(\bar{m}/M_{\text{QCD}}) \quad \Rightarrow \quad D_2 = \mathcal{O}(M_{\text{QCD}}^{-2} f_\pi^{-2}), \tag{1.85}$$

where we recalled that $\mathcal{L}_{D_2}$ breaks chiral symmetry in the EFT Lagrangian in the same way that $\mathcal{L}_{qq}$ breaks chiral symmetry in the underlying QCD Lagrangian. Hence, NDA anticipates that

$$C_2 Q^2/C_0 \sim D_2 m_\pi^2/C_0 \sim Q^2/M_{\text{QCD}}^2, \tag{1.86}$$

i.e. $\mathcal{L}_{C_2}$ and $\mathcal{L}_{D_2}$ appear two orders down with respect to $\mathcal{L}_{C_0}$. This indeed matches the Weinberg assumption.

Once the potential (1.75) is obtained up to some order, the Weinberg program postulates its insertion into the LS equation to obtain non-perturbatively the corresponding scattering amplitude, from where one can compute, in turn, predictions for the remaining observables of the system. The success of this approach comes as no surprise: besides its simplicity, it seems to achieve nice agreement with the phenomenological evidence (χ^2/d.o.f. ~ 1) [43–45].

1.2.3.2 Amending naive dimensional analysis

When applying the method described above, one implicitly expects that the resulting amplitude will obey the same expansion as the potential does,

$$T_{NN} = \sum_{\nu=0}^{\infty} T_{NN}^{[\nu]} \sim M_{\text{lo}}^{-2} \sum_{\nu=0}^{\infty} \tilde{c}_\nu \left(Q/M_{\text{hi}}\right)^\nu, \quad \tilde{c}_\nu = \mathcal{O}(1). \tag{1.87}$$

However, it is not clear at all that such an expectation will hold in an intrinsically non-perturbative problem as the *NN* one is. The iteration of singular interaction terms (those that diverge like $1/r^2$ or quicker in the limit of small r) produces ultraviolet divergences that are regularized through a momentum cutoff Λ; the cutoff dependence induced on the low-energy couplings renormalizes the one of observables, up to a small residue that becomes arbitrarily small when the cutoff is made arbitrarily large (see Section 1.1.1). Unfortunately, NDA prescribes the presence of a certain number of counterterms at a given order that, in general, is *not* sufficient to guarantee that the renormalization condition is properly fulfilled by the amplitude. As a matter of fact, already at LO NDA does not yield all the necessary short-range interactions [46–48]; similar issues reappear at higher orders [49–51] and also affect electromagnetic currents [52]. Given that non-perturbative renormalization can differ significantly from the perturbative renormalization used to infer NDA, it is perhaps unsurprising that a scheme based solely on NDA fails to produce nuclear amplitudes consistent with renormalization invariance. This poses a serious shortcoming to NDA, since such loop divergences threaten to destroy the low-energy EFT expansion, thus compromising the very consistency of the PC. Not only that, the connection with QCD is at risk. This is so because such an approach does not make for a proper EFT, where one must strive for physical predictions that are manifestly model-independent —in particular, not affected by the choices of the cutoff value and the regularization scheme [8].

Actually, cutoff independence of observables contradicts NDA already in the ${}^1S_0$ channel. The reason is that NDA prescribes that the only contact term in the LO potential should be chiral-invariant —according to Eq. (1.86), a chiral-symmetry breaking piece such as $D_2 m_\pi^2$ would appear only at N^{2}LO. The emergence of a logarithmic divergence proportional to m_π^2 as a result of the iteration of OPE, though, demands that a piece like that be present at LO [46]. This "chiral inconsistency" motivated Kaplan, Savage, and Wise [34, 35] to propose a PC where pion exchanges are treated as *perturbative* corrections starting at NLO. However, higher-order calculations soon made clear that such an approach is not valid at low momenta in certain partial waves [55].

Currently it is well-known that one low-energy coupling is required at LO to renormalize every partial wave where the potential is *singular and attractive* [47, 48]. Given that the tensor component of OPE (1.61) diverges as $1/r^3$ around $r = 0$ (see Appendix B for an illustration corresponding the ${}^3S_1$-${}^3D_1$ channel), the former implies, for example, the promotion

[8] For an alternative interpretation, see *e.g.* Refs. [53, 54].

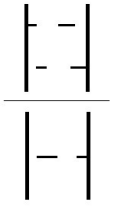

$$\sim \frac{\frac{Q^3}{4\pi} \times \left(\frac{Q}{f_\pi}\right)^4 \times \left(\frac{1}{Q^2}\right)^2 \times \frac{1}{Q^2/M_N}}{\left(\frac{Q}{f_\pi}\right)^2 \times \frac{1}{Q^2}} \sim \frac{M_N}{4\pi f_\pi} \times \frac{Q}{f_\pi} \sim \frac{Q}{f_\pi}$$

Figure 1.3: Amplitude of the one-loop OPE over the tree-level OPE, roughly computed using the usual rules of (non-relativistic) PC.

to LO of the two-derivative contact term of the ${}^3P_0$ channel [47], which NDA anticipates to be N^{2}LO. But, in fact, according to NDA there is an infinite number of partial waves where the LO potential is singular and attractive, as NDA anticipates the non-perturbativity of OPE in *any* channel at momenta $Q \gtrsim f_\pi$ (see Figure 1.3). In contrast, Refs. [47, 56–62] advocate the treat of OPE as LO only in the lower waves, where suppression by the centrifugal barrier is not effective.

As a matter of fact there exists already a consistent version of nuclear EFT [47, 56–62]. It is renormalizable, can describe the scattering amplitudes for $Q < M_{\rm QCD}$, converges well and PC is realized at the level of observables. Its foundation relies on a better understanding of the renormalization of non-perturbative physics and singular interactions [47, 48, 63–67]. The key improvements over the original Weinberg proposal are the non-perturbative renormalization of the LO amplitudes and the addition of beyond-LO contributions as perturbative corrections [9]. At LO the main difference with the Weinberg counting lies in the promotion of a series of P- and D-wave counterterms to LO in triplet partial waves for which the tensor force is attractive, a change originally proposed in Ref. [47]. At subleading orders there are more counterterms than in Weinberg counting, for instance in the attractive triplets that

[9] Actually, the reason not to resum such small corrections, as done in the Weinberg scheme, is again related to the lack of counterterms. Take for example the Long-Yang PC for the ${}^1S_0$ wave [61], where a singular two-derivative short-range interaction enters already at NLO. Such interaction will impact N^{2}LO (at second order in perturbation theory), thus producing an even more singular contribution to the amplitude, that must be canceled out by the four-derivative contact term entering at N^{2}LO —only the sum of *all* N^{2}LO terms will consistently be cutoff independent and small. In contrast, if we truncated the potential at NLO and resum *both* LO and NLO, we would be including diagrams with two (three, four...) insertions of the NLO term without the necessary four-derivative counterterm. Therefore, it would not come as a surprise if renormalization was again lost [49, 51].

already received a counterterm at LO. The convergence of the EFT expansion is acceptable and the description of the data too, but it has not achieved yet a χ^2/d.o.f. ~ 1 as in the Weinberg approach. However this is expected if we take into account that the calculations of Refs. [57–61] are still one order below the most advanced ones in the Weinberg approach.

1.3 Pionless EFT

1.3.1 Motivation

As it was discussed above, the existence of two (respectively real and virtual) bound states in the S-wave channels suffices to discard a fully perturbative treatment of the NN problem. But, actually, the binding momenta of the real bound state ($\approx 45\,\mathrm{MeV}$) and the virtual bound state ($\approx 8\,\mathrm{MeV}$) turn out to be quite smaller than the OPE scales m_π and Λ_{NN}. This implies that such states can only be reproduced at LO through some cancelation (*fine tuning*) in which the short-range component of the NN interaction is the one to blame. Physics can then be described simply by another successful, renormalizable EFT, known as Pionless (or Contact) EFT ($\not\pi$EFT) [34, 35, 68, 69]. This arises from a simple observation: in the very-low-momentum regime of nuclear physics, $Q \ll m_\pi$, pion exchange cannot be resolved. Consequently, the effective Lagrangian contains interactions of contact type only, just like Eq. (1.70), with subleading corrections consisting of four-nucleon terms including $2, 4, \ldots$ derivatives.

As usual, the off-shell amplitude is found from an LS equation analogous to Eq. (1.72); for a spherically symmetric potential, such off-shell amplitude depends only on the magnitudes of momenta and their scalar products —p', p, and $\cos\theta = \hat{\boldsymbol{p}}' \cdot \hat{\boldsymbol{p}}$. Hence, the on-shell T matrix ($p' = p = k$) can be partial-wave decomposed as

$$t_\ell(k) = \int_{-1}^{+1} \mathrm{d}\cos\theta \; T(k, \cos\theta) \; P_\ell(\cos\theta) = -\frac{4\pi/M_N}{k\cot\delta_\ell(k) - ik} = \frac{2\pi i}{M_N k}\left[S_\ell(k) - 1\right], \qquad (1.88)$$

where $P_\ell(x)$ is a Legendre polynomial, and $S_\ell(k) = \exp[2i\delta_\ell(k)]$ represents the corresponding S matrix, $\delta_\ell(k)$ being the phase shift. At sufficiently low energies,

$$k\cot\delta_\ell(k) = -a_\ell^{-1}k^{-2\ell} + \tfrac{1}{2}r_\ell k^{2(1-\ell)} + \ldots, \qquad (1.89)$$

with a_ℓ and r_ℓ the ℓ-wave scattering length and the ℓ-wave effective range [10]. The dots stand for terms proportional to $k^{2(n-\ell)}$, $n = 2, 3, \ldots$, which we omit here. This is the renowned *effective range expansion* (ERE), due to Bethe [70]. But now, contrary to the pionful case, one can derive closed, analytic expressions linking the ERE parameters to the potential parameters, which shows in a transparent way how renormalization works out. Here we will illustrate the last statement for the case of neutron-proton (np) scattering in the ${}^1S_0$ channel, where the scattering length is $a \equiv a_0 \simeq -23.7\,\mathrm{fm} \simeq -(8\,\mathrm{MeV})^{-1}$ [71], and the effective range is $r_0 \simeq 2.7\,\mathrm{fm} \simeq (73\,\mathrm{MeV})^{-1}$ [72].

The part of the Lagrangian density relevant for the ${}^1S_0$ channel is

$$\begin{aligned}\mathcal{L}^{(\not\pi)}_{{}^1S_0} &= N^\dagger\Big(i\partial_0 + \frac{\boldsymbol{\nabla}^2}{2M_N}\Big)N - C_0\left(N^{\mathrm{T}}\vec{P}_{{}^1S_0}N\right)^\dagger\cdot\left(N^{\mathrm{T}}\vec{P}_{{}^1S_0}N\right)\\ &\quad + \tfrac{1}{8}C_2\Big[\left(N^{\mathrm{T}}\vec{P}_{{}^1S_0}N\right)^\dagger\cdot\left(\boldsymbol{\nabla}^2N^{\mathrm{T}}\vec{P}_{{}^1S_0}N + N^{\mathrm{T}}\vec{P}_{{}^1S_0}\boldsymbol{\nabla}^2N\right) + \mathrm{H.c.}\Big] + \ldots,\end{aligned} \tag{1.90}$$

the ellipsis referring to terms with at least four derivatives, which we do not make explicit here. This corresponds to an interaction given by a series in even powers of p' and p,

$$V^{(\not\pi)}_{{}^1S_0}(p',p) = C_0 + \tfrac{1}{2}C_2\left(p'^2 + p^2\right) + \ldots, \tag{1.91}$$

which translates in coordinate space as an expansion consisting of a Dirac delta function plus its even derivatives. This is a highly singular potential, implying the divergence of the loop integral in the S-wave projection of the LS equation, thus the need for regularizing it somehow. Here we use a momentum cutoff Λ in the range $\Lambda \gtrsim M_{\mathrm{hi}} \gg k$ and a regulator function $f_{\mathrm{R}}(q^2/\Lambda^2)$, with q the magnitude of the off-shell nucleon momentum, that satisfies $f_{\mathrm{R}}(0) = 1$, $f_{\mathrm{R}}(\infty) = 0$. Hence,

$$T^{(\not\pi)}_{{}^1S_0}(p',p,k;\Lambda) = V^{(\not\pi)}_{{}^1S_0}(p',p;\Lambda) + \frac{1}{2\pi^2}\int_0^\infty \mathrm{d}q\, q^2 f_{\mathrm{R}}(q^2/\Lambda^2) V^{(\not\pi)}_{{}^1S_0}(p',q;\Lambda) G_0^{(+)}(q,k) T^{(\not\pi)}_{{}^1S_0}(q,p,k;\Lambda), \tag{1.92}$$

where the cutoff dependence induced on the potential must be such that the amplitude is well-defined for an arbitrarily large Λ.

Of course, the series (1.91) must be *truncated* at some point before plugging it into Eq. (1.92) to find the resulting amplitude. In the following, we will explore a few possibilities in that regard.

[10] Despite the names given here, a_ℓ and r_ℓ only have dimensions of length for $\ell = 0$. In general, $[a_\ell] = -2\ell - 1$, $[r_\ell] = 2\ell - 1$; for example, a_1 verifies $[a_1] = -3$, thus it is commonly called the scattering volume.

1.3.2 The simplest case

We start by testing the renormalizability of the simplest (non-trivial) scenario, which corresponds to the truncation of Eq. (1.91) at its first term,

$$V_{^1S_0}^{(\not\pi)}(p',p;\Lambda) \equiv C_0(\Lambda). \tag{1.93}$$

Once inserted into Eq. (1.92), this gives the simple solution

$$T_{^1S_0}^{(\not\pi)}(p',p,k;\Lambda) = T_{^1S_0}^{(\not\pi)}(k;\Lambda) = \left(\frac{1}{C_0(\Lambda)} + \frac{M_N}{4\pi}\mathcal{I}_0(k;\Lambda)\right)^{-1}, \tag{1.94}$$

with

$$\mathcal{I}_0(k;\Lambda) = \frac{2}{\pi}\int_0^\infty \mathrm{d}q\, f_\mathrm{R}(q^2/\Lambda^2)\frac{q^2}{q^2-k^2-i0^+} = ik + \theta_1\Lambda + \frac{k^2}{\Lambda}\sum_{n=0}^{\infty}\theta_{-1-2n}\left(\frac{k}{\Lambda}\right)^{2n}, \tag{1.95}$$

the numbers θ_n depending on the specific regularization employed. For example, for a sharp-cutoff prescription with a step function $f_\mathrm{R}(x) = \theta(1-x)$, it turns out that $\theta_n = 2/(n\pi)$, while in dimensional regularization with minimal subtraction we have simply $\theta_n = 0$; in general, $\theta_n \geqslant 0$ when $n > 0$. The linear divergence present needs to be canceled out by the running of the counterterm. In particular, for

$$C_0(\Lambda) = \bar{C}_0\left[-(\theta_1 a\Lambda)^{-1} + \mathcal{O}\left((a\Lambda)^{-2}\right)\right], \quad \bar{C}_0 = \frac{4\pi}{M_N}a, \tag{1.96}$$

it turns out that

$$\left[\frac{M_N}{4\pi}T_{^1S_0}^{(\not\pi)}(k;\Lambda)\right]^{-1} = \frac{1}{a} + ik + \theta_{-1}\frac{k^2}{\Lambda} + \mathcal{O}\left(\frac{k^4}{\Lambda^3}\right). \tag{1.97}$$

After taking $\Lambda \to \infty$, the above result gives

$$S_{^1S_0}^{(\not\pi)}(k) = -\frac{k+i\kappa}{k-i\kappa}, \quad \kappa = \frac{1}{a}, \tag{1.98}$$

for the corresponding scattering matrix, which exhibits a simple pole lying on the negative imaginary semiaxis, $S_{^1S_0}^{(\not\pi)}(i\kappa) \to \infty$, $\kappa \simeq -8\,\mathrm{MeV}$. This is very close to the well-known virtual shallow state present in the $^1S_0$ channel. Note that, as the residue of the scattering matrix evaluated at the pole is

$$i\,\mathrm{Res}\, S_{^1S_0}^{(\not\pi)}(i\kappa) = \frac{2}{a} < 0, \tag{1.99}$$

this state has a non-normalizable wavefunction, as it corresponds to an unbound solution.

1.3.3 Beyond the simplest case

Now, let us go one step further by truncating the series (1.91) at its second term. Much like in the pionful theory, a quandary inmediately arises: should the C_2 piece be *infinitely iterated*, just like the C_0 one in Section 1.3.2, or rather be treated as a *perturbative correction*? When *regular* potentials are considered, the difference between fully iterating or not should not be that significant (if the subleading contributions are truly small); however, in what follows we will check that is not the case at all when *singular* interactions, like the ones of ⧸EFT, are used.

1.3.3.1 Non-perturbative approach

If we decide to fully iterate the C_2 term, then we plug the interaction

$$V^{(\not\pi)}_{^1S_0}(p',p;\Lambda) \equiv \sum_{i,j=0}^{1} \mathfrak{v}_{ij}(\Lambda) p'^{2i} p^{2j}, \quad \mathfrak{v}(\Lambda) = \begin{pmatrix} C_0(\Lambda) & \frac{1}{2}C_2(\Lambda) \\ \frac{1}{2}C_2(\Lambda) & 0 \end{pmatrix}, \tag{1.100}$$

into Eq. (1.92) to solve it in a non-perturbative approach. The resulting off-shell amplitude can be put in the form

$$T^{(\not\pi)}_{^1S_0}(p',p,k;\Lambda) = \sum_{i,j=0}^{1} \mathfrak{t}_{ij}(k;\Lambda) p'^{2i} p^{2j}, \tag{1.101}$$

where Eq. (1.94) has been generalized to give the matrix identity

$$\mathfrak{t}(k;\Lambda) = \left(\mathfrak{v}^{-1}(\Lambda) + \frac{M_N}{4\pi}\mathcal{I}(k;\Lambda)\right)^{-1}, \quad \mathcal{I}(k;\Lambda) = \begin{pmatrix} \mathcal{I}_0(k;\Lambda) & \mathcal{I}_2(k;\Lambda) \\ \mathcal{I}_2(k;\Lambda) & \mathcal{I}_4(k;\Lambda) \end{pmatrix}, \tag{1.102}$$

with

$$\mathcal{I}_{2n}(k;\Lambda) = \frac{2}{\pi}\int_0^\infty \mathrm{d}q\, f_{\mathrm{R}}(q^2/\Lambda^2)\frac{q^{2(1+n)}}{q^2-k^2-i0^+} = k^{2n}\mathcal{I}_0(k;\Lambda) + \sum_{m=1}^{n}\theta_{1+2m}\Lambda^{1+2m}k^{2(n-m)}. \tag{1.103}$$

For the runnings

$$\frac{M_N}{4\pi}C_0(\Lambda) = \frac{\theta_5}{\theta_3^2}\frac{1}{\Lambda}\left[1+\left(\frac{8\theta_1^2}{\theta_3}\right)^{1/2}\left(-\frac{1}{r_0\Lambda}\right)^{1/2}+\mathcal{O}\left(\frac{1}{r_0\Lambda}\right)\right], \tag{1.104}$$

$$\frac{M_N}{4\pi}C_2(\Lambda) = -\frac{2}{\theta_3}\frac{1}{\Lambda^3}\left[1+\left(\frac{2\theta_1^2}{\theta_3}\right)^{1/2}\left(-\frac{1}{r_0\Lambda}\right)^{1/2}+\mathcal{O}\left(\frac{(a/r_0)^{1/2}}{(a\Lambda)^{3/2}}\right)\right], \tag{1.105}$$

the amplitude (1.101) verifies (when on-shell)

$$\left[\frac{M_N}{4\pi}T^{(\not\pi)}_{^1S_0}(k;\Lambda)\right]^{-1} = \frac{1}{a} + ik - \frac{r_0}{2}k^2 + \mathcal{O}\left(\frac{k^4r_0^2}{\Lambda}\right). \tag{1.106}$$

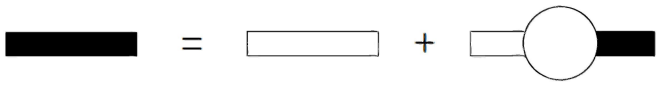

Figure 1.4: Full dibaryon propagator (solid box) resulting from the non-perturbative dressing of bare dibaryon propagator (plain box) with nucleon bubbles (circles).

But Eqs. (1.104) and (1.105) explicitly show that having $r_0 > 0$ is *incompatible* with $C_0(\Lambda), C_2(\Lambda)$ being real functions, *i.e.* with a Hermitian bare Hamiltonian [73]. This matches the so-called Wigner bound, derived from general principles for potentials that vanish identically beyond some radius [74, 75].

Yet the above issue can be bypassed if, following Ref. [76], an auxiliary "dibaryon" field $\vec{\phi}$ with quantum numbers of an isovector pair of nucleons is introduced to rewrite the non-derivative term in Eq. (1.90),

$$-C_0\left(N^{\mathrm{T}}\vec{P}_{^1S_0}N\right)^\dagger\cdot\left(N^{\mathrm{T}}\vec{P}_{^1S_0}N\right)\;\leftrightarrow\;\Delta\vec{\phi}^\dagger\cdot\vec{\phi}-g\left(\vec{\phi}^\dagger\cdot N^{\mathrm{T}}\vec{P}_{^1S_0}N+\mathrm{H.c.}\right). \tag{1.107}$$

The dibaryon residual mass Δ and the dibaryon-NN coupling g are such that

$$C_0 = g^2/\Delta, \tag{1.108}$$

as can be checked if one performs the Gaussian path integral by using $\int_{-\infty}^{+\infty}\mathrm{d}s\,\exp(as^2-2bxs)\propto\exp(-b^2x^2/a)$. The parameter redundancy (1.108) permits the convenient choice $g^2\equiv 4\pi/M_N$ [77], and the Lagrangian (1.90) may be replaced by

$$\mathcal{L}^{(\phi)}_{^1S_0} = N^\dagger\left(i\partial_0+\frac{\nabla^2}{2M_N}\right)N+\vec{\phi}^\dagger\cdot\left[\Delta+c\left(i\partial_0+\frac{\nabla^2}{4M_N}\right)\right]\vec{\phi}-\sqrt{\frac{4\pi}{M_N}}\left(\vec{\phi}^\dagger\cdot N^{\mathrm{T}}\vec{P}_{^1S_0}N+\mathrm{H.c.}\right)+\ldots, \tag{1.109}$$

where the dots account for relativistic corrections and derivative dibaryon-NN couplings. The kinetic dibaryon term has been included explicitly [11], c being a normalization (dimensionless) factor. Computing the dibaryon self-energy, *i.e.* dressing up the bare dibaryon propagator

$$\mathcal{B}_\phi(k;\Lambda) = \left[\Delta(\Lambda)+c(\Lambda)\,k^2/M_N\right]^{-1}\equiv\frac{M_N}{4\pi}\,V^{(\phi)}_{^1S_0}(k;\Lambda) \tag{1.110}$$

with nucleon loops (see Figure 1.4), yields

$$\mathcal{D}_\phi(k;\Lambda) = \left[1/\mathcal{B}_\phi(k;\Lambda)+\mathcal{I}_0(k;\Lambda)\right]^{-1}\equiv\frac{M_N}{4\pi}\,T^{(\phi)}_{^1S_0}(k;\Lambda). \tag{1.111}$$

[11] Otherwise we would be treating $\vec{\phi}$ as a static, infinitely massive field.

Taking

$$\Delta(\Lambda) = 1/a - \theta_1 \Lambda, \quad c(\Lambda)/M_N = -r_0/2 - \theta_{-1}/\Lambda, \tag{1.112}$$

the inverse amplitude becomes

$$\left[\frac{M_N}{4\pi} T^{(\phi)}_{^1S_0}(k;\Lambda)\right]^{-1} = \frac{1}{a} + ik - \frac{r_0}{2}k^2 + \mathcal{O}\left(\frac{k^4}{\Lambda^3}\right), \tag{1.113}$$

which coincides with Eq. (1.106) after taking $\Lambda \to \infty$. However, contrary to the previous case, the physical condition $r_0 > 0$ does *not* imply anymore a non-zero imaginary part of the bare potential. (In contrast, it entails the "wrong" sign of the kinetic part of the bare dibaryon.) As $V^{(\phi)}_{^1S_0}$ is momentum-independent, the only $\mathcal{I}_{2n}$ that enters the calculation is $\mathcal{I}_0$, which makes the renormalization of the amplitude much less involved. At the same time, the energy dependence of the potential is frequently a downside when one tries to apply it to the few-body sector, as it is not clear how to define the pair energy on which the pair potentials would depend.

Note that, when $\Lambda \to \infty$, Eqs. (1.106) and (1.113) allow to write the scattering matrix as

$$S^{(\not\phi,\phi)}_{^1S_0}(k) = \frac{(k+i\kappa_-)\,(k+i\kappa_+)}{(k-i\kappa_-)\,(k-i\kappa_+)}, \quad \kappa_\mp \equiv \frac{1}{r_0}\left(1 \mp \sqrt{1-2\frac{r_0}{a}}\right) = \frac{1}{r_0}\left\{1 \mp \left[1 - \frac{r_0}{a} - \frac{r_0^2}{2a^2} + \mathcal{O}\left(\frac{r_0^3}{a^3}\right)\right]\right\} \tag{1.114}$$

(with $|r_0/a| \ll 1$), from where we see that there are two simple poles, $S^{(\not\phi,\phi)}_{^1S_0}(i\kappa_\mp) \to \infty$. Again, their nature is linked to the sign of the corresponding residue,

$$i\,\mathrm{Res}\, S^{(\not\phi,\phi)}_{^1S_0}(i\kappa_\mp) = \pm 2\kappa_\mp \left(\frac{\kappa_+ + \kappa_-}{\kappa_+ - \kappa_-}\right) = \pm 2\kappa_\mp \left[1 + \mathcal{O}\left(\frac{\kappa_-}{\kappa_+}\right)\right] \tag{1.115}$$

(with $|\kappa_-/\kappa_+| \ll 1$).

- The pole at $k = i\kappa_-$, $\kappa_- = 1/a + r_0/(2a^2) + \mathcal{O}(r_0^2/a^3) \approx -8\,\mathrm{MeV}$, is nothing but the pole at $k = i\kappa$ of Eq. (1.98), that has been shifted slightly upwards,

$$\frac{\kappa_- - \kappa}{|\kappa|} = \frac{1}{2}\frac{r_0}{|a|} + \mathcal{O}\left(\frac{r_0^2}{a^2}\right) \approx 6\%, \tag{1.116}$$

  as a consequence of inputting r_0 —of course, its new location keeps being very close to the one of the physical virtual state. As $i\,\mathrm{Res}\, S^{(\not\phi,\phi)}_{^1S_0}(i\kappa_-) < 0$, this state has a non-normalizable wavefunction.

- The pole at $k = i\kappa_+$, $\kappa_+ = 2/r_0 + \mathcal{O}(1/a) \approx 146\,\text{MeV}$, lies on the positive imaginary semiaxis. It cannot be seen as physical, as it turns out that $\kappa_+ \gtrsim m_\pi$, where m_π is taken to be the pionless breakdown scale. Anyway, since $i\,\text{Res}\, S^{(\not\pi,\phi)}_{^1S_0}(i\kappa_+) < 0$, the condition to produce a normalizable wavefunction is not fulfilled, so this pole cannot correspond to a bound state, whose wavefunction has finite support in coordinate space. It is called, thus, a *redundant* pole [78, 79].

1.3.3.2 Distorted-wave Born approximation

It is much convenient, however, to further exploit the fact that the $^1S_0$ scattering length is almost ten times larger in magnitude than the $^1S_0$ effective range, which has in turn natural size, $|a|^{-1} \ll r_0^{-1} = \mathcal{O}(m_\pi)$. Indeed, the value of the inverse scattering length, very close to the one of the virtual-state binding momentum, poses the emergence of a new (accidental) momentum scale $\aleph \ll m_\pi$, which should consistently be identified with the typical size of Q in a process amenable to $\not\pi$EFT. According to this, the third term in the r.h.s. of Eqs. (1.106) and (1.113) is parametrically suppressed by $\mathcal{O}(\aleph/m_\pi)$ with respect to the first and the second one, which suggests not to treat a and r_0 on the same footing, but rather to renormalize a at LO, and r_0 at NLO.

When the potential of Eq. (1.100) is considered, the above translates into splitting

$$\left.\begin{aligned} C_0 &\to C_0^{[0]} + C_0^{[1]} + \dots \\ C_2 &\to C_2^{[1]} + \dots \end{aligned}\right\} \quad \Rightarrow \quad T^{(\not\pi)}_{^1S_0} \to T^{(\not\pi)[0]}_{^1S_0} + T^{(\not\pi)[1]}_{^1S_0} + \dots, \tag{1.117}$$

the dots accounting for beyond-NLO terms. In fact, LO has already been solved in Section 1.3.2. Taking

$$C_0^{[0]}(\Lambda) = \bar{C}_0^{[0]}\left[-(\theta_1 a\Lambda)^{-1} + \mathcal{O}\left((a\Lambda)^{-2}\right)\right], \quad \frac{M_N}{4\pi}\bar{C}_0^{[0]} = a = \mathcal{O}\left(\aleph^{-1}\right), \tag{1.118}$$

which is enhanced by $\mathcal{O}(m_\pi/\aleph)$ with respect to the NDA expectation, yields

$$\left[\frac{M_N}{4\pi}T^{(\not\pi)[0]}_{^1S_0}(k;\Lambda)\right]^{-1} = \frac{1}{a} + ik + \theta_{-1}\frac{k^2}{\Lambda} + \mathcal{O}\left(\frac{k^4}{\Lambda^3}\right). \tag{1.119}$$

In the distorted-wave Born approximation (DWBA), such LO amplitude is slightly perturbed

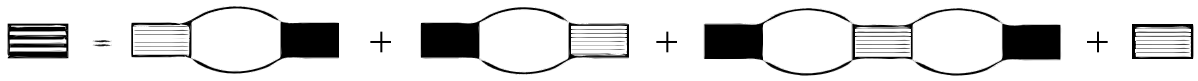

Figure 1.5: Diagrammatic representation of the distorted-wave Born approximation at first order. The LO amplitude is depicted as a solid box; the NLO potential (amplitude) is plotted as a box with thin (thick) black stripes; each bubble represents one loop insertion.

by the NLO potential $V_{^1S_0}^{(\not\pi)[1]}$, inducing a small NLO correction $T_{^1S_0}^{(\not\pi)[1]}$ (see Figure 1.5),

$$\begin{aligned} T_{^1S_0}^{(\not\pi)[1]}(p',p,k;\Lambda) = &- \frac{M_N}{4\pi} T_{^1S_0}^{(\not\pi)[0]}(k;\Lambda)\left[C_0^{[1]}(\Lambda)\mathcal{I}_0(k;\Lambda) + \tfrac{1}{2}C_2^{[1]}(\Lambda)\left(\mathcal{I}_2(k;\Lambda) + p^2\mathcal{I}_0(k;\Lambda)\right)\right] \\ &- \frac{M_N}{4\pi} T_{^1S_0}^{(\not\pi)[0]}(k;\Lambda)\left[C_0^{[1]}(\Lambda)\mathcal{I}_0(k;\Lambda) + \tfrac{1}{2}C_2^{[1]}(\Lambda)\left(p'^2\mathcal{I}_0(k;\Lambda) + \mathcal{I}_2(k;\Lambda)\right)\right] \\ &+ \left[\frac{M_N}{4\pi} T_{^1S_0}^{(\not\pi)[0]}(k;\Lambda)\right]^2\left[C_0^{[1]}(\Lambda)\mathcal{I}_0^2(k;\Lambda) + C_2^{[1]}(\Lambda)\mathcal{I}_2(k;\Lambda)\mathcal{I}_0(k;\Lambda)\right] \\ &+ \left[C_0^{[1]}(\Lambda) + \tfrac{1}{2}C_2^{[1]}(\Lambda)\left(p'^2 + p^2\right)\right]. \end{aligned} \tag{1.120}$$

Taking

$$C_0^{[1]}(\Lambda) = \bar{C}_0^{[1]}\left[\theta_1^{-3}\theta_3 + \mathcal{O}\left((r_0\Lambda)^{-1}\right)\right], \quad \frac{M_N}{4\pi}\bar{C}_0^{[1]} = -\frac{r_0}{2} = \mathcal{O}\left(m_\pi^{-1}\right); \tag{1.121}$$

$$C_2^{[1]}(\Lambda) = \bar{C}_2^{[1]}\left[(\theta_1 a\Lambda)^{-2} + \mathcal{O}\left((a^{2/3}r_0^{1/3}\Lambda)^{-3}\right)\right], \quad \frac{M_N}{4\pi}\bar{C}_2^{[1]} = \frac{a^2 r_0}{2} = \mathcal{O}\left(\aleph^{-2}m_\pi^{-1}\right), \tag{1.122}$$

it turns out that

$$\left[\frac{M_N}{4\pi} T_{^1S_0}^{(\not\pi)[1]}(k;\Lambda)\right] = \left[\frac{M_N}{4\pi} T_{^1S_0}^{(\not\pi)[0]}(k;\Lambda)\right]^2\left(\frac{r_0}{2} + \frac{\theta_{-1}}{\Lambda}\right)k^2, \tag{1.123}$$

which, combined with Eq. (1.119) (and neglecting N^{2}LO), yields, as wished,

$$\left[\frac{M_N}{4\pi} T_{^1S_0}^{(\not\pi)[0+1]}(k;\Lambda)\right]^{-1} = \frac{1}{a} + ik - \frac{r_0}{2}k^2 + \mathcal{O}\left(\frac{k^4}{\Lambda^3}\right). \tag{1.124}$$

Again, things become computationally simpler when an energy-dependent potential as the one of Eq. (1.110) is used. Now, instead of Eq. (1.117), we have

$$\left.\begin{aligned} \Delta &\to \Delta^{[0]} + \Delta^{[1]} + \ldots \\ c/M_N &\to c^{[1]}/M_N + \ldots \end{aligned}\right\} \quad \Rightarrow \quad T_{^1S_0}^{(\phi)} \to T_{^1S_0}^{(\phi)[0]} + T_{^1S_0}^{(\phi)[1]} + \ldots, \tag{1.125}$$

with $T_{^1S_0}^{(\phi)[0]}(k;\Lambda) = T_{^1S_0}^{(\not\pi)[0]}(k;\Lambda)$ (see Eq. (1.119)), provided that

$$\Delta^{[0]}(\Lambda) = \bar{\Delta}^{[0]} - \theta_1\Lambda, \quad \bar{\Delta}^{[0]} = 1/a = \mathcal{O}(\aleph) \tag{1.126}$$

(see Eqs. (1.108) and (1.118)). Besides, Eq. (1.120) now reduces to

$$\frac{M_N}{4\pi}T_{^1S_0}^{(\phi)[1]}(k;\Lambda) = -\left[\frac{M_N}{4\pi}T_{^1S_0}^{(\phi)[0]}(k;\Lambda)\right]^2\left[\Delta^{[1]}(\Lambda) + c^{[1]}(\Lambda)k^2/M_N\right], \tag{1.127}$$

and the runnings

$$\Delta^{[1]}(\Lambda) = 0; \quad c^{[1]}(\Lambda)/M_N = \bar{c}^{[1]}(\Lambda)/M_N - \theta_{-1}/\Lambda, \quad \bar{c}^{[1]}/M_N = -r_0/2 = \mathcal{O}(m_\pi^{-1}) \tag{1.128}$$

ensure that $T_{^1S_0}^{(\phi)[0+1]}(k;\Lambda) = T_{^1S_0}^{(\not\phi)[0+1]}(k;\Lambda)$ (1.124). Comparing Eq. (1.112) with Eqs. (1.126) and (1.128), we learn that, actually, $\Delta(\Lambda) = \Delta^{[0]}(\Lambda) + \Delta^{[1]}(\Lambda)$ and $c(\Lambda)/M_N = c^{[1]}(\Lambda)/M_N$, as a consequence of the momentum independence of the dibaryon potential.

Note that Eqs. (1.118), (1.121) and (1.122), one one hand, and Eqs. (1.126) and (1.128), on the other hand, confirm that

$$\frac{\bar{C}_0^{[1]}}{\bar{C}_0^{[0]}} \sim \frac{\bar{C}_2^{[1]}Q^2}{\bar{C}_0^{[0]}} \sim \frac{\bar{c}^{[1]}Q^2/M_N}{\bar{\Delta}^{[0]}} = \mathcal{O}\left(\frac{\aleph}{m_\pi}\right), \tag{1.129}$$

again at variance with NDA, which predicts $\mathcal{O}(\aleph^2/m_\pi^2)$ for the above ratios. The fact that Eq. (1.119) includes a residual effective range $\sim 1/\Lambda$ fits the need for renormalizing $r_0 \sim 1/m_\pi$ already at NLO (not at N^{2}LO), according to the argument employed in Ref. [61]; analogously, the residual dependence $\sim 1/\Lambda^3$ of Eq. (1.124) anticipates that the shape parameter P_0, present in the ERE through the term $+P_0k^4/4$, should be renormalized at N^{3}LO. (In the absence of further fine tuning, it is assumed that $P_0 \sim 1/m_\pi^3$ [34, 35, 68, 69]. Such estimate indeed works for np scattering in the $^1S_0$ channel, according to the values for P_0 obtained in Refs. [80, 81].)

Finally, at LO both the amplitude and the scattering matrix blow up (after the cutoff removal) when $k = i\kappa^{[0]} = i/a$ (see Eq. (1.98)). This pole gets a bit shallower in the imaginary momentum axis when r_0 is perturbatively included, $\kappa^{[0]} \to \kappa^{[0+1]}$, where the relative shift can be easily checked to be

$$\frac{\kappa^{[1]}}{|\kappa^{[0]}|} = \frac{r_0}{2|a|} \approx 5\%. \tag{1.130}$$

Not surprisingly, this result coincides, up to $\mathcal{O}(\aleph^2/m_\pi^2)$, with the one of Eq. (1.116).

1.3.4 Beyond the NN sector

The richness of low-energy phenomena displayed by the *three-nucleon* ($3N$) system is captured by a Lagrangian whose only degrees of freedom keep being the nucleon fields themselves, now including couplings $\sim D_{2n}\partial^{2n}(NN)^3$. It is convenient to rewrite such Lagrangian

through the inclusion of the auxiliary dibaryon field; then, the $3N$ problem amounts to the obtention of the nucleon-dibaryon scattering amplitude. And, just like the large value of the two-body scattering length enforces the non-perturbative iteration of the bare dibaryon propagator in the NN case (see Figure 1.4), now it becomes necessary to resum all the nucleon-dibaryon non-derivative diagrams [9], while subleading corrections may, as usual, be added in perturbation theory.

Again, here we will focus on the S waves —dominant due to the absence of angular-momentum repulsion— which, for the case of three spin-1/2 particles, may occupate either the doublet state ${}^2S_{1/2}$, like ^{3}H and ^{3}He nuclei, or the quartet state ${}^4S_{3/2}$, like quartet nucleon-deuteron (Nd) scattering:

- *Quartet.* In this channel, the three spins are aligned, so that the Pauli blocking prevents the three nucleons from occupying the same point, suggesting that short-range physics of the full system will not play a protagonist role. Indeed, inputting NN scattering parameters suffices to obtain a high-quality description of low-energy Nd scattering [82]. The quartet scattering length is computed in Ref. [83] to be $a_{3/2} = 6.33\,\text{fm}$ (at N^{2}LO), whose relative difference with respect to the experimental value [84] is $< 0.5\%$.

- *Doublet.* Here the Pauli principle does not forbid the three fermions to touch (the same happens in the three-boson case), thus a contact $3N$ force is anticipated to be relevant. This is confirmed by the fact that, in the absence of such interaction, the LO zero-energy nucleon-dibaryon amplitude exhibits limit-cycle-type asymptotic cutoff dependence. Such a behavior enforces the inclusion at LO of a short-range $3N$ force arising from the Lagrangian coupling $\sim D_0(NN)^3$ [85–87]. It turns out that $D_0 = \mathcal{O}((4\pi)^2/(M_N \not{\kappa}^4))$, which is enhanced by $\mathcal{O}(m_\pi^4/\not{\kappa}^4)$ with respect to the NDA expectation [9]. No three-body derivative short-range force is required at NLO, although D_0 demands a correction proportional to the two-body effective range [88]. Predictions for the three-body sector given by several models, all of them obtained using the low-energy NN phenomenology as an input, must then be correlated to a good approximation through the single three-body coupling. Thus, $\not{\pi}$EFT provides an explanation for the correlation displayed by the doublet Nd scattering length versus the ^{3}H binding energy —the so-called "Phillips line" [89]. If D_0 is fixed to reproduce the scattering length, then the binding energy is computed to be $B_{{}^3\text{H}} = 8.31\,\text{MeV}$ in Ref. [87], in very good agreement with the experimental value (2% of relative difference).

Concerning the *four-nucleon* ($4N$) system, one may inmediately ask whether an operator $\sim E_0(NN)^4$ needs to be promoted to LO in some cases. A crude but intuitive argument in support of the absence of relevant purely $4N$ forces is the following. While the kinetic repulsion is balanced by an attractive two-body potential in the NN sector, when a third particle is added the kinetic effect is multiplied only by 3/2 and the number of interacting pairs is multiplied by 3; hence, an extra repulsive $3N$ force arises to prevent the system from collapsing. As a fourth body is included, the number of attractive (repulsive) NN ($3N$) interactions is multiplied by 2 (4) with respect to the three-body case, thus no new force is required to avoid the collapse. This intuition is confirmed by the fact that no $4N$ force is needed at LO to renormalize the system [90]. The analog of the Phillips line for the four-body system, known as "Tjon line", which shows the correlation between the binding energies of ^{3}H and ^{4}He nuclei [91], is also captured by the theory. In Ref. [90] the three-body force is tuned to reproduce the experimental $B_{^3\mathrm{H}}$, resulting in a LO postdiction of $B_{^4\mathrm{He}}$ that is in good agreement (within 10%) with its phenomenological value.

Recently, the possibility of a correlation between the rough features of nuclei (at least the light ones), on one hand, and one single parameter Λ_* set by $B_{^3\mathrm{H}}$, on the other hand, has been explored [92]. In this approach, the details of the NN system are not considered as the starting point to decipher the physics of heavier systems (contrary to what has been traditionally done), but an *expansion around unitarity* —at whose LO both NN S waves exhibit bound states right at threshold and where subleading corrections are added as perturbations— is performed. The convergence pattern shown by this expansion is promising and it opens the possibility of extending such strategy to atomic and molecular physics.

In conclusion, the applications of $\not\pi$EFT to nuclear systems with $A \geqslant 3$, a couple of which we have briefly reviewed here, are particularly indicative of the power of this theory. In such a context, RG invariance proves again as the fundamental guideline from where consistent PC rules are derived.

1.4 Heavy-quark EFT

1.4.1 Introduction

As mentioned in Section 1.1.2, the QCD coupling will become smaller and smaller at the same time as the length scale of interest does, thus yielding a more easily tractable theory of strong interactions from where predictions can be made. Indeed, in an imaginary world where all quark flavors were heavy enough, *i.e.* where their Compton wavelengths were sufficiently small, the properties of heavy hadrons could be *directly* derived from first principles (if we were here to do so!). Physics of these systems would then be the strongly interacting analog of atomic physics governed by the electromagnetic force. Actually, much like the hydrogen atom is most easily understood in the rest frame of the heavy nucleus, it is very convenient to approach systems such as heavy mesons, composed of a heavy quark Q (c or b [12]) plus a light antiquark $\bar{q}$ ($\bar{u}$, $\bar{d}$ or $\bar{s}$), by assuming a (close to) static Q. Essentially, this is the strategy followed by *heavy-quark EFT* (HQEFT).

Hence, within the heavy meson one distinguishes between the massive color source and its surrounding cloud. The latter, affectionately known as "brown muck" in the literature [93], consists of the light antiquark and the associated glue. The brown muck, characterized by the infrared scale $\Lambda_{\rm QCD}$, is for sure too complicated to be explicitly solved. The key point, however, is that —much like the electronic structure of the isotope of a given element does not care about how many neutrons the nucleus contains— the brown muck will *not* see the physics of the heavy quark (except, of course, its color charge). Such an invariance goes under the name of *heavy-quark symmetry*, an old idea that dates back to the beginnings of quark models themselves [94], and was largely developed in the subsequent years [95–102]. One needs to differentiate between heavy-quark *spin* symmetry and heavy-quark *flavor* symmetry —in virtue of the former, effects that couple the heavy-quark spin $\boldsymbol{S}$ to the muck will disappear as $M_Q \to \infty$; in virtue of the latter, the muck spectrum should not look very different when the heavy quark is shifted from b to c or vice versa.

Consider the charmed pseudoscalar D mesons and the bottomed pseudoscalar $\bar{B}$ mesons, which can be arranged in SU(3) flavor space as the column vectors

$$\begin{pmatrix} D^0 & D^+ & D_s \end{pmatrix}^{\rm T} = \begin{pmatrix} c\bar{u} & c\bar{d} & c\bar{s} \end{pmatrix}^{\rm T}, \qquad \begin{pmatrix} \bar{B}^- & \bar{B}^0 & \bar{B}_s \end{pmatrix}^{\rm T} = \begin{pmatrix} b\bar{u} & b\bar{d} & b\bar{s} \end{pmatrix}^{\rm T}, \tag{1.131}$$

[12] The lifetime of the t quark is so short due to its weak decay that we do not expect it to be able to get confined into hadrons.

and similarly for the charmed vector D^* mesons and the bottomed vector $\bar{B}^*$ mesons. The correspondences

$$D(\mathbf{0}) \leftrightarrow \bar{B}(\mathbf{0}), \qquad D^*(\mathbf{0}) \leftrightarrow \bar{B}^*(\mathbf{0}), \tag{1.132}$$

where "$\mathbf{0}$" stands for the rest frame of the heavy quarks, are manifestations of heavy-quark flavor symmetry.

In a theory with N_Q heavy-quark flavors, heavy-quark flavor symmetry is an approximate $\mathrm{SU}(N_Q)$ mapping that becomes exact as $\Lambda_{\mathrm{QCD}}/M_Q \to 0$. Actually, the fact that the muck is blind to the orientation of $\boldsymbol{S}$ makes the (spin-flavor) symmetry larger, $\mathrm{SU}(2N_Q)$ [13]. Of course, this reminds us of the approximate chiral symmetry $\mathrm{SU}(N_q)_L \times \mathrm{SU}(N_q)_R$, N_q being the number of light-quark flavors (see Section 1.2.1), that becomes exact as $m_q/\Lambda_{\mathrm{QCD}} \to 0$. And, just like the mass of the s is not that small when compared to the QCD scale ($m_s/\Lambda_{\mathrm{QCD}} \sim 1/3$), which worsens the convergence of the chiral expansion at the level of the strange quark, having $\Lambda_{\mathrm{QCD}}/M_c \sim 1/3$ makes the heavy-quark expansion not as clean for the charm sector as it is for the bottom sector (since $\Lambda_{\mathrm{QCD}}/M_b \sim 1/10$).

1.4.2 HQEFT Lagrangian

In this section we will assume a top-down approach in which the starting point is the Dirac Lagrangian,

$$\mathcal{L}_Q = \bar{\Psi}_Q(i\not{\partial} - M_Q)\Psi_Q = \bar{\psi}_Q\left[i\not{\partial} + (\not{v} - 1)M_Q\right]\psi_Q, \tag{1.133}$$

where a large mechanical part of the heavy-quark field Ψ_Q was separated out analogously as it was done for the nucleon field in Eq. (1.46),

$$\Psi_Q(x) = e^{-iM_Q v^\mu x_\mu}\psi_Q(x). \tag{1.134}$$

Such field becomes (evidently) infinitely massive when $M_Q \to \infty$, which would suggest us to integrate it out from our low-energy theory. But it does not look very useful to directly eliminate the only degree of freedom present; hence, we need to first rewrite Eq. (1.133) in a suitable manner. With this purpose, use the projector $P^v_\pm$ defined in Eq. (1.48) to decompose

$$\psi_Q(x) = \left(P^v_+ + P^v_-\right)\psi_Q(x) \equiv \mathcal{Q}_v(x) + \mathcal{B}_v(x) \quad \text{with} \quad \begin{cases} \not{v}\mathcal{Q}_v = \mathcal{Q}_v & \Leftrightarrow\ P^v_+\mathcal{Q}_v = \mathcal{Q}_v,\ P^v_-\mathcal{Q}_v = 0; \\ \not{v}\mathcal{B}_v = -\mathcal{B}_v & \Leftrightarrow\ P^v_-\mathcal{B}_v = \mathcal{B}_v,\ P^v_+\mathcal{B}_v = 0. \end{cases} \tag{1.135}$$

[13] This situation is analogous to the one that gives rise to Wigner's SU(4) symmetry in nuclear physics.

Using in Eq. (1.135) in Eq. (1.133), expanding the products and simplifying,

$$\mathcal{L}_Q = \bar{\mathcal{Q}}_v \left(iv^\mu D_\mu\right) \mathcal{Q}_v - \bar{\mathcal{B}}_v \left(iv^\mu D_\mu + 2M_Q\right) \mathcal{B}_v + \bar{\mathcal{Q}}_v \left(i\not{D}^\perp\right) \mathcal{B}_v + \bar{\mathcal{B}}_v \left(i\not{D}^\perp\right) \mathcal{Q}_v, \tag{1.136}$$

with $D_\mu^\perp = D_\mu - v_\mu v^\nu D_\nu$ the orthogonal component of the covariant derivative. Equation (1.136) illustrates the splitting of the heavy-quark field into $\mathcal{Q}_v$, which is effectively massless, and $\mathcal{B}_v$, with effective mass $2M_Q$. In the rest frame, $v^\mu = (1, \mathbf{0})$, $\mathcal{Q}_v$ ($\mathcal{B}_v$) corresponds to the two upper (lower) components of the four-spinor ψ_Q. In other words, $\mathcal{Q}_v$ ($\mathcal{B}_v$) anihilates a heavy quark (creates a heavy antiquark) of four-velocity v.

Again, the fact that $\mathcal{B}_v$ becomes infinitely massive in the heavy-quark limit indicates that it may be integrated out. On a classical level —*i.e.* up to $\mathcal{O}(\alpha_s(M_Q))$ quantum corrections that can be added in perturbation theory, as $\alpha_s(M_Q \to \infty) \to 0$—, $\mathcal{B}_v$ can be easily eliminated from $\mathcal{L}_Q$ by using the equation of motion

$$\frac{\delta \mathcal{L}_Q}{\delta \bar{\mathcal{B}}_v} = \partial_\mu \frac{\delta \mathcal{L}_Q}{\delta(\partial_\mu \bar{\mathcal{B}}_v)} \quad \Rightarrow \quad i\not{D}^\perp \mathcal{Q}_v = \left(iv^\mu D_\mu + 2M_Q\right) \mathcal{B}_v, \tag{1.137}$$

hence

$$\mathcal{B}_v = \left(iv^\mu D_\mu + 2M_Q\right)^{-1} i\not{D}^\perp \mathcal{Q}_v = \frac{1}{2M_Q} \sum_{n=0}^{\infty} (-1)^n \left(\frac{iv^\mu D_\mu}{2M_Q}\right)^n i\not{D}^\perp \mathcal{Q}_v. \tag{1.138}$$

Recall that Λ_{QCD} and M_Q are the only momentum scales present. Then, in virtue of Eq. (1.134), we anticipate that each derivative in Eq. (1.138) brings down a soft momentum $\sim \Lambda_{\text{QCD}}$, implying that each term in the above sum is suppressed by $\mathcal{O}(\Lambda_{\text{QCD}}/M_Q) \ll 1$ with respect to the inmediately previous one. This guarantees the convergence of the series. Plugging Eq. (1.138) into Eq. (1.136) allows us to express our effective Lagrangian as the derivative expansion

$$\mathcal{L}_{\text{eff}} = \mathcal{L}_{\text{eff}}^{[0]} + \mathcal{L}_{\text{eff}}^{[1]} + \ldots = \bar{\mathcal{Q}}_v \left(iv^\mu D_\mu\right) \mathcal{Q}_v - \bar{\mathcal{Q}}_v \frac{\not{D}^{\perp 2}}{2M_Q} \mathcal{Q}_v + \ldots, \tag{1.139}$$

where $\mathcal{L}_{\text{eff}}^{[n]}$ contains dimension-$(4+n)$ operators suppressed by n powers of M_Q:

- Of course, the LO term is the only one that survives in the heavy-quark limit. It is nothing but the dominant kinetic piece; in the rest frame, it becomes simply $\bar{\mathcal{Q}}_v \left(iD_0\right) \mathcal{Q}_v$. The $\text{SU}(2N_Q)$ heavy-quark symmetry that was anticipated in Section 1.4.1 is manifest from this term.

- Defining $\sigma^{\mu\nu} = i\left[\gamma^\mu, \gamma^\nu\right]/2$, the NLO term may be massaged into

$$\mathcal{L}_{\text{eff}}^{[1]} = -\bar{\mathcal{Q}}_v \frac{D^{\perp 2}}{2M_Q} \mathcal{Q}_v + \bar{\mathcal{Q}}_v \frac{i\sigma^{\mu\nu} D_\mu^\perp D_\nu^\perp}{2M_Q} \mathcal{Q}_v, \tag{1.140}$$

  whose first term represents the first kinetic correction to $\mathcal{L}_{\text{eff}}^{[0]}$; in the rest frame, it collapses to $\bar{\mathcal{Q}}_v[\boldsymbol{D}^2/(2M_Q)]\mathcal{Q}_v$. The second term gives rise to the so-called "chromomagnetic" interaction, a relativistic effect that represents the most important manifestation of heavy-quark spin symmetry breaking. It is behind the small mass splitting between, for example, the heavy charmed mesons D ($J = 0$) and D^* ($J = 1$).

The situation with D and D^* is somehow similar to the one with p and n; then, just like it is useful to take advantage of the approximate isospin symmetry of nuclear physics and treat (p, n) as an isodoublet nucleon state, it results convenient to exploit approximate heavy-quark spin symmetry and combine both heavy mesons in a single "superfield". In the following, we will see how this is done.

1.4.3 Heavy-meson chiral Lagrangian

Even though heavy quarks were the only degrees of freedom we dealt with in Section 1.4.2, what we learned there turn out to be useful in the development of a low-energy EFT that encodes the coupling of heavy mesons ($Q\bar{q}$) with light mesons ($q\bar{q}$). Provided that the latter carry four-momenta that are soft compared to the chiral breakdown scale (1.32), the technology introduced in Sections 1.2.1 and 1.2.2 may be exploited to build up the Lagrangian of such EFT, as we will see.

But, as a first step, we need to construct the heavy-meson states themselves by means of a consistent formalism [5]. In the following, we will fix $Q = c$ for notation simplicity; this will not lead to any loss of generality in virtue of heavy-flavor symmetry, though. Call $|\phi^{(\pm)}\rangle$ ($|\chi^{(\pm)}\rangle$) to the spin part of the c ($\bar{q}$) wavefunction. One may use the representation

$$|\phi^{(+)}\rangle = (1\ 0\ 0\ 0)^{\mathrm{T}}, \quad |\phi^{(-)}\rangle = (0\ 1\ 0\ 0)^{\mathrm{T}}, \quad |\chi^{(-)}\rangle = (0\ 0\ -1\ 0)^{\mathrm{T}}, \quad |\chi^{(+)}\rangle = (0\ 0\ 0\ -1)^{\mathrm{T}}, \tag{1.141}$$

which make an orthonormal basis of eigenstates of the spin operator $\boldsymbol{S}$. Let us study separately the $J = 0$ and the $J = 1$ cases within the rest frame of c ($\boldsymbol{v} = \boldsymbol{0}$), for which Eq. (1.48) becomes

$$P_\pm^0 = \tfrac{1}{2}(1 \pm \gamma_0). \tag{1.142}$$

- *D mesons.* As c and $\bar{q}$ have opposite spins, the pseudoscalar spin part will be proportional to

$$|\phi^{(+)}\rangle\langle\chi^{(-)}| + |\phi^{(-)}\rangle\langle\chi^{(+)}| = P_+^0\gamma_5 \tag{1.143}$$

(see Eq. (1.142)). The full state will be thus written as

$$H_a^{(J=0)}(\mathbf{0}) = -P_+^0 D_a\gamma_5, \quad a = 1,2,3, \tag{1.144}$$

with $D_1 = D^0$, $D_2 = D^+$, $D_3 = D_s$ (see Eq. (1.131)). This state is normalized to

$$\mathrm{Tr}\left[\gamma_5(P_+^0)^2\gamma_5\right] = 2. \tag{1.145}$$

- *D^* mesons.* Since these are vector particles, three independent polarization states may take place. One can choose the polarization basis

$$\varepsilon_+ = (0, \tfrac{1}{\sqrt{2}}, \tfrac{i}{\sqrt{2}}, 0), \quad \varepsilon_0 = (0,0,0,1), \quad \varepsilon_- = (0, \tfrac{1}{\sqrt{2}}, -\tfrac{i}{\sqrt{2}}, 0), \tag{1.146}$$

which is orthonormal, $\varepsilon_{j\mu}^*\varepsilon_k^\mu = -\delta_{jk}$, and subject to the gauge constraint $v_\mu\varepsilon_j^\mu = 0$. The respective spin parts will then be proportional to

$$|\phi^{(+)}\rangle\langle\chi^{(+)}| = -\tfrac{1}{\sqrt{2}}P_+^0\not{\varepsilon}_+, \quad |\phi^{(+)}\rangle\langle\chi^{(-)}| - |\phi^{(-)}\rangle\langle\chi^{(+)}| = -P_+^0\not{\varepsilon}_0, \quad |\phi^{(-)}\rangle\langle\chi^{(-)}| = -\tfrac{1}{\sqrt{2}}P_+^0\not{\varepsilon}_-, \tag{1.147}$$

and the full state will be written as

$$H_a^{(J=1)}(\mathbf{0}) = P_+^0\not{D}_a^*, \quad a = 1,2,3, \tag{1.148}$$

with $D_1^* = D^{*0}$, $D_2^* = D^{*+}$, $D_3^* = D_s^*$. This state is normalized to

$$\mathrm{Tr}\left[\not{\varepsilon}^\dagger(P_+^0)^2\not{\varepsilon}\right] = 2. \tag{1.149}$$

In virtue of heavy-quark spin symmetry, both states (1.144) and (1.148) are coupled into a single superfield H_a. In a reference frame where the c quark has a given three-velocity $\boldsymbol{v}$,

$$H_a(\boldsymbol{v}) = P_+^v(\not{D}_a^* - D_a\gamma_5) \tag{1.150}$$

(see Eq. (1.48)). Its conjugate field is

$$\bar{H}_a(\boldsymbol{v}) = \gamma^0 H_a^\dagger(\boldsymbol{v})\gamma^0 = (\not{D}_a^{*\dagger} + D_a^\dagger\gamma_5)P_+^v. \tag{1.151}$$

The light-meson fields that couple to the heavy-meson fields (1.150) and (1.151) in the chiral Lagrangian are to be considered as pseudo-Goldstone bosons (see Section 1.2.1). Given that the heavy-meson fields transform as a triplet under $\mathrm{SU}(3)_V$, in what follows we will make use of Eq. (1.15) in the definition of the unitary matrix $\mathcal{U}$ (1.12), so that this will transform linearly under $\mathrm{SU}(3)_L \times \mathrm{SU}(3)_R$,

$$\mathcal{U}_{ab} \mapsto (U_L)_{ac}\mathcal{U}_{cd}\,(U_R^\dagger)_{db}, \tag{1.152}$$

where we kept the isospin indices explicit for later convenience. In analogy with what we imposed for the nucleon field in Section 1.2.2, the heavy-meson field H_a introduced above and its covariant derivative $(D_\mu)_{ab}H_b$ must transform non-linearly under $\mathrm{SU}(3)_L \times \mathrm{SU}(3)_R$, but linearly under $\mathrm{SU}(3)_V$. This is done via the compensator matrix $\mathfrak{h}$,

$$H_a \mapsto \mathfrak{h}_{ab}H_b, \quad (D_\mu)_{ab}H_b \mapsto \mathfrak{h}_{ab}(D_\mu)_{bc}H_c, \tag{1.153}$$

where we recalled that

$$\xi_{ab} \mapsto \mathfrak{h}_{ac}\xi_{cd}(U_R^\dagger)_{db} = (U_L)_{ac}\xi_{cd}(\mathfrak{h}^\dagger)_{db}, \quad \xi_{ac}\xi_{cb} = \mathcal{U}_{ab}. \tag{1.154}$$

The definitions of the vector current (1.41) and the axial-vector current (1.42) will be recovered, too,

$$(V_\mu)_{ab} = \tfrac{1}{2}\left[\xi^\dagger, \partial_\mu\xi\right]_{ab}, \quad (A_\mu)_{ab} = \tfrac{i}{2}\left\{\xi^\dagger(x), \partial^\mu\xi(x)\right\}_{ab}. \tag{1.155}$$

These two objects transform under $\mathrm{SU}(3)_L \times \mathrm{SU}(3)_R$ as

$$(V_\mu)_{ab} \mapsto \mathfrak{h}_{ac}\left[(V_\mu)_{cd} + \partial_\mu\delta_{cd}\right](\mathfrak{h}^\dagger)_{db}, \quad (A_\mu)_{ab} \mapsto \mathfrak{h}_{ac}(A_\mu)_{cd}(\mathfrak{h}^\dagger)_{db}, \tag{1.156}$$

and the former will be used in the definition of the covariant derivative,

$$(D_\mu)_{ab} = \partial_\mu\delta_{ab} + (V_\mu)_{ab}, \tag{1.157}$$

consistently with Eq. (1.153). With such building blocks, the most general Lagrangian coupling preserving light-quark and heavy-quark spin symmetries reads [103]

$$\mathcal{L}_{\pi H} = h\,\mathrm{Tr}\left(\bar{H}_a H_b \not{A}_{ab}\gamma_5\right) + \ldots, \tag{1.158}$$

where the traces are computed over Dirac indices, and h is a dimensionless coupling constant that must be determined through empirical data (see *e.g.* Ref. [104]). Finally, the ellipses

account for terms reflecting that both symmetries are only approximate. Being suppressed by powers of either the heavy-quark mass or the chiral breakdown scale, such terms should be added as perturbative corrections to our LO theory.

To summarize, for the last four decades HQEFT has been widely applied to the study of hadron systems in the charm and bottom sectors. Originally, this was done so in parallel with the development of χPT; in the early 90s, with the seminal work by Wise and others (see *e.g.* Ref. [105]), a new synthesis between HQEFT and χPT started to be exploited, thus opening up several unexplored directions in hadronic physics —semileptonic B and D decays with emission of a pseudo-Goldstone boson, chiral-logarithmic corrections to heavy-meson decay constants, composite states of exotic mesons and baryons, *etc.*

1.5 Outline

In this chapter, we have summarized the most general ideas behind EFT, and explained why EFT is a convenient tool in the theoretical understanding of nuclear and hadronic systems. Next, we have introduced χPT as a successful case of low-energy EFT of the $A = 0, 1$ sectors, as well as derived the corresponding PC rules. We have discussed how such rules turn out to fail already in the $A = 2$ sector due to its essential non-perturbative nature, which implies the need for generalizing the perturbative χPT to the so-called χEFT. We have also presented $\not\pi$EFT as a useful theory of few-body nuclear physics in the very-low-energy regime where the characteristic length scale is large compared to the pion Compton wavelength. Special emphasis has been made on the applications of this EFT to the $A = 2$ sector, even though a comment on more general few-nucleon systems has been included. Finally, a short introduction to HQEFT and its low-momentum connection with χEFT has been given. The basic motivation here has been to show how the heavy-meson chiral Lagrangian should be built up. This will serve us as a starting point in the description of the $DD^*_{s0}(2317)$ and $D^*D^*_{s1}(2460)$ systems.

One of the consequences of applying the χPT PC directly to NN χEFT is the predicted non-perturbativity of the OPE interaction *always*, at any partial wave. However, it is well-known that the centrifugal barrier, present whenever the orbital angular momentum is not zero, suppresses this interaction, demoting it to a perturbative effect. In Chapter 2 of the

present work, which is based on Ref. [106], this suppression is quantified for the particular case of peripheral spin-singlet channels ($^1P_1$, $^1D_2$, ...), in a way that fits consistently the EFT approach. To find the demotion of OPE with respect to LO, its strength is rescaled up to the critical point in which a bound state is produced at threshold; then, the rescaling factor determines the corresponding expansion parameter of the perturbative interaction. The results of this "peripheral demotion" may be exploited in few-body calculations, providing theoretical arguments to neglect partial waves where tree-level one-pion exchange is already higher-order than the desired calculation itself.

The $^1S_0$ partial wave was excluded from the analysis of Chapter 2, not only because the centrifugal barrier is not present in it, but also because this particular channel displays some features that are not completely understood. In particular, it is disturbing that Weinberg's prescription for the $^1S_0$ LO interaction predicts a scattering amplitude that exhibits large discrepancies with partial-wave-analysis results already at moderate scattering momenta k. In particular, the phenomenological $^1S_0$ amplitude vanishes at $k \approx 340\,\mathrm{MeV}$; since this point is quite below the assumed breakdown scale of the EFT, we would like the expansion to converge there, which requires that the amplitude zero be included at LO. This can be achieved with a two-dibaryon short-range potential. In Chapter 3, based on Ref. [107], we present a new PC in which OPE is a non-perturbative effect. It is consistent with renormalization invariance and with the symmetry properties of QCD, and its results up to NLO show remarkable agreement with phenomenology. We also include a first approach to the problem in which pions have been integrated out, just like it is done in usual $\not\pi$EFT, which allowed us to derive some analytic results that fit phenomenology surprisingly good, too.

Of course, the EFT philosophy that was exemplified in Chapters 2 and 3 is not exhausted in the nucleon sector and may be applied to more exotic physical systems, whose quark content is not the same as for ordinary matter. The opposite intrinsic parity of the $D^*_{s0}(2317)$ ($D^*_{s1}(2460)$) and the D (D^*) charmed heavy mesons enables them to exchange an S-wave kaon. The resulting one-kaon-exchange interaction has the coordinate form of an attractive Yukawa potential that turns out to be unusually strong and long-ranged due to the mass difference $M_{D^*_{s0}} - M_D$. In Chapter 4, based on Ref. [108], we develop an EFT whose degrees of freedom are the heavy mesons and the light pseudo-Goldstone bosons. The interesting feature of our proposed PC is that *only* the Yukawa potential enters at LO, while contact contributions stemming from four-meson vertices should be taken as perturbative corrections.

This implies that no non-perturbative regularization/renormalization mechanism is needed, thus allowing us to make concrete predictions. We find that one-kaon exchange almost guarantees by itself the existence of a relatively shallow $D_{s0}^* D$ ($D_{s1}^* D^*$) bound state with $J^P = 0^-$ ($J^P = 0^-, 2^-$), whose nature is probably molecular. We also anticipate the existence of its bottom counterpart $B_{s0}(5730)B$ ($B_{s1}(5776)B^*$). Here, the potential will have the same structure as before, but it will be even stronger due to the heavier masses of the bottomed mesons. Consequently, this molecular candidate will be more tightly bound and will exhibit a richer spectrum that might include an excited S-wave state and even a shallow P-wave state.

Finally, conclusions of this work are presented in Chapter 5.

Chapter 2

NN peripheral singlet waves

2.1 Introduction

One prediction of the original Weinberg counting of two-nucleon χEFT is that the OPE interaction has *always* LO nature. Nevertheless, pion exchanges have been known for a long time to be perturbative in peripheral partial waves [109, 110]. This is easy to understand in terms of the repulsive centrifugal barrier for high angular momenta ($\ell \gg k/m_\pi$, with k the center-of-mass momentum and m_π the pion mass), but we will see that, as a matter of fact, the peripheral demotion already takes place for moderate angular momenta ($\ell \sim k/m_\pi$). Even though these phenomena have been discussed in the literature from time to time [47, 56, 58, 60], it has been done rather as an afterthought, and an explanation in terms of PC has remained unexplored up to know. This chapter, based on Ref. [106], is devoted to the task of quantifying the size of the peripheral wave suppression to systematically include it in EFT calculations.

In those two-body channels where the full iteration of OPE produces short-range divergences, giving an answer to this issue is important, as it would provide a theoretically sound argument to perform or avoid the non-perturbative regularization and renormalization of the potential at a given partial wave. However, this is not the case in two-body channels where the divergences do not appear. Still, solving the issue above would find applications in few-body calculations, which usually require the inclusion of contributions arising from two-body partial waves up to a critical value of the orbital angular momentum (typically $\ell \geqslant 5$ or $j \geqslant 5$ in the three-nucleon system [111]). However, the choice of a maximum angular momentum is driven by numerical considerations, rather than by the constraints that the

EFT expansion imposes on the accuracy of physical observables.

We aim at translating the well-known peripheral wave suppression of OPE into the PC language. This will allow to discriminate, on the basis of PC arguments, which two-body partial waves are to be kept or ignored, thus improving the systematics of these calculations or even simplifying them at the lowest orders where probably very few partial waves need to be included. We will limit ourselves to the spin-singlet waves where OPE is not singular and thus can be defined without counterterms.

This chapter is structured as follows. In Section 2.2 we will compare the non-perturbative OPE predictions for the phase shifts in the singlets with their perturbative expansion, allowing us to see up to what extent OPE is perturbative. In Section 2.3 we will provide a PC explanation for the peripheral demotion of central OPE, which will be checked later against numerical calculations of the expansion parameter of central OPE. Finally we will present our conclusions in Section 2.4.

2.2 Perturbative OPE

In this section we will analyze whether the OPE potential is perturbative in the $\ell \geqslant 1$ singlet waves, *i.e.* ${}^1P_1$, ${}^1D_2$, ${}^1F_3$, *etc.* (The $\ell = 0$ singlet wave will be studied in Chapter 3.) With that purpose, we will compare the amplitudes resulting from the full iteration of OPE with the perturbative ones. The phase shifts up to fourth order in perturbation theory will be obtained. The results of these calculations will confirm that the OPE potential is definitely perturbative in all the singlet waves with $\ell \geqslant 1$. In terms of PC, the above is interpreted as the beyond-LO nature of OPE in these waves, where LO is reserved for interactions that are to be infinitely iterated to reproduce the non-perturbative physics that emerges in the S waves.

The comparison between non-perturbative and perturbative OPE can be done in a straightforward manner only in the singlets. This is due to the fact that the long-range part of the OPE potential (1.61) comprises central *and* tensor pieces. According to Eq. (1.60), the former is $\propto 1/r$ when the internucleon distance r is made arbitrarily small, thereby it is a regular interaction, but the latter gets $\propto 1/r^3$ in the short-distance regime and is thus a singular interaction. The tensor part of OPE, while playing a fundamental role in the triplet waves (see Appendix B for the case of the ${}^3S_1$-${}^3D_1$ channel), is vanishing in the singlet channels. This is what makes possible the simple analysis we pursue in this section.

2.2.1 Formalism

Here we will first solve the Schrödinger equation with the OPE potential to obtain the non-perturbative phase shift $\delta_\ell(k)$. Next, this will be perturbatively expanded as

$$\delta_\ell(k) = \delta_\ell^{[1]}(k) + \delta_\ell^{[2]}(k) + \delta_\ell^{[3]}(k) + \dots, \tag{2.1}$$

where the superindices in square brackets indicate the number of insertions of the OPE potential. Comparing the left- and right-hand sides of the equation above, we can test the convergence of the perturbative series.

Consider the reduced Schrödinger equation,

$$\left[\frac{\partial^2}{\partial r^2} + k^2 - M_N V(r) - \frac{\ell(\ell+1)}{r^2}\right] u_\ell(r;k) = 0, \tag{2.2}$$

where M_N is the nucleon mass, and $u_\ell(r;k)$ and $V(r)$ represent respectively the reduced wavefunction and the long-range component of the coordinate OPE potential (1.61). In the singlet channels, for which the tensor operator S_{12} vanishes and the spin-dependent operator $\boldsymbol{\sigma}_1 \cdot \boldsymbol{\sigma}_2$ gives -3, it turns out

$$V(r) = -\vec{\tau}_1 \cdot \vec{\tau}_2 \frac{m_\pi^2}{M_N \Lambda_{NN}} \frac{e^{-m_\pi r}}{r}, \tag{2.3}$$

where the isospin-dependent operator $\vec{\tau}_1 \cdot \vec{\tau}_2$ gives $+1$ for the isovector waves ($\ell = 0, 2, \dots$), for which $V(r)$ is attractive, and -3 for the isoscalar waves ($\ell = 1, 3, \dots$), for which $V(r)$ is repulsive. Also, recall that $\Lambda_{NN} \approx 290\,\text{MeV}$ (1.69), the characteristic momentum scale of OPE, is such that OPE is naively expected to become non-perturbative only at external momenta $Q \gtrsim \Lambda_{NN}$ (see Figure 1.3 and Refs. [34, 35]). We will check that such hypothesis does not hold in the peripheral singlets.

We solve Eq. (2.2) with the boundary conditions at the origin

$$u_\ell(0;k) = 0, \qquad \left.\frac{\partial}{\partial r} u_\ell(r;k)\right|_{r=0} = 1, \tag{2.4}$$

corresponding to a regular interaction. In virtue of the asymptotic form of the wavefunction ($m_\pi r \gg 1$),

$$u_\ell(r;k) \to \hat{\jmath}_\ell(kr) - \hat{y}_\ell(kr) \tan\delta_\ell(k), \tag{2.5}$$

$\hat{\jmath}_\ell(x) = x j_\ell(x)$, $\hat{y}_l(x) = x y_\ell(x)$ being reduced spherical Bessel functions, the non-perturbative phase shifts may be extracted by inputting u_ℓ evaluated at the infrared cutoff $R = 20\,\text{fm}$.

In contrast, the perturbative phase shifts will be found through the integral expression

$$\tan\delta_\ell(k) = -\frac{M_N}{k}\int_0^\infty \mathrm{d}r\, u_\ell(r;k)V(r)\hat{\jmath}_\ell(kr), \tag{2.6}$$

which can be easily derived from the reduced Schrödinger equation (2.2) together with its free version

$$\left[\frac{\partial^2}{\partial r^2} + k^2 - \frac{\ell(\ell+1)}{r^2}\right] v_\ell(r;k) = 0, \tag{2.7}$$

where the free wavefunction v_ℓ satisfies the regularity conditions at the origin,

$$v_\ell(0;k) = 0, \qquad \frac{\partial}{\partial r} v_\ell(r;k)\Big|_{r=0} = 1, \tag{2.8}$$

and has the asymptotic form

$$v_\ell(r;k) \to \hat{\jmath}_\ell(kr). \tag{2.9}$$

Indeed, subtracting Eq. (2.7) times u_ℓ from Eq. (2.2) times v_ℓ, integrating the result between zero and infinity, using the conditions (2.4), (2.5), (2.8), and (2.9), and recalling the property $\hat{\jmath}_\ell(x)\hat{y}'_\ell(x) - \hat{\jmath}'_\ell(x)\hat{y}_\ell(x) = 1$, Eq. (2.6) is obtained. The integral formula is very useful for a perturbative calculation: given the wavefunction of order n, the phase shift at order $n+1$ can be found.

If the potential is weak enough, the reduced wavefunction may be expressed as the perturbative sum

$$u_\ell(r;k) = u_\ell^{[0]}(r;k) + u_\ell^{[1]}(r;k) + u_\ell^{[2]}(r;k) + u_\ell^{[3]}(r;k) + \ldots, \tag{2.10}$$

with

$$\left[\frac{\partial^2}{\partial r^2} + k^2 - \frac{\ell(\ell+1)}{r^2}\right] u_\ell^{[0]}(r;k) = 0, \tag{2.11}$$

$$\left[\frac{\partial^2}{\partial r^2} + k^2 - \frac{\ell(\ell+1)}{r^2}\right] u_\ell^{[n]}(r;k) = M_N V(r) u_\ell^{[n-1]}(r;k) \text{ for } n \geqslant 1. \tag{2.12}$$

This set of differential equations is to be solved iteratively, starting with $n = 0$ for which we take $u_\ell^{[0]}(r;k) = \hat{\jmath}_\ell(kr)$ (the free solution). Then, expanding the integral expression for the phase shifts perturbatively, the Born approximation turns out,

$$\delta_\ell^{[1]}(k) = -\frac{M_N}{k}\int_0^\infty \mathrm{d}r\, \hat{\jmath}_\ell^2(kr)V(r). \tag{2.13}$$

For $n \geqslant 1$ the only subtlety is finding a suitable boundary condition for $u_\ell^{[n]}$, which can be easily done via a perturbative expansion of Eq. (2.5). At first order we find the asymptotic boundary condition

$$u_\ell^{[1]}(r;k) \to -\delta^{[1]}(k)\,\hat{y}_\ell(kr), \tag{2.14}$$

from which we can integrate $u_\ell^{[1]}$ for arbitrary r. This first correction to the wave function gives rise to the second order contribution to the phase shift, as seen by inserting $u_\ell^{[1]}$ in the perturbative expansion of Eq. (2.6):

$$\delta_\ell^{[2]}(k) = -\frac{M_N}{k}\int_0^\infty \mathrm{d}r\, u_\ell^{[1]}(r;k)V(r)\hat{\jmath}_\ell(kr). \tag{2.15}$$

Similarly, the second, third, ... order corrections to the wavefunction are obtained through the asymptotic conditions

$$u_\ell^{[2]}(r;k) \;\to\; -\delta^{[2]}(k)\hat{y}_\ell(kr), \tag{2.16}$$

$$u_\ell^{[3]}(r;k) \;\to\; -\left[\delta^{[3]}(k) + \tfrac{1}{3}\delta^{[1]3}(k)\right]\hat{y}_\ell(kr), \tag{2.17}$$

$$\dots \tag{2.18}$$

They allow to determine the third, fourth, ... order contributions to the phase shift:

$$\delta_\ell^{[3]}(k) = -\frac{M_N}{k}\int_0^\infty \mathrm{d}r\, u_\ell^{[2]}(r;k)V(r)\hat{\jmath}_\ell(kr) - \tfrac{1}{3}\delta_\ell^{[1]3}(k), \tag{2.19}$$

$$\delta_\ell^{[4]}(k) = -\frac{M_N}{k}\int_0^\infty \mathrm{d}r\, u_\ell^{[3]}(r;k)V(r)\hat{\jmath}_\ell(kr) - \delta_\ell^{[1]2}(k)\delta_\ell^{[2]}(k), \tag{2.20}$$

$$\dots \tag{2.21}$$

2.2.2 Results

As mentioned above, the calculations are always finite and well-defined for the singlet-channel OPE. Still, on a practical level, the computational expense of doing perturbation theory up to high orders decreases significantly if a *finite* cutoff is used. Hence, we have regularized the potential with a step function,

$$V(r) \to V(r)\,\theta(r - r_c), \tag{2.22}$$

which simply amounts to changing the lower limit of the perturbative integrals from $r = 0$ to $r = r_c$, and chosen $r_c = 0.3\,\mathrm{fm}$ as a reference value [1]. For this cutoff the perturbative results

[1] We are using a variable step integration method for the set of coupled differential equations (2.11) and (2.12). Owing to the number of differential equations involved, the calculation gets increasingly expensive for small cutoffs when the perturbative order considered is increased; this effect becomes more noticeable for large values of ℓ, particularly at low momenta. The chosen cutoff is actually on the limit of what we can compute at fourth order, yet it suffices for a nuclear EFT calculation. Besides, this is significantly below the standard cutoff ranges employed in previous EFT calculations in coordinate space [57, 58].

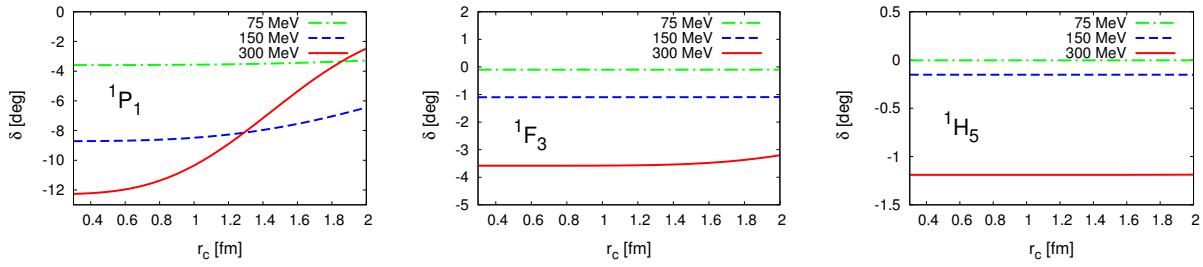

Figure 2.1: Cutoff dependence of the non-perturbative phase shifts for the OPE potential in the peripheral singlet waves $^1P_1$, $^1F_3$, $^1H_5$. We show the $0.3 \leqslant r_c \leqslant 2.0\,\text{fm}$ cutoff range for the center-of-mass momenta $k_{\text{c.m.}} = 75, 150, 300\,\text{MeV}$.

have already converged; as a matter of fact, there are only tiny differences in the results for $r_c < 1\,\text{fm}$.

In pionless calculations, the equivalence between the coordinate cutoff above and a sharp momentum cutoff Λ can be analitically derived,

$$r_c\Lambda = \left[(2\ell+1)!!^2\,\frac{\pi}{2}\right]^{\frac{1}{2\ell+1}} \tag{2.23}$$

(see Ref. [112] for details), so that $r_c = 0.3\,\text{fm}$ yields $\Lambda = 1590\,\text{MeV}$ for a P wave, $\Lambda = 2127\,\text{MeV}$ for a D wave, and higher values for $\ell \geqslant 3$. For checking purposes, in Figure 2.1 we show the cutoff dependence of the non-perturbative phase shifts corresponding to the isoscalar partial waves —it can be appreciated that, the more peripheral the wave, the weaker the cutoff dependence. We have chosen to display the cutoff dependence of the isoscalar channels ($\ell = 1, 3, 5$) because it is for these channels that the potential (2.3) is strongest, yielding more cutoff dependence. With the exception of the $^1P_1$ channel for $r_c \gtrsim 1\,\text{fm}$ (*i.e.* $\Lambda \lesssim 500\,\text{MeV}$, already quite a soft cutoff), the dependence of the phase shifts on r_c ranges from rather mild ($^1F_3$) to negligible ($^1H_5$).

For $r_c = 0.3\,\text{fm}$ we obtain the phase shifts shown in Figure 2.2, where we see how the perturbative expansion is converging extremely quickly even for the $^1P_1$ wave. The perturbative series is more convergent the higher the partial wave: with the exception of the $^1P_1$ wave, the tree-level (Born-approximation) phase shifts already match the full (non-perturbative) ones with a precision of a fraction of a degree. All this indicates that, for the particular case of the $\ell \geqslant 1$ singlet waves, the convergence parameter of the perturbative-pion expansion is certainly smaller than that of the EFT.

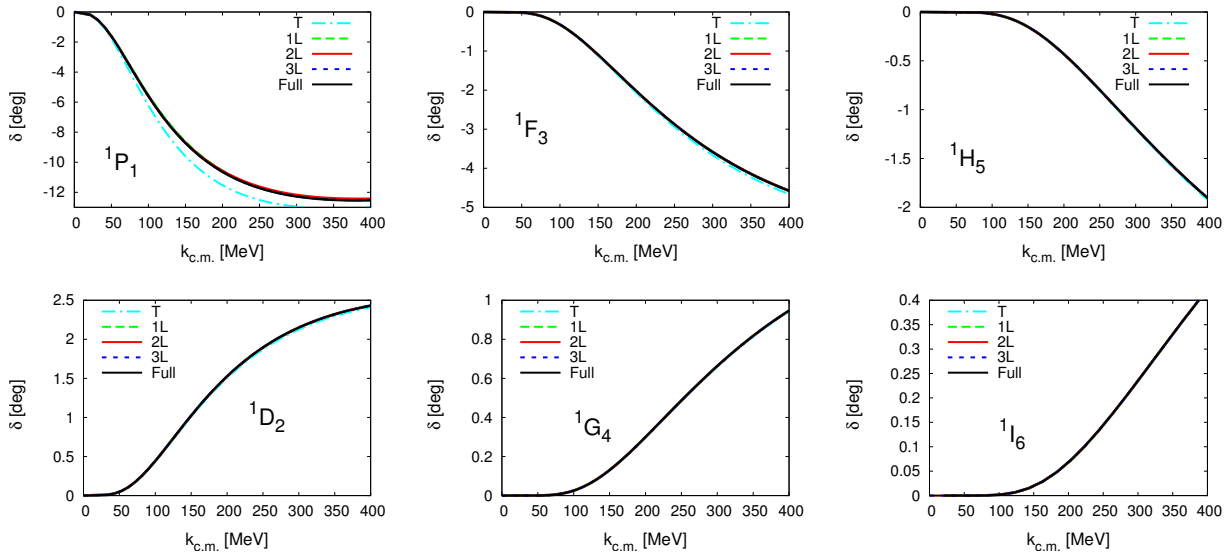

Figure 2.2: Convergence of the perturbative expansion of the phase shifts for the OPE potential in the peripheral singlet partial waves ($^1P_1$, $^1D_2$, $^1F_3$, $^1G_4$, $^1H_5$, $^1I_6$). The black solid line corresponds to the non-perturbative phase shift, while the perturbative ones are displayed at increasing orders, "T" standing for "tree level", and "1L", "2L", "3L" for the one-, two-, three-loop calculation (second, third, fourth order perturbation theory). A finite cutoff of $r_c = 0.3\,\text{fm}$ has been used.

2.3 Peripheral demotion

In this section we will discuss the role of the orbital angular momentum in the PC of the singlet channels. We have just seen that the iteration of the OPE potential is suppressed in the peripheral waves with respect to the expectations of common PC. This demands the inclusion of such "peripheral suppression" into the EFT expansion. In the following we will discuss some ideas in order to quantify an explain the origin of the factor by which the iteration of the OPE potential is suppressed in the higher partial waves.

2.3.1 Quantum-mechanical suppression

First, let us study the peripheral suppression of a finite-range potential in standard quantum mechanics. Even though the arguments presented here are relatively well-known, we will repeat them for the sake of clarity. We anticipate that this type of suppression is apparent only at momenta well below the inverse of the range of the potential, which is roughly given

by m_π for nuclear forces. This means that this kind of explanation will be useful in the context of pionless theories, but its application to pionful theories will be restricted to very peripheral waves.

We begin by considering the integral expression that allows to find the momentum-space representation of the coordinate potential $V(r)$,

$$v_\ell(p,p') \equiv \langle p,\ell|V|p',\ell\rangle = \frac{4\pi}{pp'}\int_0^\infty \mathrm{d}r\, \hat{\jmath}_\ell(pr)V(r)\hat{\jmath}_\ell(p'r), \tag{2.24}$$

which, for $p = p'$, gives the on-shell scattering amplitude in the Born approximation. Comparing $v_\ell(k) \equiv v_\ell(k,k)$ for different angular momenta, we can obtain a baseline estimation of the peripheral suppression factor. This can be done by calculating the ratio of v_ℓ against a reference partial wave, which is chosen to be the P wave as it is the smallest angular momenta considered in this chapter. There is the complication that even (odd) partial waves are isovectors (isoscalars), but this can be circumvented by taking into account the isospin factors $\vec{\tau}_1\cdot\vec{\tau}_2$ into the definition of the ratio,

$$R_\ell(k) = \frac{v_\ell(k)/(\vec{\tau}_1\cdot\vec{\tau}_2)_\ell}{v_{\ell_0}(k)/(\vec{\tau}_1\cdot\vec{\tau}_2)_{\ell_0}}, \tag{2.25}$$

where $(\vec{\tau}_1\cdot\vec{\tau}_2)_\ell$ is +1 (−3) if the total isospin is 1 (0), *i.e.* if ℓ is even (odd). Also, as $\ell_0 = 1$, $v_{\ell_0} = v_{^1P_1}$ and $(\vec{\tau}_1\cdot\vec{\tau}_2)_{\ell_0} = -3$. In Figure 2.3, the inverse of this ratio has been displayed. (The choice of the inverse is aimed at illustrating the suppression in a more transparent way.) One can see that, as the angular momentum increases, the suppression becomes much bigger, especially at low energies.

To quantify such an effect, one can use the Taylor expansion of the reduced Bessel function,

$$\hat{\jmath}_\ell(kr) = \frac{k^{\ell+1}r^{\ell+1}}{(2\ell+1)!!}\left[1+\mathcal{O}(k^2r^2)\right], \quad kr \ll \sqrt{\ell+1/2}, \tag{2.26}$$

into the on-shell version of Eq. (2.24). Recalling that the OPE potential (2.3) falls off exponentially for distances r such that $m_\pi r > 1$, it will turn out

$$v_\ell(k) = \frac{4\pi}{(2\ell+1)!!^2}\,k^{2\ell}\int_0^\infty \mathrm{d}r\, r^{2+2\ell}\left[1+\mathcal{O}(k^2r^2)\right]V(r) \tag{2.27}$$

for momenta k such that $k/m_\pi \ll \sqrt{\ell+1/2}$. We thus see that the power-law behavior of v_ℓ agrees with naive expectations, as it is consistent with the scaling of the lowest-order ℓ-wave counterterm in pionless theory ($Q^{2\ell}$). Besides, it can be explicitly checked that each term

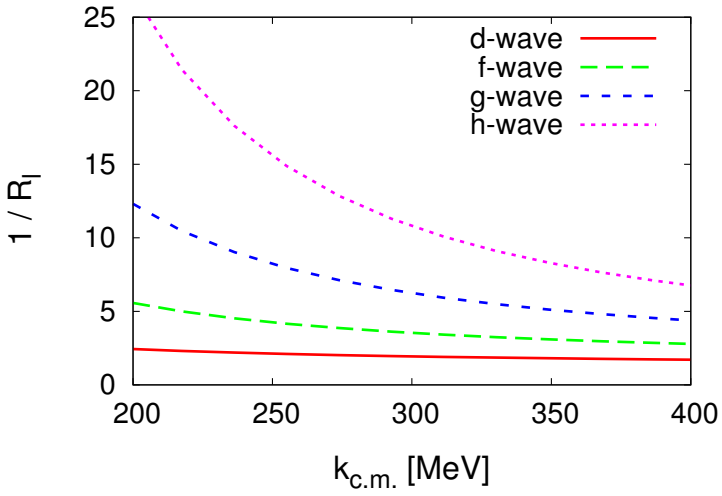

Figure 2.3: Ratio of the diagonal, momentum-space potential between the $\ell = 1$ wave and the $\ell = 2, 3, 4, 5$ waves.

in the series above is suppressed by $\mathcal{O}(k^2/m_\pi^2)$ with respect to the inmediately previous one. Thus, the expected breakdown scale of the pionless theory is come across.

Can this argument be used to justify the peripheral demotion of OPE? In principle the answer is positive: for angular momenta ℓ such that $Q/M_{\rm hi} \ll \sqrt{l+1/2}$, the argument applies over all the range of validity of the pionful theory. Taking $Q \sim m_\pi$ and $M_{\rm hi} \sim 0.5 - 1.0\,{\rm GeV}$, this happens for $\ell \gg 12 - 50$, for which a demotion of OPE similar to the one found for the pionless theory will begin to show up. Still, this range lies far beyond the point where the partial-wave expansion is truncated in three-body calculations. This means that we have to invoke a different type of argument for analyzing the demotion at moderate angular momenta. We will do this in the next section.

2.3.2 Power-counting suppression

Here we consider the peripheral wave suppression from the PC point of view. The idea is to find a relationship between the scales of a two-body system and the orbital angular momentum. The arguments we present are in principle tailored for the particular case of the OPE potential in the singlet channels, for which the issue of regularization/renormalization of divergences does not appear.

The scales that enter into the problem may be conveniently underlined by writing the OPE potential in the form

$$v_\ell(p,p') = \frac{4\pi}{M_N \Lambda_{NN}} f_\ell(p/m_\pi, p'/m_\pi), \tag{2.28}$$

f_ℓ being a dimensionless function defined as

$$f_\ell(x,x') = -\vec{\tau}_1 \cdot \vec{\tau}_2 \int_0^\infty \mathrm{d}y\, y e^{-y} \hat{\jmath}_\ell(xy) \hat{\jmath}_\ell(x'y). \tag{2.29}$$

Then, if G_0 is the Schrödinger propagator, it turns out on dimensional grounds

$$\langle p', \ell | V G_0 V | p, \ell \rangle \sim \left(\frac{4\pi}{M_N \Lambda_{NN}}\right) \times \left(\frac{M_N Q}{4\pi}\right) \times \left(\frac{4\pi}{M_N \Lambda_{NN}}\right) \sim \left(\frac{4\pi}{M_N \Lambda_{NN}}\right) \times \left(\frac{Q}{\Lambda_{NN}}\right), \tag{2.30}$$

Q standing from either k or m_π. We thus see that the decision of iterating OPE or not depends on the dimensionless ratio Q/Λ_{NN}. In the Weinberg prescription, $\Lambda_{NN} \sim Q$ and v_ℓ is to be iterated to all orders; in the Kaplan–Savage–Wise (KSW) scheme, $\Lambda_{NN} \sim M_{\rm hi}$ and v_ℓ does not require iteration. The numerical value $\Lambda_{NN} \sim 300\,\mathrm{MeV}$ lies in between of what one could consider a soft and a hard scale. As a matter of fact, none of the previous conventions works for all partial waves: on the one hand we have the ${}^3S_1$ and ${}^3P_0$ triplets where OPE is thought to be non-perturbative [47], while on the other we have the peripheral singlets where, as shown in Section 2.2, OPE is clearly perturbative and probably demoted even with respect to the $\Lambda_{NN} \sim M_{\rm hi}$ scenario.

Actually, the above mismatch between scaling expectations and numerical results lies in the dimensionless functions and numerical factors in the potential. On a PC level, it is commonly assumed that these dimensionless factors are of $\mathcal{O}(1)$ and do not affect the counting —but if that were truly the case, then OPE would be either perturbative or non-perturbative in *all* partial waves. To have a sense of what is going on here, let us consider first the ℓ-wave projection of the scattering amplitude resulting from the OPE potential in the absence of contact-range physics,

$$t_\ell(k) \equiv \langle k, \ell | T | k, l \rangle = \langle k, \ell | V | k, l \rangle + \langle k, \ell | V G_0 V | k, l \rangle + \ldots, \tag{2.31}$$

which, according to the naive analysis of Eq. (2.30), yields the expansion

$$t_\ell(k) = \frac{4\pi}{M_N \Lambda_{NN}} \sum_{n=0}^{\infty} t_\ell^{(n)}(k/m_\pi) \left(\frac{Q}{\Lambda_{NN}}\right)^n, \tag{2.32}$$

where n refers to the number of loop integrals, and the most obvious or natural expectation for the ℓ-dependent dimensionless coefficients is $t_\ell^{(n)}(x) = \mathcal{O}(1)$. If this hypothesis is correct,

the convergence radius of the series is independent of ℓ. Conversely, if the convergence depends on the particular partial wave, then the form of the loop expansion must take the alternative form

$$t_\ell(k) = \frac{4\pi}{M_N \Lambda_{NN}} \sum_{n=0}^{\infty} t_\ell'^{(n)}(k/m_\pi) \left(\frac{Q}{b_\ell \Lambda_{NN}}\right)^n, \tag{2.33}$$

where the coefficients $t_\ell'^{(n)}$ are truly $\mathcal{O}(1)$, and the factor b_ℓ accounts for the different expansion parameter and convergence radius in each partial wave ℓ. Now, Q/Λ_{NN} is not anymore the relevant ratio to check when discussing the scaling of OPE —it is rather $Q/(b_\ell \Lambda_{NN})$.

From complex analysis we know that the radius of convergence of the series above is given by the amplitude pole that is closest to threshold. However, given that the central component of the OPE potential is relatively weak, such poles will be far from threshold and not easy to find. This difficulty may be circumvented by using a different strategy —instead of finding the amplitude poles for the physical value of Λ_{NN}, we will *rescale* such physical value up to the critical point $\Lambda^*_{NN}(\ell)$ where an ℓ-wave bound state emerges at $k = 0$. The amplitude $t^*_\ell(k)$ resulting from the resized OPE will thus verify

$$t^*_\ell(0) = \frac{4\pi}{M_N \Lambda^*_{NN}(\ell)} \sum_{n}^{\infty} t_\ell'^{(n)}(0) \left(\frac{m_\pi}{b_\ell \Lambda^*_{NN}(\ell)}\right)^n \to \infty \quad \Rightarrow \quad m_\pi \sim b_\ell \Lambda^*_{NN}(\ell). \tag{2.34}$$

Consequently, at $k = 0$ the physical amplitude (2.33) becomes

$$t_\ell(0) \sim \frac{4\pi}{M_N \Lambda_{NN}} \sum_{n=0}^{\infty} t_\ell'^{(n)}(0) \left(\frac{\Lambda^*_{NN}(\ell)}{\Lambda_{NN}}\right)^n. \tag{2.35}$$

This analysis can be extended easily to finite momenta $k \neq 0$, though the conclusions are not as clear-cut. Let us explicitly disentangle the $Q = \{m_\pi, k\}$ power series in Eq. (2.33),

$$t_\ell(k) = \frac{4\pi}{M_N \Lambda_{NN}} \sum_{n=0}^{\infty} t_\ell'^{(n)}(k/m_\pi) \sum_{r+s=n} \frac{c_\ell^{(r,s)} m_\pi^r k^s}{(b_\ell \Lambda_{NN})^n}, \tag{2.36}$$

the coefficients $c_\ell^{(r,s)}$ distinguishing the contributions that stem from powers of m_π and k, respectively. But the previous expression may be rewritten by means of Eq. (2.34),

$$\begin{aligned} t_\ell(k) &= \frac{4\pi}{M_N \Lambda_{NN}} \sum_{n=0}^{\infty} t_\ell'^{(n)}(k/m_\pi) \sum_r c_\ell^{(r,n-r)} \left(\frac{m_\pi}{b_\ell \Lambda_{NN}}\right)^n \left(\frac{k}{m_\pi}\right)^{n-r} \\ &\sim \frac{4\pi}{M_N \Lambda_{NN}} \sum_{n=0}^{\infty} t_\ell''^{(n)}(k/m_\pi) \left(\frac{\Lambda^*_{NN}(\ell)}{\Lambda_{NN}}\right)^n, \end{aligned} \tag{2.37}$$

where the new coefficients $t_\ell''^{(n)}(x)$ are defined as

$$t_\ell''^{(n)}(x) = t_\ell'^{(n)}(x) \sum_r c_\ell^{(r,n-r)} x^{n-r}. \tag{2.38}$$

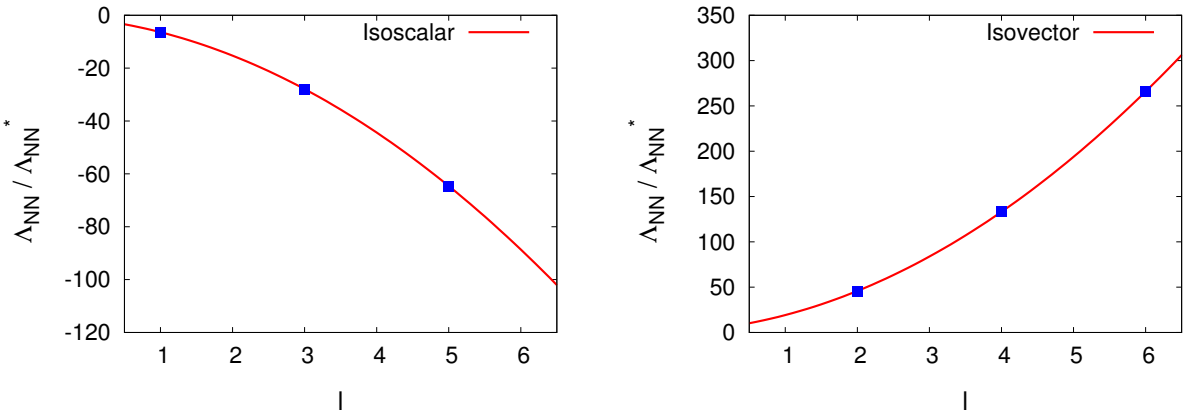

Figure 2.4: Ratio between the physical Λ_{NN} and the critical Λ^*_{NN} generating an ℓ-wave bound state at threshold. The ratio has been calculated independently for isoscalar and isovector channels.

Here, the hypothesis $c_\ell^{(r,s)} = \mathcal{O}(1)$ will amount to assuming that m_π and k always play the same role in the expansion. Yet, we cannot discard the possibility of relative numerical factors between the expansions in powers of m_π and k (one could have, for instance, $c_\ell^{(r,s)} \sim 2^s$, giving a different convergence radius in terms of k than in terms of m_π). Though this makes no difference at the conceptual level, this effect could have a moderate impact when estimating the peripheral demotion of OPE. We will briefly discuss this at the end of the section, but we anticipate that the impact is going to be small. Part of the reason lies in the fact that, at momenta $k \gtrsim m_\pi$, OPE becomes very similar to the Coulomb potential, which happens to be always perturbative except in the very-low-energy regime. This translates into the coefficients $c_\ell^{(r,s)}$ having an extremely suppressed behavior with respect to s (*e.g.* $1/s!$).

The PC demotion will be quantified by comparing the expansion parameter of perturbative OPE with the expansion parameter of pionful EFT,

$$\Lambda^*_{NN}(\ell)/\Lambda_{NN} \equiv (Q/M_{\rm hi})^{\nu(\ell)}\,, \tag{2.39}$$

which means that the order of OPE in the ℓ-wave singlet is not LO (as in the Weinberg counting) nor NLO (as in the KSW one), but $\mathrm{N}^{\nu(\ell)}$LO. Still, one needs to take into account that the scale separation in nuclear EFT is not particularly good. Putting $Q = m_\pi$ and $M_{\rm hi} \sim 0.5 - 1.0\,\mathrm{GeV}$, the expansion parameter will be $\sim 1/7 - 1/3$. Concrete EFT analyses [57–61, 113–115] suggest an expansion parameter closer to 1/3 than to 1/7.

The value of $\Lambda^*_{NN}(\ell)$ that produces the bound state at threshold is found numerically through the asymptotic condition on the zero-energy wavefunction $u_\ell(R;0) = 0$, $R = 40\,\mathrm{fm}$

Table 2.1: PC prescriptions for OPE in the singlet partial waves with $1 \leqslant \ell \leqslant 11$. We show the critical value of Λ_{NN} that renders the central potential non-perturbative in each of the singlets. The PC assignment in each partial wave depends on the expansion parameter of nuclear EFT, which is not known precisely, but expected to lie between 1/7 and 1/3. Using this range of values, we calculate the OPE demotion in each partial wave.

Isoscalar waves			Isovector waves		
$^{2S+1}\ell_J$	$\Lambda_{NN}/\Lambda^*_{NN}(\ell)$	N$^\nu$LO	$^{2S+1}\ell_J$	$\Lambda_{NN}/\Lambda^*_{NN}(\ell)$	N$^\nu$LO
$^1P_1$	−6.40	N$^{1.0-1.7}$LO	$^1D_2$	45.8	N$^{2.0-3.5}$LO
$^1F_3$	−27.9	N$^{1.7-3.0}$LO	$^1G_4$	133.1	N$^{2.5-4.5}$LO
$^1H_5$	−64.6	N$^{2.1-3.8}$LO	$^1I_6$	265.9	N$^{2.9-5.1}$LO
$^1J_7$	−116.4	N$^{2.4-4.3}$LO	$^1K_8$	444.0	N$^{3.1-5.5}$LO
$^1L_9$	−183.3	N$^{2.7-4.7}$LO	$^1M_{10}$	667.4	N$^{3.3-5.9}$LO
$^1N_{11}$	−265.4	N$^{2.9-5.1}$LO			

being the infrared cutoff. (Actually, the results are stable already for $R \geqslant 10\,\text{fm}$.) In Figure 2.4 we show the ratio $\Lambda_{NN}/\Lambda^*_{NN}$ for the peripheral singlets versus the angular momentum ℓ, which is taken as a continuous variable; the actual peripheral waves are displayed as discrete points along the curve. (Note that this ratio is negative in the isoscalar waves, as the OPE potential is actually repulsive in those channels.) The specific values of the $\Lambda_{NN}/\Lambda^*_{NN}$ are given in Table 2.1, where the effective order N$^\nu$LO at which OPE enters in each peripheral singlet is listed as well. The PC is normalized consistently with the discussion above, *i.e.* LO corresponds to a potential that has to be iterated to all orders (such as the lowest-order contact interaction in the S-wave singlet), while NLO is identified with the size of the OPE potential in the KSW counting. One can see that OPE is slightly demoted with respect to KSW even for the $^1P_1$ partial wave. Table 2.1 only shows partial waves whose average demotion does not go much beyond N^{4}LO, as contributions above this order are unlikely to enter in any practical EFT calculation in the near future. The chiral nuclear potential has not been used beyond leading three-pion exchange (or subsubleading TPE) in full EFT calculations [2]. Given that such piece of the potential enters at N^{4}LO in a Weinberg-inspired

[2]Though recently [116] the chiral potential has been calculated one order further and used in first-order perturbation theory for peripheral NN scattering.

counting [3] and at N^{5}LO in a KSW-inspired one, it does not seem necessary to go beyond that point.

The spread in the demotion emerges from the uncertainty on the expansion parameter: for each ℓ, the lowest (highest) estimation of ν results from taking the expansion parameter equal to 1/7 (1/3). (For instance, in the $^1P_1$ case N$^{1.0}$LO corresponds to 1/7 and N$^{1.7}$LO to 1/3.) If we take into account that the actual expansion parameter seems to be closer to 1/3, then the larger estimations for the demotion are expected to be more accurate than the lower ones. Still, overestimating the demotion can lead to the underestimation of the theoretical errors in a calculation, so it might be more cautious to use a value in the middle.

Apart from the uncertainty in $Q/M_{\rm hi}$, there is a second source of error in Table 2.1, namely the interplay between the k and m_π expansions that we have previously discussed qualitatively. Addressing this problem lies beyond the scope of this work, and in fact it has never been done in the literature for a pionful EFT expansion. Instead of analyzing in detail the perturbative expansion, we will explore the demotion by means of an alternative definition of $\Lambda^*_{NN}(\ell)$. We have defined $\Lambda^*_{NN}(\ell)$ as the Λ_{NN} for which a bound state appears at threshold, so that the ratio $\Lambda^*_{NN}(\ell)/\Lambda_{NN}$ corresponds to the expansion parameter of the amplitude at zero energy; however, the emergence of a low-lying virtual state or resonance *also* calls for the iteration of the potential, whose strength is now required to be smaller than in the bound-state case. Therefore one could have introduced the more general scale $\Lambda^*_{NN}(\ell, k_{\rm pole})$ as the value of Λ_{NN} for which there is a pole at $k = k_{\rm pole}$; this pole could be either a bound/virtual state or a resonance, so it would lie on the momentum complex plane in general. The new scale would have allowed us to replace the expansion (2.35) by

$$t_\ell(k_{\rm pole}) \sim \frac{4\pi}{M_N \Lambda_{NN}} \sum_{n=0}^{\infty} t_\ell^{\prime(n)}(k_{\rm pole}/m_\pi) \left(\frac{\Lambda^*_{NN}(\ell, k_{\rm pole})}{\Lambda_{NN}}\right)^n , \tag{2.40}$$

thus leading to the definition of an alternative peripheral demotion different from the one of Eq. (2.39),

$$\Lambda^*_{NN}(\ell, k_{\rm pole})/\Lambda_{NN} \equiv (Q/M_{\rm hi})^{\nu'(\ell)}. \tag{2.41}$$

If we choose the pole to be a bound state away from the threshold, then OPE will need to be stronger, amounting to a smaller Λ^*_{NN} and more demotion ($\nu' > \nu$). Conversely, imposing

[3] This corresponds to N^{3}LO in the traditional notation used in Ref. [45], which skips one order because in the Weinberg scheme the contribution linear in $Q/M_{\rm hi}$ vanishes.

the virtual-state/resonance condition implies a bigger Λ^*_{NN} ratio and less demotion ($\nu' < \nu$). Since we are more interested in the possibility that we might have been overestimating the demotion, we will consider the virtual-state/resonance hypothesis only. We have included the calculations in Appendix C and checked that the effect of a change in conditions from a threshold bound state to a resonance is quite small for $\nu(\ell)$, usually of the order of $|\Delta\nu| \sim 0.05 - 0.2$. If we compare this change to the uncertainty related to $Q/M_{\rm hi}$, which lies in the range $|\Delta\nu| \sim 0.5 - 2$, we see that corrections to the threshold bound-state condition can be safely ignored in most partial waves.

2.3.3 The peripheral perturbative expansion revisited

Now that a PC argument for the centrifugal suppression of the singlets has been provided, we test it against concrete calculations. The approach we find most convenient is the comparison of multiple iterations of the OPE potential. The ratio of iterated versus non-iterated diagrams has been already used in the past as a tool for determining the convergence of the EFT series [55], but calculations have been usually limited to just a few iterations of OPE. While this might not be a drawback in S-wave scattering, peripheral waves require the evaluation of higher orders of perturbation theory in order to get an estimation of the expansion parameter.

With that purpose, first we will introduce the diagonal matrix element of the n-iterated OPE potential as

$$\langle v_\ell^{[n]} \rangle = \langle k, \ell \,|\, \underbrace{VG_0 \dots G_0 V}_{n \text{ insertions of } V} \,|\, k, \ell \rangle = \int_0^\infty \mathrm{d}r\, u_\ell^{[0]}(r;k) V(r) u_\ell^{[n-1]}(r;k), \quad n \geqslant 1, \tag{2.42}$$

where $u_\ell^{[0]}(r;k) = \hat{\jmath}(kr)$ is the free (regular) wavefunction, while $u_\ell^{[n]}(r;k)$ is the solution of Eq. (2.12), from which

$$u_\ell^{[n]}(r;k) = M_N \int_0^\infty \mathrm{d}s\, G_\ell(r,s;k) V(s) u_\ell^{[n-1]}(s;k), \tag{2.43}$$

where the Green's function, defined by the condition

$$\left[\frac{\partial^2}{\partial r^2} + k^2 - \frac{\ell(\ell+1)}{r^2}\right] G_\ell(r,s;k) = \delta(r-s), \tag{2.44}$$

may be constructed as

$$G_\ell(r,s;k) = \frac{1}{k}\Big[\hat{\jmath}_\ell(kr)\hat{y}_\ell(ks)\theta(s-r) + \hat{\jmath}_\ell(ks)\hat{y}_\ell(kr)\theta(r-s)\Big]. \tag{2.45}$$

This allows to define the ratio of the n-iterated potential against the $(n-1)$-iterated one,

$$R_\ell^{[n]} = \langle v_\ell^{[n]} \rangle \,/\, \langle v_\ell^{[n-1]} \rangle \,. \tag{2.46}$$

Then, according to what we saw in Section 2.3.2, the initial expectation is to have

$$R_\ell^{[n]} \sim \Lambda_{NN}^*(\ell)/\Lambda_{NN}, \quad n \geqslant 1. \tag{2.47}$$

In particular, for $n = 1$ Eq. (2.46) gives

$$\begin{aligned} R_\ell^{[1]} &= \frac{M_N \int_0^\infty \mathrm{d}r\, \hat{\jmath}_\ell(kr) V(r) \int_0^\infty \mathrm{d}s\, G_\ell(r,s;k) V(s) \hat{\jmath}_\ell(ks)}{\int_0^\infty \mathrm{d}r\, \hat{\jmath}_\ell(kr) V(r) \hat{\jmath}_\ell(kr)} \\ &= \frac{\vec{\tau}_1 \cdot \vec{\tau}_2}{2\ell+1} \frac{m_\pi}{2^{2\ell+1}\Lambda_{NN}} \left[1 + \mathcal{O}\left(k^2/m_\pi^2\right)\right] \sim 2^{-2\ell-1}, \end{aligned} \tag{2.48}$$

where the low-momentum expansion of $\hat{\jmath}_\ell(kr)$ (2.26) was recalled. But, as $|\Lambda_{NN}/\Lambda_{NN}^*(\ell)| \ll 2^{2\ell+1}$ (as can be seen in Table 2.1), $R_\ell^{[1]}$ is actually very suppressed with respect to the expectation (2.47). Still, this does not necessarily mean that the peripheral demotion was underestimated in Section 2.3.2 —as we will see, lower-order perturbation theory tends to exaggerate the effect of the centrifugal barrier. The reasons of the latter are not completely clear, but it might be related to the interplay between the regular ($\hat{\jmath}_\ell(kr)$) and irregular ($\hat{y}_\ell(kr)$) components of the wavefunction at low energies ($k \ll m_\pi$), with the irregular piece giving a larger contribution and appearing only at higher-order perturbation theory. Be it as it may, the bottomline is that one needs to evaluate Eq. (2.46) at higher n to reliably probe the expansion parameter.

The results for $1/R_\ell^{[n]}$, $2 \leqslant n \leqslant 7$, are given in Figure 2.5. (The choice of the inverse is simply because the inverse of the expansion parameter is a more natural indication of the goodness of perturbation theory: the bigger $1/|R_\ell^{[n]}|$ is, the quicker the expansion converges.) The plots indicate that, as the perturbative order n gets higher and higher, the expansion parameters $R_\ell^{[n]}$ tend to agree with the results obtained in Secton 2.3.2 through a different method, thus providing a cross-check for our calculation. In principle, such agreement should be most clear at low energies ($k < m_\pi$), since at moderate energies ($k \sim m_\pi$) one needs to take into account that the $Q/(b_\ell \Lambda_{NN})$ expansion contains powers of both $m_\pi/(b_\ell \Lambda_{NN})$ and $k/(b_\ell \Lambda_{NN})$. The remarkable thing, though, is that the expansion still works rather well at larger momenta that are not far from $M_{\rm hi} \sim 0.5\,\mathrm{GeV}$. This might be puzzling from the EFT perspective but has a natural explanation in terms of the form of the central OPE potential

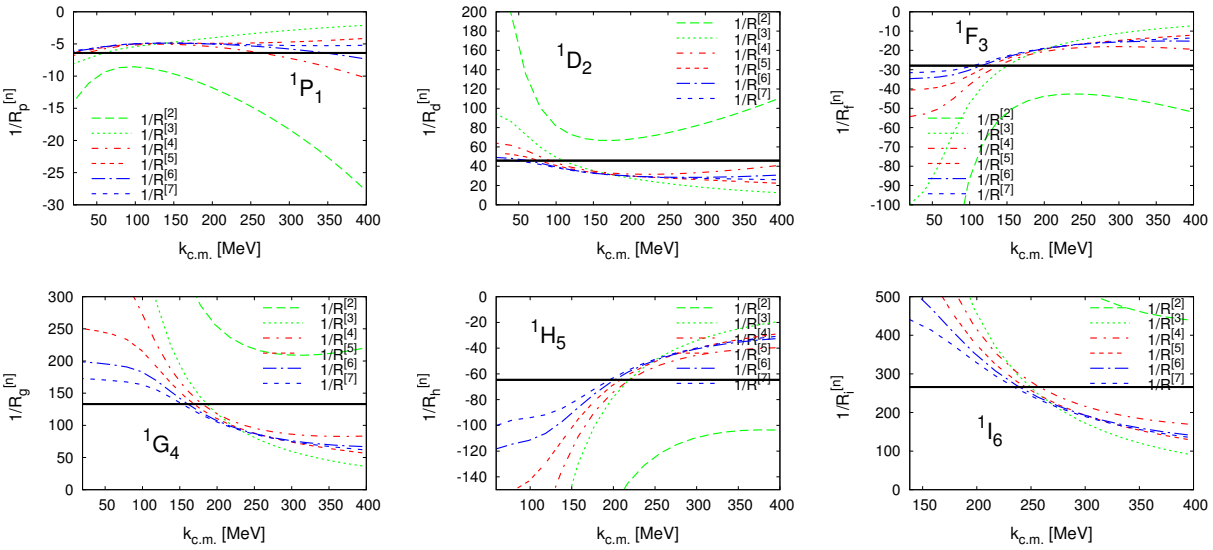

Figure 2.5: Inverse ratios $1/R_\ell^{[n]}$ (see Eq. (2.46)) in the singlet partial waves with $1 \leqslant \ell \leqslant 6$. The value of $\Lambda_{NN}/\Lambda^*_{NN}(\ell)$ (see Table 2.1), to which the ratios should converge, is shown in the black solid line.

—for momenta that are large compared to the pion mass, central OPE is almost a Coulomb-like potential ($V \sim 1/r$), which is necessarily perturbative (provided that its inverse Bohr radius is, roughly, $k_{\rm B} \sim m_\pi^2/\Lambda_{NN} < m_\pi$). However, this is a particular feature of central OPE that is not expected to happen for other contributions of the EFT nuclear potential.

From the figure we see that the convergence pattern for $\ell = 1, 2, 3$ is much more evident than for $\ell = 4, 5, 6$. In the latter cases, apparently seventh-order perturbation theory is not enough to stabilize the ratios, which nonetheless seem to converge to the predicted value. Another interesting feature is that the lower orders of perturbation theory predict actually a faster convergence than the high orders. The practical implication of this phenomenon is that results at tree level are *more* accurate than expected from the expansion parameter of the series. This might in turn point out towards choosing the higher-order estimates for the demotion.

2.3.4 Beyond central OPE

At this point a question arises: how should these ideas be extended to TPE? NDA predicts the LO (N^{2}LO) character of OPE (leading TPE); in other words, leading TPE is naively

suppressed by $Q^2/M_{\rm hi}^2$ with respect to OPE. But, since OPE is probably more demoted than that for singlet waves with $\ell \geqslant 2$ (see Section 2.3.2), it is natural to expect that a similar demotion will apply for TPE.

It is worth recalling, however, that the PC argument developed here for the peripheral demotion in the singlets relies on a particular feature of the central OPE potential: this is a regular interaction that does not require regularization. Conversely, both TPE and the non-central part of OPE are badly divergent potentials at short distances and thus require regularization. As a consequence, the arguments exploited here cannot be applied directly either to TPE or to OPE in the triplet channels. There are strategies to cope with this, though they will require serious scrutiny to check whether they work. The most obvious one is to *renormalize* these partial waves —after the inclusion of a contact-range interaction, one might be able to apply the same ideas as before. The drawback of this proposal is that it mixes short- and long-range physics, as the factor by which TPE needs to be rescaled for having a bound state at threshold depends on the scattering volume of the channel (before rescaling TPE), which fixes the contact-range coupling. This would imply that the rescaling factor is contaminated by the physical scattering volume, which is undesirable. It might happen, though, that the effect of this contamination is negligible, as it turned out for the threshold-bound-state versus shallow-resonance condition (see Appendix C).

Still, if one strives for a solution that is manifestly independent of the existence of short-range physics, two possible alternatives come to mind:

- One can invoke Birse's approach to tensor OPE [56], which adapts a series of techniques from atomic physics to study whether tensor OPE is perturbative or not. A limitation of this program is that it is formulated in the chiral limit, where the range of the OPE potential diverges and the interaction is similar to the typical potentials of atomic physics.

- A different strategy is to study the cutoff at which TPE generates deeply bound states. Deeply bound states are non-physical bound states that occur when attractive singular interactions, such as tensor OPE and TPE, are considered. As long as their binding momenta are beyond the range of applicability of EFT, they are physically meaningless, and techniques to get rid of them have been developed [47]. The point is that the more peripheral the wave, the harder the cutoff for which deeply bound states emerge. This might in turn give us quantitative information on the partial wave suppression.

2.4 Conclusion

In this chapter the EFT approach has been exploited to analyze, for the particular case of the spin-singlet channels, the common wisdom observation that pion exchanges are perturbative in peripheral waves. For this we have studied the convergence of the perturbative expansion of the phase shifts numerically up to fourth order in perturbation theory. This calculation —which has been done here for the first time up to such an order— indicates that pion exchanges are indeed perturbative in the peripheral singlets. In fact, the multiple iterations of OPE turn out to be much more suppressed than expected even in a PC such as KSW, in which OPE potential is treated as subleading.

To understand this pattern we have made use of a PC argument to determine the actual demotion of OPE potential with respect to LO. The idea is to rescale the strength of OPE up to the point in which a bound state is generated at threshold. This critical strength can be translated into a critical Λ^*_{NN} —which will be softer than the physical Λ_{NN}— such that the perturbative expansion diverges. The ratio $\Lambda^*_{NN}/\Lambda_{NN}$ corresponds to the expansion parameter of perturbative OPE, which turns out to be quickly convergent. We have checked this prediction against concrete calculations, confirming the EFT argument. Actually, even the ${}^1P_1$ partial wave is suppressed beyond NLO, and higher waves may be demoted up to the point of being less important than subleading TPE in NDA. However, the demotion of leading and subleading TPE in the peripheral waves is yet to be studied.

The importance of the peripheral demotion is not merely academic, but it has applications in few-body calculations, where the demotion can be used to improve and optimize calculations. The way in which this is achieved is by including only the necessary number of iterations in the peripheral waves and by ignoring partial waves where tree-level OPE potential is already higher-order than the order of the calculation. In fact this is analogous to the common practice of ignoring the partial waves with angular momentum larger than a certain critical value ($\ell \geqslant 5$ in most applications). The difference is that here we systematize this practice in a way that is compatible with the EFT expansion, providing guidelines for future few-body calculations in nuclear EFT.

Still, this chapter deals only with OPE in the peripheral singlets. For the peripheral demotion to be useful in few-body calculations, we need to extend the present study to peripheral triplets and also to TPE. This analysis is underway, though the tools that will be required are different that the ones we have used here due to the singular nature of tensor

OPE and TPE interactions. Hence, the calculation of their peripheral demotion will require the development of more sophisticated arguments that take into account the existence of a finite cutoff and how it relates to the other scales in the problem.

Chapter 3

NN S-wave singlet channel

3.1 Introduction

The ${}^1S_0$ partial wave was not considered in the analysis of Chapter 2. This was so because this particular channel presents, apart from the renormalization issue that was pointed out in Section 1.2.3.2, other features that remain not completely captured by the EFT approach. The understanding of these issues has not improved greatly since the late 90s, despite considerable effort [50, 61, 64, 65, 76, 112, 114, 117–140]. The present chapter, which is based on Ref. [107], aims to shed some new light in that regard.

A unique feature of this wave, which was recognized early on, is fine tuning in the form of a very shallow virtual bound state. The OPE potential (1.68) is characterized by two scales —its inverse range given by the pion mass m_π and its inverse strength given by $\Lambda_{NN} \equiv 16\pi f_\pi^2/(g_A^2 M_N) = \mathcal{O}(f_\pi)$, with $f_\pi = \mathcal{O}(M_{\rm QCD}/(4\pi))$ the pion decay constant, $M_N = \mathcal{O}(M_{\rm QCD})$ the nucleon mass, and $g_A = \mathcal{O}(1)$ the axial-vector coupling constant (see Eqs. (1.32), (1.80), and (1.81), respectively). But, at the physical pion mass, $m_\pi \simeq 140\,\text{MeV}$, the virtual state's binding momentum $\aleph \sim 10\,\text{MeV}$ is much smaller than the pion scales. It has been argued [64] that such smallness is likely due to a near coincidence between the physical values of the quark masses and their values that produce a pion attraction just enough to generate a zero-energy bound state. Be it as it may, in the very-low-energy regime, $Q \ll m_\pi$, the virtual state is well-described by an EFT where nucleons are the only explicit degrees of freedom, namely $\not\pi$EFT (see Section 1.3). To simultaneously capture the $Q \sim m_\pi$ range, however, pion exchange needs to be retained. The perturbative expansion in Q/Λ_{NN} prescribed by Refs. [34, 35] converges very slowly, if at all, in the low-energy region [64],

suggesting to identify Λ_{NN} as a low-energy scale $M_{\rm lo}$, just as indicated by NDA.

Yet, it is disturbing that the NDA-prescribed LO potential produces $^1S_0$ phase shifts showing large discrepancies with the Nijmegen partial-wave analysis (PWA) [141] even at moderate scattering energies. In Ref. [61] it was shown that, differently from what NDA anticipates, the first correction in this channel appears already at NLO, in the form of a contact interaction with two derivatives. Still, only about half of the near-threshold energy dependence exhibited by the phenomenological inverse amplitude is reproduced by LO, so Ref. [137] went a step further by promoting to LO an energy-dependent short-range interaction fixed by the effective range —a generalization of the suggestion made years before in $\not\pi$EFT [142]. Even this promotion leaves significant room for improvement when compared to the Nijmegen PWA. In particular, the empirical $^1S_0$ phase shift, thus the amplitude, vanishes at the center-of-mass momentum $k_0 \simeq 340\,\text{MeV}$. Since k_0 is only a bit above Λ_{NN}, it should be considered as a soft scale where the EFT converges, too. In contrast, we find that the LO phase shift of Ref. [137] is around 25° at $k = k_0$ and does not vanish until k reaches a few GeV. Since higher orders need to overcome LO, convergence at momenta $k \sim k_0$ will be at best very slow; besides, LO wil not provide a qualitatively correct description of the amplitude at momenta that are quite below the expected breakdown scale. This situation is unsatisfactory from the EFT point of view, and can only be remedied if LO is enforced to contain the amplitude zero. As pointed out in Ref. [69], a low-energy zero requires a different kind of fine tuning than the one giving rise to a shallow bound state. When the zero appears at very low energies, a contact EFT can be devised (the "other unnatural EFT" of Ref. [69]) which gives rise to a perturbative expansion of the amplitude around $k = k_0$. Such an expansion was developed in Ref. [124] in the presence of pions.

Here we propose a rearrangement of the short-range part of χEFT that leads to the existence of the amplitude zero at LO, in addition to the shallow virtual state. The PC of Ref. [69] is generalized with the purpose of including the non-perturbative region that contains the virtual state. This is patterned on an idea originally developed for doublet neutron-deuteron (nd) scattering at very low energies [143], where the amplitude has a zero at small imaginary momentum, in addition to a shallow virtual state. We develop an expansion in $Q/M_{\rm hi}$ for $Q \sim M_{\rm lo}$, which gives an order-by-order renormalizable amplitude. Following a successful approach to $\not\pi$EFT [144], the virtual state is assumed to be located right at threshold at LO and is moved to a binding momentum $\sim M_{\rm lo}^2/M_{\rm hi}$ at NLO. We calculate NLO corrections and show a systematic improvement in the description of the

phase shift.

A challenging feature of χEFT is that it usually does not yield analytical expressions for amplitudes. This difficulty may be evaded by exploiting also a version of our proposed PC for the theory without explicit pions, where we retain $k_0 \sim M_{\rm lo}$ but explore $\Lambda_{NN} \to \infty$. To our surprise, even though $k_0 > m_\pi$, this new version of $\not\pi$EFT also produces a good description of the empirical phase shifts.

Our approach is in line with Refs. [114, 122], which argued that short-range forces in the spin-singlet S wave must produce rapid energy dependence. It is a systematic extension of the potential proposed in Ref. [76], and it resembles the unitarized approach of Ref. [124]. More generally, it can be seen as the EFT realization of Castillejo-Dalitz-Dyson (CDD) poles [145] in S-matrix theory. Traditional S-matrix tools, such as the N/D method, have recently received renewed attention in the NN system (*e.g.* Ref. [146]). The D function is determined modulo the addition of CDD poles, which result in zeros of the scattering amplitude. In particular, the momentum k_0 may be identified with the position of a CDD pole in the $^1S_0$ channel [147]. An EFT provides a systematic description of the two-body CDD pole that can be naturally extended to more-body systems.

This chapter is structured as follows. In Section 3.2 we present an initial approach ("warm-up") to the problem on the basis of a modified organization of $\not\pi$EFT up to NLO. The proposed PC is discussed in detail, and RG invariance is demonstrated explicitly. In Section 3.3 we bring OPE into LO; also, we compare with the results of the high-quality *Nijm93* potential [148] before and after the inclusion of the NLO potential in this χEFT. Conclusions are presented in Section 3.4.

3.2 Pionless theory

Our first approach to the problem will omit explicit pion exchange (as well as electromagnetic interactions —these are small anyway for momenta $k \gtrsim \alpha M_N \sim 10\,\text{MeV}$, with $\alpha \simeq 1/137$ the fine-structure constant— and other small isospin-breaking effects [144]). Since the amplitude zero appears at a momentum above the pion mass, it is unlikely that an EFT where pions are not explicit degrees of freedom can reliably describe it. Still, our goal here is to illustrate RG invariance and PC for a systematically improvable contact theory whose amplitude includes both a near-threshold pole and a low-energy zero. The great benefit of removing pions is simply to find analytical results, which cannot be reached if one includes OPE in (fully

iterated) LO. Such results provide an important guide to the pionful analysis of Section 3.3.

As we saw in Section 1.3, in the absence of explicit pions and nucleon excitations, all interactions among nucleons are of contact type, and the part of the Lagrangian relevant for the NN ${}^1S_0$ channel reads

$$\mathcal{L}_{\not\pi}^{(\mathrm{ct})} = N^\dagger\Big(i\partial_0 + \frac{\nabla^2}{2M_N}\Big)N - C_0\left(N^{\mathrm{T}}\vec{P}_{{}^1S_0}N\right)^\dagger\cdot\left(N^{\mathrm{T}}\vec{P}_{{}^1S_0}N\right) + \ldots, \tag{3.1}$$

where N is the isodoublet, bispinor nucleon field and the NN ${}^1S_0$ projector is expressed in terms of the Pauli matrices $\boldsymbol{\sigma}$ ($\vec{\tau}$) acting on spin (isospin) space as $\vec{P}_{{}^1S_0} = \sigma_2\vec{\tau}\tau_2/\sqrt{8}$, while "..." means more complicated interactions and relativistic corrections suppressed by powers of the breakdown scale of the theory. But, as seen in Section 1.3.3.1, the interaction term in Eq. (3.1) may be rewritten by means of the isovector dibaryon field $\vec{\phi}$, so that one can use the alternative Lagrangian

$$\mathcal{L}_{\not\pi}^{(\phi)} = N^\dagger\Big(i\partial_0 + \frac{\nabla^2}{2M_N}\Big)N + \vec{\phi}^\dagger\cdot\Big[\Delta + c\Big(i\partial_0 + \frac{\nabla^2}{4M_N}\Big)\Big]\vec{\phi} - \sqrt{\frac{4\pi}{M_N}}(\vec{\phi}^\dagger\cdot N^{\mathrm{T}}\vec{P}_{{}^1S_0}N + \mathrm{H.c.}) + \ldots, \tag{3.2}$$

where Δ is the dibaryon residual mass, c is a number that normalizes the (explicitly included) dibaryon kinetic term, and higher-order contact interactions can be systematically added via the inclusion of derivative dibaryon-NN couplings.

The established PC of $\not\pi$EFT [34, 35, 68, 69] reproduces the shallow virtual state at LO, but does not generate as much energy dependence as the phenomenological phase shifts. A promotion of the dibaryon kinetic term to LO [142] allows for the reproduction of the derivative of the amplitude with respect to the energy around threshold. However, these approaches are *equivalent* to different truncations of the ERE and are unable to generate an amplitude zero at any finite momentum. This is certainly not a problem in $\not\pi$EFT, since k_0 (numerically larger than m_π) is presumably outside the scope of this theory. But here we aim at reformulating the theory in a way such that k_0 is taken below the breakdown scale, so as to illustrate the proposed reformulation of the χEFT PC in Section 3.3.

With that purpose in mind, and inspired by an EFT for very-low-energy nd scattering [143], we generalize the Lagrangian (3.2) for the case of *two* dibaryon fields, $\vec{\phi}_{1,2}$,

$$\begin{aligned}\mathcal{L}_{\not\pi}^{(2\phi)} = {} & N^\dagger\Big(i\partial_0 + \frac{\nabla^2}{2M_N}\Big)N + \sum_{j=1,2}\vec{\phi}_j^{\,\dagger}\cdot\Big[\Delta_j + c_j\Big(i\partial_0 + \frac{\nabla^2}{4M_N}\Big)\Big]\vec{\phi}_j \\ & - \sqrt{\frac{4\pi}{M_N}}\sum_{j=1,2}\left(\vec{\phi}_j^{\,\dagger}\cdot N^{\mathrm{T}}\vec{P}_{{}^1S_0}N + \mathrm{H.c.}\right) + \ldots,\end{aligned} \tag{3.3}$$

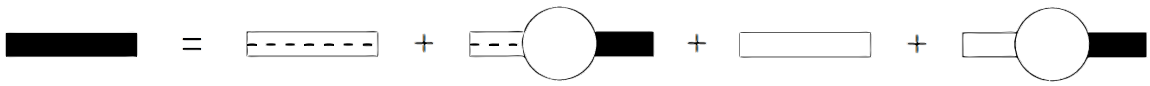

Figure 3.1: Full two-dibaryon propagator (solid box) resulting from the non-perturbative dressing of bare dibaryon-1 (dashed box) and dibaryon-2 (plain box) propagators with nucleon bubbles (circles).

Such an extension naturally allows us to reproduce the amplitude zero already at LO, greatly improving the description of the empirical phase shifts.

To illustrate the statement above, we neglect for now the interactions represented by "..." in Eq. (3.3). At momentum $k = \sqrt{M_N E}$, where E is the center-of-mass energy, the on-shell T matrix is written in terms of the S matrix and the phase shift δ as

$$T(k) = \frac{2\pi i}{M_N k}\left[S(k) - 1\right] = \frac{4\pi}{M_N}\left[-k\cot\delta(k) + ik\right]^{-1} \tag{3.4}$$

(recall Eq. (1.88)). As usual, we will regularize loop integrals through a momentum cutoff Λ in the range $\Lambda \gtrsim M_{\rm hi} \gg k$ and a regulator function $f_{\rm R}(q^2/\Lambda^2)$, with q the magnitude of the off-shell nucleon momentum, that satisfies

$$f_{\rm R}(0) = 1, \quad f_{\rm R}(\infty) = 0. \tag{3.5}$$

Much like what was done in Section 1.3.3.1 for the single-dibaryon case, here we dress up the bare two-dibaryon propagator

$$\mathcal{B}_{2\phi}(k;\Lambda) = \sum_j \left[\Delta_j(\Lambda) + c_j(\Lambda)\, k^2/M_N\right]^{-1} \equiv \frac{M_N}{4\pi} V(k;\Lambda) \tag{3.6}$$

with nucleon loops (see Figure 3.1), giving

$$\mathcal{D}_{2\phi}(k;\Lambda) = \left[1/\mathcal{B}_{2\phi}(k;\Lambda) + \mathcal{I}_0(k;\Lambda)\right]^{-1} \equiv \frac{M_N}{4\pi} T(k;\Lambda). \tag{3.7}$$

The loop integral $\mathcal{I}_0(k;\Lambda)$ was introduced already in Section 1.3.2, but we repeat it here for convenience,

$$\mathcal{I}_0(k;\Lambda) = 4\pi \int \frac{{\rm d}^3 q}{(2\pi)^3} \frac{f_{\rm R}(q^2/\Lambda^2)}{q^2 - k^2 - i\epsilon} = ik + \theta_1\Lambda + \frac{k^2}{\Lambda}\sum_{n=0}^{\infty} \theta_{-1-2n}\left(\frac{k}{\Lambda}\right)^{2n}, \tag{3.8}$$

where the dimensionless coefficients θ_n depend on the specific regularization employed. We thus arrive at

$$\left[\frac{M_N}{4\pi} T(k;\Lambda)\right]^{-1} = \frac{\left[\Delta_1(\Lambda) + c_1(\Lambda)\, k^2/M_N\right]\left[\Delta_2(\Lambda) + c_2(\Lambda)\, k^2/M_N\right]}{\Delta_1(\Lambda) + \Delta_2(\Lambda) + \left[c_1(\Lambda) + c_2(\Lambda)\right] k^2/M_N} + ik + \theta_1\Lambda + \theta_{-1}\frac{k^2}{\Lambda} + \mathcal{O}\left(\frac{k^4}{\Lambda^3}\right). \tag{3.9}$$

When the momentum k is much smaller than any other scale and the cutoff Λ is large, Eq. (3.9) reduces to the ERE (see Eqs. (1.88) and (1.89)),

$$\left[\frac{M_N}{4\pi}T(k)\right]^{-1} = \frac{1}{a} + ik - \frac{r_0}{2}k^2 - \frac{P_0}{4}k^4 + \dots \tag{3.10}$$

For low-energy np scattering, the scattering length is $a \simeq -23.7\,\text{fm} \simeq -(8\,\text{MeV})^{-1}$ [71], the effective range is $r_0 \simeq 2.7\,\text{fm} \simeq (73\,\text{MeV})^{-1}$ [72], the shape parameter is $P_0 \simeq 2.0\,\text{fm}^3 \simeq (158\,\text{MeV})^{-3}$ [80], and so on. In addition, Eq. (3.9) allows for a pole at a momentum $k_0 \simeq 340\,\text{MeV}$ [148], around which the amplitude can be expanded as [69]

$$\frac{M_N}{4\pi}\,T(k) = \frac{k^2-k_0^2}{k_0^3}\left[z_1 + z_2\frac{k^2-k_0^2}{k_0^2} + \mathcal{O}\left(\frac{(k-k_0)^2}{k_0^2}\right)\right] \tag{3.11}$$

in terms of dimensionless parameters z_n, with $|z_n| = \mathcal{O}(1)$ in the absence of further fine tuning. Such result implies that $\delta(k)$ behaves linearly around $k = k_0$,

$$\delta(k \sim k_0) = -\frac{2z_1}{k_0}(k-k_0) + \dots \tag{3.12}$$

From the *Nijm93* phase shifts [148] we find $z_1 \simeq 0.6$.

The unnaturally large value of $|a|$ has long been attributed to some fine-tuning mechanism that results into an extremely shallow virtual bound state, whose very small binding momentum poses the emergence of a new scale $\aleph \sim 10\,\text{MeV}$. In $\not\pi$EFT, one standardly assumes that the size of the higher-order ERE parameters is determined by a harder scale $\tilde{M}_{\rm hi}$, *i.e.* $1/r_0 \sim 1/P_0^{1/3} \sim \dots \sim \tilde{M}_{\rm hi}$. Then, in the $Q \sim \aleph$ momentum range, the scattering amplitude is amenable to an expansion in powers of $Q/\tilde{M}_{\rm hi}$, so that $\tilde{M}_{\rm hi}$ is the breakdown scale of the theory. Naively one expects $\tilde{M}_{\rm hi} \lesssim m_\pi$, but there is some evidence that $\not\pi$EFT works also at larger momenta. For example, the ground-state binding momenta of systems with $A = 3, 4, 6, 16$ nucleons are $\sim 100\,\text{MeV}$, and yet their physics is well described by the lowest orders of $\not\pi$EFT (see, for example, Refs. [87, 90, 149, 150]). In fact, it has been suggested that the characteristic scale of $\not\pi$EFT is set by these binding momenta through the LO three-nucleon force, so that $\aleph$ appears only at NLO or higher [92, 144].

Here we exploit the hypothesis of an enlarged range of validity of $\not\pi$EFT in the ${}^1S_0$ channel to illustrate the idea of a low-energy zero, which can be done through the replacement $\tilde{M}_{\rm hi} \to M_{\rm lo}$. Simultaneously, the smallness of $1/a$ is accounted for with the replacement $\aleph \to M_{\rm lo}^2/M_{\rm hi}$. The phenomenological parameters of the theory will then scale as

$$1/a = \mathcal{O}\left(M_{\rm lo}^2/M_{\rm hi}\right), \quad k_0 \sim 1/r_0 \sim 1/P_0^{1/3} \sim \dots = \mathcal{O}(M_{\rm lo}), \tag{3.13}$$

with $M_{\rm hi} \gg M_{\rm lo}$. In the $Q \sim M_{\rm lo}$ momentum range, the assumption (3.13) will allow us to expand the amplitude in powers of $Q/M_{\rm hi}$. Even though the usefulness of such an expansion is far from obvious, we will see below that it seems to give good results when compared to empirical low-energy data. Our prescription includes the correct position of the amplitude zero at LO, and moves the virtual state very close to its empirical position at NLO. For $Q \sim \aleph$ the NLO amplitude is similar to that of standard $\not\pi$EFT with $\tilde{M}_{\rm hi} \sim M_{\rm lo}$. The assignment $\aleph \to M_{\rm lo}^2/M_{\rm hi}$ is somewhat arbitrary but motivated by the expectations $M_{\rm lo} \sim 100\,\mathrm{MeV}$ and $M_{\rm hi} \sim 500\,\mathrm{MeV}$ [1].

Quantities in the theory can be organized in powers of the small expansion parameter $M_{\rm lo}/M_{\rm hi}$. For a generic coupling constant g, we expand formally

$$g(\Lambda) = g^{[0]}(\Lambda) + g^{[1]}(\Lambda) + \ldots, \tag{3.14}$$

where the superscript $^{[\nu]}$ indicates that the coupling appears at N$^\nu$LO. The "renormalized" coupling $\bar{g}^{[\nu]}$ —the regulator-independent contribution to the bare (running) coupling $g^{[\nu]}(\Lambda)$— is nominally suppressed by $\mathcal{O}(M_{\rm lo}^\nu/M_{\rm hi}^\nu)$ with respect to $\bar{g}^{[0]}$.

Likewise, the amplitude is written

$$T(k;\Lambda) = T^{[0]}(k;\Lambda) + T^{[1]}(k;\Lambda) + \ldots, \tag{3.15}$$

where

$$T^{[0]}(k;\Lambda) = V^{[0]}(k;\Lambda)\left[1 + \frac{M_N}{4\pi}V^{[0]}(k;\Lambda)\left(ik + \theta_1\Lambda + \frac{k^2}{\Lambda}\sum_{n=0}^{\infty}\theta_{-1-2n}\frac{k^{2n}}{\Lambda^{2n}}\right)\right]^{-1}, \tag{3.16}$$

$$T^{[1]}(k;\Lambda) = \left(\frac{T^{[0]}(k;\Lambda)}{V^{[0]}(k;\Lambda)}\right)^2 V^{[1]}(k;\Lambda), \tag{3.17}$$

etc., in terms of

$$V^{[0]}(k;\Lambda) = \frac{4\pi}{M_N}\sum_j\left(\Delta_j^{[0]}(\Lambda) + c_j^{[0]}(\Lambda)\frac{k^2}{M_N}\right)^{-1}, \tag{3.18}$$

$$V^{[1]}(k;\Lambda) = -\frac{4\pi}{M_N}\sum_j\left(\Delta_j^{[0]}(\Lambda) + c_j^{[0]}(\Lambda)\frac{k^2}{M_N}\right)^{-2}\left(\Delta_j^{[1]}(\Lambda) + c_j^{[1]}(\Lambda)\frac{k^2}{M_N}\right), \tag{3.19}$$

[1] If $\aleph$ were taken to be smaller, say $\aleph \sim M_{\rm lo}^3/M_{\rm hi}^2$, a reasonable description of observables at momenta $Q \sim \aleph$ would only emerge at N^{2}LO. Conversely, had one taken $\aleph \sim M_{\rm lo}$, the very-low-energy region would be well reproduced already at LO, but it would be more difficult to see improvements at NLO.

etc. Neglecting higher-order terms, the phase shifts at LO, LO+NLO and so on can be written as

$$\delta^{[0]}(k;\Lambda) = -\cot^{-1}\left[\frac{4\pi}{M_N k}\,\mathrm{Re}\left(\frac{1}{T^{[0]}(k;\Lambda)}\right)\right], \tag{3.20}$$

$$\delta^{[0+1]}(k;\Lambda) = -\cot^{-1}\left[\frac{4\pi}{M_N k}\,\mathrm{Re}\left(\frac{1}{T^{[0]}(k;\Lambda)} - \frac{T^{[1]}(k;\Lambda)}{T^{[0]2}(k;\Lambda)}\right)\right], \tag{3.21}$$

etc. At higher orders interactions in the "..." of Eq. (3.3) appear. We now consider the first two orders of the expansion in detail.

3.2.1 Leading order

From Eq. (3.9) we see that reproducing the amplitude zero at LO with a shallow pole requires a minimum of three bare parameters. Both residual masses, $\Delta_1(\Lambda)$ and $\Delta_2(\Lambda)$, must be non-vanishing, otherwise the resulting inverse amplitude at threshold would be proportional to Λ, *i.e.* not properly renormalized. At the same time, at least one of the dibaryon kinetic terms, which we choose to be $c_2(\Lambda)$, needs to appear at LO, otherwise the amplitude zero could not be reproduced.

Since the smallness of the inverse scattering length is attributed to a suppression by one power of the breakdown scale $M_{\rm hi}$ (see (3.13)), we take

$$\frac{1}{a^{[0]}} = 0. \tag{3.22}$$

In other words, we perform an expansion of the $NN\ {}^1S_0$ amplitude around the unitarity limit, as in Refs. [92, 144]. One of the dibaryon parameters, which turns out to be $\Delta_2(\Lambda)$, carries such an effect, so that its observable contribution vanishes at LO. The regulator-independent parts of the remaining LO parameters, Δ_1 and c_2, are assumed to be governed by the scale $M_{\rm lo}$. In a nutshell,

$$\bar{\Delta}_1^{[0]} = \mathcal{O}\left(M_{\rm lo}\right), \quad \frac{\bar{c}_1^{[0]}}{M_N} = 0, \quad \bar{\Delta}_2^{[0]} = 0, \quad \frac{\bar{c}_2^{[0]}}{M_N} = \mathcal{O}\left(\frac{1}{M_{\rm lo}}\right). \tag{3.23}$$

Because the vanishing of $c_1^{[0]}$ was imposed, eliminating dibaryon-1 via Eq. (3.2) generates a momentum-independent contact interaction. Thus, at LO we obtain the $\Lambda_{NN} \to \infty$ version of the model considered in Ref. [76], where a dibaryon (our dibaryon-2) is added to a series of nucleon contact interactions.

In order to relate $\Delta_1^{[0]}(\Lambda)$, $\Delta_2^{[0]}(\Lambda)$, and $c_2^{[0]}(\Lambda)$ —our three non-vanishing LO bare parameters— to observables, we impose on

$$F(z;\Lambda) \equiv \mathrm{Re}\left\{\left[\frac{M_N}{4\pi}\,T^{[0]}(\sqrt{z};\Lambda)\right]^{-1}\right\} \tag{3.24}$$

three renormalization conditions,

$$F(0;\Lambda) = 0, \qquad \left.\frac{\partial F(z;\Lambda)}{\partial z}\right|_{z=0} = -\tfrac{1}{2}r_0, \qquad F^{-1}(k_0^2;\Lambda) = 0. \tag{3.25}$$

The dependence of loops on positive powers of Λ is canceled by that of the bare couplings, leaving behind only the renormalized couplings and some residual cutoff dependence, which can be made arbitraly small by increasing the cutoff,

$$\Delta_1^{[0]}(\Lambda) = \bar{\Delta}_1^{[0]} - \theta_1\Lambda + \ldots, \tag{3.26}$$

$$\Delta_2^{[0]}(\Lambda) = \frac{2\theta_1}{r_0^3 k_0^2}\left[\theta_1\left(r_0\Lambda\right)^2 - \left(\tfrac{1}{2}r_0^2k_0^2 + 2\theta_1\theta_{-1}\right)r_0\Lambda + 4\theta_1\theta_{-1}^2 + \ldots\right], \tag{3.27}$$

$$\frac{c_2^{[0]}(\Lambda)}{M_N} = \frac{\bar{c}_2^{[0]}}{M_N} - \frac{2\theta_1}{r_0^3 k_0^4}\left[\theta_1\left(r_0\Lambda\right)^2 - \left(r_0^2k_0^2 + 2\theta_1\theta_{-1}\right)r_0\Lambda + 4\theta_1\theta_{-1}^2 + \ldots\right], \tag{3.28}$$

where "..." stands for terms that become arbitrarily small for an arbitrarily large cutoff. Equation (3.23) ensures that the non-vanishing renormalized couplings,

$$\bar{\Delta}_1^{[0]} = \tfrac{1}{2}r_0k_0^2, \qquad \frac{\bar{c}_2^{[0]}}{M_N} = -\tfrac{1}{2}r_0, \tag{3.29}$$

are indeed consistent with Eq. (3.13). Equations (3.26)–(3.29) yield

$$\left[\frac{M_N}{4\pi}\,T^{[0]}(k;\Lambda)\right]^{-1} = ik - \frac{r_0}{2}\frac{k^2}{1-k^2/k_0^2}\left(1 + \frac{2\theta_{-1}}{r_0\Lambda}\,\frac{k^2}{k_0^2}\right) + \mathcal{O}\left(\frac{k^4}{\Lambda^3}\right), \tag{3.30}$$

which is indeed cutoff independent up to terms that decrease as Λ increases. Although the scales and the zero location are different, Eq. (3.30) is the same that applies [143] to near-threshold nd scattering [2].

[2]Taking $A \equiv r_0k_0^2/2 \equiv -R$, Eq. (3.30) may be rewritten as

$$\left[\frac{M_N}{4\pi}\,T^{[0]}(k;\Lambda)\right]^{-1} = A + \frac{R}{1-k^2/k_0^2} + ik + \mathcal{O}\left(\frac{k^2}{\Lambda}\right),$$

which is a form used in early work on nd scattering, such as Ref. [151].

Many interesting consequences can be extracted from Eq. (3.30). For momenta below the amplitude zero, our expression reduces to the unitarity-limit version of the ERE (3.10) but with predictions for the higher ERE parameters, starting with the shape parameter

$$P_0^{[0]}(\Lambda) = \frac{2r_0}{k_0^2}\left[1 + \frac{2\theta_{-1}}{r_0\Lambda} + \mathcal{O}\left(\frac{k_0^2}{r_0\Lambda^3}\right)\right]. \tag{3.31}$$

Using the cutoff dependence to estimate the error under the assumption $M_{\rm hi} \sim 500$ MeV, the LO prediction is $P_0^{[0]}k_0^2/(2r_0) = 1.0 \pm 0.3$. These high ERE parameters are difficult to extract from data. A careful analysis in Ref. [80] obtains $P_0k_0^2/(2r_0) = 1.1$, which is well within our expected truncation error. Yet, values obtained for P_0 from the phenomenological *np* potentials *NijmII* and *Reid93* [148] are of the same order of magnitude as the value from Ref. [80], but with a *negative* sign [81].

We conjecture that, contrary to what happens in standard $\not\pi$EFT, Eq. (3.30) also applies at momenta around the amplitude zero, with terms $\mathcal{O}(M_{\rm lo})$ and corrections $\mathcal{O}(M_{\rm lo}^2/M_{\rm hi})$. Around the amplitude zero, the amplitude is perturbative [69, 124]. Indeed, a simple Taylor expansion of Eq. (3.30) gives a perturbative expansion in the region $|k - k_0| \lesssim k_0$, *i.e.* an equation of the form (3.11) with LO predictions for the coefficients,

$$z_1^{[0]}(\Lambda) = \frac{2}{r_0k_0}\left(1 - \frac{2\theta_{-1}}{r_0\Lambda} + \ldots\right), \tag{3.32}$$

$$z_2^{[0]}(\Lambda) = -\frac{2}{r_0k_0}\left[1 + \frac{2i}{r_0k_0}\left(1 - \frac{4\theta_{-1}}{r_0\Lambda}\right) + \ldots\right], \tag{3.33}$$

etc., where the "..." account for $\mathcal{O}(M_{\rm lo}^2/\Lambda^2)$. Numerically, these coefficients are $z_1^{[0]} = 0.4 \pm 0.1$ and $z_2^{[0]} = -(0.4 \pm 0.1) - i(0.2 \pm 0.1)$, which are indeed of natural size. The former is in fact reasonably close to $z_1 \simeq 0.6$ extracted from the phenomenological data. Note that we could have imposed as a renormalization condition that z_1 had a fixed value (the phenomenological one) at any Λ, thus trading the information about energy dependence carried by r_0 for that contained in the derivative of the phase shift at its zero, see Eq. (3.12).

Equation (3.30) interpolates between the two regions, $k \ll k_0$ where the amplitude is non-perturbative and $|k - k_0| \ll k_0$ where it is perturbative. Compared to standard $\not\pi$EFT, it resums not only range corrections as in Ref. [142], but also corrections that give rise to the pole at $k = k_0$. Compared to the expansion around the amplitude zero [69], it resums the terms that become large at low energies and give rise to a resonant state at zero energy. The pole structure of the LO amplitude can be made explicit by rewriting Eq. (3.30) as

$$\left[\frac{M_N}{4\pi}\,T^{[0]}(k;\Lambda)\right]^{-1} = \frac{(k - i\kappa_1^{[0]})(k - i\kappa_2^{[0]})(k - i\kappa_3^{[0]})}{i(k_0^2 - k^2)} + \mathcal{O}\left(\frac{k^2}{\Lambda}\right), \tag{3.34}$$

with

$$\kappa_1^{[0]} = 0, \quad \kappa_2^{[0]} = \frac{r_0 k_0^2}{4}\left(1 - \sqrt{1 - (4/(r_0 k_0))^2}\right), \quad \kappa_3^{[0]} = \frac{r_0 k_0^2}{4}\left(1 + \sqrt{1 - (4/(r_0 k_0))^2}\right). \quad (3.35)$$

In addition to the amplitude zero, $T^{[0]}(k_0;\Lambda) = 0$, it is apparent that there are three simple poles, $T^{[0]}(i\kappa_j^{[0]};\infty) \to \infty$. Similarly to the analysis we presented in Section 1.3, their nature depends on the sign of $i\,\mathrm{Res}\, S^{[0]}(i\kappa_j^{[0]})$:

- The pole at $k = 0$ represents a resonant state at threshold, as it induces the vanishing of $\cot\delta(0)$. Given that $i\,\mathrm{Res}\, S^{[0]}(i\kappa_1^{[0]}) = 0$, this state has a non-normalizable wavefunction. Notice that such a state can be reproduced even with a non-derivative contact potential —to check this, simply take the unitarity limit in Section 1.3.2.

- The pole at $k = i\kappa_2^{[0]}$, $\kappa_2^{[0]} \simeq 190$ MeV, lies on the positive imaginary semiaxis. However, since $i\,\mathrm{Res}\, S^{[0]}(i\kappa_2^{[0]}) < 0$, the condition to produce a normalizable wavefunction is not satisfied in this case either. Hence, this is a redundant pole —just like the pole at $k = i\kappa_+$ considered in Section 1.3.3.1.

- The pole at $k = i\kappa_3^{[0]}$, $\kappa_3^{[0]} \simeq 600$ MeV, lies deep on the positive imaginary semiaxis. It represents a bound state because $i\,\mathrm{Res}\, S^{[0]}(i\kappa_3^{[0]}) > 0$. Since no such state exists experimentally, it would set an upper bound on the regime of validity of the EFT, $M_{\rm hi} \lesssim \kappa_3^{[0]}$.

Figure 3.2 displays the phase shifts (3.20) resulting from the LO amplitude (3.30) in comparison with the *Nijm93* results [148]. As inputs, we use the empirical values of the effective range and the position of the amplitude zero. We display the cutoff band for a generic regulator by taking $\theta_{-1} = \pm 1$ and varying Λ from around the breakdown scale (500 MeV) to infinity —as the cutoff increases, our results converge, as evident in Eq. (3.30). This cutoff band provides an estimate of the LO error, except at low momentum where there is an error that scales with $1/|a|$ instead of k. The LO phase shifts are in good agreement with empirical values for most of the low-energy momentum range, except at very low momenta where the small but non-vanishing virtual-state binding energy is noticeable. Even though a plot of $k\cot\delta$ would confirm that differences at the amplitude level are indeed small, here we plot the phase shifts to better display the region around the amplitude zero, which our PC is designed to capture. There, while the phase shifts themselves are not too far off empirical values, the curvature is not well reproduced. Nevertheless, the agreement is surprisingly

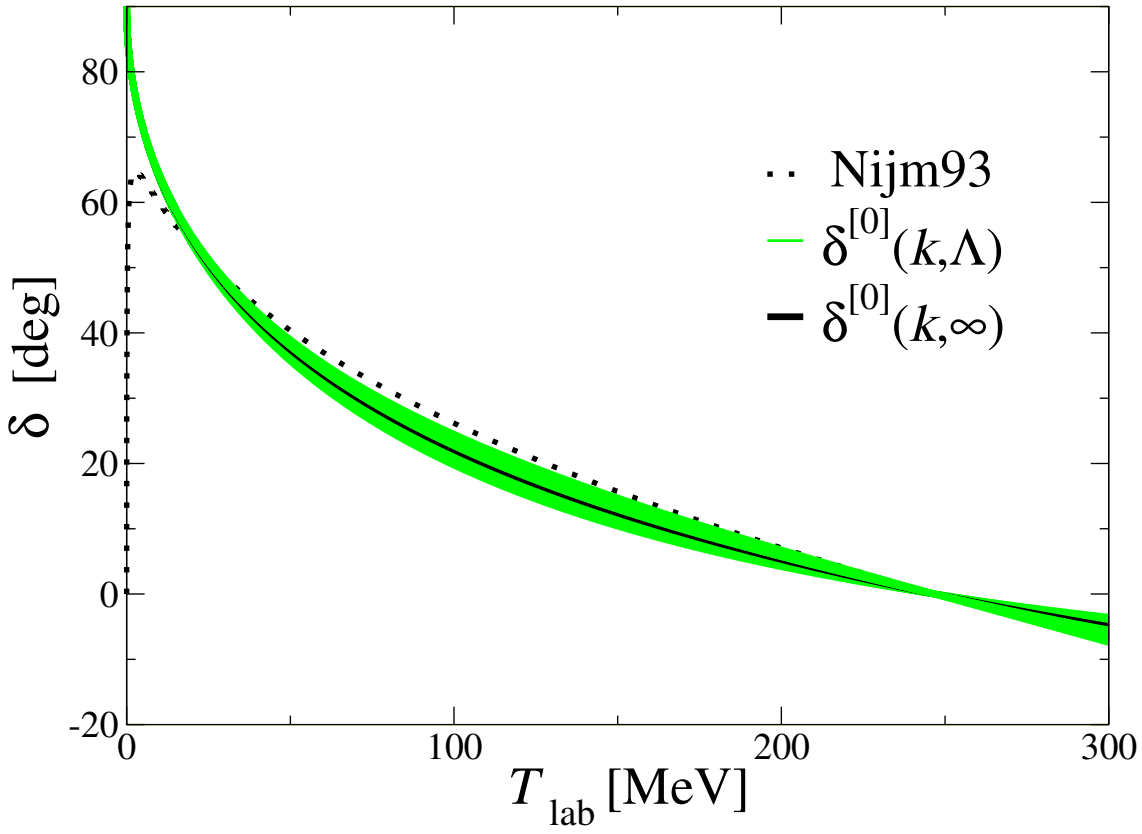

Figure 3.2: np $^1S_0$ phase shift δ (in degrees) versus laboratory energy $T_{\rm lab} = 2k^2/M_N$ (in MeV) for $\not\pi$EFT at LO in our new PC. The (black) solid line shows the analytical result (3.30) with $\Lambda \to \infty$, while the (green) band around it represents the evolution of the cutoff from 500 MeV to infinity, with $\theta_{-1} = \pm 1$. The (black) squares are the *Nijm93* results [148].

good given the absence of explicit pion fields. In the next section we examine how robust this agreement is.

3.2.2 Next-to-leading order

As pointed out in Ref. [61], the leading residual cutoff dependence of an amplitude, together with the assumption of naturalness, provides an upper bound on the order of the next correction to that amplitude. In standard $\not\pi$EFT, for example, the LO amplitude has an effective range $r_0 \sim 1/\Lambda$, indicating that there is an interaction at order no higher than NLO which will produce a physical effective range $r_0 \sim 1/\tilde{M}_{\rm hi}$ (see Section 1.3.3.2 and Refs.

[34, 35, 68, 69]). The leading residual cutoff dependence in Eq. (3.30) is proportional to k^4 and of relative order $\mathcal{O}(M_{\rm lo}/\Lambda)$. Thus, the NLO interaction must give rise to a contribution

$$P_0^{[1]}(\Lambda) \equiv P_0 - P_0^{[0]}(\Lambda) = \mathcal{O}\left(\frac{1}{M_{\rm lo}^2 M_{\rm hi}}\right) \tag{3.36}$$

to the LO shape parameter (3.31). This correction requires a higher-derivative operator. Although we could add a momentum-dependent contact operator, here we will make use instead of an energy-dependent —thus computationally simpler— strategy: we allow for a non-vanishing $c_1^{[1]}$.

In addition, given Eq. (3.13), some combination of parameters including $\Delta_2^{[1]}$ must enforce

$$\frac{1}{a^{[1]}} = \frac{1}{a} = \mathcal{O}\left(\frac{M_{\rm lo}^2}{M_{\rm hi}}\right). \tag{3.37}$$

We also introduce NLO corrections on top of the two parameters that were not zero at LO, Δ_1 and c_2, in order to keep r_0 and k_0 unchanged. Since NLO interactions must all be suppressed by $M_{\rm hi}^{-1}$, one requires

$$\bar{\Delta}_1^{[1]} = \mathcal{O}\left(\frac{M_{\rm lo}^2}{M_{\rm hi}}\right), \quad \frac{\bar{c}_1^{[1]}}{M_N} = \mathcal{O}\left(\frac{1}{M_{\rm hi}}\right), \quad \bar{\Delta}_2^{[1]} = \mathcal{O}\left(\frac{M_{\rm lo}^2}{M_{\rm hi}}\right), \quad \frac{\bar{c}_2^{[1]}}{M_N} = \mathcal{O}\left(\frac{1}{M_{\rm hi}}\right). \tag{3.38}$$

This scaling, together with what was learned at LO, is consistent with the imposition of four renormalization conditions on

$$G(z;\Lambda) \equiv -\mathrm{Re}\left\{\left[\frac{M_N}{4\pi}T^{[1]}(\sqrt{z};\Lambda)\right]\left[\frac{M_N}{4\pi}T^{[0]}(\sqrt{z};\Lambda)\right]^{-2}\right\}, \tag{3.39}$$

which ensure that a, r_0, P_0, and k_0 are fully Λ independent at NLO:

$$G(0;\Lambda) = \frac{1}{a}, \quad \left.\frac{\partial G(z;\Lambda)}{\partial z}\right|_{z=0} = 0, \quad \left.\frac{\partial^2 G(z;\Lambda)}{\partial z^2}\right|_{z=0} = -\frac{P_0^{[1]}(\Lambda)}{2}, \quad G(k_0^2;\Lambda) = 0. \tag{3.40}$$

Defining the renormalized parameters

$$\bar{\Delta}_1^{[1]} = \bar{\Delta}_2^{[1]} + \frac{3\bar{c}_1^{[1]}}{M_N}k_0^2, \qquad \frac{\bar{c}_1^{[1]}}{M_N} = -\frac{r_0}{2}\left(1 - \frac{P_0 k_0^2}{2r_0}\right), \tag{3.41}$$

$$\bar{\Delta}_2^{[1]} = \frac{1}{a} + r_0 k_0^2\left(1 - \frac{P_0 k_0^2}{2r_0}\right), \qquad \frac{\bar{c}_2^{[1]}}{M_N} = -4\left(\frac{\bar{c}_1^{[1]}}{M_N} + \frac{\bar{\Delta}_2^{[1]}}{2k_0^2}\right), \tag{3.42}$$

which with Eq. (3.38) give Eqs. (3.13) and (3.36), the cutoff dependence of the bare parameters that guarantees Eq. (3.40) is

$$\Delta_1^{[1]}(\Lambda) = \bar{\Delta}_1^{[1]} + \dots, \tag{3.43}$$

$$\frac{c_1^{[1]}(\Lambda)}{M_N} = \frac{\bar{c}_1^{[1]}}{M_N} + \dots, \tag{3.44}$$

$$\begin{aligned}\Delta_2^{[1]}(\Lambda) = {} & \bar{\Delta}_2^{[1]} - \frac{\theta_1}{r_0^4} P_0^{[1]}(\Lambda)\left[\theta_1 (r_0\Lambda)^2 + \left(r_0^2 k_0^2 - 4\theta_1\theta_{-1}\right) r_0\Lambda - 2\theta_{-1}\left(r_0^2 k_0^2 - 6\theta_1\theta_{-1}\right)\right] \\ & - \frac{4\theta_1}{a r_0^2 k_0^2}\left(r_0\Lambda - 2\theta_{-1}\right) + \dots,\end{aligned} \tag{3.45}$$

$$\frac{c_2^{[1]}(\Lambda)}{M_N} = \frac{\bar{c}_2^{[1]}}{M_N} + \frac{1}{k_0^2}\left(\bar{\Delta}_2^{[1]} - \Delta_2^{[1]}(\Lambda)\right) + \dots, \tag{3.46}$$

where the ellipsis account for terms that disappear when we take $\Lambda \to \infty$.

Using the expressions of the seven up-to-NLO counterterms in Eqs. (3.18) and (3.19), one finds in virtue of Eq. (3.17) that the NLO contribution to the amplitude verifies

$$\frac{T^{[1]}(k;\Lambda)}{T^{[0]2}(k;\Lambda)} = -\frac{M_N}{4\pi}\left[\frac{1}{a} + \frac{r_0}{2}\frac{k^4}{k_0^2 - k^2}\left(1 - \frac{P_0 k_0^2}{2r_0} + \frac{2\theta_{-1}}{r_0\Lambda}\right) + \mathcal{O}\left(\frac{k^4}{\Lambda^3}\right)\right], \tag{3.47}$$

which is indeed suppressed by one negative power of $M_{\rm hi}$. If we resum $T^{[1]}(k;\Lambda)$ while neglecting N^{2}LO terms, then

$$\left[\frac{M_N}{4\pi}\left(T^{[0]}(k;\Lambda) + T^{[1]}(k;\Lambda)\right)\right]^{-1} = \frac{1}{a} + ik - \frac{r_0}{2}k^2 - \frac{P_0}{4}\frac{k^4}{1 - k^2/k_0^2} + \mathcal{O}\left(\frac{k^6}{k_0^2\Lambda^3}\right), \tag{3.48}$$

and the ERE (3.10) is reproduced for $k < k_0$ with the experimental scattering length and shape parameter. Besides, predictions for the higher ERE parameters arise (these are hard to test given the difficulty of extracting them from phenomenological data, though), and the zero at k_0 remains unchanged due to our choice of renormalization condition. Once expanded around $k = k_0$ (see Eq. (3.11)), the distorted amplitude (3.48) yields the NLO coefficients

$$z_1^{[1]}(\Lambda) = z_1^{[0]}(\infty)\left(1 - \frac{P_0 k_0^2}{2r_0}\right) + \dots, \tag{3.49}$$

$$z_2^{[1]}(\Lambda) = z_2^{[0]}(\infty)\left(1 - i\frac{r_0 k_0}{2}\right)^{-1}\left[2\left(1 - \frac{P_0 k_0^2}{2r_0}\right) - \frac{i}{a k_0}\right] + \dots, \tag{3.50}$$

etc., where "…" stands for $\mathcal{O}(M_{\rm lo}^3/\Lambda^3)$. NLO contributions are of relative $\mathcal{O}(M_{\rm lo}/M_{\rm hi})$ with respect to their LO predictions $z_1^{[0]}$ and $z_2^{[0]}$, consistently with the residual cutoff dependence displayed in Eqs. (3.32) and (3.33). Since $z_1^{[0]}(\infty) \simeq 0.4$ underestimates by $\sim 50\%$ the slope

of the phenomenological phase shifts around the amplitude zero, a better description of data requires $z_1^{[1]}(\infty) > 0$ and thus, according to Eqs. (3.31) and (3.49), $P_0 < P_0^{[0]}(\infty)$. The value of P_0 given in Ref. [80] leads to a small change $|z_{1,2}^{[1]}(\infty)/z_{1,2}^{[0]}(\infty)| \lesssim 1/10$, but unfortunately it is $\sim 10\%$ *larger* than $P_0^{[0]}(\infty)$. Since Ref. [80] provides no error bars it is difficult to decide whether this is a real problem. We can reproduce the phenomenological z_1 by taking $P_0^{[1]}(\infty)/P_0^{[0]}(\infty) \simeq -0.6$, which is still compatible with convergence but not so small a change with respect to LO. Of course, not all the discrepancy between LO and phenomenology should be remedied by NLO, but this might indicate that something is missing. We will return to the shape parameter in the next section.

NLO also shifts the LO position of the poles (3.35) of the S matrix. One can obtain these shifts reliably by means of perturbative tools only for the two shallowest LO poles, finding in the large-cutoff limit

$$\kappa_1^{[1]} = \frac{1}{a}, \qquad \kappa_2^{[1]} = -\frac{k_0^2 + \kappa_2^{[0]2}}{k_0^2 - \kappa_2^{[0]2}} \left[\frac{1}{a} + \frac{1}{2} \frac{r_0 \kappa_2^{[0]4}}{k_0^2 + \kappa_2^{[0]2}} \left(1 - \frac{P_0 k_0^2}{2 r_0} \right) \right]. \tag{3.51}$$

We see that, as expected, $|\kappa_1^{[1]}| \sim |\kappa_2^{[1]}| = \mathcal{O}(M_{\rm lo}^2/M_{\rm hi})$, as long as $\kappa_2^{[0]} = \mathcal{O}(M_{\rm lo})$. As a consequence:

- The shallowest pole is moved from threshold to $k \simeq -8i$ MeV, and represents the well-known virtual state. Its new location almost coincides with the physical one.

- The redundant pole is moved from $k \simeq 190i$ MeV to $k \simeq 215i$ MeV, when the value of P_0 given in Ref. [80] is used. This represents a shift of relative size $\sim 15\%$ with respect to LO. Roughly two thirds of this shift are due to the finiteness of the scattering length, while the other third corresponds to the NLO correction to the shape parameter. Conversely, if we take the value of P_0 that reproduces the phenomenological z_1, then the shape correction overcomes the scattering length and the pole moves down to $k \simeq 155i$ MeV, still a modest shift.

The LO+NLO ${}^1S_0$ phase shift (3.21) can now be obtained from Eqs. (3.30) and (3.47), see Figure 3.3. Now, in addition to the empirical values of r_0 and k_0, also the values of the scattering length and the shape parameter from Ref. [80] are input, and the resulting phase shift has been called $\bar{\delta}$. We show a band around such result corresponding to a variation of $\pm 30\%$ around the P_0 value of Ref. [80] to account for its (unspecified) error. Since the cutoff

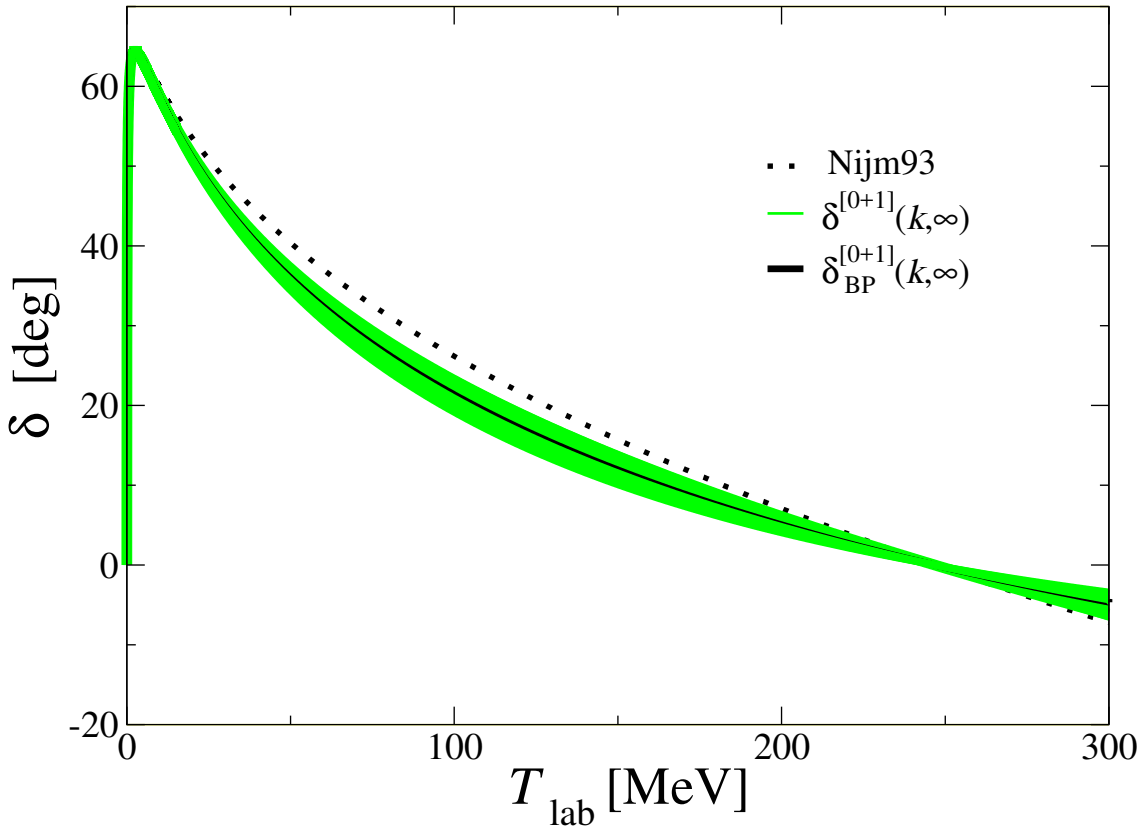

Figure 3.3: np $^1S_0$ phase shift δ (in degrees) versus laboratory energy $T_{\rm lab} = 2k^2/M_N$ (in MeV) for $\not\pi$EFT at NLO in our new PC. The (black) line shows the analytical result (3.47) with $\Lambda \to \infty$ and the value of the shape parameter from Ref. [80], while the (green) band around it represents a ±30% variation in this value. The (black) squares are the *Nijm93* results [148].

dependence of the up-to-NLO result (3.48) is very suppressed ($\sim 1/\Lambda^3$), it has been neglected in Figure 3.3. The band thus does not reflect the uncertainty of the NLO truncation, but of the input.

As expected, the physical value of a greatly improves the description of the phase shifts at very low energies ($T_{\rm lab} \lesssim 5\,$MeV, or $k \lesssim 50\,$MeV). However, already at moderate energies this improvement is much less clear. In particular, as anticipated above, only for a shape parameter ~ 30% smaller than in Ref. [80] does $\delta^{[0+1]}(k;\infty)$ get slightly closer to *Nijm93* than $\delta^{[0]}(k;\infty)$ (see Figure 3.2). Such a change is within the LO error and, overall, the reproduction of the phase shifts is very good at NLO. Agreement could be further improved, particularly around k_0, by taking an even smaller shape parameter (in particular, the one that

reproduces the phenomenological z_1); however, even in that case the curvature of the resulting phase shifts would remain different from empirical at middle energies, which suggests that our expansion is lacking terms at either LO or NLO.

3.2.3 Resummation and higher orders

The choice of identifying the fine-tuning scale $\aleph$ with $M_{\rm lo}^2/M_{\rm hi}$ implied a finite scattering length only at NLO. Alternative choices are possible, leading to slightly different amplitudes at various orders. When plotting phase shifts, these differences are amplified. For example, taking $\aleph \sim M_{\rm lo}$ would lead to the non-vanishing of $1/a$ already at LO. Then, the running and renormalized parameters given above would change by $1/a$ terms, and the amplitude (or equivalently its pole positions) would be shifted only slightly. However, in terms of phase shifts there would appear to be a large improvement around threshold.

Given our previous identification of $\aleph$ with $M_{\rm lo}^2/M_{\rm hi}$, the alternative procedure just described would amount to a resummation of higher-order corrections. Because the bare parameter $\Delta_2(\Lambda)$ exists already at LO to ensure proper renormalization, this resummation could be done without harm. However, because some NLO contributions would be shifted to LO, we would see less improvement when going from LO to NLO. Provided that one has a PC that converges, this would be just one of many ways in which we can make results at one order closer to phenomenology while remaining within the error of that order.

Regardless of such resummation, corrections at higher orders are expected to improve the situation further. The cutoff dependence of Eq. (3.48) suggests that there are no new interactions at next order, N^{2}LO, which would solely consist of one iteration of the NLO potential. However, the fact that our pionless phase shifts look too low in the middle range represents a significant, systematic lack of attraction between nucleons at $k \sim m_\pi$. This could be a reminder to include pions explicitly. Next, we consider our expansion with additional pion exchange.

3.3 Pionful theory

We now modify the theory developed in Section 3.2 to include pion exchange. This is done under the assumption that the pion mass, the characteristic inverse strength of OPE, and

the magnitude of the relevant momenta have similar sizes, not being enhanced or suppressed by powers of the hard scale,

$$m_\pi \sim \Lambda_{NN} \sim Q = \mathcal{O}\left(M_{\rm lo}\right). \tag{3.52}$$

Such an assumption has been standard in χEFT since its beginnings [36, 37]. In the NN sector, it underlies the (non-perturbative) LO character of the OPE interaction, as well as the suppression of multiple pion exchanges by powers of $(M_{\rm lo}/M_{\rm QCD})^2$. In this context, the fact that $\Lambda_{NN} \simeq 290\,\text{MeV}$ and the location of the ${}^1S_0$ amplitude zero $k_0 \simeq 340\,\text{MeV}$ are numerically close to each other suggests to consider the latter as a low-energy scale as well. Note that certain spin-triplet channels (in particular, ${}^3S_1$ and ${}^3P_0$) also have amplitude zeros at comparable momenta, but in those waves the tensor OPE suffices for a qualitatively correct description of the phase shifts already at LO in a PC consistent with RG invariance [47, 59, 60]. This is not the case of ${}^1S_0$ [61], where the conventional chiral potential is able to generate an amplitude zero only for soft momentum cutoffs $\Lambda \sim M_{\rm lo}$ [57].

The Coulomb proton-proton (pp) interaction —the dominant electromagnetic effect— scales as $\alpha M_N/M_{\rm lo} \sim \aleph/M_{\rm lo}$. As we took $\aleph = \mathcal{O}(M_{\rm lo}^2/M_{\rm hi})$, we should account for the Coulomb interaction at NLO. (Other isospin-breaking effects, such as the nucleon mass splitting, are to be accounted for perturbatively, too.) Within the $\not\pi$EFT framework, the subleading Coulomb effects were included in an expansion around the unitarity limit (regardless of the amplitude zero) in Ref. [144]. Since we anticipate no new features here, in this first approach we omit isospin breaking. Because the expansion is already quite complicated at a fixed value of m_π, we also ignore the explicit dependence on quark mass.

Pions are introduced in the usual way, by demanding that the most general effective Lagrangian transforms under chiral symmetry as does the QCD Lagrangian written in terms of quarks and gluons (see Section 1.2 and Refs. [9–11] for reviews and references). For the case of one single dibaryon field, this was done in Ref. [76], and the extension to the two-dibaryon scenario explored in Section 3.2 is straightforward. If $\vec{\pi}$ is the pion isotriplet, the effective Lagrangian reads

$$\begin{aligned}\mathcal{L}_\chi^{(2\phi)} = {} & \frac{1}{2}\left(\partial_\mu\vec{\pi}\cdot\partial^\mu\vec{\pi} - m_\pi^2\vec{\pi}^{\,2}\right) + N^\dagger\Big[i\partial_0 + \frac{\nabla^2}{2M_N} - \frac{g_A}{2f_\pi}\vec{\tau}\cdot(\boldsymbol{\sigma}\cdot\nabla\vec{\pi})\Big]N \\ & + \sum_{j=1,2}\left\{\vec{\phi}_j^{\,\dagger}\cdot\Big[\Delta_j + c_j\Big(i\partial_0 + \frac{\nabla^2}{4M_N}\Big)\Big]\vec{\phi}_j - \sqrt{\frac{4\pi}{M_N}}\left(\vec{\phi}_j^{\,\dagger}\cdot N^{\rm T}\vec{P}_{^1S_0}N + \text{H.c.}\right)\right\} + \ldots,\end{aligned} \tag{3.53}$$

in the same notation as Eq. (3.3). The omitted terms, which include chiral partners of the terms shown explicitly, are not needed up to NLO.

Inspired by the pionless theory, we take as the short-range potential of the pionful case the same dibaryon arrangement as in Section 3.2. After adding the long-range, spin-singlet projection of OPE, the LO potential is

$$\begin{aligned}\frac{M_N}{4\pi}V^{[0]}(\boldsymbol{p}',\boldsymbol{p},k;\Lambda) &= -\frac{1}{\Lambda_{NN}}\frac{m_\pi^2}{(\boldsymbol{p}'-\boldsymbol{p})^2+m_\pi^2}+\frac{1}{\Delta_1^{[0]}(\Lambda)}+\frac{1}{\Delta_2^{[0]}(\Lambda)+c_2^{[0]}(\Lambda)\,k^2/M_N}\\ &\equiv \frac{M_N}{4\pi}\left(V_{\rm L}^{[0]}(\boldsymbol{p}',\boldsymbol{p})+V_{\rm S}^{[0]}(k;\Lambda)\right),\end{aligned} \tag{3.54}$$

where $\boldsymbol{p}$ ($\boldsymbol{p}'$) is the relative momentum of the incoming (outgoing) nucleons, Λ_{NN} is the inverse OPE strength (see Eq. (1.69)), and the contact piece of OPE has been absorbed in the short-range potential $V_{\rm S}^{[0]}$ through

$$\left(1/\Delta_1^{[0]}(\Lambda)+1/\Lambda_{NN}\right)^{-1}\to\Delta_1^{[0]}(\Lambda). \tag{3.55}$$

The long-range part of OPE is the Yukawa potential represented by $V_{\rm L}^{[0]}$. Integrating out dibaryon-1 we obtain the potential of Ref. [76]. Since TPE enters only at N^{2}LO and higher [39, 41], at NLO the interaction is entirely short-ranged,

$$\frac{M_N}{4\pi}V^{[1]}(k;\Lambda)=-\frac{\Delta_1^{[1]}(\Lambda)+c_1^{[1]}(\Lambda)\,k^2/M_N}{\Delta_1^{[0]2}(\Lambda)}-\frac{\Delta_2^{[1]}(\Lambda)+c_2^{[1]}(\Lambda)\,k^2/M_N}{\left(\Delta_2^{[0]}(\Lambda)+c_2^{[0]}(\Lambda)\,k^2/M_N\right)^2}. \tag{3.56}$$

In the limit $\Delta_2^{[0]}\to\infty$ the potential is an energy-dependent version of the momentum-dependent LO+NLO interaction of Ref. [61], while the interaction of Ref. [137] emerges in the limit $\Delta_1^{[0]}\to\infty$.

Because OPE cannot be iterated analytically to all orders, we can no longer show analitically that the amplitude has a zero at LO or that the amplitude is RG invariant. However, these two features of the pionless theory are expected to be retained by the pionful theory on the basis that the strength of OPE is known to be numerically moderate in spin-singlet channels and that $V_{\rm L}^{[0]}$ is non-singular. Moreover, we continue to use the scalings (3.23) and (3.38). Below we confirm through numerical calculations that the EFT obeying such a PC indeed has an amplitude zero and preserves RG invariance.

3.3.1 Leading order

The off-shell LO amplitude is found from the LO potential (3.54) by solving the LS equation

$$T^{[0]}(\boldsymbol{p}',\boldsymbol{p},k;\Lambda)=V^{[0]}(\boldsymbol{p}',\boldsymbol{p},k;\Lambda)-M_N\int\frac{{\rm d}^3q}{(2\pi)^3}\frac{f_{\rm R}(q^2/\Lambda^2)}{q^2-k^2-i\epsilon}\,V^{[0]}(\boldsymbol{p}',\boldsymbol{q},k;\Lambda)\,T^{[0]}(\boldsymbol{q},\boldsymbol{p},k;\Lambda), \tag{3.57}$$

with $f_{\rm R}(x)$ a non-local regulator function (3.5). Defining the Yukawa amplitude,

$$T_{\rm L}^{[0]}(\boldsymbol{p}',\boldsymbol{p},k;\Lambda) = V_{\rm L}^{[0]}(\boldsymbol{p}',\boldsymbol{p}) - M_N \int \frac{{\rm d}^3q}{(2\pi)^3}\frac{f_{\rm R}(q^2/\Lambda^2)}{q^2-k^2-i\epsilon}\, V_{\rm L}^{[0]}(\boldsymbol{p}',\boldsymbol{q})\, T_{\rm L}^{[0]}(\boldsymbol{q},\boldsymbol{p},k;\Lambda), \quad (3.58)$$

the Yukawa-dressing of the incoming/outgoing NN states,

$$\chi_{\rm L}^{[0]}(\boldsymbol{p},k;\Lambda) = 1 - M_N \int \frac{{\rm d}^3q}{(2\pi)^3}\frac{f_{\rm R}(q^2/\Lambda^2)}{q^2-k^2-i\epsilon}\, T_{\rm L}^{[0]}(\boldsymbol{p},\boldsymbol{q},k;\Lambda), \quad (3.59)$$

and the resummation of NN bubbles with iterated OPE in the middle,

$$\mathcal{I}_{\rm L}^{[0]}(k;\Lambda) = 4\pi \int \frac{{\rm d}^3q}{(2\pi)^3}\frac{f_{\rm R}(q^2/\Lambda^2)}{q^2-k^2-i\epsilon}\, \chi_{\rm L}^{[0]}(\boldsymbol{q},k;\Lambda), \quad (3.60)$$

Eq. (3.57) can be rewritten as [46]

$$\left[\frac{M_N}{4\pi}\left(T^{[0]}(\boldsymbol{p}',\boldsymbol{p},k;\Lambda) - T_{\rm L}^{[0]}(\boldsymbol{p}',\boldsymbol{p},k;\Lambda)\right)\right]^{-1} = \frac{\left[M_N V_{\rm S}^{[0]}(k;\Lambda)/(4\pi)\right]^{-1} + \mathcal{I}_{\rm L}^{[0]}(k;\Lambda)}{\chi_{\rm L}^{[0]}(\boldsymbol{p}',k;\Lambda)\,\chi_{\rm L}^{[0]}(\boldsymbol{p},k;\Lambda)}. \quad (3.61)$$

This is the generalization of Eq. (3.7) for LO in the presence of pions. Because $V_{\rm L}^{[0]}$ is regular, the cutoff dependence of the integrals $T_{\rm L}^{[0]}$ and $\chi_{\rm L}^{[0]}$ is suppressed by powers of Λ. In contrast, just as the $\mathcal{I}_0$ in Eq. (3.7), $\mathcal{I}_{\rm L}^{[0]}$ has a linear cutoff dependence due to the singularity of $V_{\rm S}^{[0]}$. Additionally, it exhibits a logarithmic divergence $\sim (m_\pi^2/\Lambda_{NN})\ln\Lambda$ [46] stemming from the interference between $V_{\rm L}^{[0]}$ and $V_{\rm S}^{[0]}$. This cutoff dependence is at the root of one of the shortcomings of NDA in the NN system.

Compared to Refs. [46, 61, 137], our $V_{\rm S}^{[0]}$ has a different k dependence. As in Section 3.2, two dibaryon parameters are needed to describe the zero of the amplitude and its energy dependence near threshold, while the third parameter ensures the fine tuning that leads to a large scattering length. These three parameters are sufficient for renormalization, leaving behind only residual cutoff dependence. Our LO amplitude is analogous to that of Ref. [124], which results from the unitarization of an expansion around the amplitude zero.

Taking the sharp-cutoff function $f_{\rm R}(x) = \theta(1-x)$, we solve numerically the S-wave projection of Eq. (3.57), as done in, *e.g.*, Refs. [61, 133]. In order to determine the values of the three bare parameters at a given cutoff, three cutoff-independent conditions on the amplitude are needed. We choose them to be the same as in Section 3.2.1,

- unitarity limit, $1/a^{[0]} = 0$;
- physical effective range, $r_0 = 2.7\,{\rm fm}$;

- physical amplitude zero, $k_0 = 340.4\,\mathrm{MeV}$.

The values of $\Delta_1^{[0]}(\Lambda)$, $\Delta_2^{[0]}(\Lambda)$, and $c_2^{[0]}(\Lambda)$ in our numerical calculations must be very well tuned in order to reproduce the required values of $1/a^{[0]}$, r_0, and k_0 within a given accuracy. The need for such a tuning becomes more and more noticeable as Λ is increased [133]. But the resulting phase shift changes dramatically depending on whether $1/a^{[0]}$ is very small and negative (for a shallow virtual state) or very small and positive (for a shallow bound state). Thus, in order to facilitate the numerical solution of the LS equation, we kept the scattering length large and negative, $a^{[0]} = -600$ fm. The difference with the unitarity limit cannot be seen in the results presented below.

The LO pionful phase shift is obtained from the on-shell, S-wave-projected T matrix in the usual way (see Eq. (3.20)). The result, presented in Figure 3.4, shows little cutoff dependence, even though the cutoff parameter is varied from 600 MeV to 2 GeV. It is likely that a more realistic estimate of the systematic error coming from the EFT truncation is obtained through varying the input inverse scattering length between its physical value and zero. We will come back to such an estimate later, when we resum finite-a effects. In any case, comparing with Figure 3.2 we confirm that pions help us achieve a better description of phase shifts between threshold and the amplitude zero.

From the results in Figure 3.4 we can extract the LO shape parameter $P_0^{[0]}(\Lambda)$ using our low-energy results and the unitarity-limit version of the ERE (3.10) truncated at the level of the shape parameter. Results are shown in Figure 3.5. For Λ large enough, we find

$$P_0^{[0]}(\Lambda) \approx P_0^{[0]}(\infty)\,(1 + Q_{P_0}/\Lambda), \tag{3.62}$$

with $P_0^{[0]}(\infty) \approx -1.0\,\mathrm{fm}^3$ and $Q_{P_0} \approx 100\,\mathrm{MeV}$. Unlike the result for the shape parameter given in Ref. [80], $P_0^{[0]}(\infty)$ is *negative*, being reasonably close to $P_0 = -1.9\,\mathrm{fm}^3$, the value extracted in Ref. [81] from the *NijmII* fit [148]. The large change in the prediction for $P_0^{[0]}(\infty)$ compared to the corresponding pionless result (3.31) is confirmation of the importance of pions at LO.

3.3.2 Next-to-leading order

As in Section 3.2.2, we can infer the importance of subleading short-range contributions from the residual cutoff dependence of the LO amplitude. Figure 3.5 shows that the relative cutoff

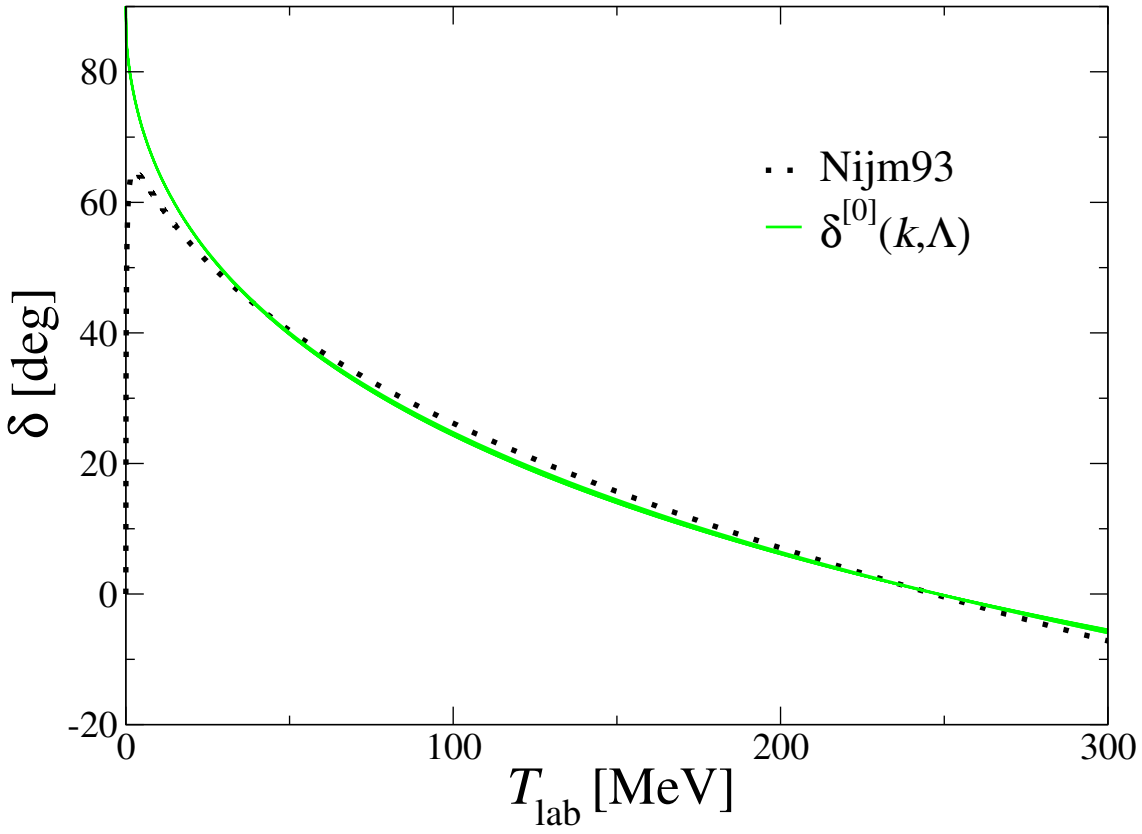

Figure 3.4: np $^1S_0$ phase shift δ (in degrees) versus laboratory energy $T_{\rm lab} = 2k^2/M_N$ (in MeV) for χEFT at LO in our new PC. The narrow (green) band represents the evolution of the sharp cutoff from 600 MeV to 2 GeV. The (black) squares are the *Nijm93* results [148].

dependence of $P_0^{[0]}(\Lambda)$ is $\mathcal{O}(M_{\rm lo}/\Lambda)$, implying that at least one extra short-range parameter needs to be included at NLO. This is represented by the NLO potential $V^{[1]}$ (3.56).

Treating $V^{[1]}$ in distorted-wave perturbation theory, we obtain a separable NLO amplitude,

$$T^{[1]}(\boldsymbol{p}',\boldsymbol{p},k;\Lambda) = \chi^{[0]}(\boldsymbol{p}',k;\Lambda)\, V^{[1]}(k;\Lambda)\, \chi^{[0]}(\boldsymbol{p},k;\Lambda), \tag{3.63}$$

where

$$\chi^{[0]}(\boldsymbol{p},k;\Lambda) = 1 - M_N \int \frac{\mathrm{d}^3q}{(2\pi)^3} \frac{f_{\rm R}(q^2/\Lambda^2)}{q^2-k^2-i\epsilon}\, T^{[0]}(\boldsymbol{p},\boldsymbol{q},k;\Lambda), \tag{3.64}$$

is defined in terms of the full LO amplitude in analogy with Eq. (3.59) for the long-range LO amplitude. As in the pionless case, we obtain the pionful LO+NLO phase shift from Eq. (3.21).

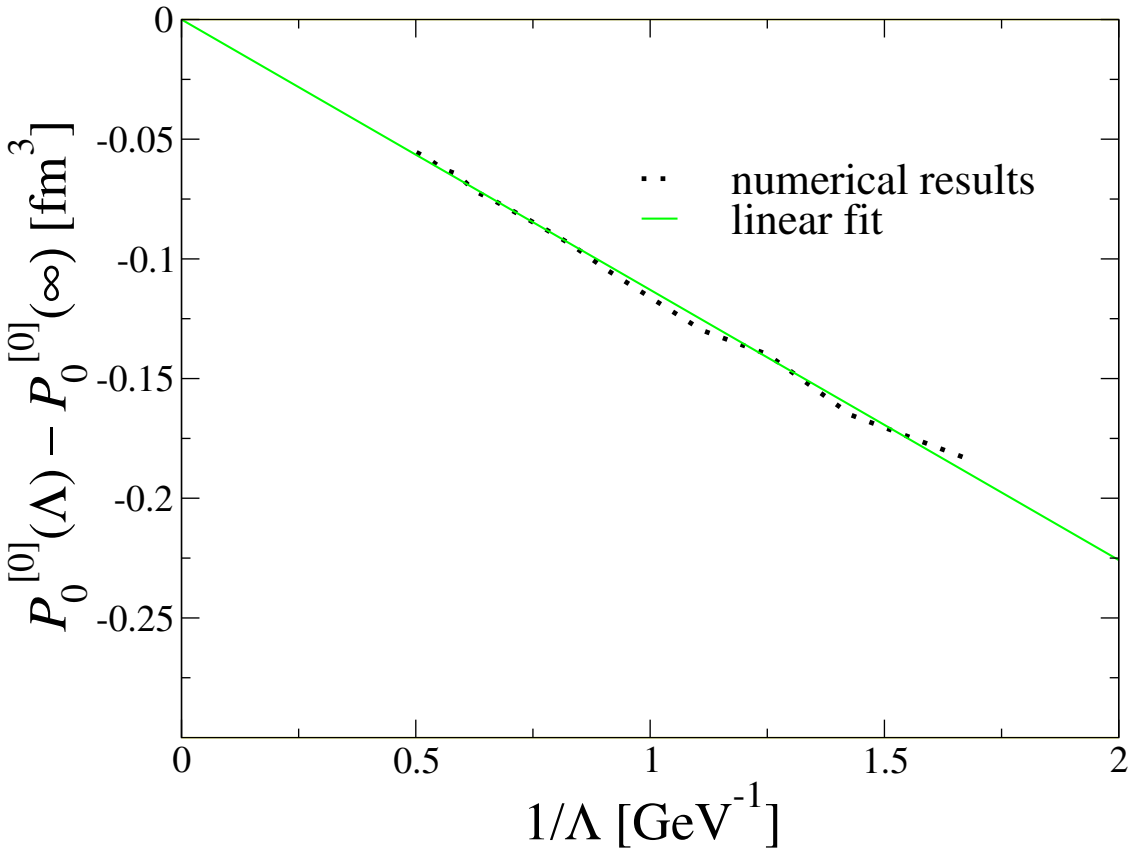

Figure 3.5: $np\,{}^1S_0$ shape parameter $P_0^{[0]}(\Lambda)$ (in fm^3) versus inverse cutoff $1/\Lambda$ (in GeV^{-1}) for χEFT at LO in our new PC. The (black) squares are the values obtained numerically in the way explained in the text; the (green) line represents the linear fit to those results.

The dibaryon parameters are fixed in virtue of four cutoff-independent conditions, which we choose to be the values of the *Nijm93* phase shifts [148] at four different momenta:

- $\delta^{[0+1]}(20.0\,\text{MeV};\Lambda) = 61.1°$;
- $\delta^{[0+1]}(40.5\,\text{MeV};\Lambda) = 64.5°$;
- $\delta^{[0+1]}(237.4\,\text{MeV};\Lambda) = 21.7°$;
- $\delta^{[0+1]}(340.4\,\text{MeV};\Lambda) = 0°$.

The LO+NLO phase shifts are shown in Figure 3.6. The narrow band when the cutoff is varied from 600 MeV to 2 GeV confirms that, as in Figure 3.4, very quick cutoff convergence

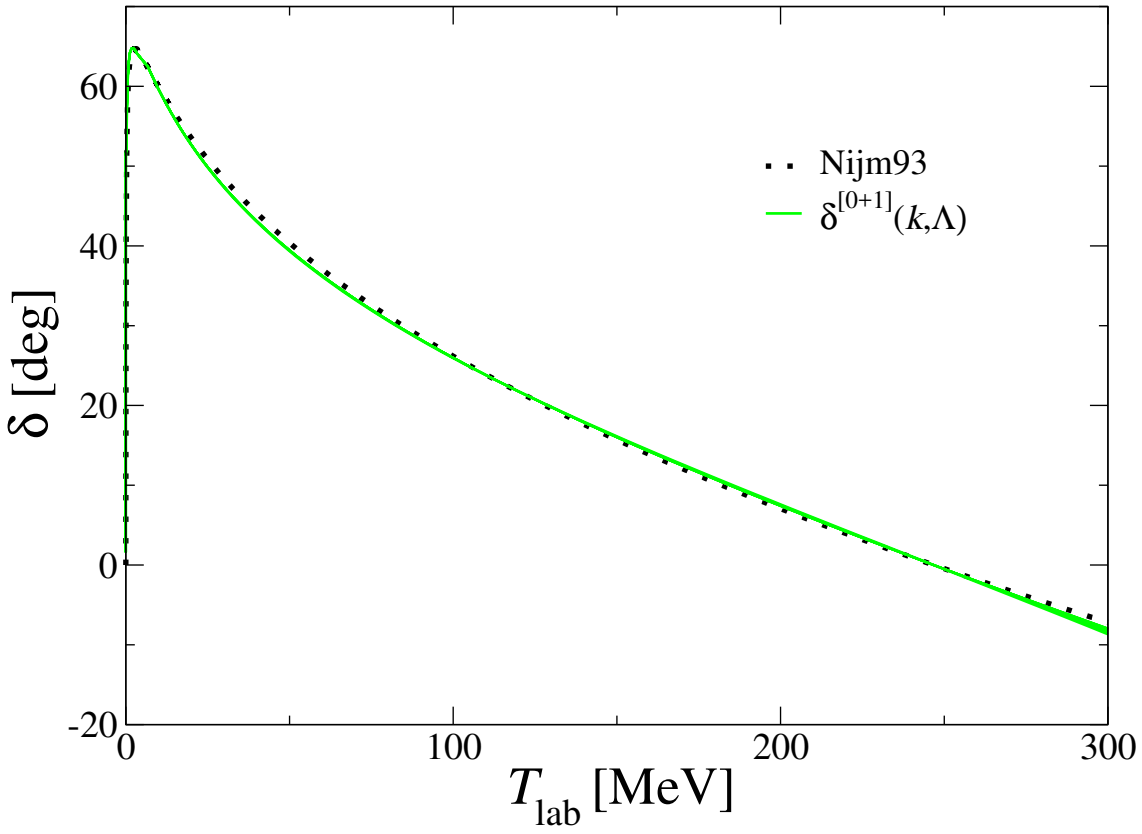

Figure 3.6: np $^1S_0$ phase shift δ (in degrees) versus laboratory energy $T_{\rm lab} = 2k^2/M_N$ (in MeV) for χEFT at NLO in our new PC. The narrow (green) band represents the evolution of the cutoff from 600 MeV to 2 GeV. The (black) squares are the *Nijm93* results [148].

takes place. The LO+NLO prediction almost lies on the *Nijm93* curve, which means that now the description of the empirical phase shifts throughout the whole elastic range $0 \lesssim k \lesssim \sqrt{M_N m_\pi}$ is much better than at LO. Indeed, the improvement is clear not only in the very-low-momentum regime (which had been expected considering that now we relaxed the unitarity-limit condition) but, more importantly from the χEFT point of view, also for momenta $k \sim m_\pi$. Comparison with the pionless result at NLO (Figure 3.3) confirms that adding OPE significantly improves predictions in this momentum range.

3.3.3 Resummation and higher orders

On the basis of the smallness of the virtual-state binding momentum when compared to the pion scales, so far we took it as an NLO parameter. We were guided by the PC presented in Section 3.2, whose consistency could be analytically demonstrated. Despite the systematic improvement and good description of data at NLO, one might be distressed by the unusual appearance of our LO phase shift (Figure 3.4) at low momentum. Within potential models, either purely phenomenological or grounded on Weinberg's prescription, it is customary to strive for a description of all regions below some arbitrary momentum on the same footing.

As emphasized in Section 3.2.3, plotting phase shifts is misleading when it comes to errors in the amplitude, which is the observable the PC is designed for; a plot of $k \cot \delta$ shows that only a small amount of physics is missed at LO even at low energies. Our strategy is a consequence of the fact that the PC assumes external momenta $Q \sim M_{\rm lo}$, and it is in principle only in this region that we expect systematic improvement order by order. The higher the momentum, the smaller the relative improvement with order, till $M_{\rm hi}$ is reached and the EFT stops working. In the other direction, that of smaller momenta, the PC may not capture the relative importance of interactions properly [3]. Therefore, the region of momenta much below the pion mass is *not* where the convergence of χEFT is to be judged.

Still, it might be of practical interest to improve the description near threshold already at LO. As in $\not\pi$EFT, we can account for non-vanishing $1/a$ already at LO without jeopardizing renormalization. Again, this is just a resummation of some higher-order contributions into LO, so that the difference with respect to what we have done earlier in this section has NLO size. As an example of this, in Figure 3.7 we show LO and LO+NLO results with an alternative fitting protocol. In the renormalization conditions at LO we replace the unitarity limit of our original fit with the physical scattering length, that is, we impose the following cutoff-independent conditions:

- $a = -23.7\,\text{fm}$;
- $r_0 = 2.7\,\text{fm}$;
- $k_0 = 340.4\,\text{MeV}$.

[3] A simple example of this is pion-nucleon scattering in χPT, where sufficiently close to threshold the LO P-wave interaction (stemming from the axial-vector coupling in Eq. (3.53)) becomes smaller than NLO corrections to the S wave.

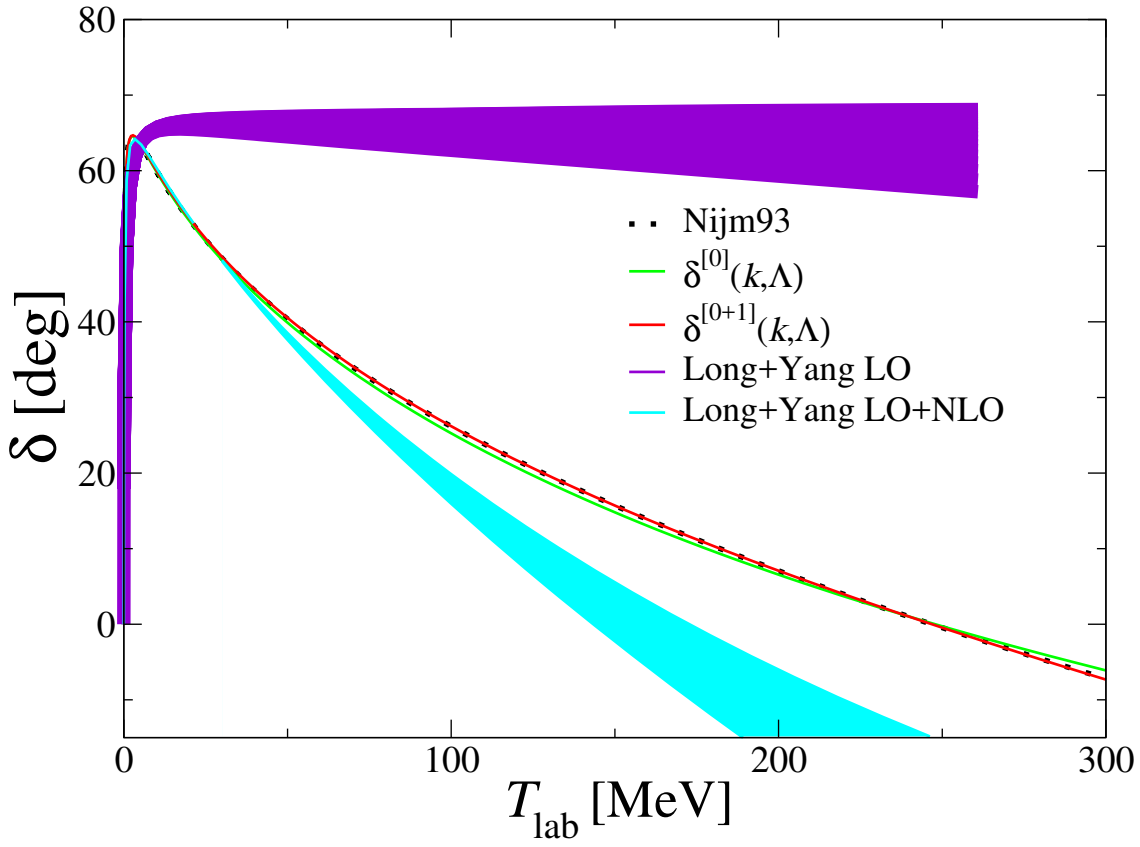

Figure 3.7: $np\ ^1S_0$ phase shift δ (in degrees) versus laboratory energy $T_{\rm lab} = 2k^2/M_N$ (in MeV) for χEFT at LO and NLO in our new PC from an alternative fitting protocol. The (green) light and (red) dark narrow bands represent, respectively, LO and LO+NLO under a cutoff variation from 600 MeV to 2 GeV. The LO and LO+NLO phase shifts from Ref. [61] have also been displayed; the upper (violet) LO band and the lower (cyan) LO+NLO band come from the same cutoff evolution as before. The (black) squares are the *Nijm93* results [148].

Likewise, at NLO we substitute the lowest *Nijm93* phase shift of our earlier fit with the physical scattering length:

- $a = -23.7\,\text{fm}$;
- $\delta^{[0+1]}(40.5\,\text{MeV}) = 64.5°$;
- $\delta^{[0+1]}(237.4\,\text{MeV}) = 21.7°$;
- $\delta^{[0+1]}(340.4\,\text{MeV}) = 0°$.

As before we vary Λ from 600 MeV to 2 GeV, but the convergence of the phase shifts is so quick that the cutoff bands cannot be resolved in our plot. The improved description of the very-low-energy region at LO compared to that seen in Figure 3.4, which is entirely due to the resummation of the finite scattering length, is evident. Besides, the alternative LO+NLO phase shifts virtually lie on the the *Nijm93* curve, so that this fit is even more phenomenologically successful than the original LO+NLO of Figure 3.6; still, the difference between both fits is modest, which attests to the fine-tuning of the ${}^1S_0$ channel, *i.e.* to the relatively low importance of $1/a$ effects. Finally, the smallness of the improvement shown by the alternative up-to-NLO curve over the alternative LO one is consequence of having resummed higher-order contributions into LO.

The ${}^1S_0$ phase shifts resulting from the PC proposed by Long and Yang for the singlet waves [61] have also been included, at both LO and NLO, in Figure 3.7. As mentioned before, the LO of such an arrangement —which, just like the LO of Weinberg's PC, consists of OPE supplemented by a short-range, momentum-independent term obtained through inputting the physical scattering length— manifestly fails in qualitatively reproducing the *Nijm93* phase shift already at laboratory energies $T_{\rm lab} \gtrsim 20\,{\rm MeV}$, *i.e.* center-of-mass momenta $k \gtrsim 100\,{\rm MeV}$; in particular, the LO phase shift does not cross zero at any finite energy (when $\Lambda \gtrsim M_{\rm hi}$ [57]). In contrast, it can be seen that, once the NLO interaction prescribed by Ref. [61] — the NLO correction to the LO counterterm, plus a two-derivative contact term determined by the empirical effective range— is added at first order in distorted-wave perturbation theory, the resulting phase shift turns out vanish at $T_{\rm lab} \sim 150\,{\rm MeV}$, *i.e.* $k \sim 250\,{\rm MeV}$ or about 25% *below* its physical location k_0. Comparing the phase shifts at LO and NLO of Ref. [61] with the ones resulting from our new proposal, we confirm that, at the price of the inclusion of k_0 as LO input and the promotion of $r_0(P_0)$ as (N)LO input, the convergence of the new results is greatly improved.

Given the importance of OPE, one expects potentially large changes in the position of the poles of $T^{[0]}$ in χEFT with respect to the $\not\pi$EFT result (3.35). Yet, the virtual state near threshold (at $k \simeq i/a$) is guaranteed by construction, as long as

$$\frac{M_N}{4\pi} T^{[0]}(k;\Lambda) \simeq \frac{1}{1/a + ik} \tag{3.65}$$

for sufficiently small k. Using the technique described in Ref. [133], one may obtain numerically the positions of the other two poles. The redundant pole seems to get deeper and deeper when the cutoff Λ is increased. This is consistent with the point of view that the redundant

pole accounts in ∉EFT for the neglected left-hand cut due to OPE. In contrast, the binding energy of the deep bound state oscillates with Λ, but we always find it to be $\gtrsim 200$ MeV, which corresponds to a binding momentum $\gtrsim 450$ MeV. This is, again, an estimate for the breakdown scale $M_{\rm hi}$.

The LO+NLO result shown in Figure 3.7 is so good that one might worry that higher orders could destroy agreement with the empirical phase shifts and undermine the consistency of our expansion. At N^{2}LO and N^{3}LO there are several contributions to account for: TPE and the associated N^{2}LO counterterms [39, 41] in first-order distorted-wave perturbation theory, as well as NLO interactions in second- and third-order distorted-wave perturbation theory. At these higher orders it might be convenient to use the perturbation techniques of Ref. [152] or to devise further resummation of NLO interactions.

We have tentatively investigated the effects of higher-order corrections by means of an incomplete N^{2}LO calculation where the long-range component of leading TPE has been included in first-order distorted-wave perturbation theory, following the analogous calculation in Ref. [61]. Since the short-range component of this potential can be absorbed in Eq. (3.56), there are no new short-range parameters and we impose the same four renormalization conditions as in NLO. We have repeated the extraction of the phase shifts and found a negligible effect on the final result, so that this incomplete N^{2}LO phase shift is at least as good as the one plotted in Figure 3.7. This might be sign that the effects of leading TPE in the $^1S_0$ channel can be compensated by a change in the strengths of our up-to-NLO short-range interactions. Of course, this is not a full calculation of the amplitude at N^{2}LO, but since the change from LO to LO+NLO is small, we might expect the iteration of NLO interactions to also produce small effects. We intend to pursue full higher-order calculations in the future.

3.4 Outlook

Despite its simplicity from the computational perspective, the NN $^1S_0$ channel has proven remarkably resistant to a systematic expansion. In this chapter we have developed a rearrangement of χEFT applied to this wave on the basis of the assumption that the sizes of the ERE parameters and the position of the amplitude zero are fixed by a single low-energy

scale $M_{\rm lo} \sim 100$ MeV. By means of two dibaryon fields, we were able to reproduce very well, already at NLO, the phenomenological phase shifts from threshold to beyond the amplitude zero at $k_0 \simeq 340\,\text{MeV}$. The existence of a spurious deep bound state at LO indicates that the expansion in powers of $M_{\rm lo}/M_{\rm hi}$ breaks down at a scale $M_{\rm hi} \sim 500$ MeV.

The new power counting is particularly transparent when pions are decoupled by an artificial decrease of their interaction strength, in which case a version of contact EFT is produced. Even in this case LO and NLO fits to empirical phase shifts look reasonable, although the lack of pion exchange is noticeable in the form of the energy dependence.

The apparent convergence of our LO and NLO results towards the empirical phase shifts suggests that our PC might be the basis for a new chiral expansion in this channel. Our new expansion relies only on the identification of the NN amplitude zero as a low-energy scale, and on the expectation that the EFT should provide a qualitatively correct description of low-energy observables already at LO. There are other NN channels, such as ${}^3S_1$ and ${}^3P_0$, whose phase shifts cross zero at some point; however, the fact that both ${}^3S_1$ and ${}^3P_0$ channels are well described already at LO in a PC consistent with RG invariance [47, 57–60, 62] suggests that the exact location of these zeros, unlike the one in ${}^1S_0$, can be reached by small, perturbative corrections.

Before a definite claim of convergence can be made, however, one or two higher orders should be calculated, where additional long-range interactions appear in the form of multi-pion exchange. Indications already exist [57, 61, 137] that TPE and its counterterms, which enter first at N^{2}LO, are amenable to perturbation theory in this channel. However, it is yet to be checked whether their contributions are small enough not to destroy the excellent agreement obtained at NLO. Doing so would require to add terms resulting from the treatment of the NLO interaction beyond first order in distorted-wave perturbation theory, but an incomplete N^{2}LO calculation without those terms suggests that higher orders might provide only very small corrections. We intend to consider also isospin-breaking corrections in the future, along the line of what was done in Ref. [144] for Pionless EFT with unitarity at LO.

If this approach succeeds, then it raises new questions. For instance, can one find an equivalent momentum-dependent approach, which would be better suited to three-body calculations and beyond? If the answer is positive, then the idea of imposing the ${}^1S_0$ zero at LO should be tested —together with consistent interactions present in other channels— in future calculations of, *e.g.*, few-body reactions or nuclear structure. Another important

element that would demand an answer is the role of the quark masses in the PC we propose here. We have worked at physical pion mass, but it remains to be seen how this new proposal can be implemented for arbitrary m_π in a renormalization-consistent manner. We intend to address these issues in future work.

Chapter 4

$D_{s0}^*(2317)D$ and $D_{s1}^*(2460)D^*$ molecules

4.1 Introduction

Already four decades ago, the existence of hadronic molecules was hypothesized [153, 154] on the basis of a simple idea: the exchange of light mesons between two heavy hadrons induces a potential that could bind them. The experimental discovery of the $X(3872)$ by the Belle group [155] provided a strong candidate for a narrow molecular state near the $D^0\bar{D}^{*0}$ threshold. Other molecular candidates have been discovered afterwards, among them the Z_c's [156, 157] (which are conjectured to be $D\bar{D}^*$ and $D^*\bar{D}^*$ molecules [158, 159]), the Z_b's [160, 161] ($B\bar{B}^*$ and $B^*\bar{B}^*$ molecules [162, 163]), and the $P_c(4450)$ pentaquark-like state [164] (a $\Sigma_c^*\bar{D}^*$ [165] or $\Sigma_c\bar{D}^*$ molecule [166–169], in the later case probably with a sizable $\Lambda_c(2590)\bar{D}$ component [170, 171]).

Making concrete predictions about hadronic molecules is a challenging task, though, given that they frequently emerge from the singular component of the hadron interaction. In particular, the OPE potential —the longest-range piece of the potential between two hadrons, provided that they contain at least one light quark— includes a tensor piece proportional to the inverse cube of the small distance (see Appendix B for an illustration corresponding to the two-nucleon case). Such force, if attractive, gives rise to an ill-defined solution [47, 48]. This is cured by means of some regularization procedure, typically an ultraviolet cutoff Λ, that renders physical predictions possible. The variation of Λ between the EFT breakdown scale $M_{\rm hi}$ and infinity provides an estimate of the systematic error of the theory at a given order.

However, the richness of the hadron spectrum allows for interactions arising from the

exchange of a pseudo-Goldstone boson that do not involve the tensor force. In particular, hadrons with opposite parities are able to exchange an S-wave pion or kaon. Provided that the hadrons have different masses, the range of the interaction might be unexpectedly large. Two examples of this have been recently given:

- In the $\Lambda_c(2590)\bar{D} \to \Sigma_c \bar{D}^*$ transition, an attractive $1/r^2$ force might take place [171]. This is a singular interaction, which makes mandatory the use of counterterms. If the attraction is strong enough, it will induce discrete scale invariance, hence the emergence of the so-called Efimov spectrum —a geometrical series of bound states analogous to the one predicted for the three-boson system in the two-body unitarity limit almost five decades ago [172].

- In the $\Lambda_c(2590)\Sigma_c$ and $\Lambda_c(2590)\bar{\Sigma}_c$ systems, an attractive $1/r$ interaction could appear [173]. As this is a regular potential, now the problem is well-defined in the absence of counterterms and results do not depend crucially on the cutoff. Still, one expects short-range physics to have some impact.

A third example, which we deal with in this chapter based on Ref. [108], might be provided by the DD^*_{s0} and $D^*D^*_{s1}$ systems, where $D^*_{s0} \equiv D^*_{s0}(2317)$ and $D^*_{s1} \equiv D^*_{s1}(2460)$. On the one hand, there are the S-wave, thus negative-parity D ($J^P = 0^-$) and D^* ($J^P = 1^-$) mesons; on the other hand, there are the P-wave, thus positive-parity D^*_{s0} ($J^P = 0^+$) and $J^P = D^*_{s1}$ ($J^P = 1^+$) mesons. Such opposite parities allow for the exchange of an S-wave kaon in the DD^*_{s0} and $D^*D^*_{s1}$ systems. As the mass differences $M_{D^*_{s0}} - M_D$ and $M_{D^*_{s1}} - M_{D^*}$ lie close to the kaon mass (only 10% of relative difference), the resulting one-kaon-exchange (OKE) interaction will have an unusually enlarged range. In addition, we will see that the $D^*_{s0}DK$ and $D^*_{s1}D^*K$ vertices are proportional to the respective mass differences, thus giving rise to an exceptionally strong Yukawa potential.

The quark content of the DD^*_{s0} and $D^*D^*_{s1}$ molecules proposed here is $c\bar{q}c\bar{s}$ with $\bar{q} = \bar{u}, \bar{d}$. (Note that the exchange of a kaon between a D (D^*) with $\bar{q} = \bar{s}$ and a D^*_{s0} (D^*_{s1}) would violate strangeness conservation.) As argued by Manohar and Wise [174], such a configuration is much more likely to form narrow molecules than compact tetraquarks. LQCD [175, 176] and quark-model calculations [177–179] seem to indicate that compact $Q\bar{q}Q\bar{q}$ objects only exist in the bottom sector, but not in the charm one (with the possible exception of a $c\bar{u}c\bar{d}$ state with $I(J^P) = 0(1^+)$). Consequently, finding a negative-parity $c\bar{q}c\bar{s}$ object would point to a molecule.

This chapter is structured as follows. In Section 4.2 the OKE potential in the DD^*_{s0} and $D^*D^*_{s1}$ systems will be derived. In Section 4.3 it will be shown that such a potential is very likely to keep both systems bound in two shallow molecular states; an EFT analysis of the results is included. Finally, conclusions are presented in Section 4.4.

4.2 OKE potential

As shown in Eq. (1.131), the pseudoscalar and vector mesons are written in SU(3) flavor space respectively as D^a and D^{*a}, whose quark content is $c\bar{q}^a$ ($\bar{q}^1 = \bar{u}$, $\bar{q}^2 = \bar{d}$, $\bar{q}^3 = \bar{s}$); they can be arranged as the single heavy-quark-symmetric superfield

$$H^a = \frac{1+\not{v}}{2}\left(\not{D}^{*a} - D^a\gamma_5\right) \tag{4.1}$$

(see Eq. (1.150)). Similarly, the scalar and pseudovector mesons are written as D_0^a and D_1^a, so that $D_0^3 \equiv D^*_{s0}$ and $D_1^3 \equiv D^*_{s1}$; they can be combined into the superfield

$$S^a = \frac{1+\not{v}}{2}\left(\not{D}^a_1\gamma_5 - D^a_0\right). \tag{4.2}$$

While the D^*_{s0} and D^*_{s1} have small widths and are consequently good candidates for being part of molecules, the D_0^a and D_1^a ($a = 1, 2$) are wide ($\Gamma \sim 200\,\text{MeV}$) and thus unlikely to form bound states (except with kaons [180]).

Recall the definition of the axial-vector current (1.155),

$$A^\mu_{ab} = -\frac{\partial^\mu \Pi_{ab}}{f_\pi}, \tag{4.3}$$

where Π is the meson-octet matrix (1.15), higher pseudo-Goldstone-boson insertions were omitted, and the pion decay constant was normalized to $f_\pi \simeq 130\,\text{MeV}$ [1]. Then, the LO heavy-meson chiral Lagrangian between the S- and P-wave heavy mesons is

$$\mathcal{L} = \frac{h}{2}\,\text{Tr}\left(\bar{H}_a S_b \not{\mathcal{A}}_{ab}\gamma_5\right) + \text{H.c.} \tag{4.4}$$

(see Section 1.4.3 and Ref. [103]). At LO in HQEFT, the four-velocity is $v^\mu = (1, \mathbf{0})$; hence, for what concerns the coupling between a non-strange D (D^*) meson and a strange D_0 (D_1) meson, the Lagrangian above collapses to

$$\mathcal{L} = \frac{h}{f_\pi}\left(D^\dagger\,\partial_0 K\,D^*_{s0} + D^{*\dagger}\,\partial_0 K\,D^*_{s1}\right) + \text{H.c.} \tag{4.5}$$

[1] One could have used the kaon decay constant f_K instead, which is $\sim 20\%$ larger than f_π. However, both constants differ only at NLO in the chiral expansion.

The coupling constant h may be inferred from the width of the pionic decay $D_0 \to D\pi$,

$$\Gamma(D_0 \to D\pi) = \Gamma(D_0 \to D\pi^0) + \Gamma(D_0 \to D\pi^\pm) = \frac{3}{2}\Gamma(D_0 \to D\pi^\pm) = \frac{3}{2}\frac{h^2}{f_\pi^2}\frac{|\boldsymbol{p}_\pi|}{2\pi}\frac{M_D}{M_{D_0}}(M_{D_0} - M_D)^2, \tag{4.6}$$

where isospin-symmetry breaking was neglected, and $|\boldsymbol{p}_\pi| = [(M_{D_0} - M_D)^2 - m_\pi^2]^{1/2}$ is the magnitude of the pion three-momentum. An analogous formula may be given for the decay $D_1 \to D^*\pi$. If the widths of the D_0 and D_1 are saturated by such decays, it turns out that h lies somewhere in between 0.5 and 0.9, where the large spread stems from the experimental uncertainties in the masses and widths of the P-wave heavy mesons, and also because the result changes according to the particular decay one considers (see *e.g.* Ref. [104]). There are also determinations of h from QCD sum rules [181, 182] and LQCD calculations [183] within the above range; the same is true if h is found from the assumption that the D^*_{s0} and D^*_{s1} are molecular [184, 185]. We will give more confidence to the central values within such an interval by using $h = 0.7 \pm 0.1$ in this chapter.

The $D^*_{s0}D$ potential is given by the amplitude of the corresponding OKE diagrams at tree level. In the $\{|DD^*_{s0}\rangle, |D^*_{s0}D\rangle\}$ basis, it reads

$$V_{D^*_{s0}D}(\boldsymbol{q}) = -\frac{1}{q^\mu q_\mu - m_K^2}\begin{pmatrix} v_{D\to DK}\, v_{D^*_{s0}K\to D^*_{s0}} & v_{D\to D^*_{s0}K}\, v_{D^*_{s0}K\to D} \\ v_{D^*_{s0}\to DK}\, v_{DK\to D^*_{s0}} & v_{D^*_{s0}\to D^*_{s0}K}\, v_{DK\to D} \end{pmatrix}, \tag{4.7}$$

where $q^\mu q_\mu = q_0^2 - \boldsymbol{q}^2$ is the squared four-momentum carried by the off-shell kaon, with $q_0^2 \approx (M_{D^*_{s0}} - M_D)^2$ (as the external three-momenta are much smaller than the masses of the heavy mesons), and $m_K \simeq 495\,\text{MeV}$ is the kaon mass. But the only non-vanishing vertices emerging from the coupling (4.5) are

$$\begin{aligned} v_{D\to D^*_{s0}K} &= i\langle D|\mathcal{L}|D^*_{s0}K\rangle = i\frac{h}{f_\pi}(iq_0) = -\frac{h}{f_\pi}\left(M_D - M_{D^*_{s0}}\right) \\ &= -v_{D^*_{s0}K\to D} = -v_{D^*_{s0}\to DK} = v_{DK\to D^*_{s0}}, \end{aligned} \tag{4.8}$$

so that

$$V_{D^*_{s0}D}(\boldsymbol{q}) = -\frac{h^2}{f_\pi^2}\frac{(M_D - M_{D^*_{s0}})^2}{\mu_K^{(0)2} + \boldsymbol{q}^2}\begin{pmatrix} 0 & 1 \\ 1 & 0 \end{pmatrix}, \tag{4.9}$$

where $\mu_K^{(0)} = [m_K^2 - (M_{D^*_{s0}} - M_D)^2]^{1/2} \simeq 206\,\text{MeV}$ represents only $\sim 40\%$ of m_K. The potential above is not diagonal, but it may be easily diagonalized by taking the (normalized) linear combination of states

$$\tfrac{1}{\sqrt{2}}(|DD^*_{s0}\rangle + |D^*_{s0}D\rangle). \tag{4.10}$$

The resulting interaction reads in coordinate space

$$\mathcal{V}_{D^*_{s0}D}(r) = -\frac{h^2}{4\pi}\frac{(M_{D^*_{s0}} - M_D)^2}{f_\pi^2}\frac{e^{-\mu_K^{(0)}r}}{r}. \tag{4.11}$$

Everything works out analogously for the $D^*_{s1}D^*$ system —for the combination

$$\tfrac{1}{\sqrt{2}}(|D^*D^*_{s1}\rangle + |D^*_{s1}D^*\rangle), \tag{4.12}$$

the potential

$$V_{D^*_{s1}D^*}(\boldsymbol{q}) = -\frac{h^2}{f_\pi^2}\frac{(M_{D^*} - M_{D^*_{s1}})^2}{\mu_K^{(1)2} + \boldsymbol{q}^2}\begin{pmatrix}0 & 1\\ 1 & 0\end{pmatrix}, \tag{4.13}$$

with $\mu_K^{(1)} = [m_K^2 - (M_{D^*_{s1}} - M_{D^*})^2]^{1/2} \simeq 206\,\mathrm{MeV}$, is diagonal and reads in coordinate space

$$\mathcal{V}_{D^*_{s1}D^*}(r) = -\frac{h^2}{4\pi}\frac{(M_{D^*_{s1}} - M_{D^*})^2}{f_\pi^2}\frac{e^{-\mu_K^{(1)}r}}{r}. \tag{4.14}$$

One sees that the interactions (4.11) and (4.14) are indeed attractive, unexpectedly long-ranged due to the effective kaon masses $\mu_K^{(0)}$ and $\mu_K^{(1)}$, and enhanced by the squared mass differences $(M_{D^*_{s0}} - M_D)^2$ and $(M_{D^*_{s1}} - M_{D^*})^2$. As a matter of fact, given that both mass differences seem to be very close to each other,

$$M_{D^*_{s0}} - M_D \simeq M_{D^*_{s1}} - M_{D^*} \simeq 450\,\mathrm{MeV} \equiv \omega_K, \tag{4.15}$$

numerically both potentials almost coincide, and we will generically denote them as

$$\mathcal{V}(r;R_c) = -\frac{h^2}{4\pi}\frac{\omega_K^2}{f_\pi^2}\frac{e^{-\mu_K r}}{r}\theta(r - R_c), \tag{4.16}$$

where $\mu_K = (m_K^2 - \omega_K^2)^{1/2}$, and a step-function regulator has been included to investigate the dependence of the results on the cutoff R_c.

The potential (4.16) is long-ranged, but what about the short-ranged component of the DD^*_{s0} and $D^*D^*_{s1}$ interaction? As a first approach, here we will follow the most economic assumption regarding it, namely that its effect may be neglected. Other possibilities will be qualitatively discussed, too.

4.3 Results

As in Chapter 2, we solve the reduced Schrödinger equation,

$$\left[\frac{\partial^2}{\partial r^2} + k^2 - \left(2\mu_H\mathcal{V}(r;R_c) + \frac{\ell(\ell+1)}{r^2}\right)\right]u(r;R_c;k) = 0, \tag{4.17}$$

where the reduced mass μ_H is $M_D M_{D^*_{s0}}/(M_D + M_{D^*_{s0}}) \simeq 1.04\,\text{GeV}$ for the DD^*_{s0} case and $M_{D^*} M_{D^*_{s1}}/(M_{D^*} + M_{D^*_{s1}}) \simeq 1.11\,\text{GeV}$ for the $D^* D^*_{s1}$ case, ℓ is the orbital angular momentum, and u is the reduced wavefunction. Yet here, contrary to Chapter 2, we are not studying the scattering problem, but looking for the bound states of the system; hence, the squared scattering momentum is written as $k^2 = -\kappa^2$, $\kappa^2 \geqslant 0$ being the squared binding momentum. We obtain this with the condition on the bound-state reduced wavefunction evaluated at the infrared cutoff $\tilde{R}_c = 10\,\text{fm} \gg 1/\mu_K$,

$$u_B(\tilde{R}_c; R_c; \kappa) = 0, \tag{4.18}$$

where u_B is found through numerical integration of the reduced Schrödinger equation with regular boundary conditions near the origin,

$$\left[-\frac{\partial^2}{\partial r^2} + \kappa^2 + 2\mu_H \mathcal{V}(r; R_c)\right] u_B(r; R_c; \kappa) = 0, \quad u_B(R_c; R_c; \kappa) = R_c, \quad \frac{\partial}{\partial r} u_B(r; R_c; \kappa)\bigg|_{r=R_c} = 1. \tag{4.19}$$

Here we restricted ourselves to the S wave, as the potential (4.16) is not so strong to overcome the centrifugal barrier and bind the system for non-vanishing orbital angular momentum. The dependence of the resulting binding energy $B = \kappa^2/(2\mu_H)$ on the ultraviolet cutoff R_c is depicted in Figure 4.1. The plot corresponding to the $D^* D^*_{s1}$ system is not given here, as it is identical except that the binding energies are slightly higher due to the increased reduced mass of the $D^* D^*_{s1}$ system.

From the figure one confirms that B is well-defined when the cutoff is removed ($R_c \to 0$), as it corresponds to a regular interaction like the Yukawa one; not surprisingly, it is in such limit that B reaches its maximum value at a given h. One can check numerically that, when the dimensionless parameter $\mu_H \omega_K^2 h^2/(2\pi\mu_K f_\pi^2)$ takes a few discrete values (1.68, 6.45, 14.34, ...), a bound state at threshold ($B = 0$) emerges in the $R_c \to 0$ limit; in other words, the first, second, third, ... bound states appear in the DD^*_{s0} ($D^* D^*_{s1}$) system for $|h| \geqslant 0.42$ ($\geqslant 0.41$), $|h| \geqslant 0.82$ ($\geqslant 0.79$), $|h| \geqslant 1.22$ ($\geqslant 1.18$), ... Given the range of possible values of h, we conclude that there is probably at least one bound state —the second one is much more unlikely but still possible, and the third one and beyond can be discarded, at least provided that the short-range component of this system is neglected in first approximation.

If one fixes $h = 0.7^{+0.1}_{-0.1}$ as in the figure and removes the cutoff, a DD^*_{s0} ($D^* D^*_{s1}$) bound state with binding binding momentum

$$\kappa(R_c \to 0) = 290^{+150}_{-120}\,\text{MeV} \quad (330^{+160}_{-130}\,\text{MeV}) \tag{4.20}$$

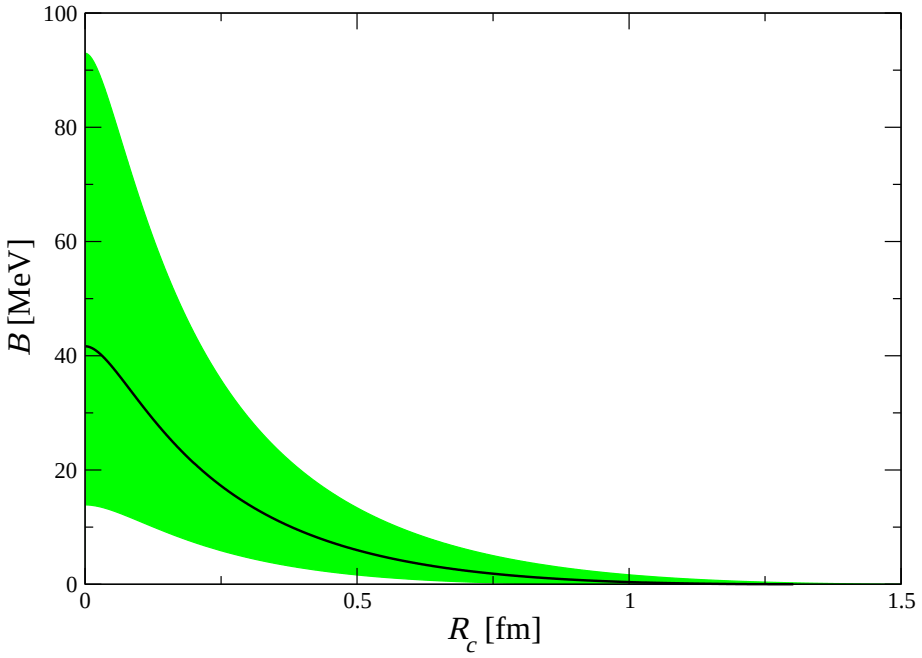

Figure 4.1: Binding energy of the DD^*_{s0} bound state versus the cutoff R_c using a sharp cutoff regulator in coordinate space. The error band corresponds to the uncertainty in the coupling $h = 0.7 \pm 0.1$.

appears. It is found that the OKE potential binds for $R_c \leqslant 1.3^{+0.3}_{-0.3}\,\text{fm}$ ($1.4^{+0.3}_{-0.3}\,\text{fm}$), from where the prediction of a bound state is deduced to be robust.

Recalling that D and D^*_{s0} have $J = 0$ while D^* and D^*_{s1} have $J = 1$, the S-wave heavy-meson bound states predicted here have spins $S = 0$ and $S = 0, 2$, respectively. For the latter case, a bound state with $S = 1$ is not possible, as it would require to replace the symmetric spin wavefunction (4.12) by the antisymmetric one

$$\tfrac{1}{\sqrt{2}}(|D^* D^*_{s1}\rangle - |D^*_{s1} D^*\rangle), \tag{4.21}$$

which diagonalizes the potential (4.13) to yield an interaction that, unlike (4.14), is repulsive and cannot bind the system.

The calculations above correspond to the LO of an EFT whose degrees of freedom are the heavy mesons and the pseudo-Golstone bosons. In this EFT, the effective kaon mass and the

heavy-meson external momenta represent soft scales ($\mu_K \sim Q \sim M_{\rm lo}$), while the breakdown is set by the QCD scale ($M_{\rm hi} \sim M_{\rm QCD}$). In analogy with the OPE potential in the NN sector (see Eqs. (1.68) and (1.69)), we write the OKE potential in momentum space in the form

$$V(\boldsymbol{q}) = -\frac{2\pi}{\mu_H \Lambda_{HH}} \frac{\mu_K^2}{\mu_K^2 + \boldsymbol{q}^2}, \tag{4.22}$$

where

$$\Lambda_{HH} = \frac{2\pi f_\pi^2 \mu_K^2}{h^2 \mu_H \omega_K^2} \simeq 50^{+40}_{-20}\,\text{MeV} \sim M_{\rm lo} \tag{4.23}$$

is the natural momentum scale of OKE in the DD_{s0} and $D^*D^*_{s1}$ systems. We conclude that the OKE potential is enhanced at low energies,

$$V(\boldsymbol{q}) \sim \frac{2\pi}{M_{\rm hi} M_{\rm lo}}. \tag{4.24}$$

As usual, a crude estimate of the EFT expansion parameter $M_{\rm lo}/M_{\rm hi}$ may be provided by the residual cutoff dependence of its LO predictions. One may take

$$\kappa\,(R_c \sim 1/M_{\rm hi}) \;\sim\; \kappa\,(R_c \to 0)\left(1 - \frac{M_{\rm lo}}{M_{\rm hi}}\right). \tag{4.25}$$

Then, combining the results for the DD^*_{s0} ($D^*D^*_{s1}$) binding momentum at $R_c = (1\,\text{GeV})^{-1} = 0.2\,\text{fm}$,

$$\kappa\,(R_c = 0.2\,\text{fm}) = 210^{+90}_{-90}\,\text{MeV} \quad (230^{+100}_{-90}\,\text{MeV}) \tag{4.26}$$

with the ones of Eq. (4.20), we get

$$\frac{M_{\rm lo}}{M_{\rm hi}} \lesssim \frac{1}{3}, \tag{4.27}$$

which is consistent with expectations.

The EFT potential also encodes contact pieces from four-meson vertices. According to heavy-quark spin symmetry, the dominant contribution from contact interactions is given by (see Refs. [186, 187] for a detailed explanation)

$$V^{(\rm ct)}_{DD^*_{s0}}(\boldsymbol{q}) = C_0^{(a)}, \qquad V^{(\rm ct)}_{D^*D^*_{s1}}(\boldsymbol{q}) = C_0^{(a)} + \boldsymbol{S}_1 \cdot \boldsymbol{S}_2\, C_0^{(b)}, \tag{4.28}$$

where the low-energy couplings $C_0^{(a)}$ and $C_0^{(b)}$, which are to be determined from available data, can display two types of scaling —natural and unnatural [188]. While the unnatural scaling requires fine tuning and is thus less probable, for the natural case we have [189]

$$C_0^{(a)} \sim C_0^{(b)} \sim \frac{2\pi}{M_{\rm hi}^2}, \tag{4.29}$$

suppressed by $\mathcal{O}(M_{\rm lo}/M_{\rm hi})$ with respect to Eq. (4.24). That is, in this PC Yukawa is LO and contact terms enter only at NLO. This possibility has been discussed in the literature [56, 189, 190], but there are very few physical realizations of it in hadron physics. From such a scheme we can deduce that at LO the $S = 0, 2$ $D^* D^*_{s1}$ states are degenerate, while at NLO the contact potential breaks the degeneracy, and there is a small energy splitting among the different spin states of the $D^* D^*_{s1}$ system.

Still, the possibility that the short-range couplings displayed unnaturally enhanced scaling cannot be discarded *a priori*. If that is the case, then one should probably keep a soft cutoff ($R_c \sim 1/M_{\rm lo}$) in the scheme followed above to get a realistic estimate of the binding energy, but an EFT-consistent prediction would be precluded. However, even in that scenario the bound states will very probably exist. The Yukawa-plus-contact potential may be regularized via a delta-shell function,

$$\hat{\mathcal{V}}(r; R_c) = \mathcal{V}(r; R_c) + C_0(R_c) \frac{\delta(r - R_c)}{4\pi R_c^2}, \tag{4.30}$$

C_0 being the coupling corresponding to the channel under consideration. In the worst case scenario, that of a repulsive contact ($C_0 > 0$), the system will bind provided that $R_c \leqslant R_c^*$ with $R_c^* \gtrsim 1\,\text{fm}$. But since this cutoff is very soft ($R_c^* \gg 1/M_{\rm hi}$), one can be relatively confident about the binding. As a matter of fact, the light-quark content of these systems —either $\bar{u}\bar{s}$ or $\bar{d}\bar{s}$— makes unlikely that there is short-range repulsion. If anything, the molecules could be more tightly bound than predicted in the first part of this section.

When going to subleading orders of the EFT, one needs to consider heavy-quark symmetry breaking corrections to the LO Lagrangian (4.4). Those are expected to provide an expansion in powers of $\Lambda_{\rm QCD}/M_c$, with $\Lambda_{\rm QCD} \sim 300\,\text{MeV}$ the non-perturbative QCD scale and $M_c \sim 1.5\,\text{GeV}$ the c quark mass. We can identify two main consequences of this:

- Probably the dominant effect is that the coupling h can differ by $\sim 10\%$ between $D D^*_{s0}$ and $D^* D^*_{s1}$, but this is likely to be inconsequential given the large uncertainty in h.

- Another effect is the mixing of the D_1 and D_1' mesons. In the heavy-quark limit, the spin of the c quark decouples from the other quantum numbers. Hence, the P-wave heavy mesons D_1 and D_1' have definite light-quark angular momentum, $J_L = 1/2$ and $J_L = 3/2$ respectively. We write

$$D_1 = D_1^{(1/2)}, \quad D_1' = D_1^{(3/2)} \quad \text{for } M_c \to \infty. \tag{4.31}$$

However, beyond the heavy-quark limit, the D_1 and D_1' contain a certain admixture of the $D_1^{(1/2)}$ and $D_1^{(3/2)}$ states,

$$D_1 = D_1^{(1/2)}\cos\theta + D_1^{(3/2)}\sin\theta, \quad D_1' = -D_1^{(1/2)}\sin\theta + D_1^{(3/2)}\cos\theta \quad \text{for } M_c \text{ finite}, \tag{4.32}$$

where the mixing angle θ is expected to be small if M_c is large. In the non-strange sector, the Belle group obtained from $B \to D^*\pi\pi$ decays that $\theta = (5.5^{+2.7}_{-2.7})^\circ$ [191], while from the widths of the D_1 and D_1' mesons it was found that $\theta = (12.1^{+6.6}_{-4.4})^\circ$ [192]. For the strange case there is no experimental information to constrain the angle, but Ref. [192] estimates it to be $\theta_s \sim 7^\circ$ from a quark-model calculation. This mixing induces a relative reduction of the strength of the OKE potential,

$$V \to V\cos^2\theta_s. \tag{4.33}$$

As $\cos^2\theta_s \sim 0.985$, the former implies a negligible 1.5% weakening of the potential.

Due to their double-charm content, probably the most effective way to produce the DD^*_{s0} and $D^*D^*_{s1}$ molecules in experiments involves heavy-ion collisions. The production yields for the theoretical T_{cc} tetraquarks ($c\bar{q}c\bar{q}$) and other exotic hadrons have been estimated for electron-positron collisions [193] and heavy-ion collisions [194], and they may be reachable by the LHC in the future (notice that double-charm baryon production has been very recently achieved by the LHCb [195]). However, we recall that the production of double charm molecules is probably different from the estimates above, which refer to the much more compact T_{cc} tetraquarks.

The ideas of this chapter may also apply to the bottom sector, where the $B_{s0} \equiv B_{s0}(5730)$ and $B_{s1} \equiv B_{s1}(5776)$ bottom-strange mesons have been theorized to have a significant molecular component and similar binding energy as the D^*_{s0} and D^*_{s1} mesons [196–198]; they also appear in LQCD calculations [199]. However, these are theoretical objects that have not been experimentally detected yet. In the hypothetical BB_{s0} and B^*B_{s1} molecules, the OKE potential is analogous to the one obtained in the charm sector, but now the spectrum is expected to be more tightly bound due to the heavier masses of the bottom mesons. The comment included here regarding these molecules is much more superficial than the analysis we developed in the charm sector. Suffice to say that for $R_c = 0$ we find a BB_{s0} bound state at $\kappa = 250^{+190}_{-150}\,\text{MeV}$, where the prediction for B^*B_{s1} is almost identical as its reduced mass virtually matches that of the BB_{s0} system. For $h = 0.8$ an excited shallow S-wave state will appear. In the P wave there is an additional bound state with $\kappa = 200^{+200}_{-200}\,\text{MeV}$, which disappears for $h = 0.6$.

4.4 Summary

As we have seen in this chapter, the DD^*_{s0} ($D^*D^*_{s1}$) system exhibits the interesting peculiarity that it can interact by means of an attractive, long-range Yukawa potential arising from the exchange of one virtual kaon. This is so because of the opposite parities and different masses of the D (D^*) and D^*_{s0} (D^*_{s1}) heavy mesons. It provides an opportunity to predict the existence of bound states, as short-range physics will not necessarily play a fundamental role, given the non-singular character of the Yukawa potential.

Two S-wave bound states with binding energies of $\sim 50\,\text{MeV}$ are found. They have respectively $S = 0$ and $S = 0, 2$, where the spectrum of the latter is spin-degenerate as a consequence of heavy-quark symmetry. These predictions are likely to represent a LO calculation within an EFT, from which we can also expect that subleading corrections will break the spin degeneracy. Even if the arrangement proposed here turns out not to hold and the short-range potential is non-perturbatively enhanced, we expect the bound states to survive since the most probable scenario is more binding.

We expect the existence of a similar situation in the bottom sector, namely the emergence of BB_{s0} and $B^*B^*_{s0}$ molecules. They will be more bound and might have a richer spectrum than their charm counterparts and there is probably a shallow P-wave bound state and an excited S-wave state. Unfortunately, however, the B_{s0} and B_{s1} heavy mesons have not been observed yet in experiments.

Chapter 5

Conclusions

The EFT philosophy offers an original and useful perspective in the theoretical comprehension of a number of very diverse physical problems. It is particularly an appropriate tool to approach strong-interacting systems in the low-energy regime, and this is so for several reasons. First, it establishes a manifest connection with the underlying theory by imposing *QCD symmetries* on the effective Lagrangian written in terms of effective degrees of freedom. Second, it exploits the separation of scales exhibited by nuclear and hadronic physics to encode *power counting* as a recipe that hierarchizes the importance of the infinite number of interactions contained in the effective Lagrangian and allows for an order-by-order improvable description of observables. Third, it is articulated in the language of *renormalization* that is widely used in quantum field theories and, most particularly, in QCD; it thus allows to interpret nuclear and hadronic physics as the renormalization-group evolution of QCD at long distances.

In the introduction to the present work, we reviewed some of the most prominent examples of EFTs that are extensively used in the modern study of few-body nuclear and hadronic systems, namely chiral EFT, pionless EFT, and heavy-quark EFT. In Chapters 2 and 3, on one hand, and Chapter 4, on the other hand, we have presented three detailed case studies of nuclear and hadronic physics, respectively, where these EFTs are used as guidelines.

The paradigmatic example of a low-energy EFT of strong interactions is chiral perturbation theory. It relies on the (approximate) chiral symmetry of QCD, which is used as a fundamental constraint on the effective Lagrangian. By means of a power counting that follows naive dimensional analysis ("naturalness"), chiral perturbation theory describes succesfully low-momentum processes (below the characteristic QCD scale $\sim 1\,\mathrm{GeV}$) that involve

one or more pseudo-Goldstone bosons plus one nucleon at most. However, processes with two and more nucleons are intrinsically non-perturbative, and thus cannot be captured by chiral perturbation theory, nor by a power counting in full correspondence with naive dimensional analysis. Indeed, already in the two-nucleon sector non-perturbative renormalization results in the fact that the number of short-range interactions prescribed at a certain order by the dimensional counting does not suffice in general to render the scattering amplitude truly renormalized. *Chiral* (or "pionful") *EFT* is the generalization of chiral perturbation theory to such non-perturbative framework.

Chiral symmetry anticipates that the longest-range component of the nuclear force has a range roughly given by the inverse pion mass ($\gtrsim 1\,\mathrm{fm}$). At distances sufficiently larger, the only effective degrees of freedom are the nucleon themselves, so that all the interactions among them are contact-type. This approach is known as *contact* (or "pionless") *EFT*. Similarly to the pionful case, the renormalization-invariance principle is used to derive the correct power counting. In the two-body sector, where the theory is equivalent to the effective range expansion of the scattering amplitude, the scaling of the couplings is again not consistent with natural expectations, which is manifest in the existence of two shallow (respectively real and virtual) bound states in the nucleon-nucleon S waves.

In Chapter 2, the power counting of two-nucleon peripheral singlet channels —those waves with zero spin angular momentum and high orbital angular momentum— was studied in the framework of chiral EFT. We explored perturbation theory up to fourth order, which allowed us to find that the one-pion-exchange potential is suppressed in these channels by the EFT expansion parameter raised to some power that grows with the orbital angular momentum. Such a suppression is, again, in contradiction with dimensional expectations and, as a matter of fact, in general turns out to be even much stronger than it is in the Kaplan–Savage–Wise scheme, in which one-pion exchange enters at next-to-leading order. This opens the door to improve the systematicity and consistency of few-body calculations, as it provides a theoretically sound guideline to include only the necessary iterations of one-pion exchange and omit those peripheral channels where the order of the tree-level potential is higher than the one of the calculation itself.

The two-nucleon ${}^1S_0$ channel —whose spin and orbital angular momenta are both zero— was not considered in Chapter 2, since it presents several features that make it quite an especial partial wave. Again in the framework of chiral EFT, Chapter 3 addressed some of these features by means of a new arrangement of short-range interactions. This was

done so in the spirit of reproducing already at leading order the qualitative behavior of the scattering amplitude all over the momentum range where the EFT is expected to hold. Since the Weinberg proposal fails to reproduce the low-energy zero exhibited by the partial-wave-analysis $^1S_0$ amplitude (center-of-mass scattering momentum $\simeq 340\,\mathrm{MeV}$), we proposed a different scheme where such zero is non-perturbatively enforced and subleading corrections are perturbatively included. Systematic improvement was shown at next-to-leading order, and we obtained results that fit phenomenological phase shifts remarkably well all the way up to the pion production threshold. We included as well a new version of contact EFT in which one-pion exchange was artificially decoupled (even though the momentum location of the zero lies beyond the inverse range of this interaction), which allowed us to derive analytic results that also fit phenomenology surprisingly well. From these phenomenological successes, we believe that the decision of imposing the $^1S_0$ zero at leading order in broader EFT-consistent calculations is worthwhile, as it may improve the description of observables in the few-body sector (light nuclei, electroweak reactions...).

Away from the nucleon sector, heavy hadrons are interesting objects by themselves, as they represent bound states of heavy and light particles. In particular, heavy mesons are composed of a heavy quark (b or c) plus a light antiquark ($\bar{u}$, $\bar{d}$ or $\bar{s}$). If one pushes the mass of the heavy quark to infinity, then the light quark will become completely insensitive to the flavor and spin of the former (heavy-quark symmetry). This scenario corresponds to the leading order of *heavy-quark EFT*; effects that break heavy-quark symmetry in the physical world are to be taken as corrections suppressed by powers of the heavy-quark mass. Also in this framework one may take advantage of chiral symmetry to construct another version of chiral EFT where pseudo-Goldstone bosons are kept as explicit degrees of freedom, but nucleons are replaced by heavy mesons.

Such an approach was used in Chapter 4. In particular, we considered the D and D^* charmed mesons, on the one hand, and the $D_{s0}^*(2317)$ and $D_{s1}^*(2460)$ charm-strange mesons, on the other hand. The opposite intrinsic parity of the D (D^*) and the D_{s0}^* (D_{s1}^*) mesons allows them to exchange an S-wave kaon, which induces a Yukawa-type potential between heavy mesons whose range is unexpectedly long (due to the closeness of their mass difference to the kaon mass) and whose strength is unusually high (as it is proportional to the square of such mass difference). This almost guarantees the existence of D_{s0}^*D and $D_{s1}^*D^*$ bound states with $J^P = 0^-$ and $J^P = 0^-, 2^-$ respectively, since calculations indicate binding energies of around 50 MeV. Such results were identified with the leading-order predictions of an

EFT whose explicit degrees of freedom are the D heavy mesons and the kaons, where the Yukawa interaction is non-perturbative while heavy-quark-symmetry-breaking contact terms are accounted for as perturbative corrections. We expect as well the existence of the bottom counterparts of the above bound states, BB_{s0} and $B^*B^*_{s1}$, which would be more tightly bound and exhibit a richer spectrum that might include a shallow P-wave state and an excited S-wave state.

We note that the three works presented respectively in Chapters 2, 3, and 4 use various theoretical techniques. For example, while Chapter 2 makes use of fully perturbative tools, Chapters 3 and 4 treat non-perturbatively their respective leading orders; while Chapters 2 and 3 study scattering problems, Chapter 4 is focused on bound states; while Chapters 2 and 4 deal with purely regular interactions, Chapter 3 includes singular terms in the potential. Still, the content of the three chapters is inspired by low-energy EFTs of strong interactions —chiral EFT in Chapters 2 and 3; pionless EFT in Chapter 3; heavy-quark (chiral) EFT in Chapter 4. This gives an idea about the versatility and richness of the EFT approach applied to nuclear and hadronic systems. We hope that the proposals we have provided in Chapters 2 and 3 will find applications beyond the two-nucleon sector, as well as that the predictions of new meson-molecular bound states that we have made in Chapter 4 will be experimentally accessed in the future.

Appendix A

Spontaneous symmetry breakdown

In this appendix we will shortly review how SSB works out by studying a few illustrative examples. First, take a relativistic scalar field theory described by the action

$$\mathcal{S}[\phi] = \int \mathrm{d}^4x \left(\tfrac{1}{2}\partial^\mu\phi\partial_\mu\phi - \tfrac{1}{2}m^2\phi^2 - \tfrac{\lambda}{4!}\phi^4 - \tfrac{3}{2\lambda}m^4\right), \tag{A1}$$

where $\phi = \phi^\dagger$ is a single field of mass m, $\lambda > 0$ is a (dimensionless) coupling parameter, and the ϕ-independent term $-3m^4/(2\lambda)$ is an irrelevant "cosmological constant". This theory remains invariant under the discrete mapping $\phi \mapsto -\phi$.

If the sign of the mass term is flipped ($m^2 \to -m^2$), Eq. (A1) becomes

$$\mathcal{S}[\phi] = \int \mathrm{d}^4x \left(\tfrac{1}{2}\partial^\mu\phi\partial_\mu\phi - \mathcal{V}(\phi)\right), \tag{A2}$$

with the interaction term

$$\mathcal{V}(\phi) = \tfrac{\lambda}{4!}\left(\phi - \phi_+\right)^2\left(\phi - \phi_-\right)^2, \quad \phi_\pm = \pm\sqrt{\tfrac{6}{\lambda}}m, \tag{A3}$$

from where $\mathcal{V}'(\phi) = 0$ for $\phi = \{0, \phi_\pm\}$. Besides, $\mathcal{V}''(0) = -m^2 < 0$ and $\mathcal{V}''(\phi_\pm) = 2m^2 > 0$, showing that the theory exhibits an unstable equilibrium at $\phi = 0$ and two degenerate stable equilibria —two different VEVs [1]— at $\phi = \phi_\pm$.

[1] Since $\phi = \phi_\pm$ are solutions of the equation of motion, classically one expects the field to occupy this value over all space. Seeing the classical theory as the $\hbar \to 0$ limit of the quantum theory, we find the average value of the field in the ground state $|\psi_\pm\rangle$,

$$\langle\phi\rangle \equiv \langle\psi_\pm|\phi|\psi_\pm\rangle = \lim_{\hbar\to 0}\int \mathcal{D}\phi\, e^{i\mathcal{S}[\phi]/\hbar}\phi = \phi_\pm.$$

This allows to identify the classical result with a quantum VEV evaluated at tree level.

Let us reshift the field ϕ via the introduction of, say, $\tilde{\phi} = \phi - \phi_+$, which has vanishing VEV. It turns out

$$\mathcal{S}[\tilde{\phi}] = \int \mathrm{d}^4x \left[\tfrac{1}{2}\left(\partial^\mu\tilde{\phi}\partial_\mu\tilde{\phi} - \tilde{m}^2\tilde{\phi}^2\right) - \sqrt{\tfrac{\lambda}{12}}\tilde{m}\tilde{\phi}^3 - \tfrac{\lambda}{4!}\tilde{\phi}^4\right], \quad \tilde{m} = \sqrt{2}m, \tag{A4}$$

whose mass term has the proper sign. However, due to the term proportional to $\tilde{\phi}^3$, the action is not invariant anymore under the reflection $\tilde{\phi} \mapsto -\tilde{\phi}$ —*the symmetry is now hidden.* By definition, such a symmetry takes both VEVs as strictly equivalent; however, the system "spontaneously" chooses one of them and thus enforces an asymmetric outcome. The symmetry exhibited by the action has been *spontaneously broken* by the ground state of the theory.

The mechanisms behind SSB are a bit more involved for continuous symmetries. To show this, consider instead the scalar field theory given by the generic action

$$\mathcal{S}[\phi] = \int \mathrm{d}^4x \left[\tfrac{1}{2}\partial^\mu\phi\partial_\mu\phi - \mathcal{V}(\phi)\right], \quad \phi = \{\phi_1, \ldots, \phi_N\}, \tag{A5}$$

which remains invariant under the continuous mapping

$$\phi_i \mapsto \phi_i + \delta\phi_i, \quad \delta\phi_i = i\epsilon\mathcal{T}_{ij}\phi_j, \tag{A6}$$

where $\epsilon = \{\epsilon_1, \ldots, \epsilon_n\}$ is an array of small space-time-independent parameters and $\mathcal{T} = \{\mathcal{T}_1, \ldots, \mathcal{T}_n\}$ is a set of $N \times N$ matrices in flavor space, called generators of the symmetry. Then, the Noether theorem predicts the emergence of n conserved currents ($\partial_\mu J^\mu = 0$) given by

$$J^\mu_A = -i\frac{\partial\mathcal{L}}{\partial(\partial_\mu\phi_i)}(\mathcal{T}_A)_{ij}\phi_j, \quad A = 1, \ldots, n. \tag{A7}$$

In particular, one has the conserved-charge operators ($\dot{Q} = 0$),

$$Q_A = \int \mathrm{d}^3x\, J^0_A = -i\int \mathrm{d}^3x\, \pi_i(\mathcal{T}_A)_{ij}\phi_j, \quad \pi_i = \frac{\partial\mathcal{L}}{\partial\dot{\phi}_i}, \tag{A8}$$

verifying

$$[Q_A, \phi_i] = i(\mathcal{T}_A)_{ij}\phi_j, \tag{A9}$$

in virtue of the canonical commutation relations between the ϕ's and the π's. Such a result motivates the introduction of a unitary object $U = 1 + i\epsilon_A Q_A$ that allows us to rewrite Eq. (A6) as a standard unitary transformation on ϕ,

$$\phi \mapsto U\phi U^{-1}. \tag{A10}$$

Now, if we assume further that the interaction term $V(\phi)$ in Eq. (A5) is (together with the kinetic term) invariant under Eq. (A6),

$$\mathcal{V}(\phi+\delta\phi) = \mathcal{V}(\phi) + \partial_i\mathcal{V}(\phi)\delta\phi_i + \mathcal{O}(\epsilon^2) = \mathcal{V}(\phi) \quad \Rightarrow \quad \partial_i\mathcal{V}(\phi)\mathcal{T}_{ij}\phi_j = 0, \tag{A11}$$

where ∂_i represents the derivative operator along the ϕ_i direction. Call ϕ_0 to the classical solution of the equations of motion, which must verify

$$\partial_i\mathcal{V}(\phi)\big|_{\phi=\phi_0} = 0, \tag{A12}$$

$$\partial_i\partial_j\mathcal{V}(\phi)\big|_{\phi=\phi_0} \geqslant 0. \tag{A13}$$

Then, if one derives Eq. (A11) with respect to ϕ_k and evaluates at $\phi = \phi_0$, it turns out in virtue of Eq. (A12)

$$\partial_k\partial_i\mathcal{V}(\phi)\big|_{\phi=\phi_0}\,\mathcal{T}_{ij}\,(\phi_0)_j = 0. \tag{A14}$$

But the potential may be represented as a series expansion in powers of $\tilde{\phi} = \phi - \phi_0$,

$$\mathcal{V}(\phi) = \mathcal{V}(\phi_0) + \tfrac{1}{2}\,\partial_i\partial_j V(\phi)\big|_{\phi=\phi_0}\,\tilde{\phi}_i\tilde{\phi}_j + \ldots, \tag{A15}$$

where the $\tilde{\phi}$-independent term is a cosmological constant, and Eq. (A12) was used again to kill the linear term. The bilinear term is in turn identified with the mass term of the $\tilde{\phi}$-theory,

$$\mathcal{M}^2_{ij} = \partial_i\partial_j V(\phi)\big|_{\phi=\phi_0}\,, \tag{A16}$$

and Eq. (A13) guarantees that $\mathcal{M}^2$ —the mass-squared matrix in flavor space— is positive-definite. This allows us to rewrite Eq. (A14) as the matrix equation

$$\mathcal{M}^2\mathcal{T}\phi_0 = 0. \tag{A17}$$

At this point, one must consider two possible, opposite scenarios: either $\mathcal{T}_A\phi_0 = 0$ for any A (so that Eq. (A17) is trivially fulfilled), or there is some A such that $\mathcal{T}_A\phi_0 \neq 0$.

- The first possibility is called the *Wigner–Weyl realization* of the symmetry; according to Eq. (A6), it implies the invariance of ϕ_0 under the symmetry ($U\phi_0U^{-1} = \phi_0$). Actually, if $|\psi_0\rangle$ is the ground state of the theory ($\langle\psi_0|\phi|\psi_0\rangle = \phi_0$), then it follows that $U\,|\psi_0\rangle = |\psi_0\rangle$, thus

$$Q_A\,|\psi_0\rangle = 0, \tag{A18}$$

i.e. the n conserved charges annihilate the (unique) vacuum. Let us prove further that the Weyl-Wigner realization implies the emergence of *degenerate states in the energy spectrum*. Take the operators ϕ_1 and $\phi_2 \equiv -i\mathcal{T}_{1i}\phi_i$; these, according to Eq. (A9), verify $[Q,\phi_1] = -\phi_2$, or equivalently $[Q,\phi_1^\dagger] = \phi_2^\dagger$, for some conserved charge Q fulfilling $[Q,H] = 0$. Assume that both operators $\phi_1^\dagger, \phi_2^\dagger$ act on the ground state as creation operators of two states $|\psi_1\rangle, |\psi_2\rangle$ with definite energies E_1, E_2,

$$\phi_i^\dagger |\psi_0\rangle = |\psi_i\rangle\,, \quad H|\psi_i\rangle = E_i|\psi_i\rangle\,, \quad i = 1,2. \tag{A19}$$

Then, it will follow from Eq. (A18)

$$\begin{aligned} E_2|\psi_2\rangle &= H|\psi_2\rangle = H\phi_2^\dagger|\psi_0\rangle = H\left(Q\phi_1^\dagger - \phi_1^\dagger Q\right)|\psi_0\rangle = HQ\phi_1^\dagger|\psi_0\rangle \\ &= QH|\psi_1\rangle = E_1 Q\phi_1^\dagger|\psi_0\rangle = E_1\left(\phi_1^\dagger Q + \phi_2^\dagger\right)|\psi_0\rangle = E_1\phi_2^\dagger|\psi_0\rangle = E_1|\psi_2\rangle\,, \end{aligned} \tag{A20}$$

thus $E_1 = E_2$ —the states $|\psi_1\rangle, |\psi_2\rangle$ are degenerate in energy.

- The second possibility is known as the *Nambu–Goldstone realization* of the symmetry. Now Eq. (A18) does not apply anymore for a given A, *i.e.* the vacuum is not left invariant by the symmetry. Let $E_0 = \langle\psi_0|H|\psi_0\rangle$ be the minimum energy the system can occupy. It is easy to see that a rotation of our original ground state, $|\psi_0'\rangle = U|\psi_0\rangle \neq |\psi_0\rangle$, is actually another ground state

$$H|\psi_0'\rangle = H(1+i\epsilon Q)|\psi_0\rangle = (1+i\epsilon Q)H|\psi_0\rangle = E_0(1+i\epsilon Q)|\psi_0\rangle = E_0|\psi_0'\rangle\,. \tag{A21}$$

That is to say, this scenario produces an *infinite set of degenerate vacua*. Again, the system needs to "spontaneously" choose one particular ground state, but now (contrary to the discrete case) the vacuum will smoothly interpolate between neighbor space-time regions due to low-energy excitations. And, precisely because of the ground-state degeneracy, such excitations must follow a massless dispersion relation. The presence of these massless objects is actually reflected by Eq. (A17), as the vector $(\mathcal{T}_A)_{ij}(\phi_0)_j \neq 0$ turned out to be an eigenstate of the $\mathcal{M}^2$ operator with zero eigenvalue. Indeed, as the Goldstone theorem stablishes, each A verifying the previous inequality (in other words, each broken generator) corresponds to a massless field $\phi_i(\mathcal{T}_A)_{ij}(\phi_0)_j$, called *Goldstone boson*, whose quantum numbers can be shown [200] to be the same as those of the broken generators. In particular, provided that the generators are space-time scalars (as it is the case in most situations of interest), the Goldstone fields need to be spinless.

Appendix B

The OPE potential in the NN $^3S_1$-$^3D_1$ channel

In the main text, we did not consider the possibility of transitions from the S wave to higher waves when deriving the OPE potential (1.62). This can always be safely done in the spin-singlet ($^1S_0$) channel. However, for the sake of completeness, here we will extend our derivation to more general transitions —those that are present in the spin-triplet ($^3S_1$-$^3D_1$) channel.

Let $\ell = 0, 2$ and $S = 1$ be the orbital and spin angular momentum numbers, and let $m_\ell = \{-\ell, -\ell+1, \ldots, +\ell-1, +\ell\}$ and $m_S = \{-1, 0, +1\}$ be their respective projections along the z-axis. We will compute the matrix element of the tensor operator S_{12} between the initial state $|\ell, m_\ell; S, m_S\rangle \equiv |\ell, m_\ell; m\rangle$ and the final state $|\ell', m'_{\ell'}; S', m'_{S'}\rangle \equiv |\ell', m'_{\ell'}; m'\rangle$. With that purpose, rewrite Eq. (1.59) as

$$S_{12} = 6\left[\tfrac{1}{3}\boldsymbol{S}_1^2 + \tfrac{1}{3}\boldsymbol{S}_2^2 + 2\left(\boldsymbol{S}_1\cdot\hat{\boldsymbol{r}}\right)\left(\boldsymbol{S}_2\cdot\hat{\boldsymbol{r}}\right)\right] - 2\boldsymbol{S}^2, \tag{B1}$$

where we recalled that $\boldsymbol{S}_j = \boldsymbol{\sigma}_j/2$ for the spin operator of the nucleon j in terms of its corresponding Pauli vector, and $\boldsymbol{S} = \boldsymbol{S}_1 + \boldsymbol{S}_2$ is the total spin operator. But

$$\left(\boldsymbol{S}_j\cdot\hat{\boldsymbol{r}}\right)^2 = \tfrac{1}{4}\sum_{k,l=1}^{3}\sigma_j^k\sigma_j^l\hat{r}^k\hat{r}^l = \tfrac{1}{8}\sum_{k,l=1}^{3}(\sigma_j^k\sigma_j^l + \sigma_j^l\sigma_j^k)\hat{r}^k\hat{r}^l = \tfrac{1}{4}\,\hat{\boldsymbol{r}}\cdot\hat{\boldsymbol{r}} = \tfrac{1}{3}\boldsymbol{S}_j^2, \tag{B2}$$

where we used that $\sigma_j^k\sigma_j^l + \sigma_j^l\sigma_j^k = 2\delta^{kl}$, and $\boldsymbol{S}_j^2 = S_j\left(S_j+1\right) = 3/4$. Hence, Eq. (B1) becomes

$$S_{12} = 6\left[\left(\boldsymbol{S}_1\cdot\hat{\boldsymbol{r}}\right)^2 + \left(\boldsymbol{S}_2\cdot\hat{\boldsymbol{r}}\right)^2 + 2\left(\boldsymbol{S}_1\cdot\hat{\boldsymbol{r}}\right)\left(\boldsymbol{S}_2\cdot\hat{\boldsymbol{r}}\right)\right] - 2\boldsymbol{S}^2 = 6\left(\boldsymbol{S}\cdot\hat{\boldsymbol{r}}\right)^2 - 2\boldsymbol{S}^2. \tag{B3}$$

Here $\boldsymbol{S}$ is the vector of 3×3 spin matrices corresponding to a particle with $S=1$,

$$S^1=\begin{pmatrix}0 & \frac{1}{\sqrt{2}} & 0\\ \frac{1}{\sqrt{2}} & 0 & \frac{1}{\sqrt{2}}\\ 0 & \frac{1}{\sqrt{2}} & 0\end{pmatrix},\qquad S^2=\begin{pmatrix}0 & -\frac{i}{\sqrt{2}} & 0\\ \frac{i}{\sqrt{2}} & 0 & -\frac{i}{\sqrt{2}}\\ 0 & \frac{i}{\sqrt{2}} & 0\end{pmatrix},\qquad S^3=\begin{pmatrix}1 & 0 & 0\\ 0 & 0 & 0\\ 0 & 0 & -1\end{pmatrix}, \tag{B4}$$

from where one may find

$$(\boldsymbol{S}\cdot\hat{\boldsymbol{r}})^2=\begin{pmatrix}\frac{2}{3}+\sqrt{\frac{4\pi}{45}}\mathcal{Y}_2^{(0)*} & -\sqrt{\frac{4\pi}{15}}\mathcal{Y}_2^{(+1)*} & \sqrt{\frac{8\pi}{15}}\mathcal{Y}_2^{(+2)*}\\ \sqrt{\frac{4\pi}{15}}\mathcal{Y}_2^{(-1)*} & \frac{2}{3}-\sqrt{\frac{16\pi}{45}}\mathcal{Y}_2^{(0)*} & \sqrt{\frac{4\pi}{15}}\mathcal{Y}_2^{(+1)*}\\ \sqrt{\frac{8\pi}{15}}\mathcal{Y}_2^{(-2)*} & -\sqrt{\frac{4\pi}{15}}\mathcal{Y}_2^{(-1)*} & \frac{2}{3}+\sqrt{\frac{4\pi}{45}}\mathcal{Y}_2^{(0)*}\end{pmatrix}, \tag{B5}$$

where $\mathcal{Y}_\ell^{(m_\ell)}(\hat{\boldsymbol{r}})=\langle\hat{\boldsymbol{r}}|\ell,m_\ell\rangle$ is a spherical harmonic. Now,

$$\langle\ell',m'_{\ell'};m'|S_{12}|\ell,m_\ell;m\rangle=6\,\langle\ell',m'_{\ell'};m'|\,(\boldsymbol{S}\cdot\hat{\boldsymbol{r}})^2\,|\ell,m_\ell;m\rangle-4\delta_{\ell,\ell'}\delta_{m_\ell,m'_{\ell'}}\delta_{m,m'}, \tag{B6}$$

where $\boldsymbol{S}^2\,|\ell,m_\ell;S,m_S\rangle=S(S+1)\,|\ell,m_\ell;S,m_S\rangle$ was recalled. But

$$\begin{aligned}\langle\ell',m'_{\ell'};m'|\,(\boldsymbol{S}\cdot\hat{\boldsymbol{r}})^2\,|\ell,m_\ell;m\rangle&=\int\mathrm{d}^2\hat{r}''\int\mathrm{d}^2\hat{r}'\,\mathcal{Y}_{\ell'}^{(m'_{\ell'})*}(\hat{\boldsymbol{r}}'')\mathcal{Y}_\ell^{(m_\ell)}(\hat{\boldsymbol{r}}')\,\langle m';\hat{\boldsymbol{r}}''|\,(\boldsymbol{S}\cdot\hat{\boldsymbol{r}})^2\,|m;\hat{\boldsymbol{r}}'\rangle\\&=\int\mathrm{d}^2\hat{r}\,\mathcal{Y}_{\ell'}^{(m'_{\ell'})*}\mathcal{Y}_\ell^{(m_\ell)}\,\langle m';\hat{\boldsymbol{r}}|\,(\boldsymbol{S}\cdot\hat{\boldsymbol{r}})^2\,|m;\hat{\boldsymbol{r}}\rangle\\&=\int\mathrm{d}^2\hat{r}\,\mathcal{Y}_{\ell'}^{(m'_{\ell'})*}\mathcal{Y}_\ell^{(m_\ell)}\left[\tfrac{2}{3}\delta_{m',m}+c_{m',m}\mathcal{Y}_2^{(m'-m)*}\right]\\&=\tfrac{2}{3}\delta_{\ell,\ell'}\delta_{m_\ell,m'_{\ell'}}\delta_{m,m'}+c_{m',m}\int\mathrm{d}^2\hat{r}\,\mathcal{Y}_{\ell'}^{(m'_{\ell'})*}\mathcal{Y}_\ell^{(m_\ell)}\mathcal{Y}_2^{(m'-m)*},\end{aligned} \tag{B7}$$

thus Eq. (B6) becomes

$$\langle\ell',m'_{\ell'};m'|S_{12}|\ell,m_\ell;m\rangle=6c_{m',m}\int\mathrm{d}^2\hat{r}\;\mathcal{Y}_{\ell'}^{(m'_{\ell'})*}\mathcal{Y}_\ell^{(m_\ell)}\mathcal{Y}_2^{(m'-m)*}, \tag{B8}$$

where we introduced the constants

$$\begin{array}{llllll}c_{+1,+1}&=\sqrt{\frac{4\pi}{45}}, & c_{+1,0}&=-\sqrt{\frac{4\pi}{15}}, & c_{+1,-1}&=\sqrt{\frac{8\pi}{15}},\\ c_{0,+1}&=\sqrt{\frac{4\pi}{15}}, & c_{0,0}&=-\sqrt{\frac{16\pi}{45}}, & c_{0,-1}&=\sqrt{\frac{4\pi}{15}},\\ c_{-1,+1}&=\sqrt{\frac{8\pi}{15}}, & c_{-1,0}&=-\sqrt{\frac{4\pi}{15}}, & c_{-1,-1}&=\sqrt{\frac{4\pi}{45}}.\end{array} \tag{B9}$$

Let us study separately the different particular cases of Eq. (B8):

- $\ell=\ell'=0$. This is of course the simplest scenario,

$$\langle 0,0;m'|S_{12}|0,0;m\rangle=\tfrac{3}{2\pi}c_{m',m}\int\mathrm{d}^2\hat{r}\,\mathcal{Y}_2^{(m'-m)*}=0. \tag{B10}$$

- $\ell = 2$, $\ell' = 0$. Taking $\tilde{m} = \{-2,-1,0,+1,+2\}$,

$$\langle 0,0;m'|S_{12}|2,\tilde{m};m\rangle = \tfrac{3}{\sqrt{\pi}} c_{m',m} \int \mathrm{d}^2\hat{r}\, \mathcal{Y}_2^{(\tilde{m})} \mathcal{Y}_2^{(m'-m)*} = \tfrac{3}{\sqrt{\pi}} c_{m',m} \delta_{m+\tilde{m},m'}. \tag{B11}$$

- $\ell = \ell' = 2$. Taking $\hat{m}, \tilde{m} = \{-2,-1,0,+1,+2\}$,

$$\langle 2,\tilde{m};m'|S_{12}|2,\hat{m};m\rangle = 6 c_{m',m} \int \mathrm{d}^2\hat{r}\, \mathcal{Y}_2^{(\tilde{m})*} \mathcal{Y}_2^{(m'-m)*} \mathcal{Y}_2^{(\hat{m})}, \tag{B12}$$

from where, using the general result

$$\int \mathrm{d}^2\hat{r}\, \mathcal{Y}_{j_1}^{(m_1)*} \mathcal{Y}_{j_2}^{(m_2)*} \mathcal{Y}_{\mathcal{J}}^{(\mathcal{M})} = \sqrt{\tfrac{(2j_1+1)(2j_2+1)}{4\pi(2\mathcal{J}+1)}} \mathcal{C}(j_1,m_1;j_2,m_2|\mathcal{J},\mathcal{M})\, \mathcal{C}(j_1,0;j_2,0|\mathcal{J},0), \tag{B13}$$

with $\mathcal{C}(j_1,m_1;j_2,m_2|\mathcal{J},\mathcal{M}) \equiv \langle j_1,m_1;j_2,m_2|\mathcal{J},\mathcal{M}\rangle$ a (real) Clebsch–Gordan coefficient, it turns out

$$\langle 2,\tilde{m};m'|S_{12}|2,\hat{m};m\rangle = -\sqrt{\tfrac{90}{7\pi}} \mathcal{C}(2,\tilde{m};2,m'-m|2,\hat{m}) c_{m',m}. \tag{B14}$$

However, the basis of eigenstates of the orbital angular momentum, the spin angular momentum, and their respective third components, does not correspond to the basis of eigenstates employed by the usual spectroscopic notation. Let J be the total angular momentum,

$$|^{2S+1}\ell_J\rangle_M \equiv |[\ell,S]\,J,M\rangle\,, \tag{B15}$$

where $M = \{-J,-J+1,\ldots,+J-1,+J\}$, the third component of the total angular momentum, verifies $M = m_\ell + m_S$. Generically,

$$|[\ell,S]\,J,M\rangle = \sum_{m_\ell,m_S} \mathcal{C}(\ell,m_\ell;S,m_S|J,M)\,|\ell,m_\ell;S,m_S\rangle\,, \tag{B16}$$

so that

$$\left\{\begin{array}{ll} |^3S_1\rangle_{-1} & (m_\ell = 0, m_S = -1), \\ |^3S_1\rangle_{0} & (m_\ell = 0,\, m_S = 0), \\ |^3S_1\rangle_{+1} & (m_\ell = 0,\, m_S = +1), \end{array}\right. \qquad \left\{\begin{array}{llll} |^3D_1\rangle_{-1} & (m_\ell = -2, m_S = +1; & -1,0; & 0,-1), \\ |^3D_1\rangle_{0} & (m_\ell = -1, m_S = +1; & 0,0; & +1,-1), \\ |^3D_1\rangle_{+1} & (m_\ell = 0, m_S = +1; & +1,0; & +2,-1), \end{array}\right. \tag{B17}$$

become respectively ($S = 1$)

$$\left\{\begin{array}{lcl} |^3S_1\rangle_{-1} &=& |0,0;-1\rangle\,, \\ |^3S_1\rangle_{0} &=& |0,0;0\rangle\,, \\ |^3S_1\rangle_{+1} &=& |0,0;+1\rangle\,, \end{array}\right. \qquad \left\{\begin{array}{lcl} |^3D_1\rangle_{-1} &=& \sqrt{\tfrac{3}{5}}\,|2,-2;+1\rangle - \sqrt{\tfrac{3}{10}}\,|2,-1;0\rangle + \sqrt{\tfrac{1}{10}}\,|2,0;-1\rangle\,, \\ |^3D_1\rangle_{0} &=& \sqrt{\tfrac{3}{10}}\,|2,-1;+1\rangle - \sqrt{\tfrac{2}{5}}\,|2,0;0\rangle + \sqrt{\tfrac{3}{10}}\,|2,+1;-1\rangle\,, \\ |^3D_1\rangle_{+1} &=& \sqrt{\tfrac{1}{10}}\,|2,0;+1\rangle - \sqrt{\tfrac{3}{10}}\,|2,+1;0\rangle + \sqrt{\tfrac{3}{5}}\,|2,+2;-1\rangle\,. \end{array}\right. \tag{B18}$$

With the ingredients above, the obtention of the matrix element $\langle {}^3\ell_1'|S_{12}|{}^3\ell_1\rangle$ is straightforward:

- $\ell = \ell' = 0$. In virtue of Eq. (B10), it is clear that

$$\langle {}^3S_1|S_{12}|{}^3S_1\rangle = 0 \tag{B19}$$

—here we have provided an alternative, more involved proof of what we had already shown in the main text.

- $\ell = 2$, $\ell' = 0$; $\ell = 0$, $\ell' = 2$. Take for instance $M = M' = 0$. Using Eq. (B11),

$${}_0\langle {}^3S_1|S_{12}|{}^3D_1\rangle_0 = \sqrt{\tfrac{27}{10\pi}}(c_{0,+1} + c_{0,-1}) - \sqrt{\tfrac{18}{5\pi}}c_{0,0} = \sqrt{8}. \tag{B20}$$

The same result can be obtained for $M = M' = -1, +1$, so that

$$\langle {}^3S_1|S_{12}|{}^3D_1\rangle = \langle {}^3D_1|S_{12}|{}^3S_1\rangle = \sqrt{8}, \tag{B21}$$

where $S_{12}^\dagger = S_{12}$ was used.

- $\ell = \ell' = 2$. Take for instance $M = M' = 1$. Given Eq. (B14),

$$\begin{aligned}{}_{+1}\langle {}^3D_1|S_{12}|{}^3D_1\rangle_{+1} = &\sqrt{\tfrac{9}{245\pi}}c_{+1,+1} + \sqrt{\tfrac{27}{245\pi}}c_{0,+1} + \sqrt{\tfrac{81}{980\pi}}c_{0,0} \\ &- \sqrt{\tfrac{324}{245\pi}}c_{-1,-1} - \sqrt{\tfrac{972}{245\pi}}c_{0,-1} - \sqrt{\tfrac{216}{245\pi}}c_{+1,-1} = -2.\end{aligned} \tag{B22}$$

The same result can be obtained for $M = M' = -1, 0$, so that

$$\langle {}^3D_1|S_{12}|{}^3D_1\rangle = -2. \tag{B23}$$

Next, we compute the matrix element of the operator $\boldsymbol{\sigma}_1 \cdot \boldsymbol{\sigma}_2$ between the initial and the final state,

$${}_{M'}\langle {}^3\ell_1'|\boldsymbol{\sigma}_1 \cdot \boldsymbol{\sigma}_2|{}^3\ell_1\rangle_M = 2\,\langle [\ell', 1]\,1, M'|\left(\boldsymbol{S}^2 - \boldsymbol{S}_1^2 - \boldsymbol{S}_2^2\right)|\,[\ell, 1]\,1, M\rangle = \delta_{\ell,\ell'}\delta_{M,M'}, \tag{B24}$$

i.e. (conservation of the third component of the total angular momentum is understood)

$$\langle {}^3S_1|\boldsymbol{\sigma}_1 \cdot \boldsymbol{\sigma}_2|{}^3S_1\rangle = \langle {}^3D_1|\boldsymbol{\sigma}_1 \cdot \boldsymbol{\sigma}_2|{}^3D_1\rangle = +1, \qquad \langle {}^3S_1|\boldsymbol{\sigma}_1 \cdot \boldsymbol{\sigma}_2|{}^3D_1\rangle = \langle {}^3D_1|\boldsymbol{\sigma}_1 \cdot \boldsymbol{\sigma}_2|{}^3S_1\rangle = 0. \tag{B25}$$

Similarly, but now recalling that $I = 0$ and $I_1 = I_2 = 1/2$, the matrix elements of the operator $\vec{\tau}_1 \cdot \vec{\tau}_2$ turn out to be (spin and isospin conservations are understood)

$$\langle {}^3S_1|\vec{\tau}_1 \cdot \vec{\tau}_2|{}^3S_1\rangle = \langle {}^3S_1|\vec{\tau}_1 \cdot \vec{\tau}_2|{}^3D_1\rangle = \langle {}^3D_1|\vec{\tau}_1 \cdot \vec{\tau}_2|{}^3S_1\rangle = \langle {}^3D_1|\vec{\tau}_1 \cdot \vec{\tau}_2|{}^3D_1\rangle = -3. \tag{B26}$$

Using Eqs. (B19), (B21), (B23), (B25), and (B26) in Eq. (1.61), we finally get for the coordinate OPE potential in the $^3S_1$-$^3D_1$ channel:

$$\langle {}^3S_1|\mathcal{V}_{\rm OPE}(\boldsymbol{r})|{}^3S_1\rangle = -\tfrac{g_A^2 m_\pi^3}{16\pi f_\pi^2} Y(m_\pi r) + \tfrac{g_A^2}{4f_\pi^2}\delta(\boldsymbol{r}), \tag{B27}$$

$$\langle {}^3S_1|\mathcal{V}_{\rm OPE}(\boldsymbol{r})|{}^3D_1\rangle = \langle {}^3D_1|\mathcal{V}_{\rm OPE}(\boldsymbol{r})|{}^3S_1\rangle = -\tfrac{\sqrt{2} g_A^2 m_\pi^3}{8\pi f_\pi^2} T(m_\pi r) Y(m_\pi r), \tag{B28}$$

$$\langle {}^3D_1|\mathcal{V}_{\rm OPE}(\boldsymbol{r})|{}^3D_1\rangle = -\tfrac{g_A^2 m_\pi^3}{8\pi f_\pi^2}\left[\tfrac{1}{2} - T(m_\pi r)\right] Y(m_\pi r) + \tfrac{g_A^2}{4f_\pi^2}\delta(\boldsymbol{r}). \tag{B29}$$

Appendix C

Peripheral demotion and resonances

In this appendix we discuss the different choices for the definition of Λ_{NN}^* and the effect they have on the peripheral demotion of the OPE potential. We will see that the impact of changing the threshold-bound-state assumption by a different condition is rather small. Consider a bound state with binding energy $B \geqslant 0$ at $k_{\rm pole} = i\kappa_B$, $\kappa_B = \sqrt{M_N B} \geqslant 0$. If such bound state emerges from the OPE potential, we will need to consider three scales (m_π, Λ_{NN}^*, and κ_B) in the EFT expansion. Hence, in this context two opposite options appear:

- By requiring $B = 0$, we eliminate one of the variables in the problem, leaving only m_π and Λ_{NN}^*, which combine by means of a numerical factor to give an expansion parameter equal to one (see Eq. (2.34)). This scenario is the easiest and most convenient choice to isolate the scale Λ_{NN}^*, and thus it was exploited in the main text.

- If $B > 0$, conversely, the EFT expansion will involve two different ratios, m_π/Λ_{NN} and κ_B/Λ_{NN}. The breakdown of the amplitude expansion at a particular Λ_{NN} for $k = k_{\rm pole}$ does not necessarily mean that Λ_{NN} is the Λ_{NN}^* we are looking for. There could be a (probably small) mismatch between the two owing to the different numerical factors in each subexpansion. If we were able to take these details into account, it might very well happen that we recovered the original scale generating the threshold bound state.

Yet we will ignore these complications here, and focus instead on checking the robustness of the estimations we presented in the main text. For that we will consider the case of a virtual state or resonance, $k_{\rm pole} = -i\kappa_V$ or $k_{\rm pole} = \kappa_R$, where κ_V is real and positive and κ_R is complex. This will translate into a new value of the critical Λ_{NN}^* that depends on the

Table C.1: Inverse expansion parameter of perturbative OPE and corresponding shift in its peripheral demotion if the threshold-bound-state condition is replaced by the shallow-resonance condition.

Isoscalar waves			Isovector waves		
$^{2S+1}\ell_J$	$\Lambda_{NN}/\Lambda^*_{NN}(\ell, m_\pi)$	$\Delta\nu = \nu' - \nu$	$^{2S+1}\ell_J$	$\Lambda_{NN}/\Lambda^*_{NN}(\ell, m_\pi)$	$\Delta\nu = \nu' - \nu$
$^1P_1$	–4.86	$-(0.14 - 0.25)$	$^1D_2$	33.31	$-(0.16 - 0.29)$
$^1F_3$	–24.9	$-(0.06 - 0.10)$	$^1G_4$	119.7	$-(0.05 - 0.10)$
$^1H_5$	–59.1	$-(0.05 - 0.08)$	$^1I_6$	250.2	$-(0.03 - 0.05)$

position of the pole, $\Lambda^*_{NN} = \Lambda^*_{NN}(\ell, k_{\rm pole})$, $|k_{\rm pole}| \sim Q$. Proceeding as in the $k_{\rm pole} = 0$ case, we define the peripheral demotion as

$$\Lambda^*_{NN}(\ell, k_{\rm pole})/\Lambda_{NN} = (Q/M_{\rm hi})^{\nu'(\ell, k_{\rm pole})}, \tag{C1}$$

where the $'$ distinguishes the new estimations from the old ones (see Table 2.1).

Virtual states and resonances are amplitude poles in the second Riemann sheet of the complex momentum plane. While they are easy to locate in the case of contact-range potentials, finding them for a finite-range potential is technically more challenging, due to the difficulty of choosing the second Riemann sheet in a numerical calculation. As we are interested in peripheral waves, the most natural outcome when the strength of the potential is reduced is that a bound state eventually becomes a resonance. This can be easily traced because the scattering amplitude saturates the unitarity bound and the phase shift reaches 90° at some momentum k close to $\mathrm{Re}[\kappa_R]$. Therefore, the criterion we are going to use for $\Lambda^*_{NN}(\ell, \kappa_R)$ will be

$$\cot \delta_\ell(k = m_\pi) = 0\,, \tag{C2}$$

which in general will imply $|\kappa_R| > m_\pi$, but only by a small amount if the resonance is narrow, $\mathrm{Im}[\kappa_R]^2 \ll \mathrm{Re}[\kappa_R]^2$.

The changes in $\nu(\ell)$ when the resonance condition is imposed are shown in Table C.1. In general the new condition only entails a tiny change in $\nu(\ell)$ in the $-(0.05 - 0.2)$ range. This change is an order of magnitude smaller than the changes in $\nu(\ell)$ related to the uncertainty in the EFT expansion parameter $Q/M_{\rm hi}$ and hence can be safely ignored.

Appendix D

Résumé en français

La philosophie des théories effectives des champs (EFT, de l'anglais *Effective Field Theories*) offre une perspective originale et utile dans la compréhension théorique de problèmes physiques très divers. Il s'agit d'un instrument particulièrement approprié pour l'étude des systèmes avec interaction forte à basse énergie, et ceci pour plusieurs raisons:

- Il établit une connexion manifeste avec la théorie plus fondamentale en imposant les *symétries de QCD* sur le lagrangien effectif exprimé en termes de degrés de liberté effectifs.

- Il exploite la séparation des échelles de la physique nucléaire et hadronique au travers du *power counting*, une recette qui hiérarchise l'importance du nombre infini d'interactions contenues dans le lagrangien effectif et permet une description des observables qui est améliorable ordre par ordre.

- Il est articulé dans le langage de la *renormalisation* qui est largement utilisé dans les théories quantiques des champs et, plus particulièrement, dans QCD; il permet donc d'interpréter la physique nucléaire et hadronique comme l'évolution du groupe de renormalisation de QCD à longues distances.

Dans l'introduction au présent travail, nous avons passé en revue quelques des exemples les plus remarquables d'EFT qui sont largement utilisés dans l'étude moderne des systèmes nucléaires et hadroniques à petit nombre de corps, à savoir l'EFT chirale, l'EFT sans pions et l'EFT de quarks lourds. Dans les chapitres 2 et 3, d'une part, et le chapitre 4, d'autre part, nous avons présenté trois études de cas détaillées de la physique nucléaire et hadronique, respectivement, lorsque ces théories sont utilisés comme lignes directrices.

L'exemple paradigmatique d'une EFT d'interactions fortes à basse énergie est la théorie chirale des perturbations. Il repose sur la (approximative) symétrie chirale de QCD, qui est utilisée comme contrainte fondamentale sur le lagrangien effectif. Au moyen d'un *power counting* qui suit une analyse dimensionnelle naïve («naturel»), la théorie chirale des perturbations décrit des processus réussis à faible impulsion (en dessous de l'échelle caractéristique de QCD, vers 1 GeV) avec un pseudo-boson de Goldstone au minimum plus un nucléon au maximum. Cependant, les processus avec deux nucléons et plus sont intrinsèquement non-perturbatifs, et ne peuvent donc pas être capturés par la théorie chirale des perturbations, ni par un *power counting* en pleine correspondance avec l'analyse dimensionnelle naïve. En effet, déjà dans le secteur de deux nucléons, la renormalisation non-perturbative fait que le nombre d'interactions à courte portée prescrites à un certain ordre par le *counting* dimensionnel ne suffise pas en général à rendre l'amplitude de diffusion véritablement renormalisée. L'*EFT chirale* (ou *pionful*) est la généralisation de la théorie chirale des perturbations à un tel cadre non-perturbatif.

La symétrie chirale prévoit que la portée maximum de la force nucléaire est approximativement donnée par l'inverse de la masse du pion. À des distances suffisamment grandes, les seuls degrés de liberté effectifs sont les nucléons eux-mêmes, de sorte que toutes les interactions entre eux sont de contact. Cette approche est connue sous le nom de *EFT de contact* (ou *pionless*). De même façon que dans le cas *pionful*, le principe d'invariance de renormalisation est utilisé pour dériver le *power counting*. Dans le secteur de deux nucleons, où la théorie est equivalente au développement de portée effective, la mise à l'échelle des couplages n'est pas conforme aux attentes naturelles, ce qui se manifeste par l'existence de deux peu profonds (respectivement réel et virtuel) états liés dans les ondes S.

Dans le chapitre 2, le *power counting* des canaux nucléon-nucléon singulets périphériques —ces ondes avec un moment cinétique de spin nul et un moment cinétique orbital élevé— a été étudié dans le cadre de l'EFT chirale. Nous avons exploré la théorie des perturbations jusqu'au quatrième ordre, ce qui nous a permis de constater que le potentiel d'échange d'un pion est supprimé dans ces canaux par le paramètre d'expansion de l'EFT élevé à une puissance qui croît avec le moment cinétique orbital. Une telle suppression est, encore une fois, en contradiction avec les attentes dimensionnelles et, en fait, s'avère en général beaucoup plus forte que dans le schéma de Kaplan–Savage–Wise, dans lequel l'échange d'un pion entre à deuxième (*next-to-leading*) ordre. Cela ouvre la porte à l'amélioration de la systématique et de la cohérence des calculs dans le secteur de quelques corps, car il fournit une ligne

directrice théorique qui n'inclut que les itérations nécessaires du potentiel d'échange d'un pion et omet les canaux périphériques où l'ordre du potentiel sans itérations est plus élevé que celui du calcul lui-même. Toutefois, pour que ces idées soient pleinement rentables, il faudrait étendre cette analyse à l'échange d'un pion dans les ondes triplets périphériques et aux interactions d'échange de plusieurs pions.

Le canal nucléon-nucléon ${}^1S_0$ —dont le moment cinétique de spin et le moment cinétique orbital sont zéro— n'a pas été considéré dans le chapitre 2, car il présente plusieurs caractéristiques qui en font une onde partielle particulière. Dans le cadre de l'EFT chirale, le chapitre 3 a abordé certaines de ces caractéristiques au moyen d'un nouvel arrangement d'interactions à courte portée. Cela a été fait dans l'esprit de reproduire déjà à premier (*leading*) ordre le comportement qualitatif de l'amplitude sur tout l'interval d'impulsion où l'EFT devrait se maintenir. Puisque la proposition de Weinberg ne reproduit pas le zéro présenté à basse energie par l'amplitude de l'onde ${}^1S_0$ selon l'analyse des ondes partielles (impulsion du centre de masse $\simeq 340\,\mathrm{MeV}$), nous avons proposé un schéma différent où un tel zéro est imposé de manière non-perturbative et les corrections à ordres supérieurs sont incluses de manière perturbative. L'amélioration systématique a été montrée jusqu'au le deuxième ordre, et nous avons obtenu des résultats qui correspondent remarquablement bien aux déphasages phénoménologiques jusqu'au seuil de production de pions. Nous avons également inclus une nouvelle version de l'EFT de contact dans laquelle l'échange des pions était artificiellement découplé (même si la localisation de l'impulsion du zéro se situe au-delà de l'inverse de la masse du pion), ce qui nous a permis d'obtenir des résultats analytiques qui reproduisent l'analyse des ondes partielles assez bien aussi. De ces succès phénoménologiques, nous croyons que la décision d'imposer le zéro du ${}^1S_0$ à premier ordre dans des calculs plus générales et aussi cohérentes avec EFT vaut la peine, car ça peut améliorer la description des observables dans le secteur de quelques corps (noyaux légers, réactions électrofaibles...).

Hors du secteur des nucléons, les hadrons lourds sont des objets intéressants par eux-mêmes, car ils représentent des états liés de particules lourdes et légères. En particulier, les mésons lourds sont composés d'un quark lourd (b ou c) plus un antiquark léger ($\bar{u}$, $\bar{d}$ ou $\bar{s}$). Si la masse du quark lourd est pris suffisament grande, alors le quark léger deviendra insensible à la saveur et au spin du premier (symétrie de quarks lourds). Ce scénario correspond à le premier ordre de l'*EFT de quarks lourds*; les effets qui brisent la symétrie de quarks lourds dans le monde physique doivent être considérés comme des corrections supprimées par les puissances négatives de la masse des quarks lourds. Dans ce cadre, on peut utiliser la symétrie

chirale pour construire une autre version de l'EFT chirale où les pseudo-bosons de Goldstone sont conservés comme degrés de liberté explicites, mais les nucléons sont remplacés par des mésons lourds.

Une telle approche a été utilisée dans le chapitre 4. En particulier, nous avons considéré les mésons charmés D et D^*, d'une part, et les mésons charmés et étranges $D_{s0}^*(2317)$ et $D_{s1}^*(2460)$, d'autre part. La parité intrinsèque opposée des mésons D (D^*) et D_{s0}^* (D_{s1}^*) leur permet d'échanger un kaon d'onde S, qui induit un potentiel de type Yukawa entre des mésons lourds dont la portée est étonnamment longue (en raison de la proximité de leur différence de masse avec la masse du kaon) et dont la force est anormalement élevée (car elle est proportionnelle au carré de cette différence de masse). Ceci presque garantit l'existence des états liés D_{s0}^*D et $D_{s1}^*D^*$ avec $J^P = 0^-$ et $J^P = 0^-, 2^-$ respectivement, puisque les calculs indiquent des énergies de liaison d'environ 50 MeV. Ces résultats ont été identifiés avec les prédictions à premier ordre d'une EFT dont les degrés de liberté explicites sont les mésons lourds et les kaons, où l'interaction de Yukawa est non-perturbative tandis que les termes de contact qui brisent la symétrie de quarks lourds sont pris en compte comme corrections perturbatives. Nous envisageons également l'existence des contreparties des états liés ci-dessus dans le secteur *bottom*, BB_{s0} et $B^*B_{s1}^*$, qui seraient plus fortement liés et présenteraient un spectre plus riche qui pourrait inclure un état d'onde P peu profond et un état d'onde S excité.

Nous notons que les trois travaux présentés respectivement dans les chapitres 2, 3 et 4 emploient diverses techniques théoriques:

- Alors que le chapitre 2 utilise des outils totalement perturbatifs, les chapitres 3 et 4 traitent de façon non-perturbative leurs premiers ordres respectifs.

- Tandis que les chapitres 2 et 3 étudient les problèmes de diffusion, le chapitre 4 est axé sur les états liés.

- Alors que les chapitres 2 et 4 traitent d'interactions purement régulières, le chapitre 3 inclut des termes singuliers dans le potentiel.

Pourtant, le contenu des trois chapitres est inspiré par des EFT d'interactions fortes à faible énergie —EFT chirale dans les chapitres 2 et 3; EFT sans pions dans le chapitre 3; EFT (chirale) de quarks lourds dans le chapitre 4. Cela donne une idée de la polyvalence et de la richesse de l'approche des EFT appliquée aux systèmes nucléaires et hadroniques. Nous

espérons que les propositions fournies dans les chapitres 2 et 3 trouveront des applications au-delà du secteur de deux nucléons, ainsi que les prédictions de nouveaux états liés moléculaires aux mésons lourds que nous ont fait dans le chapitre 4 seront confirmés à l'avenir.

Bibliography

[1] H. Georgi. Effective field theory. *Ann. Rev. Nucl. Part. Sci.*, 43:209, 1993.

[2] A. Pich. Effective field theory. *arXiv:9806303 [hep-ph]*, 1998.

[3] D.B. Kaplan. Five lectures on effective field theory. *arXiv:0510023 [nucl-th]*, 2005.

[4] I.W. Stewart. Effective field theory. *http://ocw.mit.edu*, 2014.

[5] A.A. Petrov and A.E. Blechman. *Effective Field Theories*. World Scientific Publishing Co. Pte. Ltd., 2016.

[6] M. Srednicki. *Quantum Field Theory*. Cambridge University Press, 2007.

[7] S.R. Beane, W. Detmold, K. Orginos, and M.J. Savage. Nuclear physics from lattice QCD. *Prog. Part. Nucl. Phys.*, 66:1, 2011.

[8] C. Alexandrou. Hadron structure in lattice QCD. *Prog. Part. Nucl. Phys.*, 67:101, 2012.

[9] P.F. Bedaque and U. van Kolck. Effective field theory for few-nucleon systems. *Ann. Rev. Nucl. Part. Sci.*, 52:339, 2002.

[10] E. Epelbaum, H.-W. Hammer, and U.-G. Meißner. Modern theory of nuclear forces. *Rev. Mod. Phys.*, 81:1773, 2009.

[11] D.R. Entem and R. Machleidt. Chiral effective field theory and nuclear forces. *Phys. Rept.*, 503:1, 2011.

[12] W. Leidemann and G. Orlandini. Modern *ab initio* approaches and applications in few-nucleon physics with $A \geqslant 4$. *Prog. Part. Nucl. Phys.*, 68:158, 2013.

[13] S. Scherer. Introduction to chiral perturbation theory. *Adv. Nucl. Phys.*, 27:277, 2003.

[14] C.G. Callan, N. Coote, and D.J. Gross. Two-dimensional Yang-Mills theory: A model of quark confinement. *Phys. Rev. D*, 13:1649, 1976.

[15] C. McNeile. An estimate of the chiral condensate from unquenched lattice QCD. *Phys. Lett. B*, 619:124, 2005.

[16] C. Patrignani and others (Particle Data Group collaboration). Review of particle physics. *Chin. Phys. C*, 40:100001, 2016.

[17] J. Gasser and G.R.S. Zarnauskas. On the pion decay constant. *Phys. Lett. B*, 693:122, 2010.

[18] M. Gell-Mann, R.J. Oakes, and B. Renner. Behavior of current divergences under $\mathrm{SU}(3) \times \mathrm{SU}(3)$. *Phys. Rev.*, 175:2195, 1968.

[19] S. Weinberg. Non-linear realizations of chiral symmetry. *Phys. Rev.*, 166:1568, 1968.

[20] S.R. Coleman, J. Wess, and B. Zumino. Structure of phenomenological Lagrangians. I. *Phys. Rev.*, 177:2239, 1969.

[21] C.G. Callan, S.R. Coleman, J. Wess, and B. Zumino. Structure of phenomenological Lagrangians. II. *Phys. Rev.*, 177:2247, 1969.

[22] N.H. Fuchs, H. Sazdjian, and J. Stern. How to probe the scale of $\langle \bar{q}q \rangle$ in chiral perturbation theory. *Phys. Lett. B*, 269:183, 1991.

[23] M. Knecht, H. Sazdjian, J. Stern, and N.H. Fuchs. A possible experimental determination of $m_s/\bar{m}$ from $K_{\mu 4}$ decays. *Phys. Lett. B*, 313:229, 1993.

[24] S. Pislak and others (BNL-E865 collaboration). A new measurement of K^+_{e4} decay and the S-wave $\pi\pi$ scattering length a^0_0. *Phys. Rev. Lett.*, 87:221801, 2001.

[25] G. Colangelo, J. Gasser, and H. Leutwyler. The quark condensate from K_{e4} decays. *Phys. Rev. Lett.*, 86:5008, 2001.

[26] H. Georgi. *Weak Interactions and Modern Particle Theory.* Dover Books, 2009.

[27] A. Manohar and H. Georgi. Chiral quarks and the nonrelativistic quark model. *Nucl. Phys. B*, 234:189, 1984.

[28] H. Georgi. Generalized dimensional analysis. *Phys. Lett. B*, 298:197, 1993.

[29] J. Gasser, M. Sainio, and A. Svarc. Nucleons with chiral loops. *Nucl. Phys. B*, 307:779, 1988.

[30] V. Bernard, N. Kaiser, and U.-G. Meißner. Chiral dynamics in nucleons and nuclei. *Int. J. Mod. Phys. E*, 4:193, 1995.

[31] A. Pich. Chiral perturbation theory. *Rept. Prog. Phys.*, 58:563, 1995.

[32] G. Ecker. Chiral perturbation theory. *Prog. Part. Nucl. Phys.*, 35:1, 1995.

[33] H. Yukawa. On the interaction of elementary particles. *Proc. Phys. Math. Soc. Japan*, 17:48, 1935.

[34] D.B. Kaplan, M.J. Savage, and M.B. Wise. A new expansion for nucleon-nucleon interactions. *Phys. Lett. B*, 424:390, 1998.

[35] D.B. Kaplan, M.J. Savage, and M.B. Wise. Two-nucleon systems from effective field theory. *Nucl. Phys. B*, 534:329, 1998.

[36] S. Weinberg. Nuclear forces from chiral Lagrangians. *Phys. Lett. B*, 251:288, 1990.

[37] S. Weinberg. Effective chiral Lagrangians for nucleon-pion interactions and nuclear forces. *Nucl. Phys. B*, 363:3, 1991.

[38] M. Rho. Exchange currents from chiral Lagrangians. *Phys. Rev. Lett.*, 66:1275, 1991.

[39] C. Ordóñez, L. Ray, and U. van Kolck. Chiral Lagrangians and nuclear forces. *Phys. Lett. B*, 291:459, 1992.

[40] C. Ordóñez, L. Ray, and U. van Kolck. Nucleon-nucleon potential from an effective chiral Lagrangian. *Phys. Rev.Lett.*, 72:1982, 1994.

[41] C. Ordóñez, L. Ray, and U. van Kolck. The two-nucleon potential from chiral Lagrangians. *Phys. Rev. C*, 53:2086, 1996.

[42] V.R. Pandharipande, Daniel R. Phillips, and U. van Kolck. Delta effects in pion-nucleon scattering and the strength of the two-pion-exchange three-nucleon interaction. *Phys. Rev. C*, 71:064002, 2005.

[43] D.R. Entem and R. Machleidt. Chiral two-pion-exchange at order four and peripheral nucleon-nucleon scattering. *Phys. Rev. C*, 66:014402, 2002.

[44] D.R. Entem and R. Machleidt. Accurate charge-dependent nucleon-nucleon potential at fourth order of chiral perturbation theory. *Phys. Rev. C*, 68:041001, 2003.

[45] E. Epelbaum, W. Glockle, and U.-G. Meißner. The two-nucleon system at next-to-next-to-next-to-leading order. *Nucl. Phys. A*, 747:362, 2005.

[46] D.B. Kaplan, M.J. Savage, and M.B. Wise. Nucleon-nucleon scattering from effective field theory. *Nucl. Phys. B*, 478:629, 1996.

[47] A. Nogga, R.G.E. Timmermans, and U. van Kolck. Renormalization of one-pion exchange and power counting. *Phys. Rev. C*, 72:054006, 2005.

[48] M. Pavón Valderrama and E. Ruiz Arriola. Renormalization of nucleon-nucleon interaction with chiral two-pion-exchange potential: Non-central phases. *Phys. Rev. C*, 74:064004, 2006. [Erratum: *Phys. Rev. C*, 75:059905, 2007].

[49] C.-J. Yang, Ch. Elster, and D.R. Phillips. Subtractive renormalization of the chiral potentials up to next-to-next-to-leading order in higher nucleon-nucleon partial waves. *Phys. Rev. C*, 80:034002, 2009.

[50] C.-J. Yang, Ch. Elster, and D.R. Phillips. Subtractive renormalization of the nucleon-nucleon interaction in chiral effective theory up to next-to-next-to-leading order: S waves. *Phys. Rev. C*, 80:044002, 2009.

[51] Ch. Zeoli, R. Machleidt, and D.R. Entem. Infinite-cutoff renormalization of the chiral nucleon-nucleon interaction up to next-to-next-to-next-to-leading order. *Few-Body Syst.*, 54:2191, 2013.

[52] M. Pavón Valderrama and D.R. Phillips. Power counting of contact-range currents in effective field theory. *Phys. Rev. Lett.*, 114:082502, 2015.

[53] E. Epelbaum and U.-G. Meißner. On the renormalization of the one-pion-exchange potential and the consistency of Weinberg's power counting. *Few-Body Syst.*, 54:2175, 2013.

[54] E. Epelbaum and J. Gegelia. Regularization, renormalization and 'peratization' in effective field theory for two nucleons. *Eur. Phys. J. A*, 41:341, 2009.

[55] S. Fleming, T. Mehen, and I.W. Stewart. Next-to-next-to-leading order corrections to nucleon-nucleon scattering and perturbative pions. *Nucl. Phys. A*, 677:313, 2000.

[56] M.C. Birse. Power counting with one-pion exchange. *Phys. Rev. C*, 74:014003, 2006.

[57] M. Pavón Valderrama. Perturbative renormalizability of chiral two-pion exchange in nucleon-nucleon scattering. *Phys. Rev. C*, 83:024003, 2011.

[58] M. Pavón Valderrama. Perturbative renormalizability of chiral two-pion exchange in nucleon-nucleon scattering: P and D waves. *Phys. Rev. C*, 84:064002, 2011.

[59] B. Long and C.-J. Yang. Renormalizing chiral nuclear forces: A case study of $^3P_0$. *Phys. Rev. C*, 84:057001, 2011.

[60] B. Long and C.-J. Yang. Renormalizing chiral nuclear forces: Triplet channels. *Phys. Rev. C*, 85:034002, 2012.

[61] B. Long and C.-J. Yang. Short-range nuclear forces in singlet channels. *Phys. Rev. C*, 86:024001, 2012.

[62] Y.-H. Song, R. Lazauskas, and U. van Kolck. Triton and neutron-deuteron scattering up to next-to-leading order in chiral effective field theory. *Phys. Rev. C*, 96:024002, 2017.

[63] S.R. Beane, P.F. Bedaque, L. Childress, A. Kryjevski, J. McGuire, and U. van Kolck. Singular potentials and limit cycles. *Phys. Rev. A*, 64:042103, 2001.

[64] S.R. Beane, P.F. Bedaque, M.J. Savage, and U. van Kolck. Towards a perturbative theory of nuclear forces. *Nucl. Phys. A*, 700:377, 2002.

[65] M. Pavón Valderrama and E. Ruiz Arriola. Renormalization of nucleon-nucleon interaction with chiral two-pion exchange potential: Central phases and the deuteron. *Phys. Rev. C*, 74:054001, 2006.

[66] M. Pavón Valderrama and E. Ruiz Arriola. Renormalization-group analysis of boundary conditions in potential scattering. *Ann. Phys.*, 323:1037, 2008.

[67] B. Long and U. van Kolck. Renormalization of singular potentials and power counting. *Ann. Phys.*, 323:1304, 2008.

[68] U. van Kolck. Nucleon-nucleon interaction and isospin violation. *Lect. Notes Phys.*, 513:62, 1998.

[69] U. van Kolck. Effective field theory of short-range forces. *Nucl. Phys. A*, 645:273, 1999.

[70] H. Bethe. Theory of the effective range in nuclear scattering. *Phys. Rev.*, 76:38, 1949.

[71] L. Koester and W. Nistler. New determination of the neutron-proton scattering amplitude and precise measurements of the scattering amplitudes on carbon, chlorine, fluorine, and bromine. *Z. Phys. A*, 272:189, 1975.

[72] E. Lomon and R. Wilson. Neutron-proton scattering at a few MeV. *Phys. Rev. C*, 9:1329, 1974.

[73] D.R. Phillips, S.R. Beane, and T.D. Cohen. Non-perturbative regularization and renormalization: Simple examples from non-relativistic quantum mechanics. *Ann. Phys.*, 263:255, 1998.

[74] E.P. Wigner. Lower limit for the energy derivative of the scattering phase shift. *Phys. Rev.*, 98:145, 1955.

[75] D.R. Phillips and T.D. Cohen. How short is too short? Constraining zero-range interactions in nucleon-nucleon scattering. *Phys. Lett. B*, 390:7, 1997.

[76] D.B. Kaplan. More effective field theory for nonrelativistic scattering. *Nucl. Phys. B*, 494:471, 1997.

[77] H.W. Grießhammer. Improved convergence in the three-nucleon system at very low energies. *Nucl. Phys. A*, 744:192, 2004.

[78] S.T. Ma. Redundant zeros in the discrete energy spectra in Heisenberg's theory of characteristic matrix. *Phys. Rev.*, 69:668, 1946.

[79] S.T. Ma. On a general condition of Heisenberg for the S matrix. *Phys. Rev.*, 71:195, 1947.

[80] V.A. Babenko and N.M. Petrov. Determination of low-energy parameters of neutron-proton scattering in the shape-parameter approximation from present-day experimental data. *Phys. Atom. Nuc.*, 73:1499, 2010.

[81] M. Pavón Valderrama and E. Ruiz Arriola. Determination of low energy parameters for nucleon-nucleon scattering at next-to-next-to-next-to-next-to-leading order in all partial waves with $j \leqslant 5$. *arXiv:0407113 [nucl-th]*, 2004.

[82] P.F. Bedaque, H.-W. Hammer, and U. van Kolck. Effective theory for neutron-deuteron scattering: Energy dependence. *Phys. Rev. C.*, 58:641, 1998.

[83] P.F. Bedaque and U. van Kolck. Nucleon-deuteron scattering from an effective field theory. *Phys. Lett. B*, 428:221, 1998.

[84] W. Dilg, L. Koester, and W. Nistler. The neutron-deuteron scattering lengths. *Phys. Lett. B*, 36:208, 1971.

[85] P.F. Bedaque, H.-W. Hammer, and U. van Kolck. Renormalization of the three-body system with short range interactions. *Phys. Rev. Lett.*, 82:463, 1999.

[86] P.F. Bedaque, H.-W. Hammer, and U. van Kolck. The three-boson system with short-range interactions. *Nucl. Phys. A*, 646:444, 1999.

[87] P.F. Bedaque, H.-W. Hammer, and U. van Kolck. Effective theory of the triton. *Nucl. Phys. A*, 676:357, 2000.

[88] H.-W. Hammer and T. Mehen. Range corrections to doublet S-wave neutron-deuteron scattering. *Phys. Lett. B*, 516:353, 2001.

[89] A.C. Phillips. Consistency of the low-energy three-nucleon observables and the separable interaction model. *Nucl. Phys. A*, 107:209, 1968.

[90] L. Platter, H.-W. Hammer, and U.-G. Meißner. On the correlation between the binding energies of the triton and the α-particle. *Phys. Lett. B*, 607:254, 2005.

[91] J.A. Tjon. Bound states of ^{4}He with local interactions. *Phys. Lett. B*, 56:217, 1975.

[92] S. König, H.W. Grießhammer, H.-W. Hammer, and U. van Kolck. Nuclear physics around the unitarity limit. *Phys. Rev. Lett.*, 118:202501, 2017.

[93] J.M. Flynn and N. Isgur. Heavy-quark symmetry: Ideas and applications. *J. Phys. G*, 18:1627, 1992.

[94] Á. de Rújula, H. Georgi, and S.L. Glashow. Hadron masses in a gauge theory. *Phys. Rev. D*, 12:147, 1975.

[95] E. Eichten and F.L. Feinberg. Spin-dependent forces in heavy-quark systems. *Phys. Rev. Lett.*, 43:1205, 1979.

[96] E. Eichten and F.L. Feinberg. Spin-dependent forces in QCD. *Phys. Rev. D*, 23:2724, 1981.

[97] M. Suzuki. Spectator theory of final-state spins in semileptonic decays of heavy-flavored mesons. *Nucl. Phys. B*, 258:553, 1985.

[98] B. Grinstein, M.B. Wise, and N. Isgur. Weak mixing angles from semileptonic decays in the quark model. *Phys. Rev. Lett.*, 56:286, 1986.

[99] T. Altomari and L. Wolfenstein. Comment on "Weak mixing angles from semileptonic decays in the quark model". *Phys. Rev. Lett.*, 58:1583, 1987.

[100] H.D. Politzer and M.B. Wise. Leading logarithms of heavy quark masses in processes with light and heavy quarks. *Phys. Lett. B*, 206:681, 1988.

[101] H.D. Politzer and M.B. Wise. Effective field theory approach to processes involving both light and heavy fields. *Phys. Lett. B*, 208:504, 1988.

[102] N. Isgur, D. Scora, B. Grinstein, and M.B. Wise. Semileptonic B and D decays in the quark model. *Phys. Rev. D*, 39:799, 1989.

[103] A.F. Falk and M.E. Luke. Strong decays of excited heavy mesons in chiral perturbation theory. *Phys. Lett. B*, 292:119, 1992.

[104] P. Colangelo, F. de Fazio, F. Giannuzzi, and S. Nicotri. New meson spectroscopy with open charm and beauty. *Phys. Rev. D*, 86:054024, 2012.

[105] M.B. Wise. Chiral perturbation theory for hadrons containing a heavy quark. *Phys. Rev. D*, 45:2188, 1992.

[106] M. Pavón Valderrama, M. Sánchez Sánchez, C.-J. Yang, B. Long, J. Carbonell, and U. van Kolck. Power counting in peripheral partial waves: The singlet channels. *Phys. Rev. C*, 95:054001, 2017.

[107] M. Sánchez Sánchez, C.-J. Yang, B. Long, and U. van Kolck. The two-nucleon amplitude zero in chiral effective field theory. *arXiv:1704.08524 [nucl-th]*, 2017.

[108] M. Sánchez Sánchez, L.-S. Geng, J.-X. Lu, T. Hyodo, and M. Pavón Valderrama. Exotic doubly charmed $D^*_{s0}(2317)D$ and $D^*_{s1}(2460)D^*$ molecules. *arXiv:1707.03802 [hep-ph]*, 2017.

[109] N. Kaiser, R. Brockmann, and W. Weise. Peripheral nucleon-nucleon phase shifts and chiral symmetry. *Nucl. Phys. A*, 625:758, 1997.

[110] N. Kaiser, S. Gerstendorfer, and W. Weise. Peripheral nucleon-nucleon scattering: Role of Delta excitation, correlated two-pion and vector-meson exchange. *Nucl. Phys. A*, 637:395, 1998.

[111] H. Witala, W. Gloeckle, J. Golak, A. Nogga, H. Kamada, R. Skibinski, and J. Kuros-Zolnierczuk. Nucleon-deuteron elastic scattering as a tool to probe properties of three-nucleon forces. *Phys. Rev. C*, 63:024007, 2000.

[112] D.R. Entem, E. Ruiz Arriola, M. Pavón Valderrama, and R. Machleidt. Renormalization of chiral two-pion-exchange nucleon-nucleon interactions. Momentum versus coordinate space. *Phys. Rev. C*, 77:044006, 2008.

[113] M.C. Birse. Deconstructing triplet nucleon-nucleon scattering. *Phys. Rev. C*, 76:034002, 2007.

[114] M.C. Birse. Deconstructing $^1S_0$ nucleon-nucleon scattering. *Eur. Phys. J. A*, 46:231, 2010.

[115] K.L. Ipson, K. Helmke, and M.C. Birse. Effective short-range interaction for spin-singlet P-wave nucleon-nucleon scattering. *Phys. Rev. C*, 83:017001, 2010.

[116] D.R. Entem, N. Kaiser, R. Machleidt, and Y. Nosyk. Peripheral nucleon-nucleon scattering at fifth order of chiral perturbation theory. *Phys. Rev. C*, 91:014002, 2015.

[117] T.D. Cohen and J.M. Hansen. Systematic power counting in cutoff effective field theories for nucleon-nucleon interactions and the equivalence with PDS. *Phys. Lett. B*, 440:233, 1998.

[118] J.V. Steele and R.J. Furnstahl. Removing pions from two-nucleon effective field theory. *Nucl. Phys. A*, 645:439, 1999.

[119] T. Mehen and I.W. Stewart. Renormalization schemes and the range of two-nucleon effective field theory. *Phys. Rev. C*, 59:2365, 1999.

[120] T. Frederico, V.S. Timóteo, and L. Tomio. Renormalization of the one-pion-exchange interaction. *Nucl. Phys. A*, 653:209, 1999.

[121] J. Gegelia. Nucleon-nucleon scattering and effective field theory: Including pions non-perturbatively. *Phys. Lett. B*, 463:133, 1999.

[122] D.B. Kaplan and J.V. Steele. The long and short of nuclear effective field theory expansions. *Phys. Rev. C*, 60:064002, 1999.

[123] C.H. Hyun, D.-P. Min, and T.-S. Park. A higher-order calculation of neutron-proton scattering in cutoff effective field theory. *Phys. Lett. B*, 473:6, 2000.

[124] M. Lutz. Effective chiral theory of nucleon-nucleon scattering. *Nucl. Phys. A*, 677:241, 2000.

[125] J.M. Nieves. Renormalization of the one-pion-exchange nucleon-nucleon interaction in presence of derivative contact interactions. *Phys. Lett. B*, 568:109, 2003.

[126] J.A. Oller. Nucleon-nucleon interactions from effective field theory. *Nucl. Phys. A*, 725:85, 2003.

[127] M. Pavón Valderrama and E. Ruiz Arriola. Renormalization of singlet nucleon-nucleon scattering with one-pion exchange and boundary conditions. *Phys. Lett. B*, 580:149, 2004.

[128] M. Pavón Valderrama and E. Ruiz Arriola. Renormalization of nucleon-nucleon scattering with one-pion exchange and boundary conditions. *Phys. Rev. C*, 70:044006, 2004.

[129] V.S. Timóteo, T. Frederico, A. Delfino, and L. Tomio. Recursive renormalization of the singlet one-pion exchange plus point-like interactions. *Phys. Lett. B*, 621:109, 2005.

[130] J.-F. Yang and J.-H. Huang. A Padé-aided analysis of non-perturbative nucleon-nucleon scattering in $^1S_0$ channel. *Commun. Theor. Phys.*, 47:699, 2007.

[131] J. Soto and J. Tarrús. Taking dibaryon fields seriously. *Phys. Rev. C*, 78:024003, 2008.

[132] D. Shukla, D.R. Phillips, and E. Mortenson. Chiral potentials, perturbation theory, and the $^1S_0$ channel of nucleon-nucleon scattering. *J. Phys. G*, 35:115009, 2008.

[133] C.-J. Yang, Ch. Elster, and D.R. Phillips. Subtractive renormalization of the nucleon-nucleon scattering amplitude at leading order in chiral effective theory. *Phys. Rev. C*, 77:014002, 2008.

[134] K. Harada, H. Kubo, and Y. Yamamoto. Pions are neither perturbative nor non-perturbative: Wilsonian renormalization-group analysis of nuclear effective field theory including pions. *Phys. Rev. C*, 83:034002, 2011.

[135] S.-I. Ando and C. H. Hyun. Effective range corrections from effective field theory with dibaryon fields and perturbative pions. *Phys. Rev. C*, 86:024002, 2012.

[136] S. Szpigel and V.S. Timóteo. Power counting and renormalization-group invariance in the subtracted kernel method for the two-nucleon system. *J. Phys. G*, 39:105102, 2012.

[137] B. Long. Improved convergence of chiral effective field theory for $^1S_0$ of nucleon-nucleon scattering. *Phys. Rev. C*, 88:014002, 2013.

[138] K. Harada, H. Kubo, T. Sakaeda, and Y. Yamamoto. Convergent perturbative nuclear effective field theory. *arXiv:1311.3063 [nucl-th]*, 2013.

[139] E. Epelbaum, A.M. Gasparyan, J. Gegelia, and H. Krebs. $^1S_0$ nucleon-nucleon scattering in the modified Weinberg approach. *Eur. Phys. J. A*, 51:71, 2015.

[140] X.-L. Ren, K.-W. Li, L.-S. Geng, B. Long, P. Ring, and J. Meng. Leading-order covariant chiral nucleon-nucleon interaction. *arXiv:1611.08475 [nucl-th]*, 2016.

[141] V.G.J. Stoks, R.A.M. Klomp, M.C.M. Rentmeester, and J.J. de Swart. Partial-wave analysis of all nucleon-nucleon scattering data below 350 MeV. *Phys. Rev. C*, 48:792, 1993 (http://nn-online.org).

[142] S.R. Beane and M.J. Savage. Rearranging pionless effective field theory. *Nucl. Phys. A*, 694:511, 2001.

[143] A. Vaghani, R. Higa, G. Rupak, and U. van Kolck. In preparation.

[144] S. König, H.W. Grießhammer, H.-W. Hammer, and U. van Kolck. Effective theory of ^{3}H and ^{3}He. *J. Phys. G*, 43:055106, 2016.

[145] L. Castillejo, R.H. Dalitz, and F.J. Dyson. Low's scattering equation for the charged and neutral scalar theories. *Phys. Rev.*, 101:543, 1956.

[146] D.R. Entem and J.A. Oller. The N/D method with non-perturbative left-hand-cut discontinuity and the $^1S_0$ nucleon-nucleon partial wave. *arXiv:1610.01040 [nucl-th]*, 2016.

[147] M.I. Krivoruchenko. Remarks on the origin of Castillejo-Dalitz-Dyson poles. *Phys. Rev. C*, 82:018201, 2010.

[148] V.G.J. Stoks, R.A.M. Klomp, C.P.F. Terheggen, and J.J. de Swart. Construction of high-quality nucleon-nucleon potential models. *Phys. Rev. C*, 49:2950, 1994 (http://nn-online.org).

[149] I. Stetcu, B.R. Barrett, and U. van Kolck. No-core shell model in an effective-field-theory framework. *Phys. Lett. B*, 653:358, 2007.

[150] L. Contessi, A. Lovato, F. Pederiva, A. Roggero, J. Kirscher, and U. van Kolck. Ground-state properties of ^{4}He and ^{16}O extrapolated from lattice QCD with pionless EFT. *Phys. Lett. B*, 772:839, 2017.

[151] W.T.H. van Oers and J.D. Seagrave. The neutron-deuteron scattering lengths. *Phys. Lett.*, 36B:208, 1967.

[152] J. Vanasse. Fully perturbative calculation of neutron-deuteron scattering to next-to-next-to-leading order. *Phys. Rev. C*, 88:044001, 2013.

[153] M.B. Voloshin and L.B. Okun. Hadron molecules and charmonium atom. *JETP Lett.*, 23:333, 1976.

[154] Á. de Rújula, H. Georgi, and S.L. Glashow. Molecular charmonium: A new spectroscopy? *Phys. Rev. Lett.*, 38:317, 1977.

[155] S.K. Choi and others (Belle collaboration). Observation of a new narrow charmonium-like state in exclusive $B^{\pm} \to K^{\pm}\pi^{+}\pi^{-}J/\psi$ decays. *Phys. Rev. Lett.*, 91:262001, 2003.

[156] M. Ablikim and others (BESIII collaboration). Observation of a charged charmonium-like structure in $e^{+}e^{-} \to p^{+}p^{-}J\psi$ at $\sqrt{s} = 4.26\,\mathrm{GeV}$. *Phys. Rev. Lett.*, 110:252001, 2013.

[157] Z.Q. Liu and others (Belle collaboration). Study of $e^{+}e^{-} \to \pi^{+}\pi^{-}J/\psi$ and observation of a charged charmonium-like state at Belle. *Phys. Rev. Lett.*, 110:252002, 2013.

[158] Q. Wang, C. Hanhart, and Q. Zhao. Decoding the riddle of $Y(4260)$ and $Z_c(3900)$. *Phys. Rev. Lett.*, 111:132003, 2013.

[159] F.-K. Guo, C. Hidalgo-Duque, J. Nieves, and M. Pavón Valderrama. Consequences of heavy-quark symmetries for hadronic molecules. *Phys. Rev. D*, 88:054007, 2013.

[160] A. Bondar and others (Belle collaboration). Observation of two charged bottomonium-like resonances in $\Upsilon(5S)$ decays. *Phys. Rev. Lett.*, 108:122001, 2012.

[161] I. Adachi and others (Belle collaboration). Evidence for a $Z_b^0(10610)$ in Dalitz analysis of $\Upsilon(5S) \to \Upsilon(nS)\pi^0\pi^0$. *arXiv:1207.4345 [hep-ex]*, 2012.

[162] M.B. Voloshin. Radiative transitions from $\Upsilon(5S)$ to molecular bottomonium. *Phys. Rev. D*, 84:031502, 2011.

[163] M. Cleven, F.-K. Guo, C. Hanhart, and U.-G. Meißner. Bound state nature of the exotic Z_b states. *Eur. Phys. J. A*, 47:120, 2011.

[164] R. Aaij (LHCb collaboration). Observation of $J/\psi p$ resonances consistent with pentaquark states in $\Lambda_b^0 \to J/\psi K^{-} p$ decays. *Phys. Rev. Lett.*, 115:072001, 2015.

[165] R. Chen, X. Liu, X.-Q. Li, and S.-L. Zhu. Identifying exotic hidden-charm pentaquarks. *Phys. Rev. Lett.*, 115:132002, 2015.

[166] M. Karliner and J.L. Rosner. New exotic meson and baryon resonances from doubly-heavy hadronic molecules. *Phys. Rev. Lett.*, 115:122001, 2015.

[167] H.-X. Chen, W. Chen, X. Liu, T.G. Steele, and S.-L. Zhu. Towards exotic hidden-charm pentaquarks in QCD. *Phys. Rev. Lett.*, 115:172001, 2015.

[168] L. Roca, J. Nieves, and E. Oset. LHCb pentaquark as a $\bar{D}^*\Sigma_c - \bar{D}^*\Sigma_c^*$ molecular state. *Phys. Rev. D*, 92:094003, 2015.

[169] C.W. Xiao and U.-G. Meißner. $J/\psi(\eta_c)N$ and $\Upsilon(\eta_b)N$ cross sections. *Phys. Rev. D*, 92:114002, 2015.

[170] T.J. Burns. Phenomenology of $P_c^+(4380)$, $P_c^+(4450)$ and related states. *Eur. Phys. J. A*, 51:152, 2015.

[171] L.S. Geng, J.X. Lu, and M. Pavón Valderrama. Scale invariance in heavy hadron molecules. *arXiv:1704.06123 [hep-ph]*, 2017.

[172] V. Efimov. Energy levels arising from resonant two-body forces in a three-body system. *Phys. Lett. B*, 33:563, 1970.

[173] L.-S. Geng, J.-X. Lu, M. Pavón Valderrama, and X.-L. Ren. Are there near-threshold Coulomb-like baryonia? *arXiv:1705.00516 [hep-ph]*, 2017.

[174] A.V. Manohar and M.B. Wise. Exotic $QQ\bar{q}\bar{q}$ states in QCD. *Nucl.Phys. B*, 399:17, 1992.

[175] P. Bicudo, K. Cichy, A. Peters, B. Wagenbach, and M. Wagner. Evidence for the existence of $ud\bar{b}\bar{b}$ and the non-existence of $ss\bar{b}\bar{b}$ and $cc\bar{b}\bar{b}$ tetraquarks from lattice QCD. *Phys. Rev. D*, 92:014507, 2015.

[176] A. Francis, R.J. Hudspith, R. Lewis, and K. Maltman. Lattice prediction for deeply bound doubly heavy tetraquarks. *Phys. Rev. Lett.*, 118:142001, 2017.

[177] J. Carlson, L. Heller, and J.A. Tjon. Stability of dimesons. *Phys. Rev. D*, 37:744, 1988.

[178] B.A. Gelman and S. Nussinov. Does a narrow tetraquark $cc\bar{u}\bar{d}$ state exist? *Phys. Lett. B*, 551:296, 2003.

[179] J. Vijande, A. Valcarce, and N. Barnea. Exotic meson-meson molecules and compact four-quark states. *Phys. Rev. D*, 79:074010, 2009.

[180] F.-K. Guo and U.-G. Meißner. More kaonic bound states and a comprehensive interpretation of the D_{sJ} states. *Phys. Rev. D*, 84:014013, 2011.

[181] P. Colangelo, F. de Fazio, G. Nardulli, N. di Bartolomeo, and R. Gatto. Strong coupling of excited heavy mesons. *Phys. Rev. D*, 52:6422, 1995.

[182] P. Colangelo and F. de Fazio. QCD interactions of heavy mesons with pions by light cone sum rules. *Eur. Phys. J. C*, 4:503, 1998.

[183] D. Becirevic, E. Chang, and A. Le Yaouanc. Pionic couplings to the lowest heavy-light mesons of positive and negative parity. *arXiv:1203.0167 [hep-lat]*, 2012.

[184] D. Gamermann and E. Oset. Axial resonances in the open and hidden charm sectors. *Eur. Phys. J. A*, 33:119, 2007.

[185] A. Martínez Torres, E. Oset, S. Prelovsek, and A. Ramos. Reanalysis of lattice QCD spectra leading to the $D_{s0}^*(2317)$ and $D_{s1}^*(2460)$. *JHEP*, 05:153, 2015.

[186] M. Pavón Valderrama. Power counting and perturbative one-pion-exchange in heavy meson molecules. *Phys. Rev. D*, 85:114037, 2012.

[187] J.-X. Lu, L.-S. Geng, and M. Pavón Valderrama. Heavy-baryon molecules in effective field theory. *arXiv:1706.02588 [hep-ph]*, 2017.

[188] M.C. Birse, J.A. McGovern, and K.G. Richardson. A renormalization-group treatment of two-body scattering. *Phys. Lett. B*, 464:169, 1999.

[189] M. Pavón Valderrama. Power counting and Wilsonian renormalization in nuclear effective field theory. *Int. J. Mod. Phys. E*, 25:1641007, 2016.

[190] T. Barford and M.C. Birse. A renormalization-group approach to two-body scattering in the presence of long-range forces. *Phys. Rev. C*, 67:064006, 2003.

[191] K. Abe and others (Belle collaboration). Study of $B^- \to D^{**0}\pi^-$ ($D^{**0} \to D^{(*)+}\pi^-$) decays. *Phys. Rev. D*, 69:112002, 2004.

[192] H.-Y. Cheng. Hadronic b decays involving even parity charmed mesons. *Phys. Rev. D*, 68:094005, 2003.

[193] T. Hyodo, Y.-R. Liu, M. Oka, K. Sudoh, and S. Yasui. Production of doubly-charmed tetraquarks with exotic color configurations in electron-positron collisions. *Phys. Lett. B*, 721:56, 2013.

[194] S. Cho and others (ExHIC collaboration). Exotic hadrons from heavy-ion collisions. *Prog. Part. Nucl. Phys.*, 95:279, 2017.

[195] R. Aaij and others (LHCb collaboration). Observation of the doubly-charmed baryon Ξ_{cc}^{++}. *Phys. Rev. Lett.*, 119:112001, 2017.

[196] F.-K. Guo, P.-N. Shen, H.-C. Chiang, R.-G. Ping, and B.-S. Zou. Dynamically generated 0^+ heavy mesons in a heavy chiral unitary approach. *Phys. Lett. B*, 641:278, 2006.

[197] F.-K. Guo, P.-N. Shen, and H.-C. Chiang. Dynamically generated 1^+ heavy mesons. *Phys. Lett. B*, 647:133, 2007.

[198] M. Altenbuchinger, L.-S. Geng, and W. Weise. Scattering lengths of Nambu-Goldstone bosons off D mesons and dynamically generated heavy-light mesons. *Phys. Rev. D*, 1:014026, 2014.

[199] C.B. Lang, D. Mohler, S. Prelovsek, and R.M. Woloshyn. Predicting positive-parity B_s mesons from lattice QCD. *Phys. Lett. B*, 750:17, 2015.

[200] S. Weinberg. *The Quantum Theory of Fields. Vol. 2: Modern Applications*. Cambridge University Press, 1996.

université PARIS-SACLAY | ÉCOLE DOCTORALE PHENIICS

Titre : *Théories effectives des champs pour systèmes avec interaction forte : diffusion des nucléons et états liés de quarks lourds*

Mots clés : théorie effective ; nucléons ; mesons lourds ; renormalisation ; symétrie chirale ; pions

Résumé : Au cours des dernières décennies, des théories effectives des champs (TEC) ont été largement utilisées comme approche de la physique à interaction forte et à faible énergie (régimes nucléaires et hadroniques). Dans cette thèse, nous explorons en detail trois exemples d'application du programme des TEC au système nucléon-nucléon dans l'état de spin singulet (onde S et ondes périphériques respectivement) et aux molécules théorisées de mésons lourds DD_{s0}* et D^*D_{s1}*.

Title : *Effective field theories of strong-interacting systems in nucleon scattering and heavy-quark bound states*

Keywords : effective theory ; nucleons ; heavy mesons ; renormalization ; chiral symmetry ; pions

Abstract : Effective field theories (EFT) have been widely used as an approach to strong-interacting physics in the low-energy region (nuclear and hadronic regimes). In this thesis, we explore in detail three examples of application of the EFT program to the two-nucleon spin-singlet state (S wave and peripheral waves, respectively) and to the theorized heavy meson molecules DD_{s0}* and D^*D_{s1}*.

Université Paris-Saclay
Espace Technologique / Immeuble Discovery
Route de l'Orme aux Merisiers RD 128 / 91190 Saint-Aubin, France